A Scientific Approach to EMI Reduction in Switching Power Supplies

by

Thomas Farkas

B.S., Massachusetts Institute of Technology (1989)

Submitted to the Department of Electrical Engineering and Computer Science
in partial fulfillment of the requirements for the degree of

Master of Science in Electrical Engineering

at the

MASSACHUSETTS INSTITUTE OF TECHNOLOGY

September 1991

Author .....
Department of Electrical Engineering and Computer Science
August 30, 1991

Certified by .....
Martin F. Schlecht
Associate Professor of Electrical Engineering
Thesis Supervisor

Accepted by .....
Campbell L. Searle
Chairman, Departmental Committee on Graduate Students

A Scientific Approach to EMI Reduction in Switching Power Supplies

by

Thomas Farkas

Submitted to the Department of Electrical Engineering and Computer Science
on August 30, 1991, in partial fulfillment of the
requirements for the degree of
Master of Science in Electrical Engineering

Abstract

The increasingly larger scale of integration in electronic systems has demanded a corresponding increase in the density of the power supplies of these systems. To some extent, this demand has been met by resorting to higher switching frequency power converters ($\sim$1 MHz). One of the major problems with high frequency switching converters is the generation of radio frequency signals which may interfere with communication broadcasts. The amount of this electromagnetic interference (EMI) which a product may generate is subject to governmental regulations throughout much of the world. The regulatory standards can generally be met with the addition of an EMI filter on the line side of the power supply. EMI filters may be quite large due to the large storage elements needed to filter the power line.

The application of EMI filters is generally quite unscientific and often results in costly iterations and suboptimal results. Power supply and EMI filter designs might be significantly improved by investigation of some of the issues associated with these filters, development of some useful instrumentation procedures, and the application of some methodology and innovation to the design of these filters.

This document proposes a strategy for EMI research, outlining the major issues to be investigated. Some of this research has been undertaken in the work of this thesis. A project to characterize and understand the performance of EMI filters led to some understanding of the influence of component parasitics and electromagnetic coupling on filter performance. Work on characterization of power supply EMI sources has also been undertaken. The other major aspect of this work is an investigation into the practical application of active circuitry to EMI filtering at the utility interface of a switching power supply. The major problem addressed is compensation of the feedback loop of the active filter, which includes the variable external impedance of the utility. For the specific application considered herein, that of a conventional switching frequency of 75 kHz, the active filters were not found to be practical. Extending analysis up to higher switching frequencies, however, to which the power supply industry is moving anyway, shows potential for active filtering as a viable means for controlling EMI more effectively with lower cost and volume.

Thesis Supervisor: Martin F. Schlecht
Title: Associate Professor of Electrical Engineering

Contents

List of Figures

Chapter 1

Introduction

1.1 Motivations for Research

As the scale of integration in computer systems continues to increase, these systems require larger amounts of power in smaller volumes. To truly take advantage of this miniaturization, the power supplies in such systems must therefore process more power in smaller volumes. Aside from heatsinks, energy storage elements occupy most of the volume of power converters. By increasing the converter's switching frequency, these storage elements can be made many times smaller. With recent advances, converters can now operate well into the radio frequency range ($\frac{1}{2}$ - 10 MHz).

A significant problem associated with high frequency switching converters, is the generation of electromagnetic interference (EMI) by the action of the switching. EMI signals may be currents which are conducted through the power line, or electromagnetic waves which are radiated into the environment. If conducted through the line, these signals can interfere with other electronic circuits operating on the same line and, at high enough frequencies, they will result in radiated EMI. Excessive levels of radiated noise in the radio frequency range will, of course, interfere with communication signals.

In order to prevent these problems associated with excessive EMI from power supplies, as well as from other parts of electronic systems, various national and international regulatory agencies have set up standards limiting conducted and radiated EMI generated by electronic equipment, as well as test procedures to determine whether or not systems meet these standards. While radio frequency noise may be reduced at its source to some extent through careful design techniques, some form of low-pass filter between the power supply and the

line is generally required to meet the standards. Because this EMI filter requires energy storage elements and carries high currents and voltages, it may be quite large; like the rest of the power supply, its size reduction may significantly reduce the size and cost of the system for which it operates.

For the most part, the design and application of EMI filters to power supplies for computer systems is surprisingly unscientific in practice. The regulatory standards are generally met through costly trial and error methods, starting with "what worked last time." The goals of this ongoing research are to develop more scientific methods for the design of EMI filters and to use these methods to develop practical designs for EMI filters with greater cost and size efficiency. Although radiated emissions will be considered too, most of this work has focused on conducted EMI, since it is more directly affected by the EMI filters.

1.2 Background

1.2.1 Standards and Test Procedures

Standards limiting radio frequency emissions from commercial electronic equipment are set by the Federal Communications Commission (FCC) in the United States and by similar agencies throughout the world. Many countries have adopted the standards set by the International Special Committee on Radio Interference (CISPR), and products to be marketed internationally are generally tested to meet its EMI limits. Figure 1-1 shows the strictest compilation of international limits which apply to residentially marketed computing devices. An important characteristic of these standards is that in the low frequency

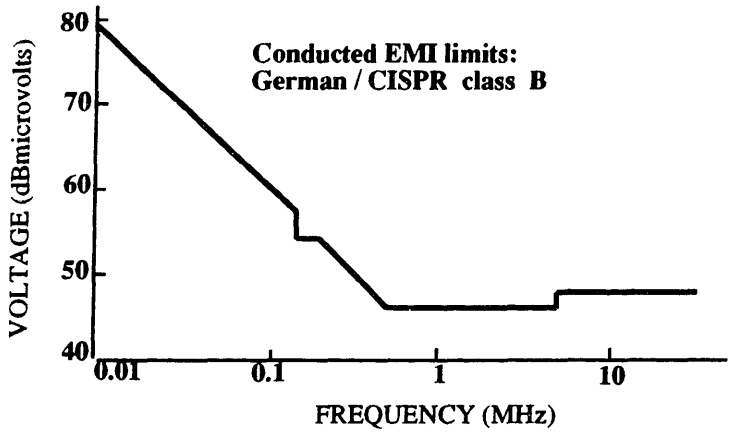

Figure 1-1: Strictest international commerce standards for conducted emissions

range, the limits become stricter by 20 dB per decade as frequency increases. They then level off for frequencies above 500 kHz, except for a small step at 5 MHz.

Typical commercial standards, including those of CISPR and the FCC, specify limits on conducted emissions in terms of a voltage measured across a specific line impedance of 50Ω shunting each phase (hot and neutral) to ground. In accordance, a line impedance stabilization network (LISN) is usually used in testing for EMI requirements. The LISN interfaces the power line, the test product, and a spectrum analyzer used to determine EMI levels throughout the RF range. Besides providing a standardized impedance to the unit under test, the LISN low-pass filters the incoming power line from external noise and protects the instrumentation from the large 60 Hz voltage of the power line with a high-pass filter. A typical circuit for one phase of a LISN is shown in Fig. 1-2, taken from [9]. Each phase of the power line interfaces with the test item through one of these circuits. The common connection shown in the circuit is tied to earth ground and the corresponding connection in the unit under test.

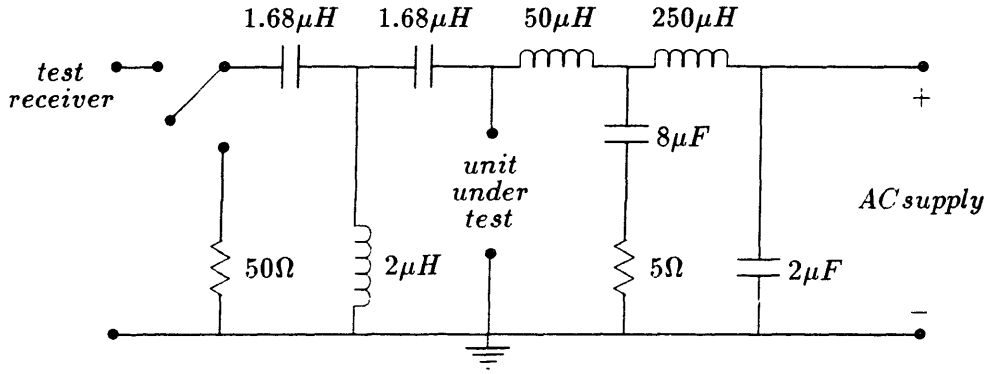

Figure 1-2: Single phase of a LISN

The switch at the test receiver port of the LISN toggles the termination of the high-pass filter between the 50Ω resistor shown and the test receiver input, which should also be 50Ω for standard testing. The magnitude of the transfer function between the EMI source voltage and the voltage at the measurement port is shown in Figure 1-3. Due to the large difference in order of magnitude between the 60 Hz power line frequency and the EMI measurement frequencies, this third-order high-pass filter is sufficient to attenuate the 60 Hz signal by 100 dB and still have a flat pass-band above 10 kHz.

An important function of the LISN is to present the test item with a standardized

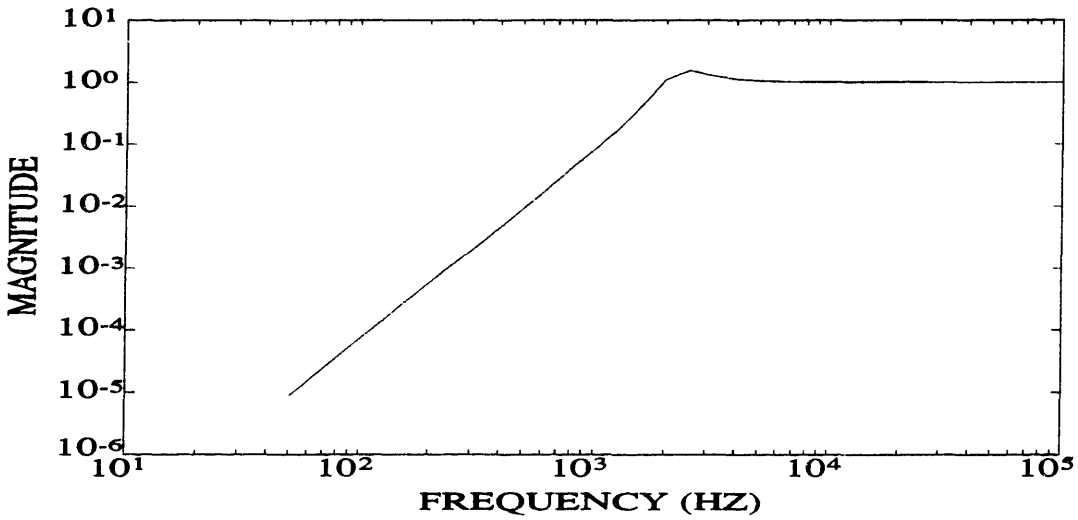

Figure 1-3: LISN transfer function from EMI source to measurement

impedance which is also typical of the impedance that may be seen looking into the ac power line. Figure 1-4 shows the LISN's input impedance at the test unit port over the specified EMI measurement frequency range. Over this range the line impedance seen by the unit is approximated by the parallel combination of a 50Ω resistor and the series combination

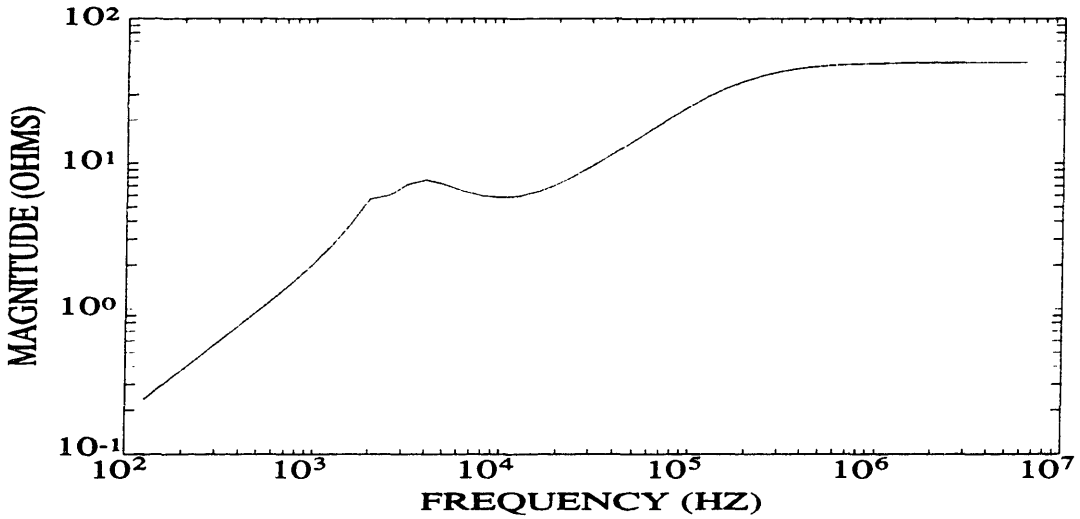

Figure 1-4: Impedance of LISN to test item with AC power line connection shorted

of a 5Ω resistor and a 50μH inductor, which is the simulated impedance required if all major commercial specifications, including those of the FCC, VDE, and CISPR, are to be met between 9 kHz and 30 MHz. At high frequencies (above 1 MHz) this simulated line impedance becomes a purely resistive 50Ω.

Equipment designed for United States military applications is subject to a different set of requirements on noise emissions. These specifications, given by [10] and shown in Fig. 1-5, are more stringent in that they fall by 30 dB per decade up to a frequency of 2 MHz.[3] Unlike the commercial standards which specify the maximum voltage across a specified impedance, the military specifies a current ripple limit which is 10 μA at 2 MHz and above. The line impedance used, a 10 μF feedthrough capacitor [10], is essentially a short circuit at these frequencies.

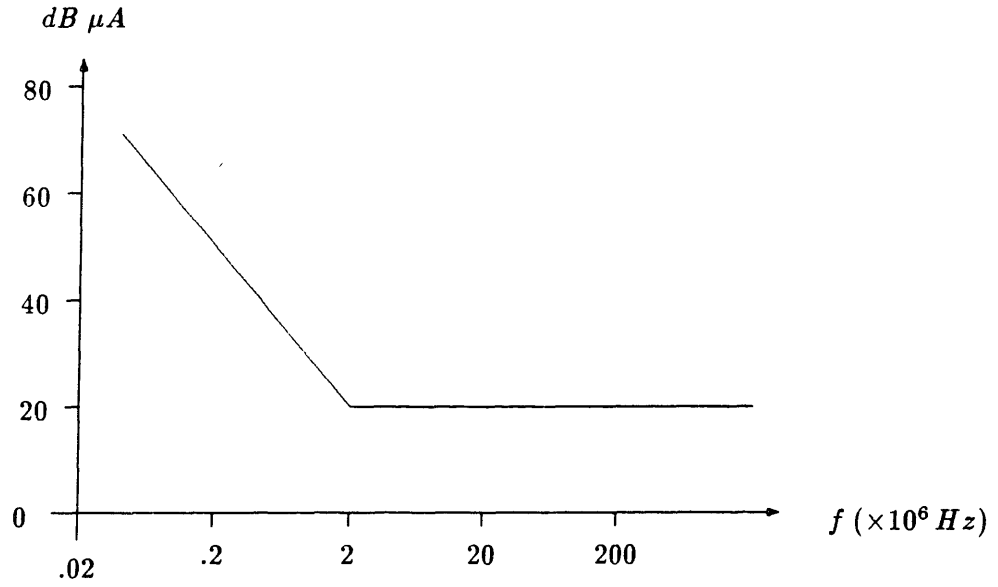

Figure 1-5: MIL-STD-461B CE03 Current Ripple Specification

Measurements of conducted emissions are performed over a ground plane to reduce the effects of external EMI. Radiated emissions in the frequency range of 30 to 1000 MHz are measured over a larger ground plane using a receiver and an antenna located a few meters from the test unit.[1]

1.2.2 Common-Mode and Differential-Mode EMI

Although the EMI standards specify limits on the EMI measured between each phase and neutral, it is very useful to consider EMI as consisting of two orthogonal components: differential-mode and common-mode. The differential-mode current is that current which flows in through either the hot or neutral wire of the utility connection and returns through the other. The common-mode current flows in through both hot and neutral and returns

through the third, or ground wire. While the differential-mode currents are generally a direct result of the on-off switching of the current flow through the power supply, the common-mode currents result mostly from stray capacitances to ground which conduct current when nodes are switched between different voltage levels. Both types of conducted EMI therefore have spectra dominated by the switching frequency and, to a lesser extent, by the harmonics of that frequency.

1.2.3 Basic EMI Filters

The basic building block of an EMI filter is a low-pass stage containing a series impedance that is large at the switching frequency and a shunt impedance that is small at that frequency. Thus, a series inductor L and a shunt capacitor C usually form the ideal block. The order of the two components depends on whether current or voltage is to be filtered, which is a function of the type of EMI source. Since any source has some impedance and may be expressed as either a Thevenin equivalent voltage source with some impedance or as a Norton equivalent current source with the same impedance, this impedance characteristic of the source is what determines the order of components. In order to take advantage of the source impedance, a low source impedance should be followed by a high (series) impedance and a high source impedance should be followed by a low (shunt) impedance. In certain applications, lossy components, including ferrites as well as resistors, may also be useful filter elements to limit resonances. [8]

An important point to note about the simple L-C filter is that while it has 0 dB attenuation well below the resonant frequency $\omega_o = 1/\sqrt{LC}$, at the higher frequencies of interest, it will attenuate (ideally) by a factor of $\omega^2 LC$, which increases by 40 dB with each decade in frequency. This characteristic is quite useful, given the fact that most EMI standards have limits that drop with frequency as well.

When a very large amount of attenuation is desired, two or more filter stages may be cascaded to obtain this attenuation with much smaller components than would be needed using only one stage.[2] However, care must be taken, particularly with multiple stages and smaller components, that L-C resonances do not occur at EMI frequencies and that they are reasonably damped in any case.

1.2.4 Components

While an EMI filter could be designed to simply filter each phase with respect to ground, filters typically distinguish between common-mode and differential-mode EMI. A major reason for this distinction is that safety limits on levels of currents from either phase to ground restrict the size of capacitors connected from the hot or neutral wires to ground. These capacitors are commonly referred to as 'Y' capacitors if they have been designed and approved for this use. Larger valued capacitors, known as 'X' capacitors, may be connected between the phases, however, to filter differential-mode emissions in conjunction with relatively small inductors. Still, the common-mode filtering requires large inductors to make up for the small capacitors to ground. Because these inductors must also support the low frequency line current, they must have relatively heavy wire as well as large cores to support the low frequency magnetic field without saturating. Part of this problem is solved by using a relatively large-valued common-mode inductor. A common-mode inductor, as shown in Fig. 1-6, is simply a N:N transformer connected in series with the two phases of the power line so that the fluxes from oppositely-directed (differential-mode) currents, labeled i_{DM}, cancel each other. Thus, for reasonably good coupling the large low-frequency differential mode current sees very little inductance and does not create a magnetizing flux in the core. Of course, there will be some leakage inductance; in fact, this leakage is often large enough to contribute to the differential-mode filtering function. The common-mode current i_{CM}, however, sees this differential inductance plus the much larger common-mode inductance.

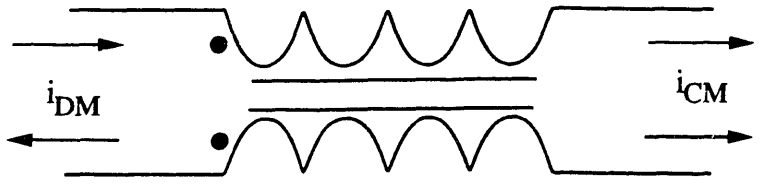

Figure 1-6: Connection of a transformer as a common-mode inductor

1.2.5 Filter Design

While the ideal performance of a filter may be easily predicted based on the values of inductance and capacitance used, there are many parasitic effects in components and layouts which drastically affect the actual performance of typical EMI filters. Besides accounting

for these effects, the design of an EMI filter should be tailored to the relevant EMI standards and the EMI source in the power supply. The external impedances of the power line and the EMI source also need to be considered. Typically, however, the EMI filter is designed on a trial-and-error basis, often starting with some other filter that may have been used for a similar power supply and then making necessary additions or changes until the unit passes the required emission tests. Often, little attention is paid to whether the EMI problems are due to differential-mode or common-mode noise. By the time the tests have been passed, the resulting filter design is usually far from optimal.

1.3 Outline

This thesis is divided into several distinct sections. Chapter 2 sets forth a proposed research strategy for EMI reduction, discussing the categories of issues associated with this topic. This chapter also provides a useful overview of much of the results discussed in Chapter 3. The rest of the chapters discuss work which was undertaken as part of this EMI research plan. Chapter 3 reports the results of a filter measurement study and touches upon a great many of the EMI issues. Chapter 4 concerns instrumentation methods to characterize power supplies. Chapter 5 introduces the topic of active EMI filtering by discussing its basic principles and the issues of its practical application, as well as some previous work on the topic. This chapter sets the stage for the following chapter which analyzes some active circuits and their problems in attempting to develop practical applications. Chapter 7 attempts to tie this work together with some conclusions and to suggest directions for continuing the study of EMI reduction in power supplies.

Chapter 2

Issues for EMI Filter Design Research

As part of this thesis, we propose the development of a scientific strategy for designing filters to meet EMI standards for power supplies. This strategy may be the basis for a filter design software package which would interact with instrumentation. This package might develop into a knowledge-based CAD system. Fig. 2-1 expresses the relationship between the fundamental objectives of this strategy. At the very least, this strategy requires a deeper understanding of many issues associated with EMI filters.

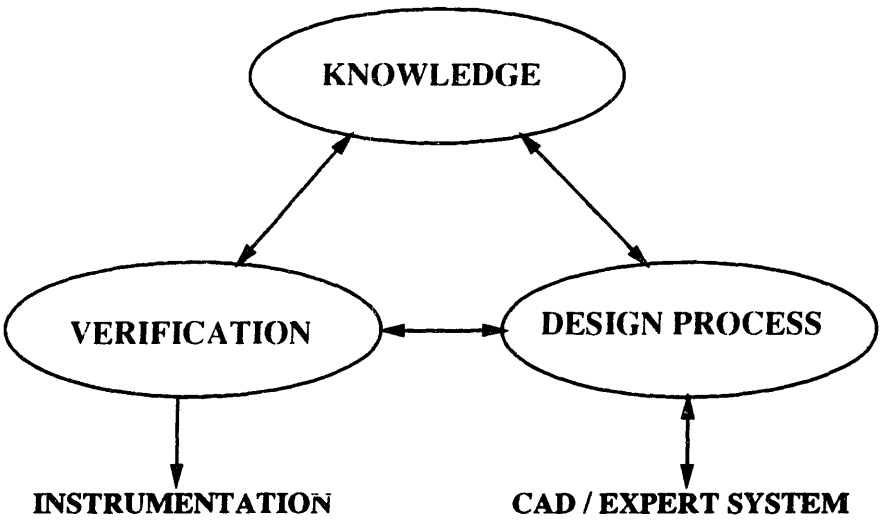

Figure 2-1: Objectives of EMI research

This work started with the study of EMI and the performance of EMI filters. Attempts were made to measure the actual performance of a filter and to understand deviations from what one would predict. This work, which is documented in Chapter 3, provided an understanding of the issues involved in the performance of EMI filters and the types of investigations which need to be performed. The important issues to be considered in a grand strategy for EMI filter design may be categorized into the following areas:

1. Source Reduction
2. Instrumentation
3. Components
4. Topology
5. Active Filtering
6. Layout
7. Radiated EMI

This chapter highlights these topics in the following seven sections and then ties this outline to the work of this thesis.

2.1 Reduction of EMI Sources

A good place to attack a problem is usually at the source. The requirements of the EMI filter would certainly be eased by design techniques which reduce the amplitude of high frequency waveforms generated by the power supply. Qualitative and quantitative understanding of the sources of EMI in the power supply is essential to reducing these sources. As mentioned earlier, it is helpful to discuss EMI in terms of common-mode and differential-mode components. The reduction of EMI sources is thus considered in terms of these two components in the following subsections. A third subsection considers coupling to the filter as a type of EMI source, although this coupling of signals through magnetic or electric fields may result in both common-mode and differential-mode emissions.

2.1.1 Common-Mode Sources

Common-mode EMI is a completely parasitic and unnecessary problem, which is a function of the layout and construction of the power supply and filter. This type of noise is generated by the normal differential operation of the power circuit in which nodes that are capacitively coupled to ground are switched. Typically, these nodes are associated with a transformer whose secondary is grounded, or with switching device heatsinks which need to be connected to the grounded chassis to dissipate heat. Common-mode noise may be reduced by installing shields between the switching nodes and ground, and connecting these shields to the return node of the respective side of the power circuit. The common-mode source of the power supply is often complicated by other impedances in the unit. Local capacitive filtering, that is, at the source of the EMI rather than at the external filter, may therefore be a good way to eliminate or reduce the need for common-mode EMI filter components.

2.1.2 Differential-Mode Sources

While common-mode EMI is a purely parasitic problem, differential-mode EMI is inherent in the operation of the switching power supply circuit and therefore has a well-defined source and network. Nevertheless, differential-mode EMI may be reduced by using control schemes such as continuous conduction, harmonic cancellation, or resonant-mode switching. Another source of EMI which may be reduced by good component design is the ringing between a transformer's winding capacitance and leakage inductance.[7]

2.1.3 Coupling to Filter

Coupling (magnetically or electrically) to the filter from the power supply may be considered as another type of EMI source, and one whose reduction is crucial. Particularly on the AC line side of the filter, this source may be very important because coupled noise bypasses much or all of the filter, rendering it useless. The issues associated with this problem are basically related to the layout of the power supply and its arrangement with respect to the filter. Components, such as transformers or other magnetics, which may have relatively large external fields, need to be kept away from the filter. In addition, some type of shielding may be necessary between the power supply and the filter. Shielding and other noise reduction techniques, such as the use of feedthrough capacitors for improved filter performance, are

described in [1].

2.2 Instrumentation

Instrumentation is an area of work fundamental to the development of a strategy for EMI filter design, because instrumentation techniques developed could be used to study other issues by experimentation. Besides the required regulatory tests on each phase referenced to ground, the filter design process should take into account common-mode and differential-mode EMI emission levels. The advantages of determining levels of both modes of EMI are the facilitation of diagnosis of EMI problems and the subsequent prevention of the use of unnecessary extra or excessively large components to reduce a mode of EMI which has a negligible effect on the total EMI.

These levels may be obtained by simply adding or subtracting the phase and neutral to ground signals. Most spectrum analyzers have these basic arithmetic functions, but many of them just add or subtract magnitudes, ignoring phase angles.[5] In addition, the subtraction of two nearly identical signals to obtain the differential mode EMI when common-mode noise dominates may be a challenge to the common-mode rejection capability of the analyzer's arithmetic function. The opposite is true for the calculation of common-mode EMI. In recent work by others [5], a circuit using high frequency transformers to either add or subtract signals, depending on a switch position, was used to convert the signals between the two phases and ground to one common-mode or differential-mode signal.

In addition to measuring the EMI generated by the final product, a more scientific design process would take advantage of precise information concerning the (unfiltered) EMI source. This information would aid in the design of both filters and the actual power supplies generating the EMI. For a specific filter design, knowledge of the EMI source would allow the design to be tailored to its specific function. More generally, measurement of EMI sources could provide information on the characteristics of power supply EMI that would be useful in developing new designs which generate less EMI.

Measurement of an EMI source should include the source impedance, as well as the source value, since the impedance affects both the measurement of the source and the requirements of the filter. In fact, Thevenin or Norton equivalent models of both the common-mode and differential-mode source would be ideal for use in the filter design process

because of their compatibility with circuit simulations and intuition. While simple circuit and waveform analysis may prove useful to some extent [7], particularly with regard to the differential-mode EMI, generation of an EMI source model for each power supply would be greatly aided by the development of instrumentation techniques to determine equivalent source values and impedances of both types of sources. This task is complicated by the large EMI levels of an unfiltered power supply and the presence of the large line voltages necessary to get the power supply to produce the EMI.

Investigation of EMI filters might also address the measurement of the frequency response, as well as the input and output impedance, of isolated filters. If this type of measurement could be proven reliable, filters and power supplies could be measured prior to integration and matched by a software package based on impedances, source level, attenuation of the filter, and applicable EMI standards. While measuring the common-mode response of a filter is relatively straightforward, it is much more difficult to take reliable measurements of the differential-mode response, particularly for a high attenuation filter. This is largely because, unlike the common-mode for which the signal is referenced to ground on both ends, the differential-mode measurement requires that both sides of of the filter be isolated from one another. Even with this accomplished, questions remain as to what sort of coupling there would be between filtered and unfiltered neutrals in the actual system containing the filter, since the unfiltered neutral capacity couples to ground in the system and the filtered neutral connects to ground through the utility. In both types of measurements, the effects such as inductor saturation due to power line currents are necessarily neglected. If proven reliable to a good extent, however, the measurements on the isolated filter could be checked against measurements of an EMI source with and without the filter.

Figure 2-2 shows the models employed for both the common-mode and differential-mode networks. We would like to characterize each block and then verify our understanding by comparing results with measurements of conducted emissions. Note that the line impedance ought to be a known function of frequency for a given test, (i.e. LISN). All of these instrumentation capabilities would be very useful tools in the investigation of EMI filters, as well as in the design process.

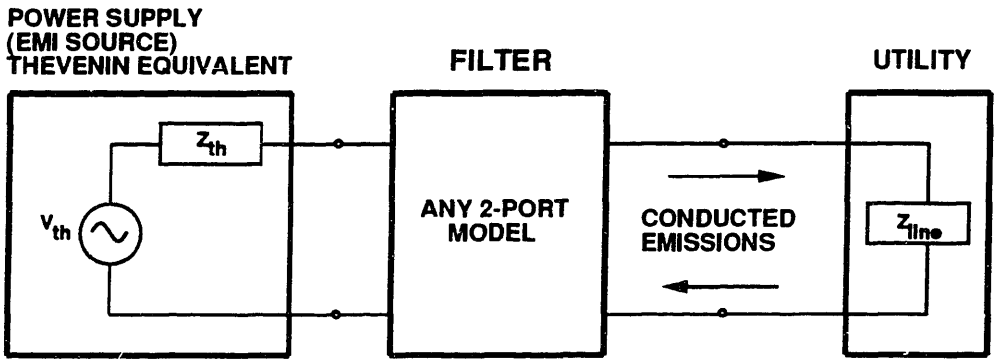

Figure 2-2: Power supply and filter system component models (differential-mode or common-mode)

2.3 Component Issues

Also essential to the design of effective EMI filters is a good understanding of the components used in the filters, namely inductors and capacitors. Because these energy storage components tend to be fairly large due to both required element values and high voltage or current levels, operating them in the radio frequency range generally takes these components beyond the limits of their expected behavior. Parasitic inductance in series with a capacitor, for example, will cause its impedance to increase with frequency above its self-resonant frequency. Similarly, parasitic capacitance across the windings of filter inductors dominates the behavior of those components at high frequencies. The design of filters could be aided by techniques to predict the values of these and other parasitic elements and to understand component behavior at higher frequencies (beyond 10 MHz) where second-order models including the parasitic elements seem to break down.

Many topics which need to be studied are specific to common-mode inductors. Because of their large inductance values, these components play an important part in the common-mode filtering of EMI. At the same time, however, common-mode inductors may also cause problems associated with their leakage inductance. This leakage inductance gives external fields which may couple to other areas of the filter. The extent of this coupling needs to be investigated. Tighter windings can lower the leakage inductance, but it is possible that this may result in local saturation of the outer portion of the core, as more of the leakage inductance becomes partly associated with the core, reducing the effectiveness of the inductor. Both problems might be eliminated if the leakage inductance is made negligible

by using bi-filar windings, which would have the advantages of considerably lower leakage, less inter-winding capacitance, and more inter-winding capacitance, the latter of which is advantageous in that it makes the choke an Nth order LC filter (where N is the number of turns on each winding), at least at high enough frequencies.

One problem that may be associated with the bi-filar winding of inductors is the issue of safety regulation, which is an important topic that bears upon the design of power supply filters since they generally connect directly to power lines and carry reasonably high voltages. The bi-filar windings reduce leakage by bringing the windings closer together, but this may require extra insulation for safety and this, in turn, may restrain heat flow from the windings. Another safety-related issue is that of 'X' and 'Y' capacitor standards which place limits on the types and values of these capacitors between the lines or to ground.

2.4 Topology Issues

Several problems and issues worthy of study relate to the topological design of EMI filters. The performance of a particular topology certainly depends on the terminating impedances on either side of the filter. While effects on ideal performance may be understood in terms of analysis of the schematic, the effect of line impedance on actual filter performance, particularly at high frequencies, may actually be dominated by inductive coupling from previous filter stages; and this coupling will depend on the impedance with which the filter terminates, since a lower impedance output loop will pick up less magnetic field. Measurement of the source impedance, as discussed above, would allow for the design to account for the type and level of this impedance. While the line side should also be characterized, since it is generally not a perfect voltage source (short circuit at high frequencies), it has a much more varying and difficult to measure impedance. Some study to generate a probable range of values would certainly be useful, particularly in the development of alternate topologies.

Various alternate topologies should be considered in studying the improvement of EMI filters. In addition to the basic topology of the alternating series inductor and shunt capacitor network, filters might contain stages or components tailored to particular frequencies or frequency ranges. For example, part of the filter may be designed to filter low-frequency EMI and the other might be tailored for high frequencies. One such method would use a series combination of inductor and capacitor as a low impedance shunt element at the

resonant frequency or a parallel combination as a high impedance series element at resonance. While these combined elements would only be of much use for one small frequency range, a high Q resonance tuned to the right frequency could provide a large attenuation at the fundamental frequency with small components, as the LC product may be considerably smaller than for the standard filter topology and only one of the resonant components needs to store energy at the power-frequency. Using a resonant combination to filter the lowest EMI frequency might allow a substantial reduction of the remaining filtering components if their sizes are driven by EMI levels at this frequency and the next frequency of concern is two or three times as high and has lower levels of EMI. In addition to the cost of the required high-Q, tuned resonant filter, the biggest problem with this type of filter is keeping it tuned over product, temperature, and age variations.

One interesting and promising type of alternate filter topology, which may reduce cost as well as size of EMI filters, involves the use of active devices to enhance energy storage components. Through the use of transistor circuits, inductors or capacitors can be made to appear much larger than their actual size over a reasonably large frequency range, so that required filter performance may be achieved with a smaller circuit. This approach was considered in previous work by [2] and [18], and is considered below as an additional topic on its own.

2.5 Active Filtering

An example of an active filter topology is the inductor-enhancing circuit shown in Figure 2-3. The independent current source I_{sw} represents the source of conducted EMI, a high frequency switching current. The capacitor C_f absorbs most of this current, generating a ripple voltage v_r, which must be dropped across the inductor-enhancement circuit with a minimal ripple current i_r passed on to the utility. This function is realized by the active circuitry which senses the voltage v_{in} across the inductor L_s with the large impedance Z_{in} and drives a current $g_m v_{in}$ through inductor L_d to drop ripple voltage without generating ripple current i_r through the utility. Ideally, with infinite transconductance g_m, the input voltage v_{in} would be driven to zero, as would the ripple current.

The key advantage of the active filter is that it makes it possible to use smaller energy storage components with correspondingly smaller parasitics. Because these smaller compo-

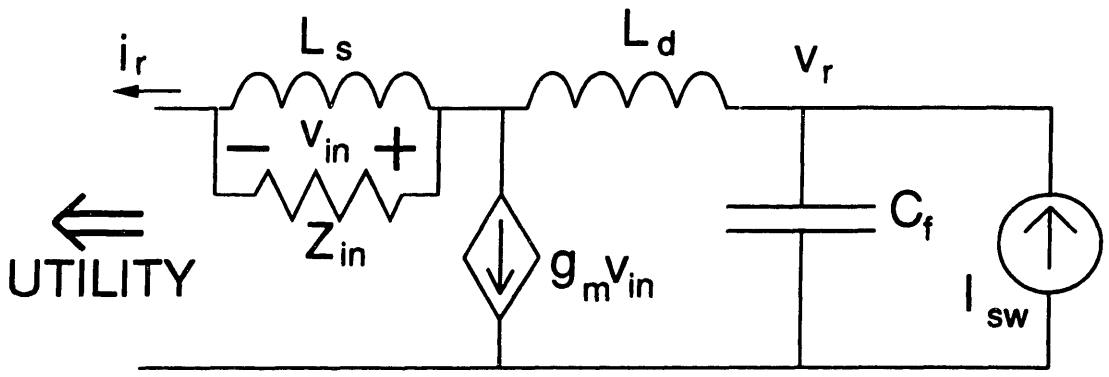

Figure 2-3: Example of active filter: inductor-enhancing circuit

nents remain effective at higher frequencies, they need only be actively enhanced at lower frequencies, so that they can be just as effective as the larger components which they would replace.

One of the major design issues associated with the active EMI filter circuit is that of compensating the feedback loop associated with the active circuit. In the circuit of Fig. 2-3, for example, the driving current $g_m v_{in}$ from the active circuit splits between the two inductors, so that some of it passes through the sense inductor L_s, generating voltage which feeds back into the input of the voltage-to-current amplifier. With a reasonably large gain, such a feedback loop may be susceptible to stability problems which would require compensation.

In previous work on this topic, a stable active circuit which enhanced inductance by a factor of over 500 at a frequency of 1 MHz was designed and demonstrated. [2] A major problem with the practical use of that circuit is that the loop transmission includes the impedance of the power line, and the stability of the closed loop therefore depends on this impedance. While the previously built circuit was tested in a laboratory with a very low simulated line impedance, an actual filter will be terminated by some undetermined line impedance. A practical design must ensure loop transmission stability for the wide range of possible line impedances.

Other issues that need to be addressed in developing the active power filter concept into a practical design include transient protection, biasing of the active circuitry, susceptibility to external EMI, and power dissipation. It is worth noting that the extra filtering performance of the active circuit is achieved by dissipating much of the ripple energy that would otherwise be filtered by larger storage components. Nevertheless, by using actively-enhanced elements

in the latter part of a filter (towards the line side), where ripple energies are already quite small, the effects of large storage components may be achieved with reasonably low power dissipation. Under these circumstances, the extra power dissipation of the active circuitry may, in fact, be offset by the decreased line frequency dissipation in the scaled down parasitic resistances of the energy storage components.[2]

Another way in which the active filter concept might be expanded would be in the enhancement of two or more components in the same circuit. In fact, the impedance of one active sub-circuit may prove useful in controlling the loop transmission stability of the other active sub-circuit. The interactions between the active circuitries as well as with external impedances certainly need to be considered.

With a better understanding of the applications of active filters and other topological issues, a general strategy to determine the optimal topology for the filter may be generated and possibly implemented into some computer-aided-design software. The first step in such a design process would be to compare measurements of the EMI source magnitude with applicable EMI standards which need to be met and determine the level of attenuation required of the filter across the EMI spectrum. Based on the level of attenuation, the number of (LC) stages or a number of components, as well as the applicability of active devices, might be determined. Finally, the distribution of filtering among components would be determined and any active circuitry would be designed.

2.6 Layout Issues

The issues associated with the layout of EMI-filter circuits are chiefly related to inductive and capacitive coupling. While reduction of loop areas and increased spacing between nodes seem like appropriate objectives, they often conflict with each other or with other goals. Various issues need to be studied and tested so that more optimal layouts may be implemented.

Significant magnetic coupling may occur between any loops including circuit paths or actual inductive components. The extent of this coupling and its effect on filter performance should be determined through analysis and testing. The orientation of the inductors should be considered, as it may result in constructive or destructive interference of fields from common-mode or differential-mode currents. If inductive coupling significantly deteriorates

circuit performance, which is likely in high attenuation filters (more than 80 to 100 dB), then a shield between stages or around an inductor may be a useful remedy.

Capacitive coupling may also hamper the achievement of high attenuation in filters. In preliminary research work, coupling was observed across a filter on the order of a fraction of a picoFarad, limiting its performance above 1 MHz. In fact, for a filter with a capacitor across the power line in its final stage, the effect of a parasitic capacitance across the filter is easily predicted by a voltage divider. If the final filter capacitor is 1 μF, for example, the parasitic capacitance of 1 pF will limit the attenuation of the filter to a maximum of 120 dB. While a filter is not as sensitive to parasitic capacitances between relatively adjacent nodes, this sort of coupling may be much greater and may have the effect of adding to the parasitic capacitance of components, particularly inductors, or it may couple nodes within different components to one another. Again, the orientation of components may be used to minimize the loss of attenuation due to coupling, in this case, by making for small voltage differences between the most highly coupled nodes.

Another way in which the layout, and more so the actual construction, of the circuit can affect filter performance is through the impedances of connections. The impedance in the fastening of shields may affect their performance and the connection resistance of low impedance components (capacitors) may, in fact, dominate over the actual impedance of the component at high enough frequencies. This is of particular concern in the context of actively enhanced capacitors, where an effective 100 or 1000 μF capacitance value is conceivable. Even the 100 μF capacitor, for example, would have an impedance magnitude at 1 MHz of less than 2 mΩ, which could easily be dominated by the resistance and reactance of component connections and leads.

Clearly, connections and field coupling may lead to many non-idealities in EMI filters which must be understood and accounted for in the design process. As with component parasitics, prediction of the parasitics which model layout non-idealities would certainly be helpful in the design and layout of EMI filters. These parasitics could be nicely incorporated into a computer-aided-design package.

2.7 Radiated EMI

Although most of this research has been focused on conducted EMI, it is essential to consider radiated EMI due to the relationship between the two types of emissions. Unlike conducted EMI which must flow through the power supply filter, radiated EMI may result from any part of a system, particularly digital circuits with clock cycles or other transitions in the radio frequency range. It is also possible that much of the EMI radiated by electronic systems is due to high frequency EMI from signal switching or power switching harmonics conducted onto power cords, as well as other connections between subsystem units.

In any case, radiated EMI must be considered in the context of the overall system and its configuration. While the relative importance of conducted EMI in determining the total radiated EMI has yet to be experimentally verified, its likelihood suggests that EMI filters should be designed with criteria for reasonable performance at frequencies above the 30 MHz tested range of conducted EMI. This objective requires research towards understanding the behavior of the large components used in typical filters, but also makes a case for the small components allowed by active filter designs. Possibly more important may be the determination of the electromagnetic interactions in filters, as they may be strong enough to bypass the components, rendering their behavior irrelevant.

2.8 Scope of This Thesis

While a comprehensive set of issues to be investigated in working towards the goal of improved EMI reduction has been outlined herein, the study of all of these topics is well beyond the scope of this work. Instead, a subset of this research, principally including instrumentation and active filter development, has been performed.

The initial work on EMI filter measurement, which led to the development of the set of issues to address was an important part of the work documented in here and touches upon many of the fundamental topology, component, and layout issues. Essential to much of the proposed work is a conducted EMI measurement facility to test ideas and develop some useful instrumentation techniques as described earlier. Such a facility, similar to standard test facilities used in industry to meet regulatory standards, was built in the laboratory and used in the development of power supply characterization techniques. The other major area of this work was in the development of more optimal EMI filter topologies. Much

attention was given in particular to the practical application of the active filter concept as described earlier. To develop practical circuits, however, all aspects including components and layout need to be considered in order to obtain an optimal design. Thus, while the work documented herein is divided into three projects, many common issues are investigated or somehow involved in these projects.

Chapter 3

Measurement of EMI Filters

3.1 Overview

An essential aspect of a scientific approach to EMI reduction is the study of each of the parts of the system as well as their interactions within the system. The system associated with conducted EMI consists mainly of the power supply, the EMI filter, and the external impedance of the utility. Thus, the EMI filter is the link through which EMI is transmitted (and hopefully attenuated). An understanding of the performance of the EMI filter is therefore essential for optimal EMI reduction.

3.1.1 Factors Affecting Filter Performance

Several factors influence the performance of an EMI filter, the most obvious of which is the topology. The topological connection of elements of particular values is certainly critical, but the parasitic effects of the actual components used in the filter play an important role, as well, and may even come to dominate the filter's performance at higher frequencies. In addition, the layout may also strongly influence the terminal characteristics of the filter due to electromagnetic coupling between nodes or loops of the filter. Shielding, the arrangement of the components and conductors, and grounding techniques are all aspects of the filter design which bear upon these parasitic layout effects, thereby influencing the performance of the filter.

3.1.2 Motivations

Measurements to characterize the frequency response of an EMI filter are useful for several reasons. The effects of the filter network on common-mode and differential-mode signals may be isolated from the power supply and understood. The influence of component and layout parasitics may be studied through such characterizations. With measurements of filter performance, the filter design may be optimized so that requirements are met without wasteful overdesign of the filter in either its common-mode or differential-mode subcircuit.

3.1.3 Approach

To study the EMI problem and the measurement of EMI filters, a project was undertaken to characterize and understand the performance of a typical filter. The filter was examined first to consider the common-mode and differential-mode subcircuits it contained and the ideal behavior which would be expected of these subcircuits. The actual impedances of the components were then measured and modeled. Simulations of the resulting circuit model were compared to the ideal performance and the measured performance of the filter to determine, respectively, the effects of the components' parasitics and the effects of the layout parasitics. Various challenges involved in the measurement of the frequency response of the circuit contributed to the learning which resulted from this study.

This chapter is concerned primarily with the EMI filter as an isolated unit which processes the signal from an EMI source in the power supply. Accordingly, the load side of the filter will be considered the input and the utility side will be referred to as the output of the filter.

3.2 The Ideal EMI Filter

The "typical" EMI filter considered in this study is one that would be used for a switch-mode power supply converting about 500 to 1000 watts from a 120 to 240 volt utility mains at a switching frequency on the order of 100 kHz. Such a power supply usually has a rectifier front-end which allows the use of a fairly large-valued unipolar capacitor on the dc side. Connected across this capacitor is the dc/dc switching converter that steps the 300 Vdc down to the required 5 Vdc. The large amount of ripple on this capacitor due to the ac currents drawn by the converter are large enough relative to the low levels required to pass

the EMI test that the addition of a third or fourth order EMI filter between the rectifier and the utility is generally required. In order to filter both common-mode and differential-mode EMI, the filter is balanced. Series inductance in any stage is split evenly between the hot and neutral phases and capacitance to ground is similarly split. The schematic for the particular filter studied is shown in Fig. 3-1. This filter is designed to give sufficient attenuation for a converter switching at 75 kHz. The structure of the filter is best understood by separately considering its common-mode and differential-mode subcircuits.

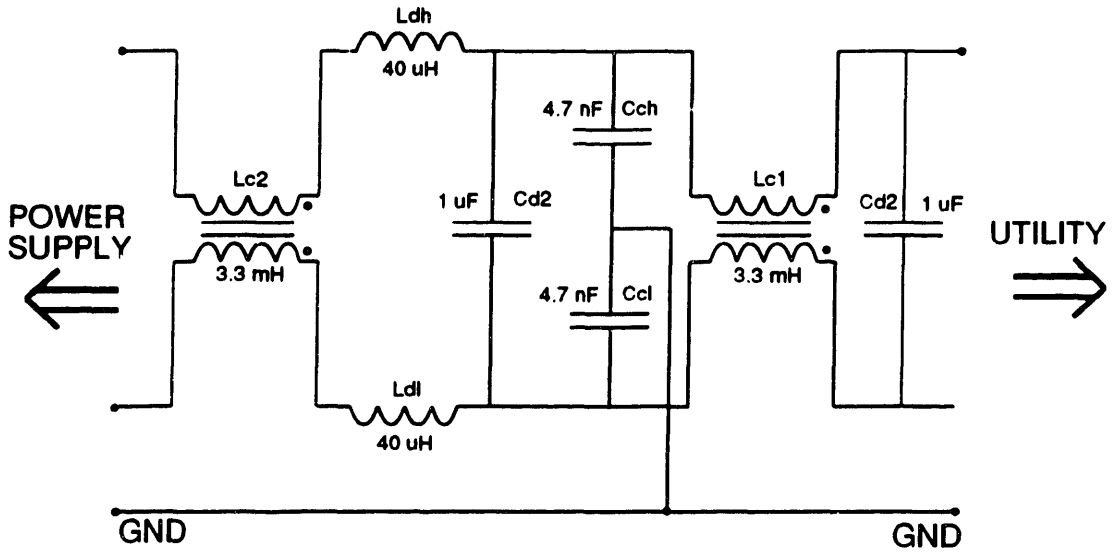

Figure 3-1: Schematic of EMI filter studied

3.2.1 The Common-Mode Subcircuit

The common-mode subcircuit is obtained by considering the hot and neutral wires as being shorted together on each end of the filter and, consequently, across all points of symmetry as well. The result of this folding of the circuit is that all pairs of balanced inductors and Y-capacitors appear to be in parallel and line-to-line capacitors are short-circuited. The schematic for the common-mode subcircuit of the filter in Fig. 3-1 is shown in Fig. 3-2.

Note that the value of the coupled inductor pair was already given in terms of its common-mode inductance in Fig. 3-1, so that this value of 3.3 mH does not change during the transformation to common-mode circuit. While the uncoupled inductors do contribute to common-mode filtering, their effect is negligible, since the pair effectively appears in

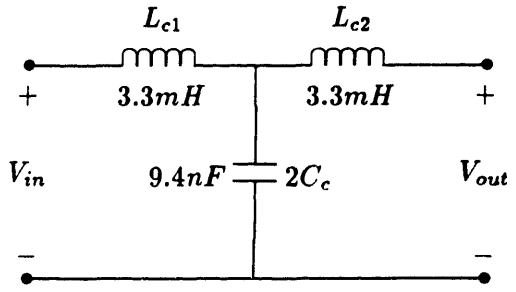

Figure 3-2: Schematic of common-mode subcircuit of EMI filter studied

parallel and the resulting 20 μH is much smaller than the 3.3 mH common-mode inductor.

Common-Mode Filter Design

The common-mode topology and component values designed into this circuit are largely a result of the limited amount of capacitance to ground allowed by safety restrictions on current conducted to earth ground. The limit on this leakage current is 0.5 mA, so the maximum acceptable common-mode capacitors (Y-capacitors) are about 5 nF for a filter that operates at 60 Hz and 120 VAC or 50 Hz and 240 VAC. [11] In order to get reasonable attenuation at the switching frequency, any adjacent series inductor must be large enough so that it resonates with the shunt capacitor well below the switching frequency. The limited size of the shunt capacitors to ground therefore necessitates relatively large common-mode inductance; hence the need for relatively large-valued inductors which are coupled so that the core does not saturate from the flux generated by the large differential-mode power-level currents. Despite the reduced load on the core, these components are fairly large. Splitting the allotted ground capacitance into more than one place in the circuit would require these inductors to be even larger just to keep the resonant frequency at least a factor of 2 to 3 below the switching frequency. Note that the common-mode resonant frequency of the 10 nF shunt capacitance with either 3.3 mH common-mode inductor is about 30 kHz and cannot be pushed higher without losing significant attenuation at 75 kHz due to resonance, as well as the lower LC product. In addition, capacitors to ground at more than one point on the hot or neutral line of the filter would combine in series in the differential-mode network to shunt the inductance with a capacitance much larger than that of its parasitic

winding capacitance. Thus, this effective allotment of only one common-mode capacitance shapes the common-mode filter into a third order L-C-L topology, like that of Fig. 3-2.

Although not shown here, a ground-wire inductor is commonly included in the system to enhance the attenuation of common-mode signals. This inductor is placed at the outermost part of the system ground. Because it is in the ground wire, its energy storage requirements may be relatively small since it need not be rated to carry much current.

Ideal Common-Mode Frequency Response

The expected frequency response of the common-mode filter network, depends on the external line impedances to which it is connected, particularly because of the high impedance inductors on both sides of the filter. The case which was considered here is the application of a voltage source at the rectifier end and a 50Ω load impedance on the utility side. The choice of 50 Ω allowed simulation of a typical LISN test impedance and eased comparison with measurements, which are typically done with a 50 Ω input impedance (or a very large impedance on the order of megaohms). Given this test configuration, the expected frequency response of the filter from input to output voltage was unity magnitude at low frequencies, with a pole between the load resistance and the adjacent inductor at around 2.4 kHz, and a resonant peaking around 30 kHz, followed by a 60 dB per decade roll-off. Results of a spice simulation of the network confirming this analysis are shown in the plot of Fig. 3.2.1.

3.2.2 The Differential-Mode Subcircuit

The differential-mode subcircuit consists of all uncoupled series inductances and all line-to-line capacitances. Because the common-mode inductances are very large, the leakage inductances associated with these chokes contribute substantially to the uncoupled (differential-mode) inductances. While this leakage inductance is, in fact, a parasitic component, its size may require that it be considered along with the main elements of the circuit, rather than as a second-order effect. The differential-mode subcircuit for the sample EMI filter, a fourth order L-C-L-C topology, is shown in Fig. 3-4.

The design of the differential-mode sub-circuit of the filter is certainly more flexible than the common-mode. Line-to-line capacitors on the ac side of the rectifier must be approved as X-capacitors rated for the line voltage by the applicable regulatory agencies, but the

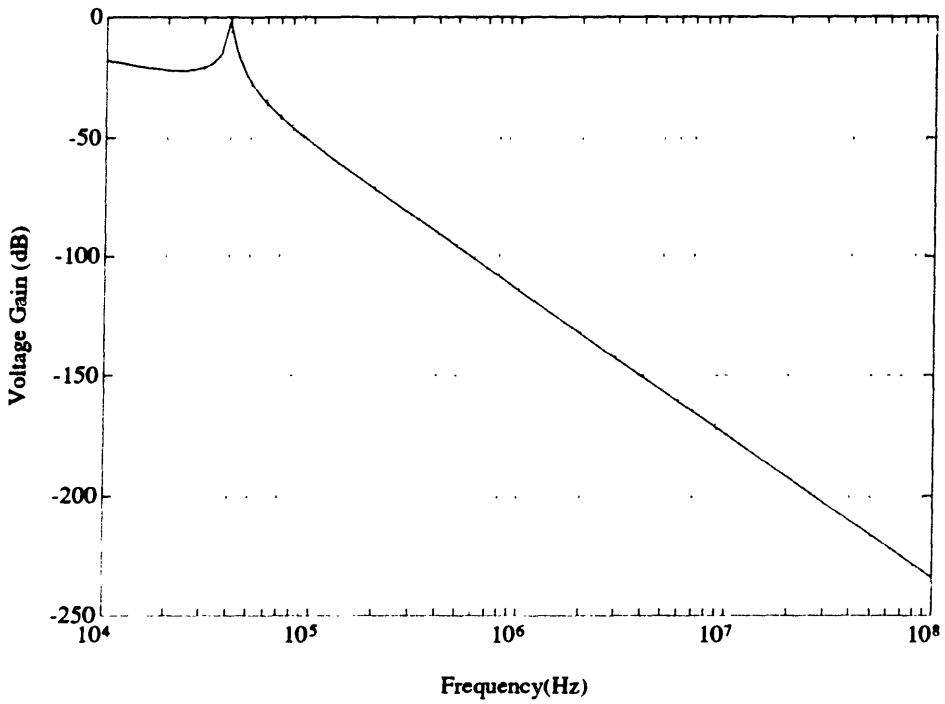

Figure 3-3: Ideal common-mode frequency response of studied filter

values of these capacitors are limited only by power factor requirements, cost, size and availability of only certain discrete values. While there are many important issues involved in selecting capacitors and inductors and trading off between the relative sizes of the two types of energy storage components in the circuit, as detailed in [12] and [1], a simple rough idea of the optimal split between inductance and capacitance per filter stage is obtained by

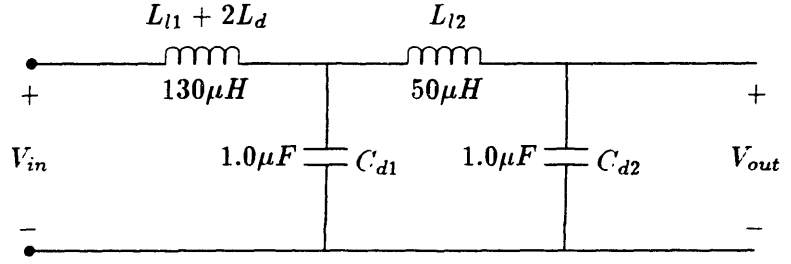

Figure 3-4: Schematic of differential-mode subcircuit of EMI filter studied

setting the magnetic and electrical energy storage amounts to be equal:

$$\frac{1}{2}LI^2 = \frac{1}{2}CV^2 \tag{3.1}$$

where I and V are the peak or rms current and voltage ratings required for the components. The result of this equation is that the characteristic impedance of the filter, $\sqrt{L/C}$, should be equal to the impedance of the power supply, V/I. This result makes sense: if the line voltage, for example, is increased, more inductance and less capacitance should be used rather than re-sizing the capacitor to handle the higher voltage with the same capacitance. For example, a filter which operates on a 120 V rms line and carries 10 Amperes of rms current would have an optimal L/C ratio of about 140, which is not much larger than the ratio in the second stage of the differential-mode filter of Fig. 3-4.

Ideal Differential-Mode Frequency Response

The ideal performance of this differential-mode sub-filter is considered in the same external source and load impedance as the common-mode circuit. The 50 Ω load impedance is of little importance except at very low frequencies where it is close to the impedance of the large X capacitor. As a fourth-order L-C network with two different inductances, this filter has two resonant frequencies. Above these resonances, its frequency response should drop by 80 dB per decade at higher frequencies. Results of SPICE calculations confirming this analysis are shown in Fig. 3.2.2.

3.3 Component Parasitic Effects

The deviation of an EMI filter from its expected frequency responses based on the topology might be largely explained by the characteristics of the components. Knowledge of the parasitic effects associated with the components is therefore important. Acquiring and applying this knowledge requires appropriate measurement and modeling procedures. Although most parasitic effects are distributed throughout the components, modeling them with lumped elements may be sufficiently accurate. Lumped parameter models are more preferable since they allow for simpler hand calculations or simulations to relate the characteristics of the components to the performance of the filter.

The approach taken here was to develop simple models for the components and to choose

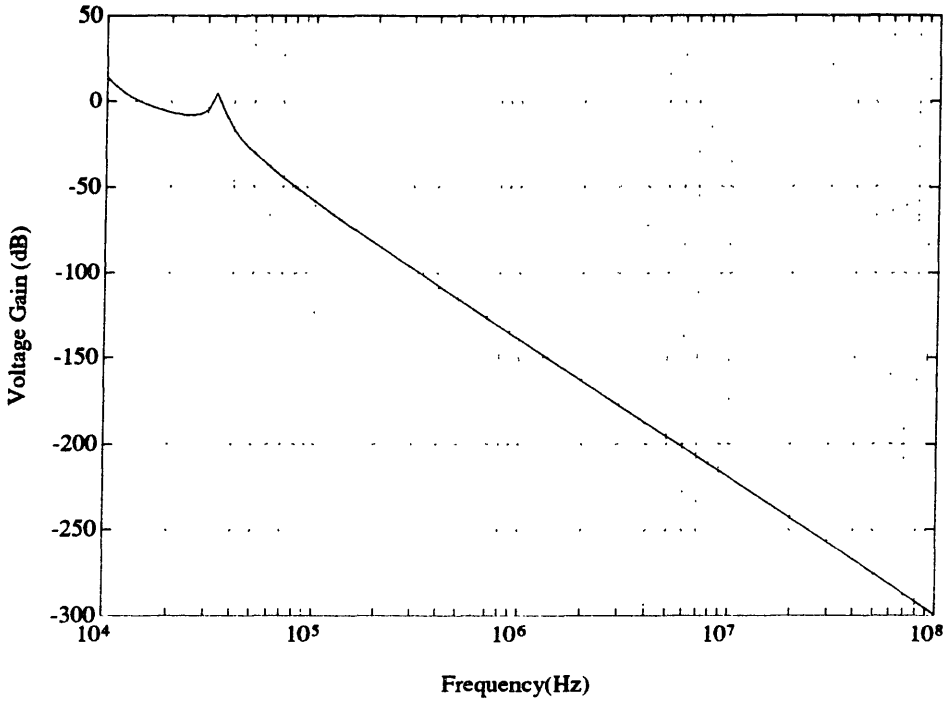

Figure 3-5: Ideal differential-mode frequency response of studied filter

parameters for the models based on measurements. The impedances given by the resulting models were then compared with the measured impedances to test the accuracy of the models. These models were then used to account for parasitic effects in the circuit simulations. Impedance magnitude and phase measurements of components could be made at selected frequencies between 5 Hz and 13 MHz with an HP 4192A LF Impedance Analyzer.

3.3.1 Capacitors

Modeling of Parasitics

An actual capacitor includes several parasitic effects. One of these is the series inductance of the leads and the internal structure. This inductance may dominate the impedance of the component above the self resonant frequency where it rings with the capacitance unless sufficiently damped by resistive effects. There are several types of resistive effects in a capacitor. Dielectric losses and the non-zero resistance of the leads contribute to an effective series resistance (ESR). Dielectric losses, which dominate the ESR, cause it to increase with frequency. [1] A parallel resistance may be used to model the leakage of the

capacitor due to the finite resistivity of the dielectric material. This parallel resistance is negligible, however, at the EMI frequencies of interest where the capacitor is used as a low impedance element. The series R-L-C model shown in Fig. 3-6 was therefore chosen to model the filter capacitors and their parasitic effects.

Figure 3-6: Series R-L-C model for capacitor with parasitic effects

Measurement Results

Measurements of one of the 1μF X capacitors showed a self-resonant frequency of 1 MHz, suggesting a series parasitic inductance of 22.5 nH. The impedance of the component at the self resonant-frequency indicated that the ESR of the capacitor was about 25 mΩ . The plots of Fig. 3-7 compare the data from measurements of the capacitor with calculations based on an ideal 1μF and based on the series RLC model. Clearly, the parasitic effects of this large capacitor seem important: above the resonant frequency, which is well in the middle of the filter's operating range, the impedance of the component deviates from its ideal value by 40 dB per decade in the undesirable direction of increasing impedance. Although the impedance of the capacitor is considerably lower than its ideal value over a small frequency range in the vicinity of resonance, this range of about an octave does not compare to the decade and more in which the inductive impedance of the capacitor deteriorates its attenuation performance.

Despite its short leads, this performance is typical of such a large-valued RFI capacitor.[16] The smaller Y capacitors, behave like ideal capacitors up to a much higher frequency, the main reason being that the larger impedance of the capacitor makes it less sensitive to parasitics rather than that the parasitics are any lower. In fact, the particular common-mode capacitor measured here had a slightly larger parasitic inductance, as well as series resistance, yet it retained its predominantly capacitive characteristics beyond 13 MHz, as shown in Fig. 3-8.

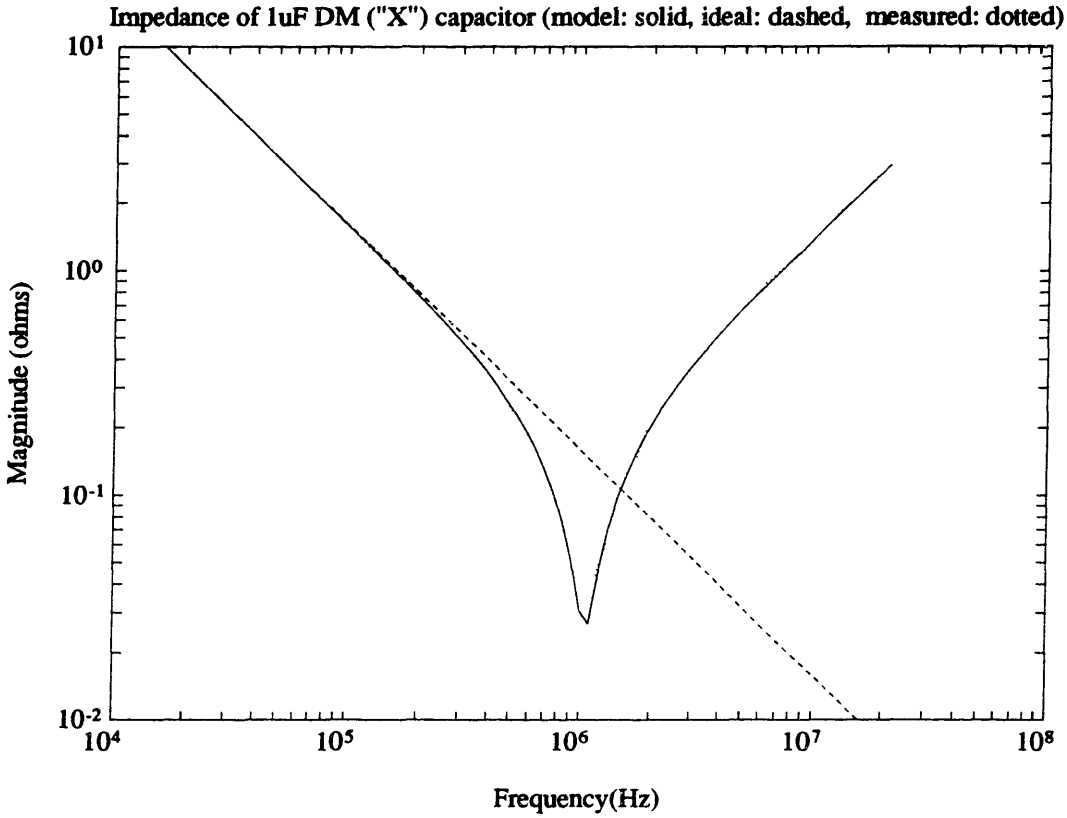

Figure 3-7: Comparison of ideal and measured impedance to series RLC model: 1 uF, 22.5 nH, .025 ohms

3.3.2 Inductors

Modeling of Parasitics

The parasitic effects of inductors are quite complex. An inductor has winding capacitance distributed throughout the component. For simplicity, this effect is modeled with a parasitic shunt capacitor. This parasitic capacitance may resonate with the main inductor at a frequency well within the range of operation of the filter, giving the component capacitive characteristics above this frequency. This resonance may be damped or even dominated, however, by lossy parasitic effects.

The resistive impedance of an inductor, comprising both wire and core losses, is a complicated function of frequency. At low frequencies, losses are dominated by the series wire resistance which may be on the order of the inductive reactance at the low frequencies of power transmission. This was, in fact, the case for several measured EMI filter inductors

of values 40, 50, and 160 μH, which had resistances equal to 50 to 80% of the impedance magnitude at 60 Hz. At higher frequencies, however, the series resistance becomes less important. Although the skin effect increases this resistance at higher frequencies, the skin depth is only a weak function of frequency, inversely proportional to its square root, and the dependence of the resistance on this skin depth, although inversely proportional at high frequencies, is negligible below the kHz range for the wire dimensions of interest. The skin depth of copper, for example, is about 0.75cm at 60 Hz [14], and doesn't fall below 1 mm until over 3 kHz. The inductive reactance, on the other hand, is directly proportional to frequency. As the reactive impedance rises, however, the second type of loss, core loss, becomes important. Cores losses, including both hysteris effects and eddy currents induced in the core material, may be modeled by a shunt resistance; however, this resistance is a function of both frequency and flux level. [14]

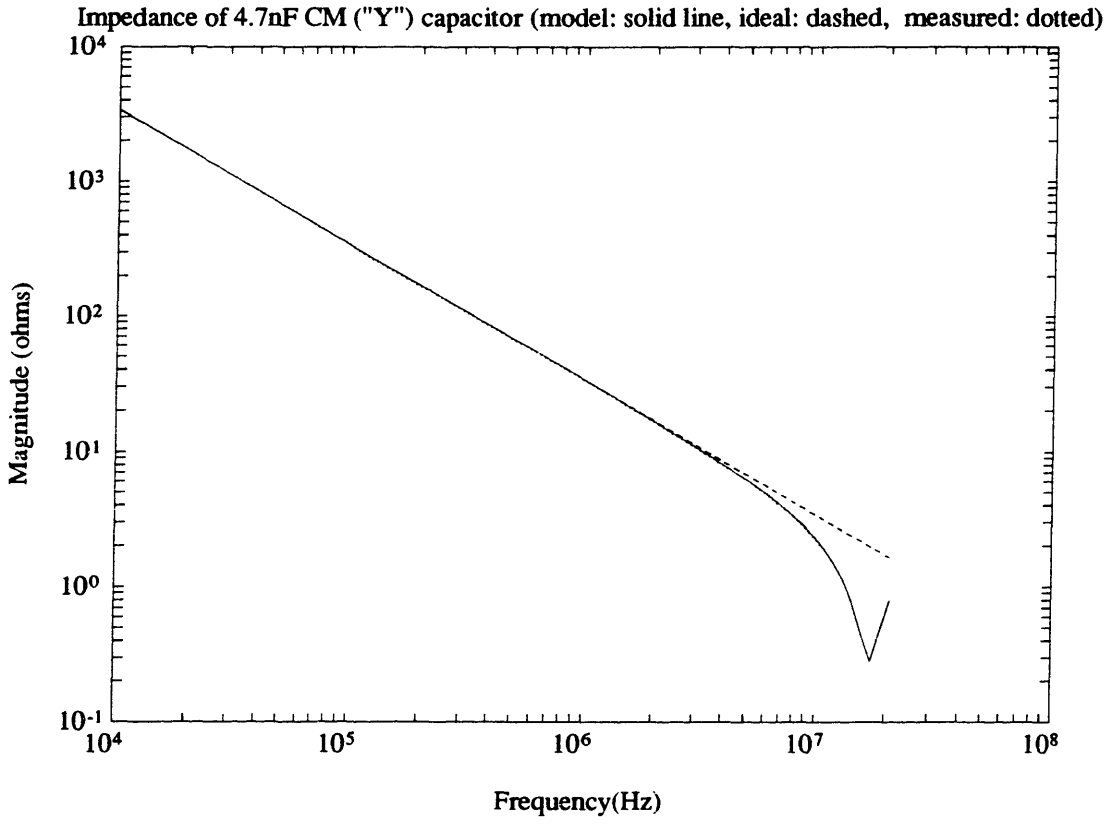

Figure 3-8: Comparison of ideal and measured impedance to series RLC model: 4.7 nF, 18 nH, .028 ohms

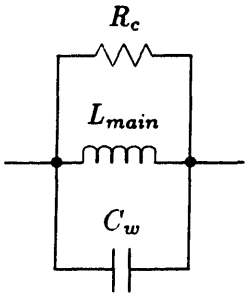

Figure 3-9: Parallel R-L-C model for inductor with parasitic effects

In addition to these parasitic effects, variations of core permeability over frequency and changes in current densities due to skin effects may change the actual inductance of a component over frequency. For simplicity, however, these effects were neglected in modeling the inductors. The core resistance was also assumed to be independent of frequency. The circuit shown in Fig. 3-9 was therefore chosen as a convenient and reasonably accurate model for inductors over the measurable EMI frequency range (10 kHz to 30 MHz). In this parallel R-L-C model, C_w represents the effects of the distributed winding capacitance and R_c predominantly represents the core loss effects.

The Common-Mode Inductor The common-mode inductor, being comprised of two coupled inductors is more complicated to model. Since it is essentially a series-connected transformer, an appropriate model might be similar to that of a transformer. An alternate approach which was taken was to consider the component as two separate components, a common-mode one and a differential-mode one, and use the inductor model of Fig. 3-9 for each of these. Accordingly, measurements were made on the choke with both a common-mode connection and a differential-mode connection.

Measurement Results

Results for the modeling and measurement of the differential-mode inductor are shown in Fig. 3-10. There is some deviation between the model and the measurements, especially over the megaHertz range. The simple model chosen could not account for a gradually increasing reduction in the inductance with frequency from 37.6μH at 10 kHz to 36.6μH at 100 kHz, and 27.1μH at 1 MHz, while the component remained predominantly inductive

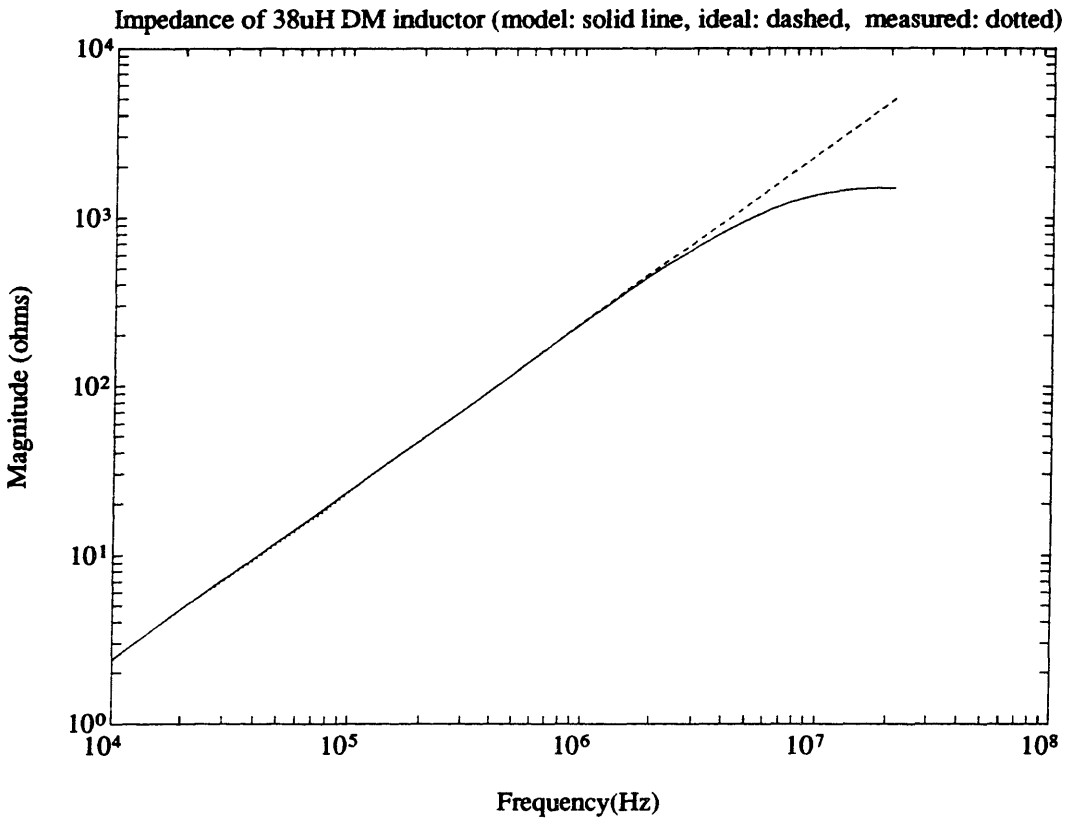

Figure 3-10: Comparison of ideal and measured impedance to parallel RLC model: 38 uH, 2 pF, 1.5 kohms

(phase between +45deg and +90deg) up to 10 MHz. Results of the measurements and comparisons for the the two connections of the common-mode inductor are shown in Figs. 3-11 and 3-12. While the differential-mode and common-mode study of the components

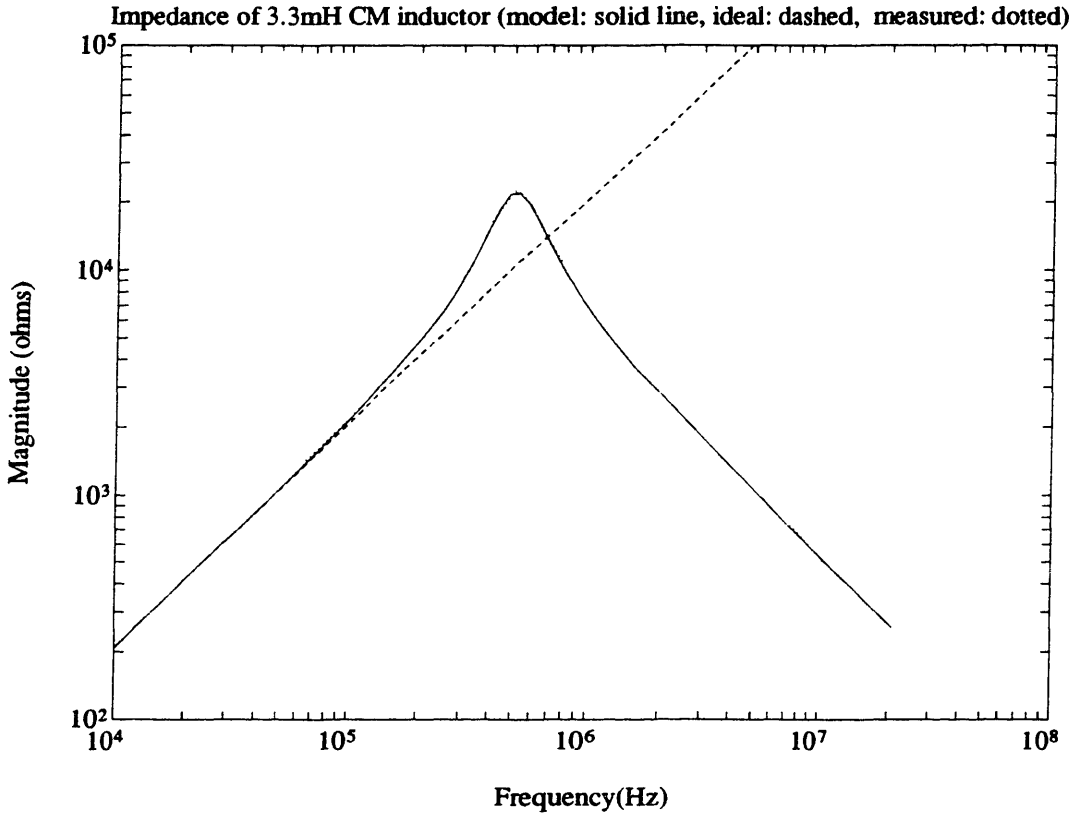

Figure 3-11: Comparison of ideal and measured common-mode impedance to parallel RLC model: 3.3 mH, 30 pF, 22.3 kohms

were done independently, it is useful to note the relationships between the parasitics of the components. The winding capacitance, in particular, is exactly four times as large for the common-mode inductance as for the differential-mode inductance. This result makes sense, since the common-mode value is based on two (ideally) identical windings in parallel and the differential mode value depends on the two windings in series. The parasitic parallel resistances are difficult to correlate, since they depend on the flux levels coupled into the core, and the differential component, being a leakage inductance couples only partially to the core. As with the differential-mode capacitor, the very large common-mode component of the choke is very susceptible to parasitics; it resonates with its winding capacitance at about 500 kHz. Inspection of the component shows that its high inductance per unit volume

was achieved partially by crowding many turns onto each half of the toroid, placing them adjacent and layering many of them one on top of another. This construction explains the relatively large winding capacitance and leakage inductance measured. Another common-mode inductor from a different EMI filter was measured on the impedance analyzer. This slightly larger component with an only slightly smaller inductance of 3 mH had fewer turns which were more carefully wound. The measured results were about one-third the leakage inductance ($\approx 15\mu$H) and half the winding capacitance (15 pF).

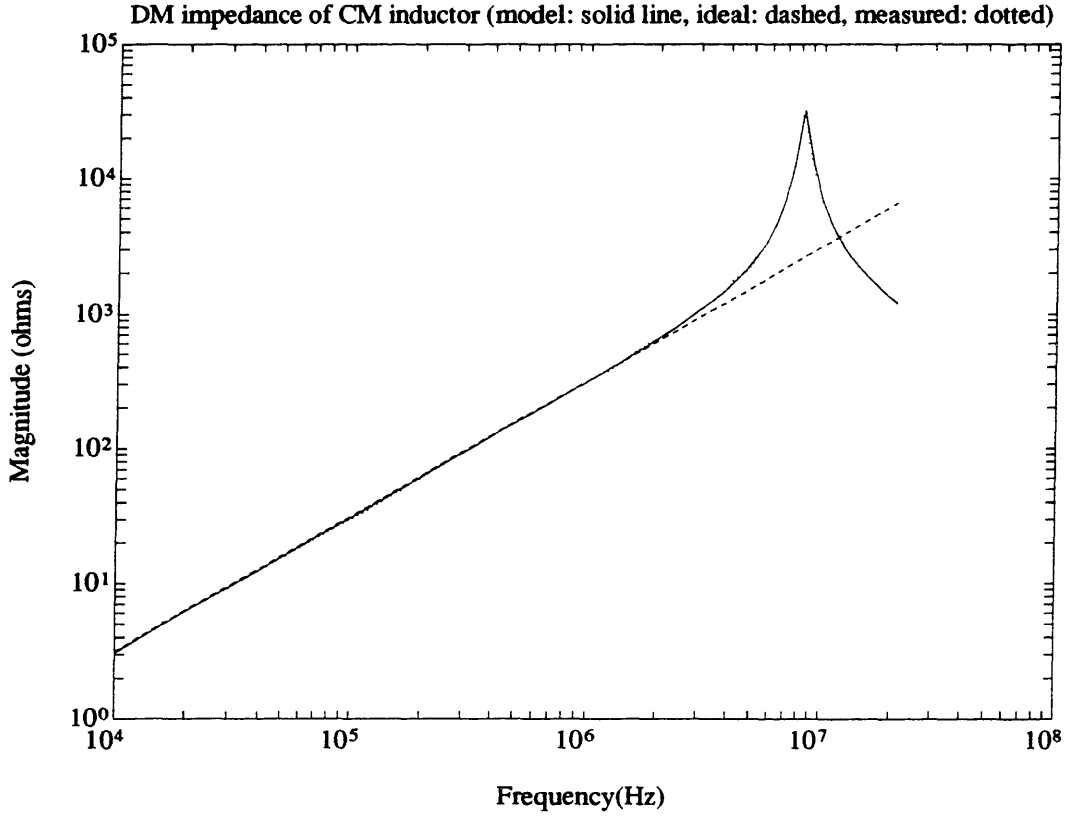

Figure 3-12: Comparison of ideal and measured differential-mode impedance to parallel RLC model: 49 uH, 7.5 pF, 32 kohms

3.3.3 Implications

These measurements illustrate an important aspect of filter design: few components can be relied on for attenuation over a very large frequency range. The low end of this range is limited by the usefulness of (relatively small) components for low-frequency attenuation and the high end is governed by parasitics and especially limited for larger components.

In fact, smaller, high-frequency back-up components are often used, particularly in the case of a filter capacitor [1, p. 142], which might have a smaller less inductive capacitor placed in parallel with it. In the particular filter studied, some of the most poorly behaved components, including one of the common-mode inductors, as well as one of the differential-mode capacitor, do, in fact, have such high-frequency back-up components due to the effects of common-mode components on differential-mode filtering and vice-versa. The differential-mode inductors may be considered as backing up the common-mode inductor and the smaller common-mode capacitors appears in parallel with the differential-mode capacitor. The usefulness of these backup components may be very limited, however, unless the components are carefully chosen. The two small Y capacitors, for example, having larger parasitics than the X capacitor and being connected in series with respect to the differential-mode network, actually have a larger impedance than the X capacitor throughout the whole range of frequencies considered, and therefore do not contribute much to the differential-mode attenuation.

3.3.4 Effects of Component Parasitics on Filter Performance

To determine the potential effects of the component parasitics on filter performance, the common-mode and differential-mode frequency responses of the filter were considered using the above component models in place of each circuit element. Results of SPICE simulations with these component parasitics were then compared with the results of calculations based on ideal circuit elements. Note that all components were included in both the differential-mode and common-mode networks so as to include any effects, particularly at high frequencies, by which a component of one network may become important in the other network, as described in the previous section.

Common-Mode Parasitic Effects

The plot of Figure 3-13 shows a comparison of the ideal and actual common-mode responses. As would be expected, the self-resonance of the common-mode inductor at 500 kHz increases the attenuation somewhat over a small range but results in great losses of potential attenuation at higher frequencies. In fact, over the low MHz range all of the filter components are capacitive, so the slope of the frequency response is 20 dB per decade due to the voltage divider between the load resistance and the dominant parasitic capacitance of

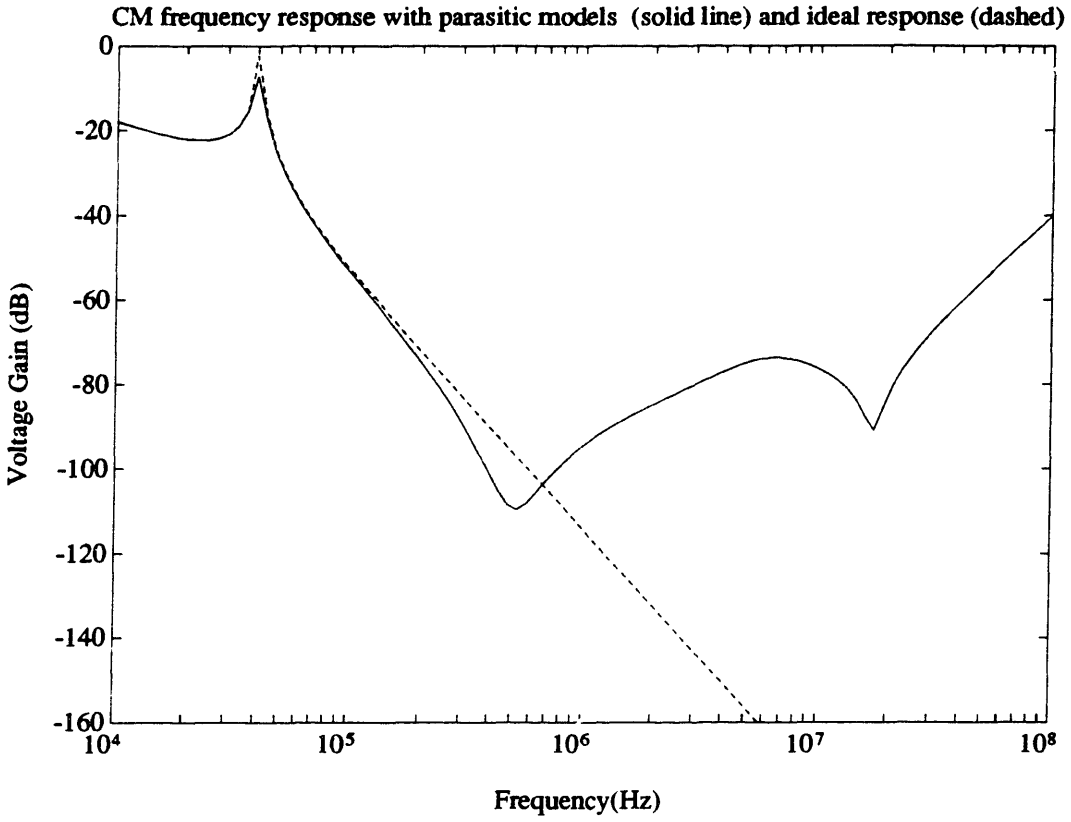

Figure 3-13: Calculated CM gain of EMI filter with and without parasitic elements

the output inductor. At the higher self-resonant frequency of the common-mode capacitors, the filter attenuation begins to deteriorate even more rapidly; the ideally L-C-L low-pass filter turns into a C-L-C high-pass-filter with a cut-off frequency of a few hundred MHz.

Differential-Mode Parasitic Effects

Fig. 3-14 compares the calculated differential-mode attenuation of the filter circuit with

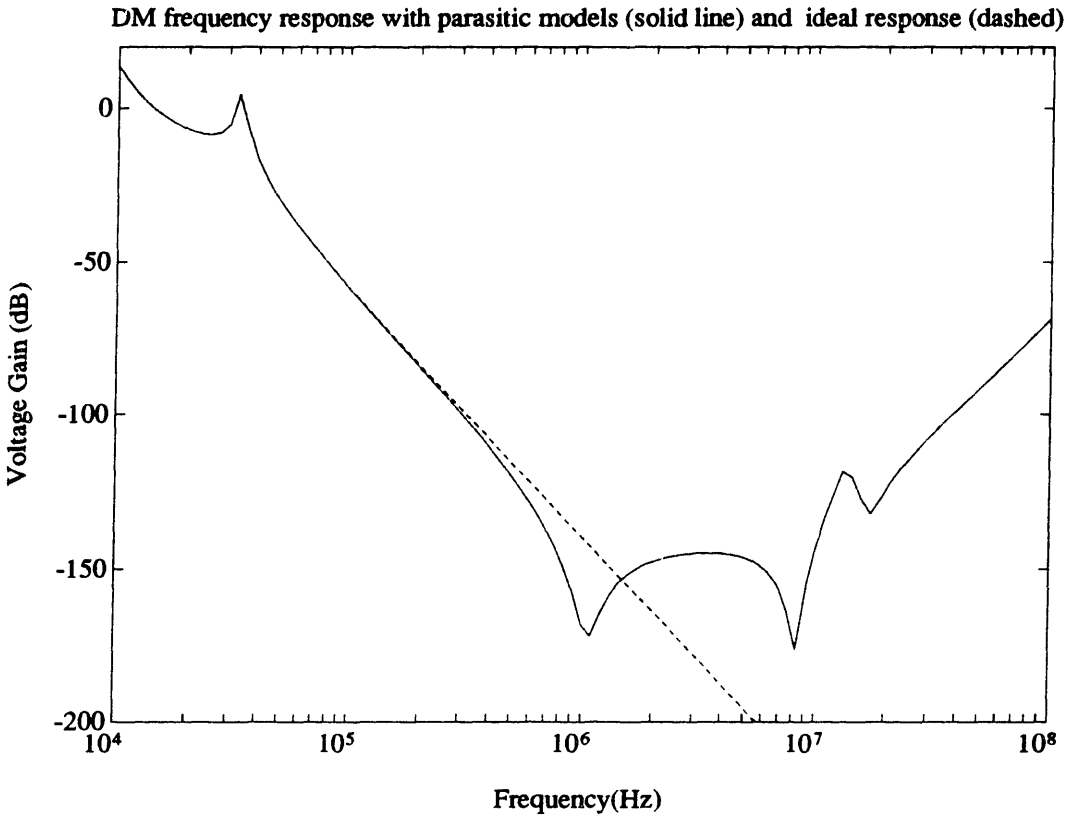

Figure 3-14: Calculated DM gain of EMI filter with and without parasitic elements

and without the inclusion of component parasitic effects. Again, the self-resonances of the filter components, first the two capacitors at 1 MHz, and then the leakage inductance of the common-mode choke at 8 MHz, followed by the (well-damped) differential-mode inductors, deteriorate the performance of the filter above a few megaHertz. Much like the common-mode filter's parasitic effects, those of the differential-mode network transform this fourth order low-pass filter into a fourth order high-pass filter at very high frequencies.

A notable feature on the model-based differential-mode plot is a positive resonant peak at 13 MHz. This peak illustrates a subtle but fundamental problem with the inclusion

of smaller high frequency back-up components. Since all component self-resonances would cause shunt capacitors to be very small impedances or series inductors to be very large impedances, self-resonant frequencies should give frequency response peaks in the negative direction. Thus, the oppositely-directed peak at 13 MHz must be a resonance between parasitic or principal elements of different component, such as series inductors or parallel capacitors. In order for a high-frequency backup component to be helpful, it must have lower parasitics than the larger component, but this automatically implies that the parasitic of the large one will resonate with the small component before the smaller's self-resonant frequency. If the deterioration of attenuation that results from this peaking is troublesome, this plot illustrates the need for damping of such parasitic resonances and hence very careful selection of those components which are to share series or shunt positions in either the common-mode or the differential-mode network.

The large dynamic range of the scale of the plot of Fig. 3-14 should be noted. Even with the parasitic effects included, the expected attenuation of this fourth order filter is very large over a sizable portion of the EMI frequency range, being in excess of 140 dB between 800 kHz and 10 MHz.

3.4 Frequency Response Measurements of the EMI Filter

Measurements of the frequency response of the EMI filter were made using a HP 3577A Network Analyzer. This instrument has a source and three receivers with input impedance options of 50 Ω or 1 MΩ || 30 pF, and features including arithmetic capabilities and data storage registers. The analyzer's source, a frequency-sweeping sinusoidal voltage signal generator, was applied at the filter input (rectifier side). Since this source has a substantial output impedance, measurements were made at the input as well as the output of the filter. While the receiver impedance at the input was inconsequential, the impedance used at the output was 50Ω , as suggested in Section 3.2.1. The frequency response was then computed by the network analyzer as a ratio of the two measurements.

3.4.1 Common-Mode Measurement

As in the analysis of the common-mode subcircuit, measurements of the common-mode filtering performance involved assuming a sufficient degree of symmetry in the filter and

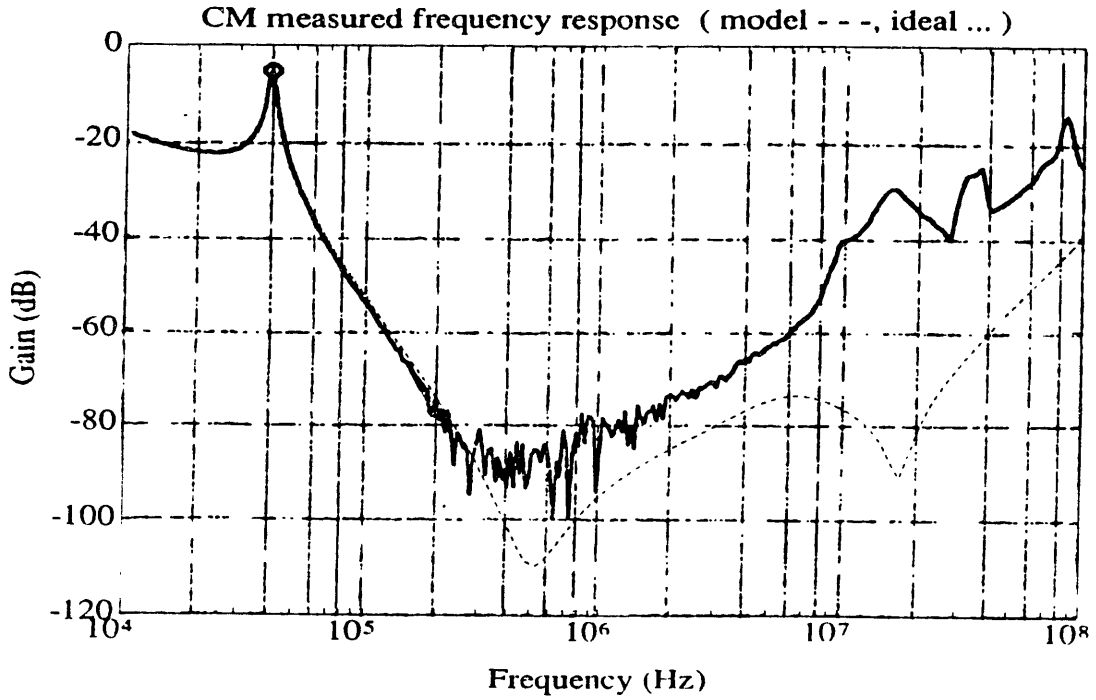

Figure 3-15: Measured CM frequency response compared to model-based calculation

shorting together the hot and neutral phases on each end of the filter. Measurements were made from these shorted together nodes to the third wire of the filter, the earth ground connection.

Sweeping the range of 10 kHz to 100 MHz and and displaying the ratio of the output to the input voltage of the common-mode-connected filter, the resulting data agreed with the model-based calculations to within 1 or 2 dB up to about 400 kHz. Fig. 3-15 shows the two curves for a broad frequency range, but the measured signal on this plot is limited at the low-end by the dynamic range of the analyzer. Results of a second measurement in which a larger input voltage was applied, swept only above 100 kHz, and measured with a 46 dB voltage divider, are shown in Fig. 3-16.

While the general shapes of the measured and calculated curves of Fig. 3-15 and 3-16 are similar up to about 15 MHz many of the key features are shifted to lower frequencies, and hence lesser attenuations, for the measured version. This type of correlation would seem to indicate the types of models of the component parasitic chosen for the common-mode circuit were reasonable ones, but that the values used in the calculations were not quite accurate. One reason for this inaccuracy may be the fact that only one of each type of component was

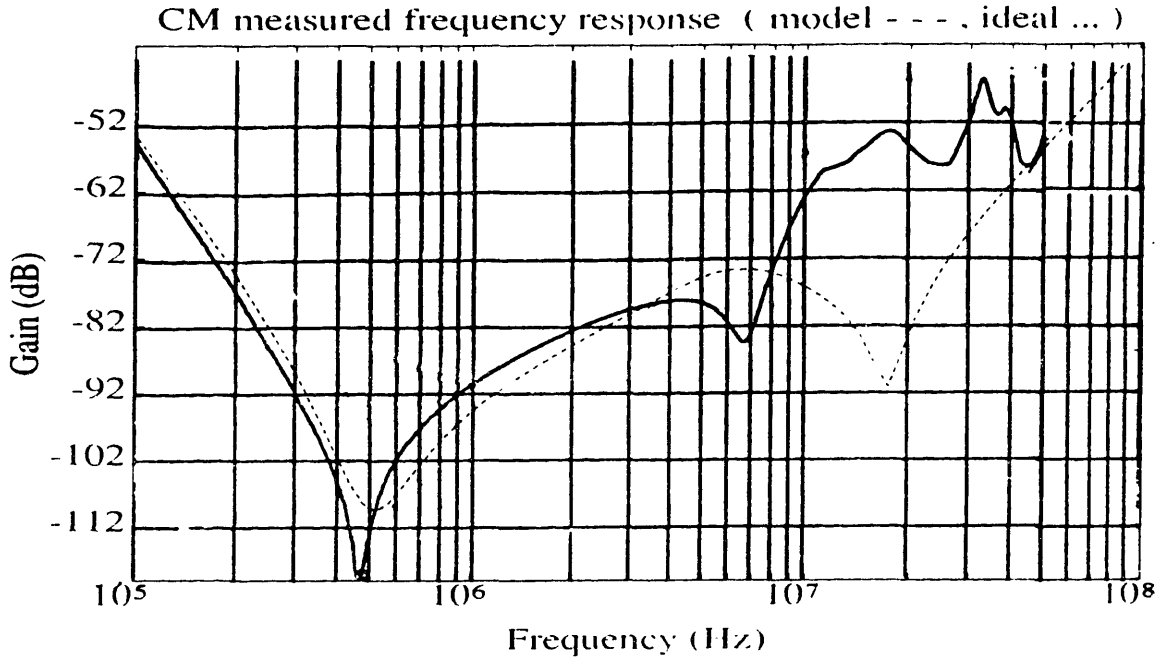

Figure 3-16: High-frequency measured common-mode frequency response compared to model-based calculations

measured, neglecting tolerances and differences in parasitics. Another possible cause for this error is that the effective values of the parasitic elements were greater when the components were placed in the actual circuit. Capacitance between pc board traces, for example, may have added to the effective capacitance in parallel with the inductors, and the inductance of the traces connecting to capacitors may have added extra series inductance to these components. In addition, some model deficiency is evident, as the discrepancy between 100 and 500 kHz corresponds well to the inaccuracy of the oversimplifying modeling of the common-mode choke, as evident over the same range in Fig. 3-11. At frequencies above 15 MHz, the correlation between prediction and measurement was very poor with possible causes including the uncertainty of the component models beyond the 13 MHz limit of the impedance analyzer and the likelihood of other parasitic effects in the layout of the circuit, as well as in the components.

3.4.2 Differential-Mode Measurement

Measurements similar to those of the common-mode frequency response were attempted for the differential-mode frequency response. This involved applying and measuring signals between the hot and neutral phases of the filter. Several practical issues made this a much

more complex task than the common-mode measurement. In particular, the large expected attenuation and the balanced four-terminal topology of the differential-mode filter caused difficulty in determining a measurement method and uncertainty in accepting results.

Large Expected Attenuation

Much greater attenuation was expected from the differential-mode network, which, even with parasitics, is a fourth-order low-pass-filter up to 1 MHz, as compared to the common-mode circuit which was expected to have only third-order characteristics, only up to 500 kHz, and with a somewhat higher cut-off frequency. As evident in Fig. 3-14, the model for the differential-mode network predicts attenuations of as much as 160 dB around 1 MHz. Such a large attenuation is very difficult to measure, as even a signal of 10 volts would be attenuated to the sub-microvolt range, making it very susceptible to noise as well as coupling within the measurement configuration. The dynamic range of the network analyzer between overload levels and the noise floor was, in fact, measured to be about 90 dB. By measuring the input voltage with a voltage divider and putting in the largest possible input signal, an extra 21 dB of dynamic range can be added, since the source is capable of supplying this much more than the maximum trip voltage of the receivers(-13 dBV), but this is still well short of the expected 160 dB attenuation which would need to be measured.

Trouble Due to Topology

The other cause for difficulty in measuring the differential-mode attenuation of the EMI filter was the symmetric topology of the differential network. Since the filter is balanced, it is a four-terminal network without the common neutrals shared by the two ports of a three terminal one like the common-mode T-network. Source and receiver instruments connected to each side of the filter therefore need to be neutral- (and ground-) isolated from one another. The type of measurement configuration used for the common-mode would connect the neutral terminals of each side of the differential-mode circuit through the low impedance of the network analyzer ground.

To see the effect of any finite (or zero) impedance between these nodes, consider the fourth-order balanced filter schematic of Fig. 3-17, redrawn in Fig. 3-18 with an external impedance Z_{gnd} connecting the two neutrals. To the extent that this external ground impedance is a short circuit, the inductors on the neutral side of the filter L_{d1l} and L_{d2l}

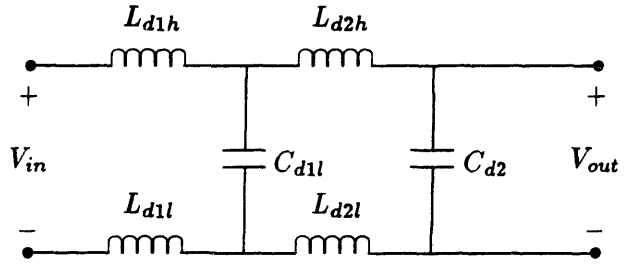

Figure 3-17: Fourth-order balanced differential filter

are in series with one of the X capacitors, C_{d1}, thus reducing the effective filter order to second-order and the measured attenuation accordingly. Similarly, for non-zero but finite Z_{gnd}, there will be some loss of attenuation. For this loss of attenuation to be negligible, a rough approximation would say that the impedance of Z_{gnd} must be much larger than the sum of the impedances of the neutral-side inductors. For the filter under study, this sum of these inductances was about 100μH, so that sufficient isolation at 10 MHz would require that this impedance be greater than about 6kΩ . Even if this external impedance was reduced to a parasitic capacitive coupling across an isolation transformer or between the chassis of an instrument and ground, the corresponding requirement on this capacitance would be that it be much less than 2.5 pF.

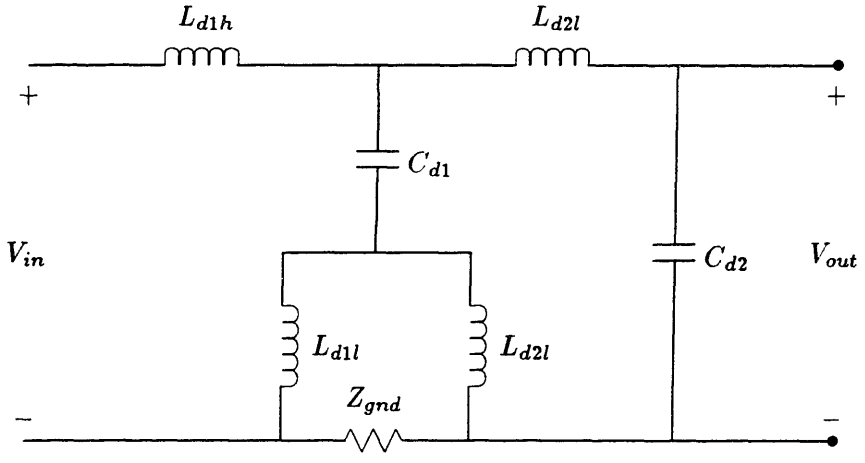

Figure 3-18: Fourth-order balanced filter redrawn with external impedance between neutrals

Differential Measurement Attempts

In addition to these isolation schemes, various differential measurement configurations were considered in attempting to circumvent this "ground impedance" problem. Most of these involved one or both of two techniques: (1) the application of a differential voltage to the filter input, and (2) the differential measurement of the input and output voltages. Figure 3-19 shows a measurement circuit configuration in which both of these schemes were attempted. A transformer was used to convert a ground referenced voltage signal into a differential signal with respect to ground. Both the input and output voltages were measured with respect to the same ground using two receiver channels with the high input impedance of $Z_m = 1M\Omega \parallel 30$ pF selected, and adding the two resulting traces.

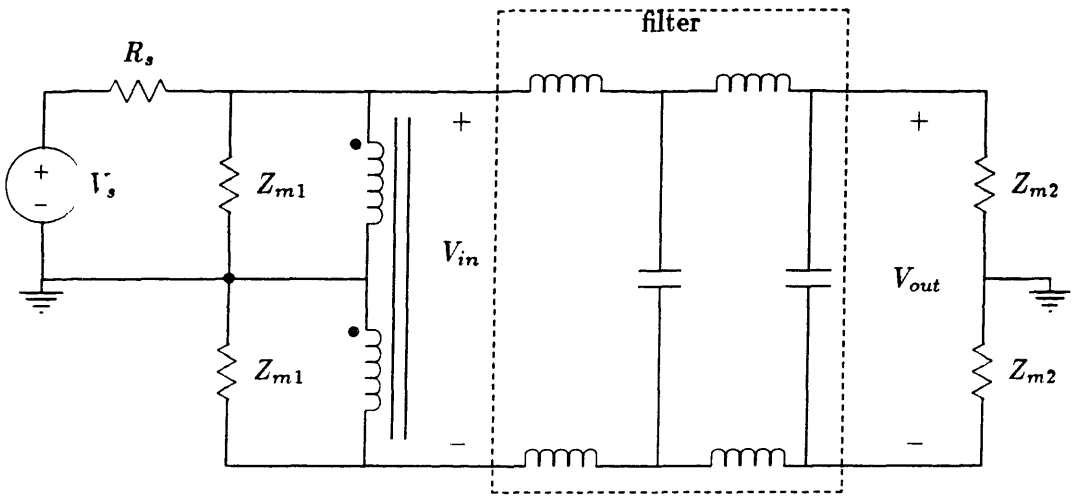

Figure 3-19: Configuration for differential measurement of differential-mode attenaution

The availability of only three receiver inputs on the analyzer precluded the simultaneous measurement of the input and output voltages, so that any effects due to the measurement impedances resulted in ratios of input and output voltages that do not correspond to one another. The measurement impedances between terminals of opposite ports, in fact, could have affected the circuit, as they were significantly smaller than the sum of the impedances on the upper or lower half of the filter, particularly in the MHz range where the impedance of the 30 pF input capacitance was relatively small. Of course, the measurement impedances should have no effect for a truly differential-mode network and a truly differential-mode

input voltage. However, imbalance in the input voltage resulted from transformer leakage inductance. as well as the output impedance of the voltage source; and asymmetry due to component tolerances would have resulted in uneven splitting of currents even if the input voltage were truly differential-mode. The non-differential-mode nature of the real configuration was verified by observing substantial differences in the two channels being used to measure the input or output voltage.

Shorting of Low-Side Inductors

The measurement method finally used involved shorting out the inductors on the neutral side of the filter, and measuring the frequency response between the ports of the resulting three terminal network. If the series inductance for each filter stage was effectively halved, the error associated with this modification to the circuit would be 6 dB for each stage, or 12 dB for the whole filter, at frequencies well above the main L-C resonances; also, the filter resonances would be at frequencies roughly 3 dB higher.

The measurements made on the resulting three-terminal network disagreed with this analysis, however. Further analysis revealed that the leakage inductance associated with the low-side winding of each common-mode choke was not eliminated from the circuit by shorting the winding. A model for the common-mode inductor is shown in Fig. 3-20 along with part of the filter configuration in which it would appear with the low side inductor windings shorted. While the coupled pair of inductors has no effect for a truly differential-mode current through the component, a current passing through only one winding sees the very large magnetizing inductance of these coupled inductors. Thus, even with one of the windings shorted, the lower impedance path is that which passes through both windings, seeing only the leakage inductances, rather than through the short-circuit across the lower winding.

Looking at this somewhat differently, the leakage inductance of the lower winding is reflected across the transformer and seen by the current in the upper winding. In addition, the transformer makes an equal current flow through the secondary (lower) winding. This current circulates through the short circuit, canceling the returning differential-mode current, so that this short-circuit has no effect, at least to the extent that the magnetizing inductance which may divert some of the secondary current is much larger than the leakage inductance of the alternate path. The result is that the leakage inductance, being inherently

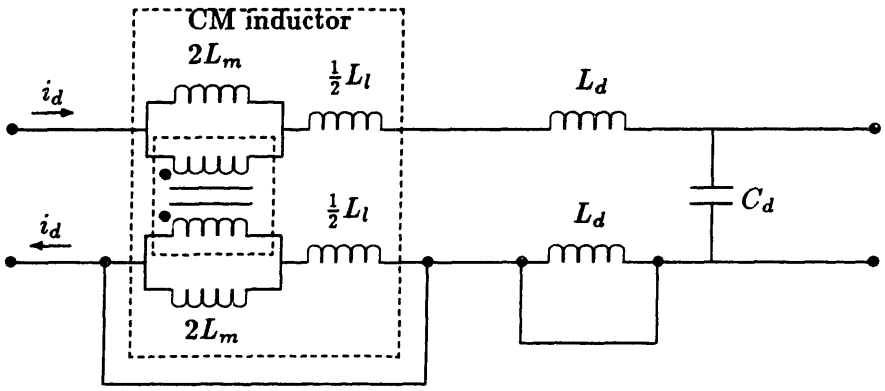

Figure 3-20: Better model for common-mode inductor used in filter with neutral-side inductors shorted

in series with the transformer cannot be directly shorted. Consequently, short-circuiting the low-side windings eliminates only the 40μH low-side differential mode inductor from the circuit, so that the only effect is a 30%, or 3 dB, reduction in the inductance of the first stage and the resulting gain. The associated resonant frequency would be changed by only half this amount, or 1.5 dB.

Results

The understanding of the above section complicates the ground impedance effect discussed earlier, and will therefore be taken up later during the discussion of parasitic coupling effects. Nevertheless, the three terminal measurement method described above eliminates this effect and allows for measurements of something very close to the true differential-mode filter to be made with more certainty as to what is being measured.

After dealing with some parasitic coupling-related problems, which will be discussed in the following section, the frequency responses shown in Figs. 3-21 and 3-22 were obtained. The calculated ideal- and model-based responses for the three-terminal differential filter as analyzed above are also shown in these figures. The measurements and model-based calculations agree up to about 150 kHz to within a few dB. Both show the exact same location for the 28 kHz resonance. Above 150-200 kHz, however, it is clear that the measured component parasitics do not account for the differential-mode filter performance.

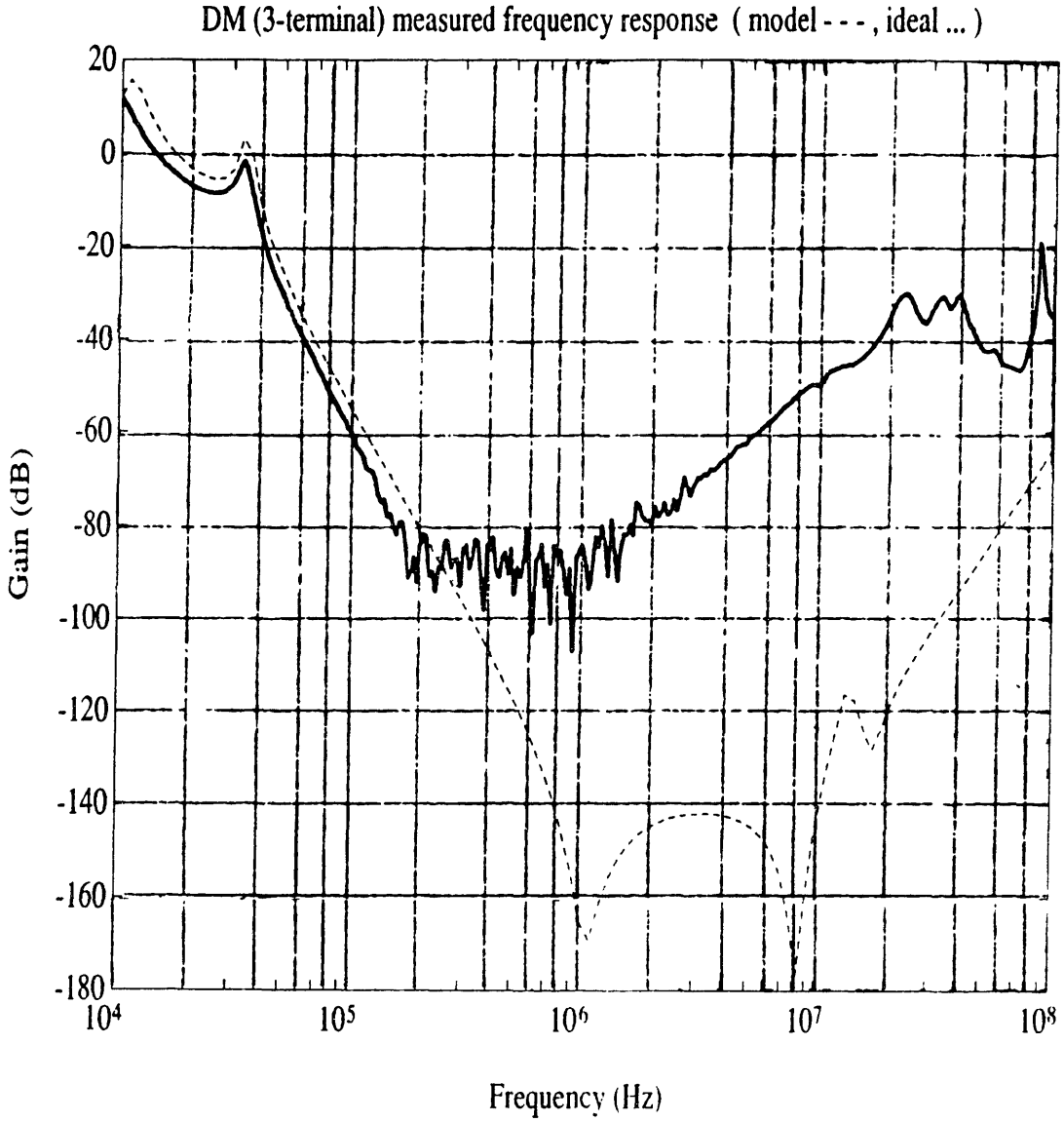

Figure 3-21: Measured DM frequency response compared to model- based calculation

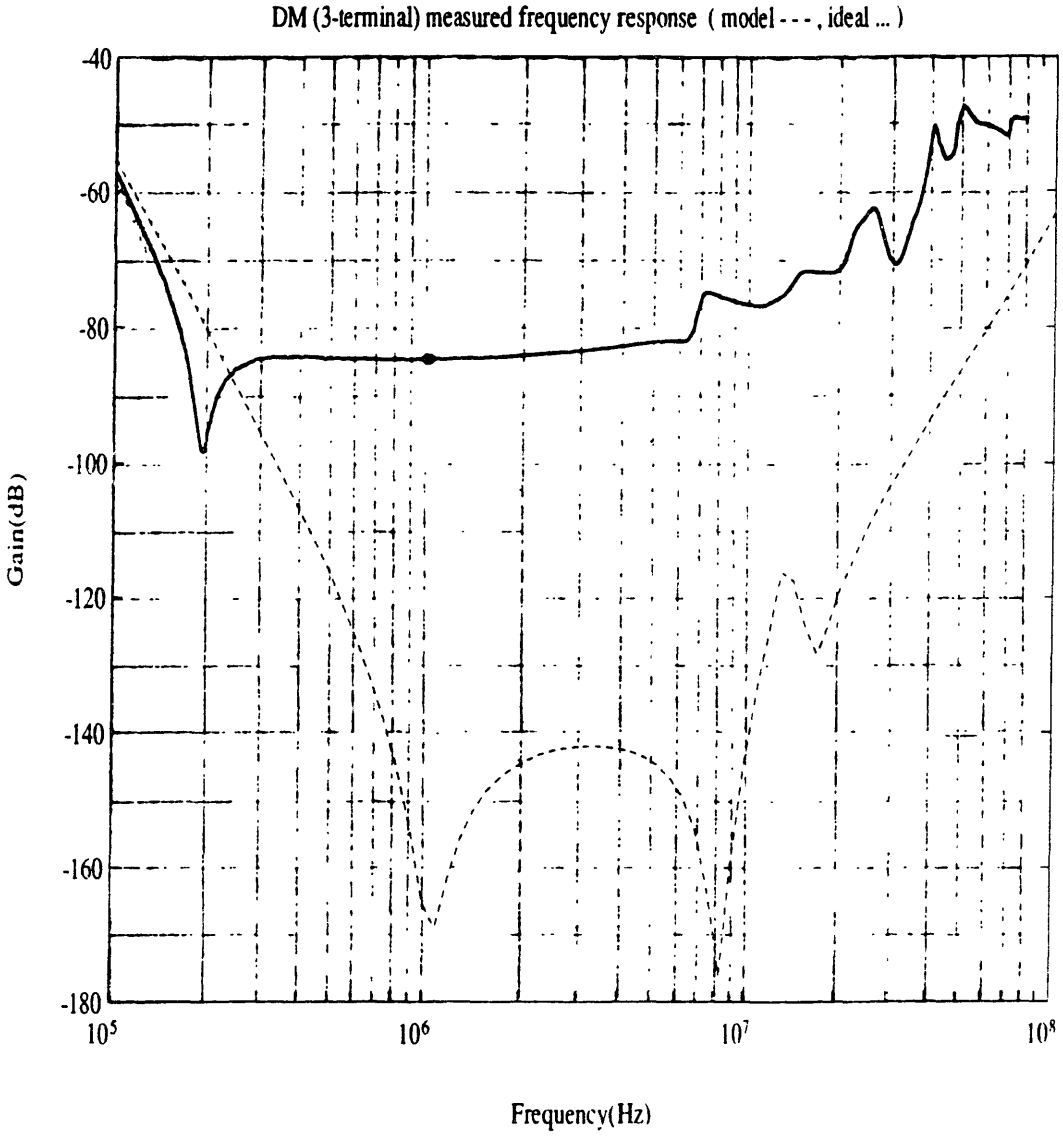

Figure 3-22: High-frequency measured differential-mode frequency response compared to model-based calculation

3.5 Parasitic Coupling In the Filter And In Measurements

The shortcomings of the circuit model based on the components and their parasitic elements suggests the importance of parasitic effects associated with the physical realization of the circuit in which these components are used. Two forms of such phenomena, capacitive coupling and inductive coupling, are considered here in terms of their effects on filter performance, as well as observed effects on measurements of filter performance. Capacitive coupling is due to the energy storage in time-varying electric fields between circuit nodes at different potentials. Inductive coupling involves magnetic flux due to current flowing in a circuit loop linking into a loop in another part of the circuit, and thereby causing current to flow in this secondary loop. Because the output side of the filter has much smaller currents and voltages than the input side at EMI frequencies by the nature of it being an attenuator, the nodes and loops associated with this output side are very sensitive to electromagnetic coupling from the large input voltage or current on the input side, as noted in Section 3.4.2. The ground impedance problem discussed in Section 3.4.2, in fact, illustrated the great influence that a small capacitance between the input and output of a filter can have on the attenuation of the filter.

Resistive Attenuator

The "fourth-order" resistive attenuator shown in Fig. 3-23 was used to study the problems of filter measurement experimentally. For the purpose of observing some of the parasitic effects associated with a filter, this circuit was very useful to consider as a simplified substitute for the EMI filter, since it has a flat frequency response with zero phase to the extent that the resistors have flat frequency responses. The ideal attenuation is $A_o = R_b^2/R_s^2$, and if these carbon resistors are reasonably small in value, good frequency responses may be obtained from the components.

The resistive attenuator built used 50Ω resistors, which were ideal for all practical purposes, and 10kΩ resistors which were ideal up to about 10 MHz, where their parasitic capacitance became a significant effect. The 10kΩ value was chosen since it is on the order of the value of the impedance of the series inductance of each stage around 10 MHz. Thus, with no other parasitic couplings, this attenuator would be expected to have an attenuation of 92 dB (or 98 dB if measured with an additional 50Ω across the output), and a bandwidth

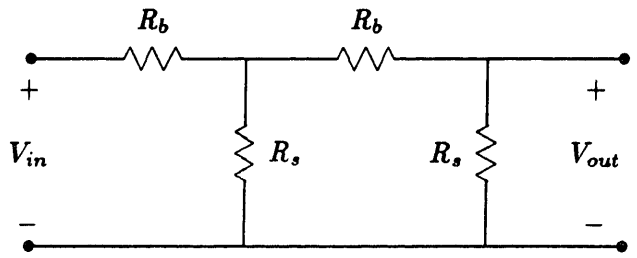

Figure 3-23: Resistive attenuator used to study measurement of filters

of around 10 MHz. A balanced version of this attenuator, having 10kΩ resistors on both the high and low side of each stage was also used in studying some of the various differential and isolation techniques discussed in section 3.4.2 for measuring the differential-mode frequency response of the filter.

3.5.1 Capacitive Coupling

Capacitive Coupling in Resistive Attenuator

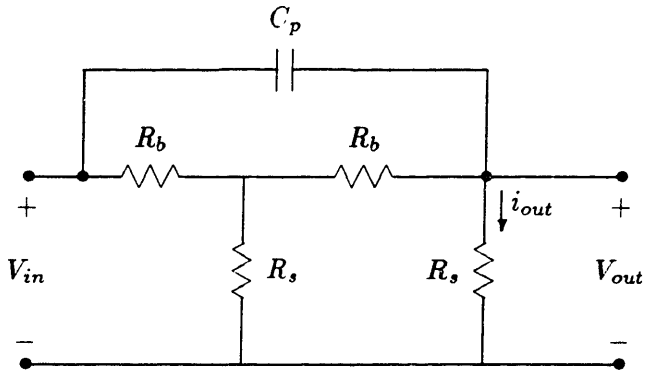

Figure 3-24: Capacitive coupling across resistive attenuator

To consider the effect of a parasitic capacitance across the resistive attenuator, as shown in Fig. 3-24, the larger resistance, R_b is assumed to be much larger than the smaller one, R_s. The current, i_{out} through the small output resistor then has two components, one from the resistive attenuator and one from the parasitic capacitor, which is essentially driven by

v_{in} for reasonable attenuations:

$$i_{out} = (\frac{R_s}{R_b^2} + sC_p)v_{in} \tag{3.2}$$

where C_p is the parasitic capacitance. The gain of the attenuator is thus given by

$$\frac{v_{out}}{v_{in}} = (\frac{R_s}{R_b}^2 + sC_pR_s) = \frac{1}{A_o}(1 + sC_pR_sA_o) \tag{3.3}$$

where A_o is the ideal attenuation of the network. Thus, (3.3) shows the effect of capacitive coupling on a network's attenuation as a function of only the capacitance, the ideal attenuation, and the output impedance.[1] A magnitude bode plot of this result is shown in Fig. 3-25. Another, perhaps more intuitive way of getting this result is to say that the attenuation of the filter will have a pole where the voltage divider between the parasitic capacitor and the output impedance, R_s, gives the same attenuation as the attenuator would ideally, for then the RC divider is the dominant effect at higher frequencies, decreasing the attenuation by 20 dB per decade. Of course, the approximations made in either case break down at high frequencies where the resulting attenuation becomes closer to one and the voltage across the parasitic capacitor cannot be assumed equal to the input voltage, but this merely adds a zero to cancel the pole and leave the gain flat at unity. Besides, at these frequencies, the resistive components would be completely dominated by parasitics anyway.

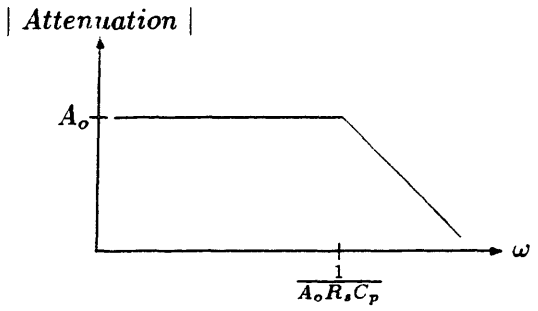

Figure 3-25: Bode plot for resistive attenuator with capacitive coupling

[1] A related result is derived in [1. p. 31] considering the capacitive coupling as a noise voltage source.

According to (3.3), for the 98 dB resistive attenuator constructed with 25Ω of output impedance, a parasitic capacitance of of about 8 fF across the attenuator would be sufficient to reduce the bandwidth of the network to below 10 MHz. This is an incredibly small amount of capacitance, even in free space, where $\epsilon \approx 100$ fF/cm. Using a parallel-plate approximation, two nodes of soldered wires each having an area of 0.4 cm^2 and spaced 5 cm apart would have a capacitance of 8 fF.

Experiments with the resistive network of Fig. 3-23 confirmed the potential application of the above analysis. Measurements were made with a 50Ω receiver impedance. With the two stages of the attenuator separated by a twisted pair connection a few feet long, the 98 dB attenuation was measured with a 3 dB bandwidth of about 10 MHz. Connecting the two stages adjacently, however, resulted in a much lower bandwidth of 1 MHz, which was reduced to as low as 300 kHz by bringing the input and output nodes close together to a separation of only about 1 cm.

Capacitive Coupling in Differential-Mode Filter

The capacitive coupling analysis for the resistive network applies to the EMI filter, except that the output impedance (for the differential-mode network) equals the impedance of the X-capacitor, C_{d2}. Thus, the level of the coupling depends on a capacitive voltage divider between this capacitor and the parasitic capacitor across the filter, and would theoretically be independent of frequency, although its effect on the frequency-dependent attenuation would not be. For instance, a parasitic capacitance of 10 fF across the filter to a 1 μF output capacitor would limit the maximum attenuation of the filter to 160 dB. This is not quite true at high frequencies where the output impedance is no longer a capacitance, but is instead the parasitic inductance of the X capacitor. The measured 1 MHz self-resonant frequency of this capacitor indicates that the impedance of the capacitor at 10 MHz is 40 dB larger than if it had remained capacitive. Thus, the maximum attenuation of 160 dB decreases by 40 dB per decade to 120 dB at 10 MHz. A fairly large parasitic capacitance has been assumed here, and still the measured differential-mode attenuation of the filter is limited to even lower levels than these. This example suggests that, while capacitive coupling across the filter may have been a dominant mechanism in the resistive attenuator, it is probably only a second-order effect in the differential-mode filter measurements due to its lower output impedance.

Capacitive Coupling in Common-Mode Filter

The common-mode network, on the other hand, terminates with the relatively large impedance of the common-mode inductor and so capacitive coupling to the output node would depend on the 50Ω measurement impedance, thus leading to a situation similar to that of the resistive attenuator (except twice as much output impedance), so that 100 dB of attenuation becomes susceptible to a few fF of capacitive coupling over the MHz range. Because of the poor frequency performance of the common-mode chokes, the expected attenuation in the MHz range was not large enough to make any capacitive coupling noticeable.

Other Types of Capacitive Coupling

Other levels of parasitic capacitance certainly cannot be ruled out from being influential. The parasitic capacitances of the components, and, most likely, some of the traces connecting them, as suggested in Section 3.4.1, certainly limit the filter's attenuation. In addition, other parasitic capacitances within the circuit, such as between the windings of two inductors, may influence the filter's performance. These types of coupling, which would be distributed parasitic effects between components or traces, were not considered in detail during this investigation.

3.5.2 Inductive Coupling

Inductive, or magnetic, coupling is the other type of layout parasitic mechanism considered in this study of filter measurement. Such coupling may be between any current-carrying loops in the circuit, parts of which may be within a component such as the turns of an inductor. The basic mechanism of this coupling is the magnetic flux generated by current flowing in one loop, which by Faraday's Law induces a voltage in another loop.

Magnetic Coupling Between Non-Adjacent Loops

A simple way to model the phenomenon of magnetic coupling is with a mutual inductance. For non-adjacent loops, this is done with a transformer, as shown in Fig. 3-26 for magnetic coupling between the input and the output loop of the resistive attenuator circuit. The measurement impedance is shown in this figure because it is part of the output loop and is therefore fundamental to the inductive coupling effect. The inductance of the input loop

is split into a self inductance L_s, and a much smaller mutual inductance L_m which is that part of the inductance which couples (through the transformer) to the secondary loop, or the output loop in the case considered here. Because the impedances of these parasitic inductances, especially the mutual inductances, are typically very small compared to other impedances in the loop, the rest of the input loop may be considered to be a current source, and the output loop surrounding the transformer may be neglected in determining the voltage across the mutual inductance. A result of these approximations is the simplified model of Fig. 3-27, in which the current i_{in} produces a voltage $L_m \frac{di_{in}}{dt}$. [2] The mutual inductance term L_m, which determines the level of the magnetic coupling between loops, is a complicated function of the geometry and other layout effects such as shielding.

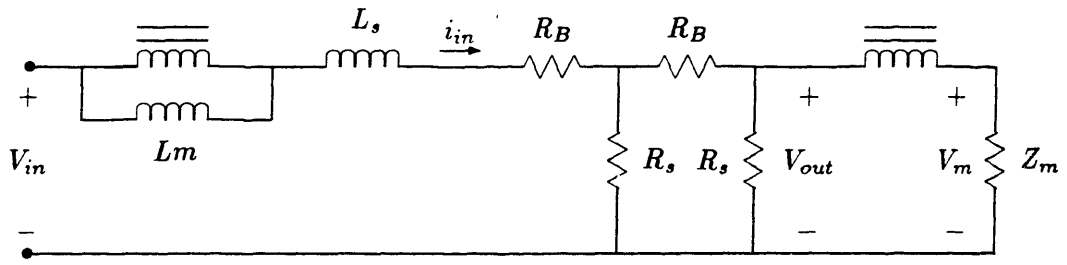

Figure 3-26: Inductive coupling in resistive attenuator

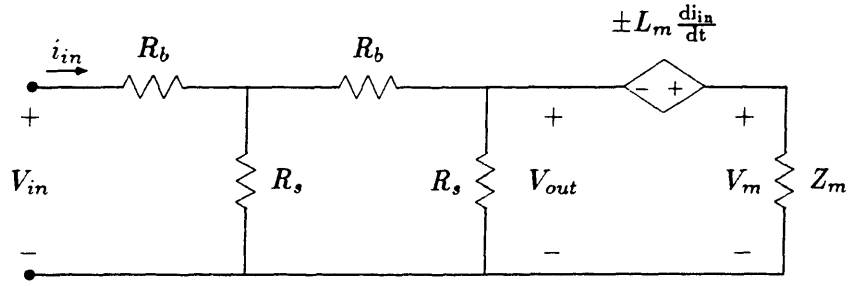

Figure 3-27: Model for inductive coupling in resistive attenuator

The relative size of the measurement impedance Z_m with respect to the output impedance

[2] A similar result is derived in [1, pp. 37-38].

of the attenuator (R_s here) determines the effect of the inductive coupling on the measured voltage. For example, the 50Ω impedance of the attenuator or the even smaller output impedance of the differential-mode EMI filter would cause at least half of the induced voltage to drop across the measurement impedance, whether it is 50Ω or of some greater magnitude. Common-mode measurements of the filter, however, include the much larger output impedance of the second common-mode inductor, so that most of any induced voltage in the output loop will drop across this inductor, at least at high frequencies where the induced voltage is more likely to be significant anyway.

While the resistive network example involves coupling between circuit loops, either the primary or the secondary loop may include inductor windings. Looking at it differently, the mutual inductance of Fig. 3-26 may include a filter inductor's leakage which couples into a secondary loop or a leakage inductance into which flux from another loop couples. In fact, the involvement of actual inductors is more likely to be the case in the EMI filter, where fairly large inductors appear in the high-current input loops of both the common-mode and the differential-mode filter and in the sensitive output loop of the common-mode network. Also note the large amount of leakage inductance of the common-mode inductor, which is certain to be larger than the parasitic inductance of a circuit loop, and through which both common- and differential-mode currents flow.

Magnetic Coupling Between Adjacent Loops

The simplest case of magnetic coupling between adjacent loops is the measurement of the voltage across a solenoidal inductor, as shown schematically in Fig. 3-28. Supposing that the measurement resistor R_m is large compared to the impedance of the inductor, the ac current source i_a drives a current through the solenoid, thereby generating magnetic flux through the turns of this solenoid which are part of loop A. These same turns are also part of loop B, so that this flux also couples into loop B, where it induces a voltage across R_m.

Of course, simple circuit theory makes this result obvious, but a similar issue is illustrated in a more subtle way by the circuit of Fig. 3-29 in which the inductor is replaced by a wire. Now circuit theory would say that no voltage would be measured across R_m; however, the current i_a circulating in loop A generates flux, which might be substantial if A contains thin wire and has a large loop area. Some of this flux returns through loop B

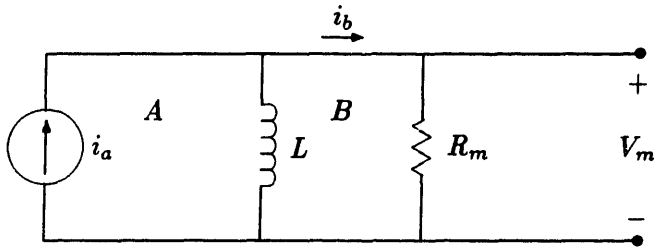

Figure 3-28: Inductor measurement circuit

and creates a voltage around it. Note that the current direction and the voltage polarity are opposite from those of Fig. 3-28, since the flux is coupled here in its return path. This voltage, and hence the inductance measured, does not depend on how much wire of loop A is shared with loop B but instead on how much of the flux in loop A couples to loop B.

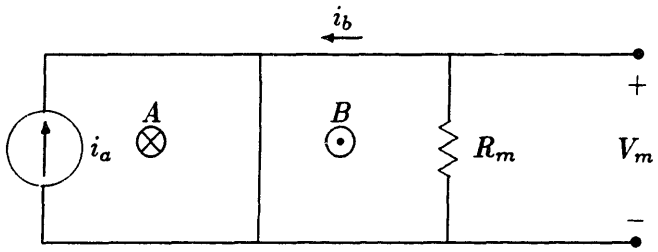

Figure 3-29: Inductive coupling between adjacent loops

Ground Impedance Revisited

This understanding is now applied to the differential-mode filter ground impedance problem discussed earlier in Section 3.4.2. The differential-mode filter with the neutral sides shorted is shown again in Fig. 3-30, this time with the coupled inductors of the common-mode choke included in the circuit model. To emphasize the symmetry of the filter, the magnetizing and leakage inductances of each winding are shown separately. The three loops in the resulting circuit are labeled A, B, and C.

The input voltage drives a current i_a through loop A, with the voltage dropping predominantly across the differential-mode and leakage inductances. Without the neutral- shorting

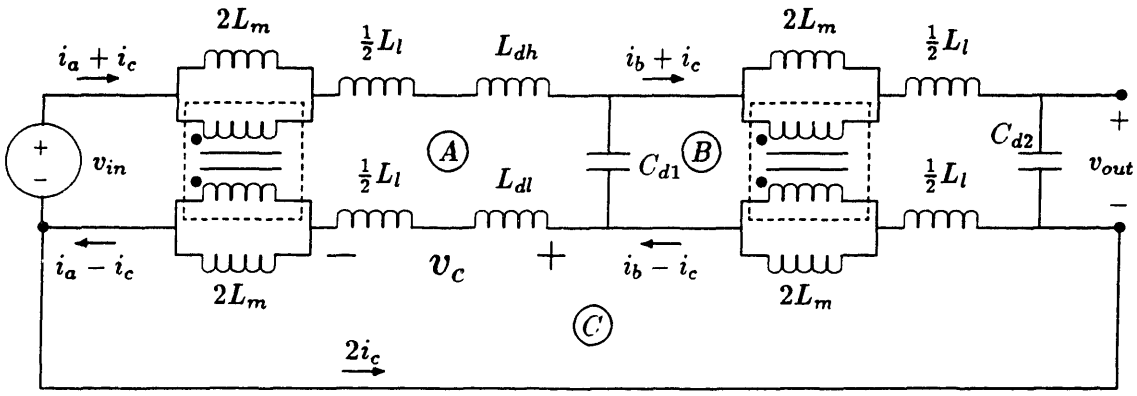

Figure 3-30: Better model for differential-mode filter with neutrals shorted

connection, the remainder of the voltage would drop across the differential-capacitor C_{d1} in the loop A, and this small voltage would drive current i_b through the second loop B. With the neutral connection creating loop C, however, the current in the lower differential and leakage inductors of loop A creates flux that couples into loop C, driving voltage v_c across the rest of the loop. If the coupled inductors are neglected as done earlier in Fig. 3-18, this voltage v_c, which is approximately half of the input voltage, would appear across the lower inductors of loop B, thus driving this loop with a much larger voltage than that across C_{d1}, leading to a loss of nearly half the (dB) attenuation, (i.e., the magnitude of the attenuation will be decreased to the square root of what what it would have been without the ground impedance coupling.) Using the more accurate model of Fig. 3-30, however, and realizing that the impedances of the individual common-mode inductor windings in loop C are those of their very large magnetizing inductances, it is clear that the resulting current i_c flowing in this ground loop will be much smaller than i_a. Also note that the flow of i_c through each of the loop C magnetizing inductances creates flux that couples to the opposite windings in the A and B loops, so that no net flux is coupled into these loops by i_c. This transformer effect maintains no additional net voltage drop in loops A or B by forcing a current equal to i_c through the magnetizing inductances of the upper windings. This current circulates through the voltage source, the output capacitor, and the neutral-shorting connection. Thus, the coupled inductors limit the extra output current and resulting output voltage due to the shorted neutrals by effectively placing the common-mode inductance in series with this neutral connection.

A few important points deserve mention here. In terms of the measurement method used

and described in section 3.4.2, note that by shorting all inductor windings, the coupling between loops A and B through loop C is eliminated, as illustrated in Fig. 3-31.

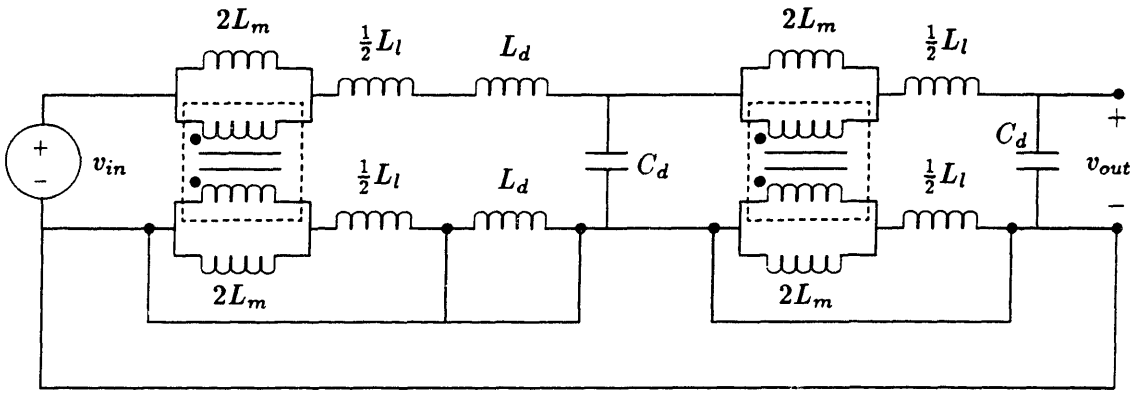

Figure 3-31: Better model for differential-mode filter with neutral-side inductors shorted

Also, while the coupling of the inductors effectively places the common-mode chokes in series with the neutral connection, the common-mode choke was shown in section 3.3.2 to have a large winding capacitance and therefore a low self-resonant frequency, so that at higher frequencies, the neutral connection could significantly reduce the attenuation of the four-terminal filter.

Probably more applicable to the actual use of the EMI filter in a power supply would be the inclusion of some finite coupling impedance rather than a short-circuit between the two neutrals. This impedance may be some sort of capacitive coupling from the rectifier-side neutral to ground which may have a low impedance through the utility to the neutral at the other end of the filter. This capacitance or any other ground impedance would appear in series with the common-mode-inductor (or its winding capacitance at high frequencies) in determining how much current couples from loop A to loop B, which, if significant, deteriorates the attenuation of the filter. A series resonance between this capacitance and the common-mode impedance would leave the situation of Fig. 3-18 in which dB attenuation is roughly halved by the ground impedance effect.

Magnetic Coupling in the Ground Loop

One interesting case of magnetic coupling observed while attempting to measure the differential-mode frequency response of the filter involved coupling to a ground loop, probably from

the leakage of the common-mode inductor in the input loop. The ground loop was part of a measurement configuration shown in Fig. 3-32. Leakage flux from the inductor L coupled into a loop consisting of the ground wires of coaxial cables connecting the circuit

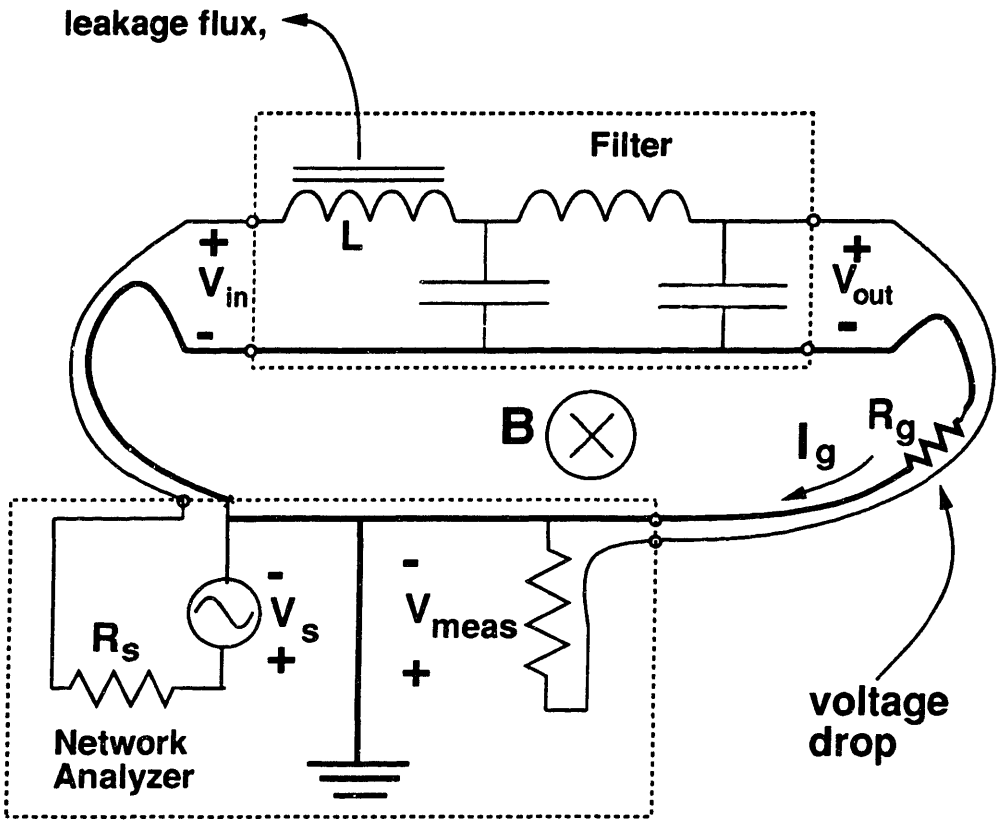

Figure 3-32: Magnetic coupling to the ground loop in a measurement configuration

to the network analyzer, the conductors of the side of the pc board with low-side inductors shorted, and the internal connection between signal grounds within the network analyzer. The area of this loop may be fairly large – on the order of a few 100 cm^2– without special efforts to keep it low, since the coaxial cables connect to different ends of the filter. In this case the dominant impedance of the secondary loop at frequencies in the MHz range may actually be the self-inductance, but the conductor resistance is also substantial due to the skin effect. A resistance of about 50mΩ was measured at 1.6 MHz for the ground conductor of the cable used to measure the output voltage of the filter. With 1 volt at the input of the filter, an attenuation of 100 dB would have given an output of $v_{out} \approx 10\ \mu V$. Any voltage dropped across the 50Ω resistance in the cable due to current in the ground loop generated by inductive coupling added to or subtracted from the measured value of the 10 μV signal.

The 1 volt across the input loop splits between the 50μH of common-mode choke leakage inductance and the 40μH of the high-side differential-mode inductor, so that about 0.55 volts generated leakage flux in the common-mode inductor. To determine the fraction, α, of this flux which was needed to significantly affect the filter measurements, the relationship between voltage and flux is first considered:

$$V = \frac{d\lambda}{dt} = j\omega(N\Phi) \tag{3.4}$$

where $\lambda = N\Phi$ is the flux linkage of N turns and sinusoidal steady state has been assumed assumed. For voltage V_1 and flux Φ_1 in the primary winding (input loop) and V_2 and $\Phi_2 = \alpha\Phi_1$ in the single-turn secondary (ground loop), the following equations may thus describe the magnetic coupling

$$\Phi_1 = \frac{v_1}{j\omega N} \tag{3.5}$$

$$V_2 = j\omega\Phi_2 = j\omega\alpha\Phi_1 = \frac{\alpha}{N}v_1 \tag{3.6}$$

Each of the windings of the common-mode inductor has about 50 turns, but most of the leakage flux, in addition to not coupling through both windings, does not couple to all the turns of either winding, so the effective number of turns N would be somewhat smaller but quite difficult to calculate. If values of N=20 and $v_1 = 0.5$ V are assumed, then a small coupling fraction of $\alpha = .001$ is sufficient to generate 25 μV in the ground loop, of which 10 μV could drop across the output measurement cable. Of course, this explanation was difficult to directly verify, but the case is supported by the differential-mode frequency response curves compiled in Fig. 3-33, which were taken with the different measurement cable configurations such that the area of the ground loop and its location and orientation with respect to the filter were varied, thus changing the sign and magnitude of the coupling fraction α in (3.6). From the shapes of the curves, it appears that there are other significant effects on the filter attenuation or the amount of coupling to the ground loop, but it is likely that very low output voltages may be due the voltage drop in the ground cable effectively canceling the filter output voltage at that particular frequency and cable configuration, while this drop may add to or even dominate over the true filter output in other cases.

With some understanding of this ground loop coupling and some other parasitic effects, the differential-mode filter measurements of Figs. 3-21 and 3-22 were made with special

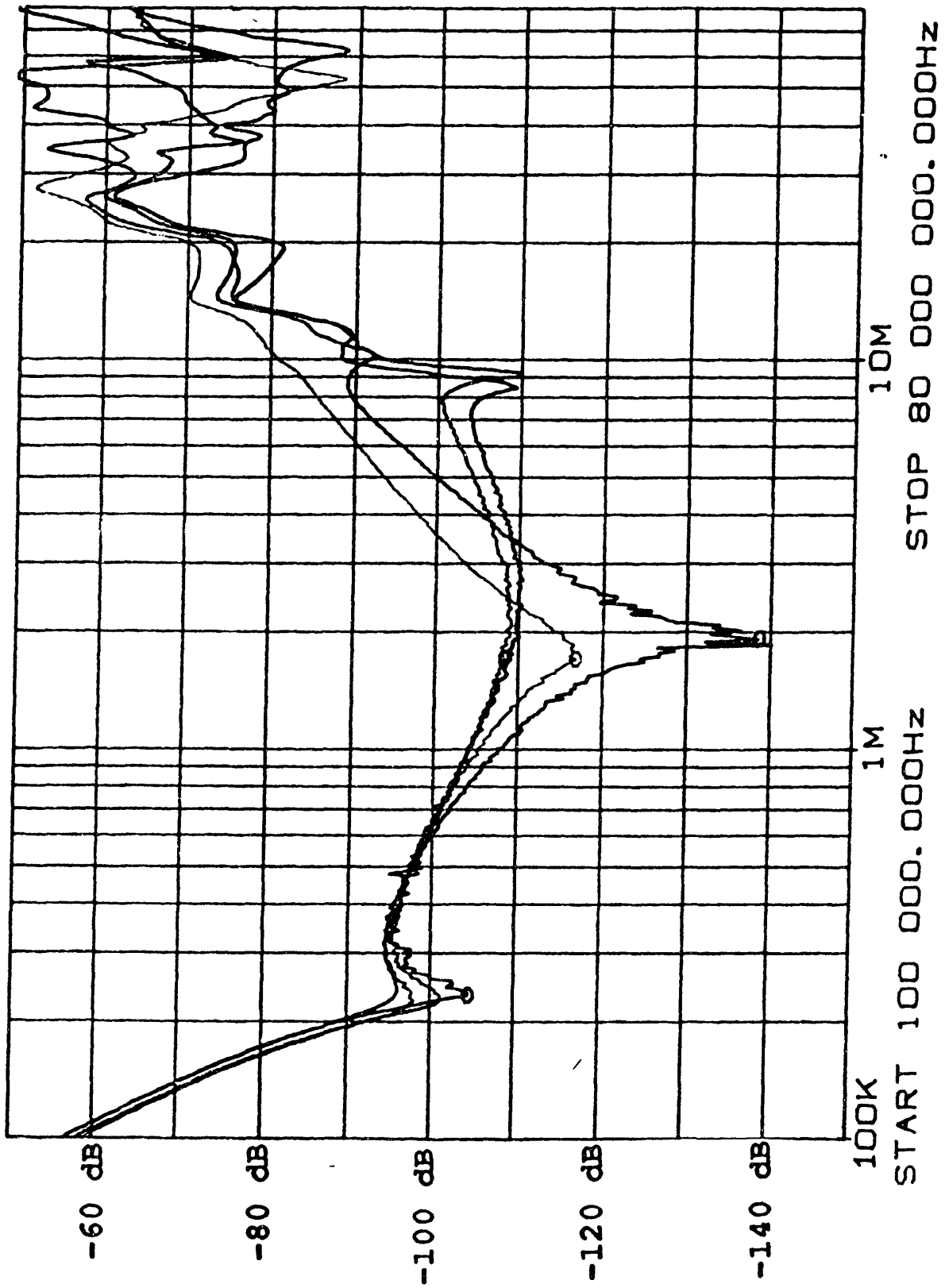

Figure 3-33: Differential-mode filter measurements with various cable configurations

precautions. The filter was mounted on a thin slab of wood with a sheet of metal underneath as a shield shorted to the (earth) ground plane, which was also connected to the signal ground (neutral) input. The output cable was fastened so that it ran underneath the metal sheet alongside the input signal and measurement cables.

3.6 Conclusions

3.6.1 Understanding of Filter Performance

The results of this EMI filter measurement study include a fairly good qualitative understanding and at least a rough quantitative understanding of many of the phenomena which influence the performance of an EMI filter or affect the measurement of this performance. Components of the sample EMI filter were measured and fit to simple models with reasonable accuracy to 13 MHz. The performance of the common-mode filter was measured and quantitatively understood to the extent that its components were characterized. The differential-mode attenuation of the filter was much more difficult to measure, however, due to a combination of the topology and the layout of the circuit, which led to the dominance of parasitic effects which were extraneous to components and therefore difficult to quantify. The low output impedance of the differential-mode filter, as well as its significantly larger component-based attenuation, seemed to make it more susceptible to magnetic coupling to the output loop. While this statement was verified only in terms of its potential effects on measurements through ground loop coupling, magnetic coupling to the output measurement loop seems to be a plausible explanation for the lower attenuation finally measured. While capacitive coupling was studied through analysis and the use of a resistive attenuation network, its effects on filter attenuation were not noticeable from the measurements performed.

Filter Design Implications

In terms of the implications on the design of the filter considered, the volume of the filter is occupied mostly by four very large components, two differential-mode capacitors and two common-mode inductors. While such large components might be needed to meet EMI ripple specifications at the converter's switching frequency, their sizes seem to cause the deterioration of the high-frequency performance of the filter due to their large parasitics, as

well as extraneous parasitic couplings which are exacerbated by their characteristics. The low impedance of the differential-mode capacitor at the output increases the coupling of magnetic flux to the differential output loop and the large leakage inductance of the input common-mode inductor is probably the major source for this magnetic flux.

3.6.2 Suggestions for Future Work

A retrospective analysis of this investigation leads to several suggestions for any future work which attempts to repeat or continue this study. This effort might include a better quantitative understanding and verification of parasitic coupling, and a more accurate measurement and understanding of filter performance at higher frequencies.

Components might be characterized up to higher frequencies using the Network Analyzer to comparve the components to the input impedance of the analyzer receiver or the output impedance of the source. Carrying out such measurements would require special attention to and accounting for any parasitics in the measurement configuration to be sure that the true component impedances are measured. Measurements may be performed on resistors of similar impedances to test procedures and configurations as was done in the filter study herein. In addition, both phase and magnitude measurements must be used to develop component models from the resulting data. More likely, however, as shown by some preliminary high frequency component measurements of this form, the components will not lend themselves to simple models; thus, accurate determination of component-based frequency response expectations of the filter may require calculations directly using the measured complex impedance values. In addition, for greater accuracy of predicted performance, especially at high frequencies where parasitics may be less controlled, measurements should be made on all components rather than assuming components of the same make and size have identical impedance profiles.

Study of the parasitic effects which are associated with the layout or the interactions among components may include measurements of the pc board and frequency response or impedance measurement effects of removal or replacements of certain components. Furthermore, interesting, and perhaps useful, information may come of measurements of the cross-coupling between modes of the filter, such as, the common-mode output resulting from a differential-mode input, for example. Although the study done herein assumed isolation of the common-mode and differential mode signals and their respective networks, there is

certainly cross-talk between the networks due to electromagnetic coupling and component mismatches in the practical use of the EMI filter.

3.6.3 Perspective Considerations

While the results of this study are certainly of theoretical interest at least, their practical importance depends on the application of the filter. The environment in which the filter is placed affects the results obtained. Parasitic coupling directly from the power supply to the filter output, for example could render the filter useless. Also of fundamental importance are the filtering needs, as well as the output impedance, of the power supply, which need to be clearly understood, so that the filter is optimally designed to meet its requirements without costly added-on revisions or overdesign for unnecessary performance at certain frequencies which may likely sacrifice performance at more critical frequencies. The characterization of power supply EMI is, in fact the topic of the following chapter.

Chapter 4

Measurement of power supply EMI sources

Introduction

The standard procedure to test for EMI compliance is to measures the EMI using a LISN network with an EMI filter in between the power supply and the LISN. As discussed in Chapter 3, the network of a typical EMI filter disproportionately attenuates and cross-couples the common-mode and differential-mode EMI signals with a frequency dependence that is difficult to predict. While a better understanding of EMI filters is therefore desirable, measurements to characterize the EMI source in the power supply itself are an important part of a scientific approach to EMI reduction. In simplest form, the models developed by such characterizations should include a source and an impedance whose values vary with frequency.

The motivation to directly characterize the power supply's EMI source are twofold. First, such measurement would give the power supply designer a tool to more directly study aspects of the power supply design which affect its EMI performance, as well as to give a final evaluation of its performance for comparison with other types of designs. Second, as mentioned at the end of Chapter 3, such measurements give specific requirements of the EMI filter, allowing for its more optimal design.

This chapter discusses the understanding and modeling of power supply EMI sources and suggests instrumentation methods to determine the parameters of the EMI source models. Various issues associated with the practical implementation of these methods are

considered.

4.1 The Power Supply as an EMI Source

4.1.1 Differential-Mode EMI Source

The differential-mode component of the EMI is generated mainly by the chopping of the input line current. Based on the current levels and the control technique, the waveform for the differential current is relatively easy to predict. A Fourier analysis of this waveform should give the spectrum of the EMI source with good accuracy at low frequency, but less so at the highest frequency. Similarly, the differential-mode impedance of the power supply can generally be determined as a function of the input rectifier capacitance and the control strategy. Since it attempts to maintain constant input power, the converter should look like a negative resistance over a time scale larger than the power frequency cycle, increasing current as the voltage decreases. At frequencies higher than this but smaller than the switching frequency of the power supply, the impedance depends on the control technique used. If there is a power-factor correction circuit shaping the output current waveform, it might be controlled by a fixed pre-programmed sinusoid, in which case it will be a stiff current source and the rectifier capacitor will dominate the impedance. Alternately, it could operate as a positive resistor, increasing or decreasing the current as the voltage waveform rises or falls; in this case, the resistance would depend on the load level, which determines the amount of current being drawn. In any case, the impedance would be dominated by the capacitor and its parasitics at the higher frequencies, especially above the switching frequency.

4.1.2 Common-Mode EMI Source

While the source voltage and source impedance of differential-mode EMI may be fairly well-understood, those of the common-mode EMI component are a complex function of parasitic elements such as heatsink and transformer capacitances, as well as the voltage changes on switched nodes. As suggested in Section 2.1, the common-mode network of the power supply (excluding the EMI filter) is a purely parasitic one. Thus, the topology and control strategy have no direct bearing on this impedance. While speculation may be made, perhaps confirmed with measurements, as to the values of some of the parasitic

capacitances and other elements of the common-mode network, work is clearly needed to better understand the common-mode source and output impedance of the power supply.

4.1.3 Narrowband and Broadband EMI Characteristics

EMI may be categorized into broadband and narrowband EMI, where these relative terms describe the bandwidth of the EMI with respect to that of the receiver. The spectra of both common-mode and differential-mode EMI mostly include energy at the fundamental switching frequency and its harmonics. To the extent that the switching frequency is constant, this spectrum consists of narrowband 'spikes' at these discrete frequencies. Particularly at high frequencies, however, where many of the harmonics may be bunched together, the EMI tends to become more broadband. In addition, the ringing of parasitic components often results in high frequency EMI that is broadband due to the damping of the ringing and the nonlinearity of some of the components.

4.1.4 EMI Modeling of the Power Supply

A fundamental basis of this work is the Thevenin and Norton equivalent models of circuit theory. These models are applied to the power converter by assuming linearity and employing frequency-dependent sources and impedances. Figure 4-1 shows a model for the power supply which contains generic Thevenin models for both the differential- and common-mode EMI sources, including their Thevenin voltages v_{DM} and v_{CM} and Thevenin impedances Z_{DM} and Z_{CM} . A basic Thevenin equivalent of v_{DM} and Z_{CM} appears across the hot and neutral terminals so long as the hot and neutral external impedances to ground are equal. Similarly, if the hot and neutral nodes are connected, the common-mode Thevenin equivalent appears between this terminal and ground.

The dual Norton equivalent models for each mode of the EMI source could just as well be used in generating a model for the power supply. In fact, at least for the differential-mode, such a model might be closer to the operation of the actual power supply. Except for pathological cases of zero or infinite Thevenin/Norton impedance, however, the two models are completely interchangeable, although one may be more convenient than the other from a practical standpoint.

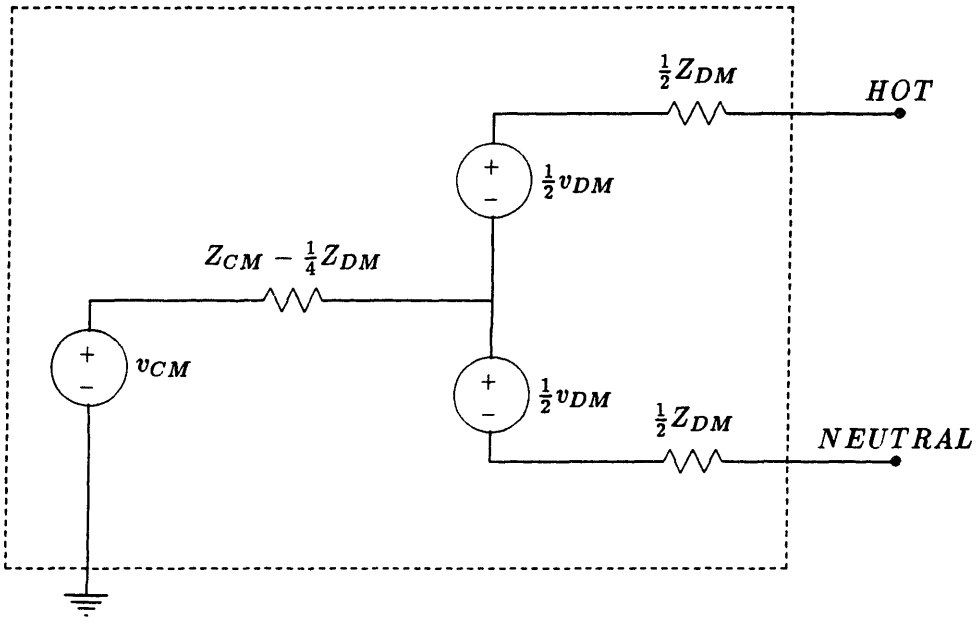

Figure 4-1: Thevenin model for the power supply as an EMI source

4.2 Basic methods

The common-mode and differential-mode terminal pairs may each be considered as 'black box' Thevenin or Norton equivalents and tests may thus be devised to characterize the two 'black boxes'. Two basic methods to characterize a 'black box' are passive measurements and signal injection. Passive measurements across known impedances are useful only if there is a power source inside, which is the case for the application here. Active measurements involve the injection of test signals and measurement of the responses of the network at its terminals. The injected signal and its source impedance are essentially a known Thevenin or Norton equivalent circuit which is used to determine one that is unknown. Both types of tests require at least two measurements to find the two parameters in the model for each mode. The measurement procedures developed herein are all based on one or both of these test methods.

4.2.1 Graphical Interpretations

The two techniques described above are illustrated graphically in the i-v plot of Fig. 4-2. The dark solid line represents the i-v characteristics of the unknown two-terminal EMI

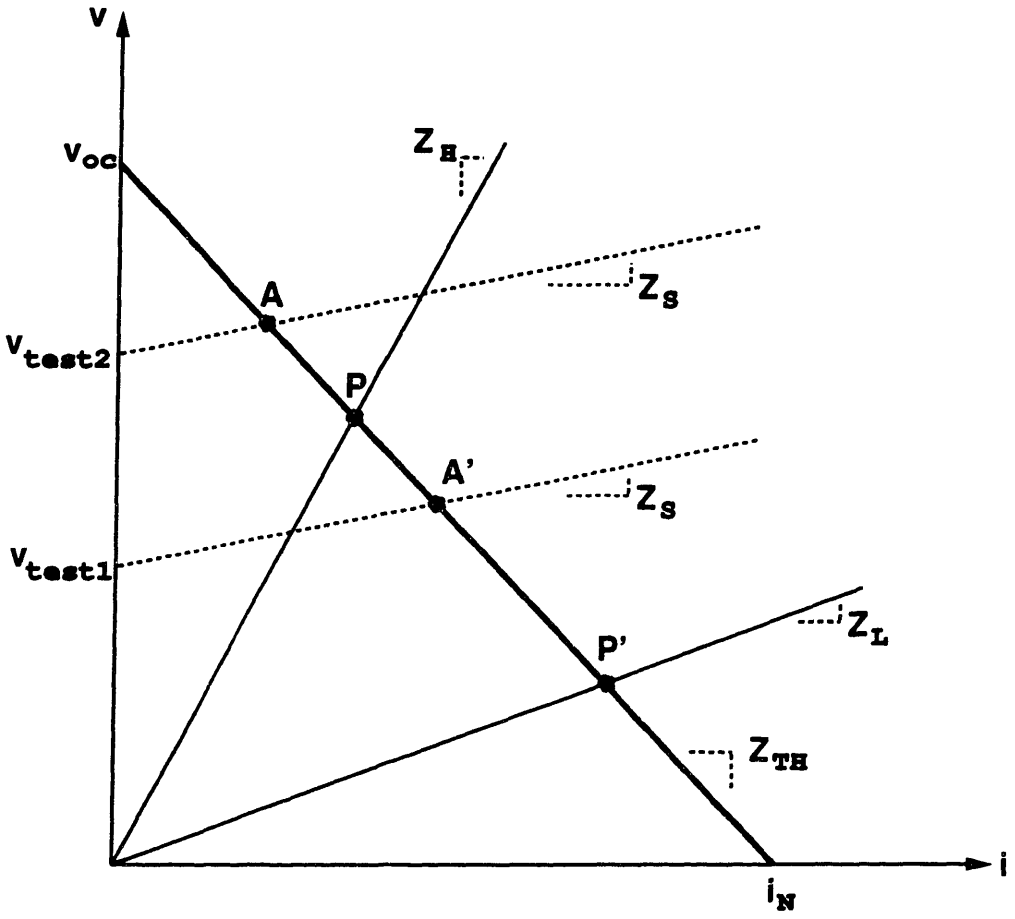

Figure 4-2: Graphical representation of active and passive power supply measurement procedures

source at a particular frequency, so its slope is $-Z_{TH}$ and its v axis intercept is the open-circuit voltage v_{OC}. The thin solid lines represent the two impedances of the passive test, a high impedance Z_H and a lower impedance Z_L . The slopes of these lines are equal to the corresponding impedances. The two intersecting points P and P' determine the load line of the unknown impedance. Similarly, the two dotted lines represent the injected signals V_{test1} and V_{test2} with source impedance Z_S for the active test; their intersections with the load line of the EMI source at A and A' determine that line. Note that that this plot assumes all impedances are purely real. While it might be possible to make the test impedances resistive, the test should account for complex Thevenin impedances.

Despite the assumption of purely real impedances, Fig. 4-2 is useful to illustrate the basic idea of the measurement techniques and some important issues. In particular, the selection of test impedances and signal levels requires some consideration, as it affects the

spacing between intersection points. If this spacing is too small, the determination of the unknown i-v characteristic will be too sensitive to noise and errors. On the other hand, if extreme values are used, the validity of the linearity assumptions made may be called into question. It might be helpful to target the intersecting points to be spaced apart a bit but around the typical region of operation of the power supply, perhaps based on the input impedance of the typical EMI filter. Of course, accomplishing this requires some trial and error, since the location of the curve is initially unknown. While the two curves for the passive test always diverge, the two test signal injection networks must be chosen carefully so that they either stay nearly parallel or diverge. One way to do this is to use the same source impedance, but different magnitudes for the two injected signals.

4.2.2 Passive Measurement

Testing With Two Impedances

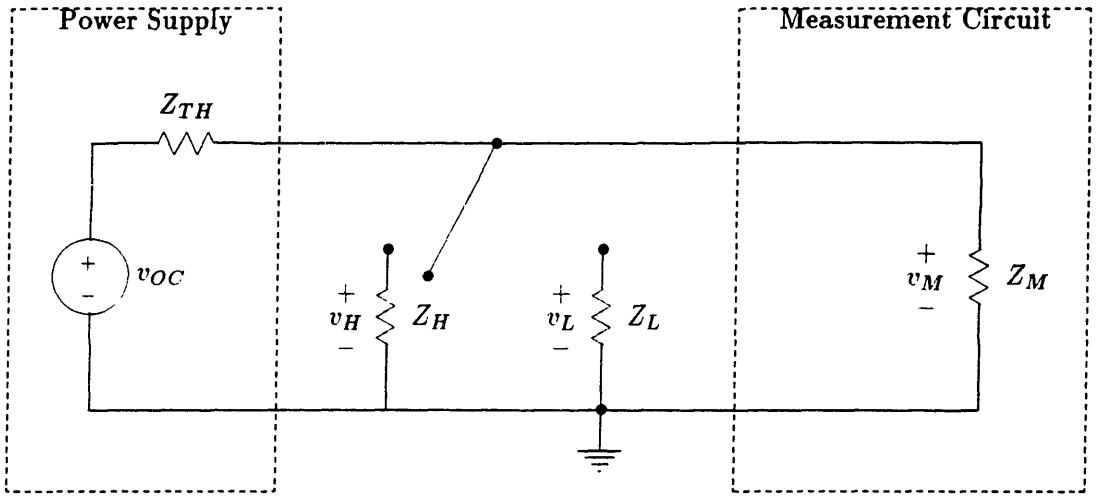

Figure 4-3: Model for high and low impedance measurements on each phase

A basic circuit for the passive measurement test is shown in Fig. 4-3. The high and low impedances are manually switched and the corresponding output voltages are measured. Neglecting the presumably large measurement impedance Z_M, a simple voltage divider describes the relationship for either of the tests and is written here for the high impedance

case:

$$v_H = \frac{Z_H}{Z_H + Z_{TH}} v_{OC} \tag{4.1}$$

Combining (4.1) with its low impedance counterpart and solving for the unknowns gives two of the possible equations which may be used to get the desired information:

$$v_{OC} = v_H \left(\frac{1 - \frac{Z_L}{Z_H}}{1 - \frac{V_H Z_L}{V_L Z_H}} \right) \tag{4.2}$$

$$Z_{TH} = Z_L \left(\frac{1 - \frac{v_H}{v_L}}{1 - \frac{V_H Z_L}{V_L Z_H}} \right) \tag{4.3}$$

Note that both of these expressions have the same denominator. More important, however, is the fact that they both contain the ratio $\frac{V_H}{V_L}$. Because the impedance expression in (4.1) is a complex expression whose phase may depend on the high or low test impedance, even if the test impedance is resistive, v_H and and v_L have different phases with respect to v_{OC}. Because the measurements are taken at different times so their phases cannot be compared, and the phase of the source impedance cannot be determined, any phase measurements of v_H and v_L have no useful reference; thus the ratio $\frac{V_H}{V_L}$, which appears throughout the expressions of (4.2) and (4.3) contains a random phase error. As the expressions subtracted from 1 in the denominators may be near unity, this phase error can change the values of the expressions dramatically.

Testing With Three Impedances

This phase error problem calls for a different approach. One such approach would be to make three measurements and use the extra information to figure out the unknowns of the circuit. Since the phase of v_H (4.1) is the source of trouble, a new equation is written from (4.1) to give an expression for the magnitude of v_H in terms of the real and imaginary parts of the impedance:

$$\mid v_H \mid = \frac{\sqrt{(\Re Z_H)^2 + (\Im Z_H)^2}}{\sqrt{[\Re Z_H + \Re Z_{TH}]^2 + [\Im Z_H + \Im Z_{TH}]^2}} v_{OC} \tag{4.4}$$

Thus, the three unknowns are v_{OC} , $\Re Z_{TH}$, and $\Im Z_{TH}$. Alternately, (4.4) could be written in terms of v_{OC}, $\angle Z_{TH}$, and $\mid Z_{TH} \mid$, and then solved along with two similar equations for these three variables. In either case, the algebra for this solution is quite messy; since it is

straightforward but tedious it will not be included here.

Open Circuit Test

The 'open circuit' test is a special case of the passive measurement test in which the test impedance is made large enough for Z_{TH} in (4.1) to be neglected. The result is a direct measurement of the Thevenin equivalent voltage, allowing solution of only two equations from two additional measurements to find the complex Thevenin impedance. Experimental measurements would be necessary to verify that the test impedance is sufficiently high to conclude that the measured voltage is equal to the open-circuit voltage. As will be discussed in Section 4.3, implementation of the open-circuit test may involve more practical difficulties as well.

4.2.3 Signal Injection Test

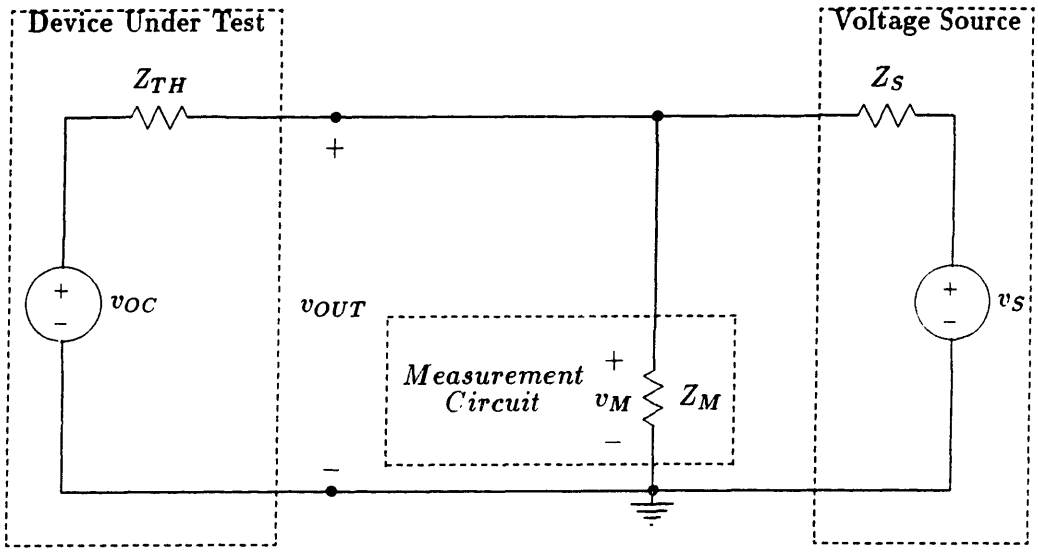

Figure 4-4: Model for the injected signal test

The signal injection method as described earlier and shown schematically in Fig. 4-4 also requires two measurements and the solution of two equations for two unknowns. For the basic circuit of Fig. 4-4, the measured voltage is a superposition of the open-circuit

voltage and the test signal voltage (again neglecting Z_M):

$$v_M = (\frac{Z_S}{Z_{TH} + Z_S})v_{OC} + (\frac{Z_{TH}}{Z_{TH} + Z_S})v_S \tag{4.5}$$

Again, the problem of a random phase exists in this equation. While the phase difference between v_S and v_M can be measured, the phase of v_{OC} with respect to either of these voltage is unknown. Furthermore, the extra complications of the injected source begs the question of why this method would be advantageous.

Approximation Method

By varying the injected signal between two extremes, however, two simple tests can be made which determine the parameters of the Thevenin model. First, a very large signal, $v_S \gg v_{OC}$ is applied. More specifically, this equality should be satisfied with the respective voltage divider factors of (4.5), so that the contribution of v_{OC} to the measured voltage v_M is negligible. In this case, the network under test is treated as a passive one; with the first term of (4.5) eliminated, the measured voltage carries meaningful information on both phase and magnitude that may be used to directly calculate the complex Thevenin impedance. For the second test, a test voltage $v_S \ll v_{OC}$ is applied or it is simply removed from the circuit, so that the second term in (4.5) may be neglected. The result is identical to the passive measurement test described above, except that prior knowledge of Z_{TH}, both $\Re Z_{TH}$ and $\Im Z_{TH}$, makes only one passive measurement necessary. The major advantages of this test are the simplicity of the algebra and the need for only one impedance, which may be present throughout both measurements and accounted for in calculations.

4.3 Practical Implementation Issues

4.3.1 Equipment

Measurement and Computation Equipment

The main piece of equipment used in this work is the HP 3577A Network Analyzer, also used for the filter measurement described in Chapter 3. This instrument has magnitude and phase computation capabilities which allow measurement of common-mode and differential-mode signals without the use of a magnetic addition/subtraction circuit as required in [5]

and the algebraic manipulation of traces to perform functions such as those in (4.2) and (4.3). The instrument's voltage source sweeps through up to 401 frequencies within a programmed band and its three receivers simultaneously measure signals at these frequencies. While its network analysis and computation features are very useful for the signal injection procedure when the EMI source is neglected, the use of this equipment for spectrum analysis is limited due to its low resolution bandwidth capability. The largest setting is 1 kHz for this parameter which determines the bandwidth of the bandpass filtering used to obtain each data point. With a maximum of 401 data points per screen, this means that a linear sweep of a range wider than 400 kHz can miss narrowband information that is between the 1 kHz-wide measurement bands. For a logarithmic sweep, this limit is even more severe. Thus, for high-frequency measurement of signals of spectral content that is random with respect to the network analyzer's source, this instrument is inadequate.

While some exploratory work was done using only the Network Analyzer, more recent work uses a digitizing oscilloscope as well. Both instruments are linked to a PC with a GPIB interface. The available oscilloscopes may sample at rates in excess of 100 MHz. The resulting data can then be transferred to the PC and manipulated for spectral analysis by a software package such as Matlab.

The Power Source

The discussions of Section 4.2 assumed that the power supply was a source of EMI on its own. Of course, it is only through the interaction of the power converter with a source of power that it produces the high frequency signals to be measured in this piece of work. In a sense, the power source is needed to bias the power converter into the Thevenin equivalent network of Fig. 4-1.

Two power sources are considered here. The 60 Hz 120 V (or 220 V) utility is useful for measurements to determine the EMI source during the standard operation of the power supply. Also useful are tests which use a variable DC power source to 'bias' the power supply at different levels to study its EMI source at particular parts of the 60 Hz cycle to better understand the operation of the power supply in terms of EMI generation. The HP 6477C power supply used has a maximum of 220 V output, but two of these supplies are available so that testing at the peak levels of the higher foreign utility systems may be done by connecting the power sources in series.

4.3.2 An Interface Network

The same needs which lead to the use of a LISN in standard EMI testing also call for some sort of interface network between the power source, the unit under test, and the measurement apparatus. Aside from the transmission of power and coupling of the EMI signals to the measurement apparatus, the interface needs include the provision of a required power source impedance to the converter, filtering of external EMI from the power source, and protection of the EMI instrumentation from overvoltages. As will be shown throughout this section, the LISN is an inadequate interface network for this instrumentation work.

Test and Power Source Impedance

The measurement methods described in Section 4.2 require either that the power source impedance be negligibly large or that it be used as part of the measurement test impedance. In any case, since this test impedance needs to be on the order of the input impedance of an EMI filter, which is usually a large inductor, the 50 Ω of the LISN is too small. Instead, a large inductance needs to be used as a DC/60 Hz link. The series impedance used consisted of a 3 mH common-mode inductor and a pair of 85 μH inductors in series with each line for a total of about 350 μH of high-frequency differential-mode inductance.

Using the large source inductance as part of the test impedance, resistors are added in parallel. These resistors, chosen properly, provide damping of resonances between the power source inductance and any capacitive EMI source impedance. If undamped, such a resonance could give misleading measurement results or make computation difficult. While, resonance should not matter theoretically if the complex test impedance is characterized and included in the computation, the extremely small or large voltages may challenge dynamic range limits of the measurement instrument or of the computation functions. For the passive test requiring several different impedances, using different values of the resistance in parallel with the series inductance, may be the means of changing the test impedance.

Filtering of the Power Source

Both the utility and the DC power supply are themselves sources of undesired EMI as well. Due to FCC regulations, their EMI levels should be substantially lower than the unfiltered EMI of the power converter being tested. To be safe, however, an EMI filter should be

added to ensure the use of a clean power source. While the LISN could be used as a filter with the required inductance added in series, it was found that the LISN is not a sufficient line filter to protect the measurement apparatus. While it does an excellent job of filtering at EMI frequencies well up into the megaHertz range, the low-pass line filter and the high-pass measurement coupling filter both have cut-off frequencies in the low kiloHertz range. Cascaded in the power source to measurement path, they pass power line noise in this range, which is large enough at the site of our measurement facility to overload the inputs of the network analyzer.

The line filter used instead includes a low-pass stage with a 700 Hz cutoff frequency consisting of a 26 mH series inductor and a 20 μF capacitor to ground on each line. While this would be a blatant violation of capacitance to ground standards in commercial equipment, it is acceptable for a laboratory test facility. The series inductance described above for the purpose of providing a large source impedance supplements this filter, particularly in its high frequency performance, so that the LISN is not needed for this function.

Protection of Measurement Apparatus

The interface network needs to protect the measurement equipment from large EMI levels to be measured, as well as from the high voltage of the power source. The high-pass-filter to attenuate the power voltage may be a simple capacitor. This capacitor must be sized to give sufficient attenuation at 50-60 Hz and very little at the EMI frequencies, unless some attenuation of the EMI is desired.

The maximum acceptable voltage level at the input of the network analyzer is 225 mV, even with a 20 dB input attenuation option. This figure is typically much larger than the few millivolts or less of EMI at the filtered output of a power supply. With the filter removed, however, the levels of the EMI to be measured may be several volts. A voltage divider between the coupling capacitor and the measurement impedance is therefore taken advantage of in the interface network. If the receiver input impedance of 1 MΩ || 30 pF is selected, the effective measurement impedance throughout the EMI frequency range was found to be a capacitance on the order of 200 pF due to the low RC pole of the input impedance and the relatively large additional capacitance of the measurement cable. Thus, a capacitance of 5 pF in series with each input should provide a sufficient attenuation, which is also conveniently frequency-independent over a wide range. At 60 Hz, this capacitance is

about 500 MΩ and should therefore give enough attenuation in a divider with the 1 MΩ of the measurement impedance.

4.3.3 Common-Mode and Differential-Mode Testing

Figure 4-5 shows a configuration for the measurement of a power supply, including the unit under test, a DC power source, instrumentation apparatus, and the required interface network components, as well as a source for signal injection. Two measurement input channels with impedance Z_M couple to the hot and neutral lines through blocking capacitors, each shown in the figure as a voltage divider impedance Z_D. The common-mode or differential-mode ripple voltage at the power supply input may be obtained from the resulting measurements of v_H and v_N by adding or subtracting them and dividing by a stored pre-measured trace which characterizes the voltage divider relationship between Z_D and Z_M.

Note that the source shown in the figure is connected for the injection of a common-mode signal through two capacitors. If the two capacitors and the hot and neutral RF impedances to ground are matched, this will be a truly common-mode signal. As discussed in Section 3.4.2, the application of a differential voltage is more difficult due to the connection between the low-side of the voltage source and ground. If the network analyzer, which contains the signal injection source, is connected to the utility through a two wire 'cheater', and its signal ground are connected to the neutral of the power converter, the problem may not be as severe as in Chapter 4, where we wanted the differential current to flow through high-impedance inductors (although the neutral-connected chassis would require safety precautions). Here, the desired path of the differential current is through the low-impedance of the power supply, rather than the EMI filter.

Another type of measurement problem is specific to the common-mode measurement. This problem is that of common-mode current which returns through a ground path other than the ground wire at which voltage measurements are made. Capacitance to the ground plane over which the testing is done may be one such path. This coupling would also exist, however, in standard EMI testing of the power supply, as well as in the actual application of the power supply, where walls or floors may include 'ground planes' capable of conducting substantial common-mode currents. The result is that, for common-mode measurements at least, the entire system in which the power supply is used and tested for EMI compliance,

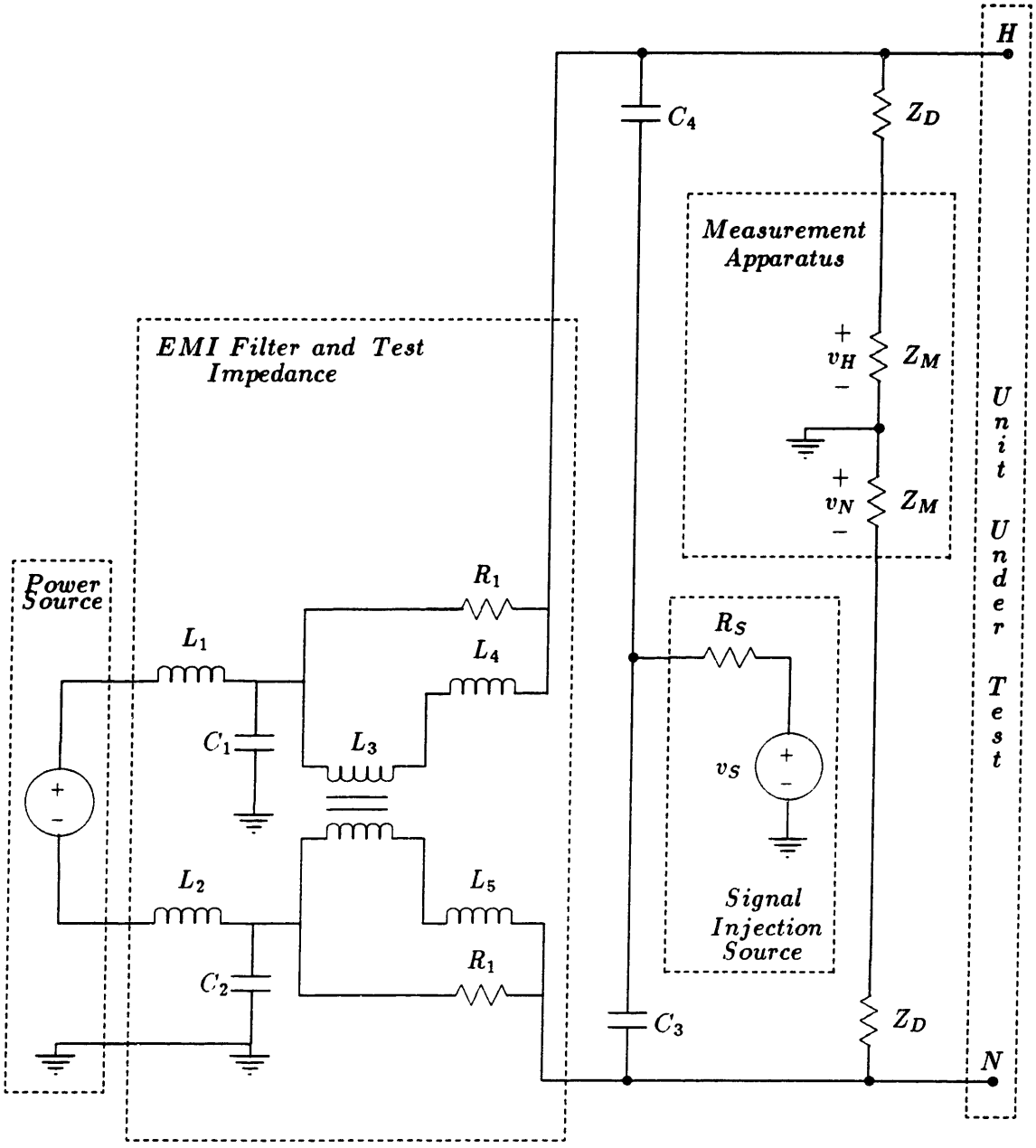

Figure 4-5: Circuit configuration for measurement of power supply EMI source

should be the unit under test.

4.3.4 Characterization of Impedances

The computation of v_{OC} and Z_{TH} from the measurements made requires characterization measurements of the test impedance, the measurement voltage divider between Z_M and Z_D, and the signal injection source impedance, if the injection method is used. Characterizations of an impedance are made by comparing the impedance to the source or receiver impedance of the network analyzer, as suggested for component study in Section 3.6.2. Characterization of a voltage divider involves the straight use of the network analyzer.

To the extent that it is possible, characterizations should be done with the same configuration as used in the actual power supply measurement to account for any parasitic effects. The effective values of the small capacitors used for Z_D, for example, may likely be significantly increased above their nominal 5 pF by parasitic capacitance between connecting wires and soldering joints.

For characterizations of the test impedance, the network analyzer input should be placed directly across the hot- and neutral-to-ground impedances, as well as the hot to neutral impedance. The impedance of the network analyzer measurement and voltage divider impedance , $Z_M + Z_D$ may be neglected for low frequency measurements. Above 500 kHz, however, as the resonance of the common-mode filter inductor is approached, its roughly 10 pF of common-mode capacitance may become significant. To include this in the test impedance characterization, the Z_D's may be connected from each line to ground, neglecting the effect of the much smaller analyzer impedance Z_M. If an injected signal is to be used, it should be removed from the circuit for characterization of the test impedance. While the source impedance of the actual DC power supply should not matter through the L-C-L filter, this assumption might be confirmed by comparing characterizations with the connections shorted and open-circuited.

4.3.5 Other Practical Considerations

Selection of Test Impedance

Depending on the type of test method used, extremely large or small impedances may lead to inaccuracies due to dynamic range problems. In the passive test, if two or more of the

test impedances used are much larger than the Thevenin impedance, even if they are a few factors apart from each other, the voltage dividers between each of them and the Thevenin impedance may be numerically too close to each other, so that the difference is masked by noise in the computation of Z_{TH}. Alternately, if this test impedance is too small during the active injection test, the current divider between the test impedance and the Thevenin impedance will cause the same problem. Of course, selection of a test impedance that is neither too large or or too small before setting up a test requires a rough order of magnitude a priori knowledge of the Z_{TH}. Otherwise, some experimental measurements may be needed with different test impedances.

Practical Application of the Signal Injection Method

The signal injection method was shown in Section 4.2.3 to reduce the required computation and eliminate the need for extra test impedances if the injected signal could alternately be made much larger and much smaller than the open circuit voltage. Given that the fundamental component of the ripple voltage of the power supply may be a few volts, an injected signal that is much larger than it would be at least about 20 volts. Besides requiring a high frequency amplifier to generate what is above the range of typical signal generators, this injected high-frequency voltage would have a magnitude on the order of that of the power source and would therefore significantly affect the operation of the power supply. This, of course, violates the notion that a measurement procedure should have a minimal disturbance effect on the thing it is trying to measure.

A variation on this approximation takes advantage of the narrowband characteristics of typical power supply EMI, at least at the lower frequencies where the levels of this EMI are likely to be on the order of volts. The narrow spikes at the fundamental frequency and its harmonics are the only items of interest in calculating v_{OC}. The Z_{TH}, however, is the input impedance of the power supply and should be a continuous function of frequency even where there is no v_{OC}. Thus, the method suggested here involves injection of a signal that is only on the order of a volt to obtain Z_{TH} at all measured frequencies that do not contain EMI spikes from the power supply. This may require an initial rough measurement of the power supply's EMI to determine these frequencies, but it allows the power supply to be considered as a passive element at all other frequencies. The resulting Z_{TH} may then be processed by replacing values at the fundamental and harmonic frequencies with

interpolations based on measurements at nearby frequencies. These Z_{TH} values can then be used to determine v_{OC} by using a passive measurement.

While this discussion has assumed narrowband spikes of EMI, broadband EMI which may exist at higher frequencies will have lower levels than that at higher frequencies. In fact, if the EMI is broadband at any frequency, it is unlikely to contain a very large component at any of the particular measured frequencies within the band. If the EMI levels are much smaller than the injected signal then this technique becomes the basic approximation method described earlier in Section 4.2.3.

Low Frequency Stability of Test Circuit

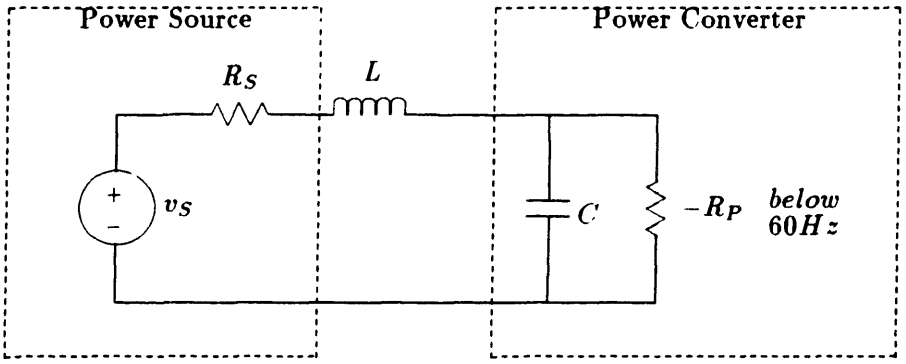

Figure 4-6: Low frequency model for power supply measurement

Particularly if the open circuit voltage test is attempted, the large amount of inductance placed between the power source and the converter may lead to stability trouble in the test circuit. A source of this trouble would be the negative resistance of the power supply below the power frequency, as shown in the simplified low frequency model of the test circuit in Fig. 4-6. Even for a very large inductance of several milliHenries, the typical input capacitance of a few microfarads will resonate with it at around 1 kHz. Thus, assuming a reasonably small power source resistance R_s, C can be neglected from the circuit, leaving a series L-R circuit. The pole of this circuit is of course at $-\frac{R}{L}$ where $R = R_s - R_p$, so that if $R_p > R_s$ then this pole is in the right-half-plane and the circuit is unstable with a natural response of a growing exponential. Of course, if L is sufficiently small, then this exponential is on a time scale shorter than the power frequency cycle in which case the impedance of

the power supply is not a negative resistance, and the instability does not occur. Thus, one of two conditions must be satisfied to ensure the stability of the test circuit:

$$R_p < R_s$$

and

$$\frac{R_s - R_p}{L} < \omega_p$$

where ω_p is the power frequency in radians per second, or 377 for a 60 Hz system.

4.4 Conclusion

The need has been shown for direct measurement of the unfiltered EMI source in a power supply to improve both filter and power supply designs. The power supply has been modeled by distinguishing between common-mode and differential-mode EMI and modeling each of these with a Thevenin equivalent voltage source and impedance. Active and passive measurement techniques have been presented, along with various practical considerations of the measurement methods to determine the parameters of this model for the power supply.

Chapter 5

Active Filtering

5.1 Introduction

In addition to the development of better instrumentation techniques, as discussed in chapters 3 and 4, EMI reduction in power supplies may stand to benefit from novel techniques which use alternate topologies to increase the performance per size and cost of EMI filters. In the signal processing area, active devices are employed to reduced the size and cost of filter circuits by reducing the size of, or eliminating some of, the energy storage components, particularly the inductors. [17] Active techniques might also bring similar advantages if applied to power electronic circuits to reduce EMI. In fact, because the energy storage components are sized for the large voltage and current levels of the power circuit, it seems that the advantages of active power filters for EMI reduction could be even greater. Of course, this application of active filtering also involves many different challenges associated with the levels of current and voltage in the power circuit, as well as other aspects of the environment in which the active circuit is to be placed.

This chapter explores the basic principles, motivations, and challenges of active filtering as applied to power circuits for EMI reduction. Included is a review of some previous work in this area by others. The remaining challenges of practical active filter development will then be discussed, along with other important design issues. In addition, one of the challenges of active filtering, the uncertainty of the utility line impedance, required some investigation, the results of which are presented herein. Finally, a discussion of the requirements and expectations of a practical activc EMI filter sets the stage for the following chapter in which some active filter circuits are analyzed and considered as replacements for a passive EMI

filter similar to one studied in chapter 3.

5.2 Overview: Principles Of Active Filtering

5.2.1 Objective

To develop the basic principles of active filtering, the functions of the components of a passive L-C filter are first considered. An ideal capacitor serves as a current filtering shunt element by rejecting power-frequency currents while shunting ripple current to ground (or neutral for differential-mode) with a minimal voltage ripple generated. The dual element, the ideal inductor, serves as a series voltage filter by passing power-frequency currents while dropping ripple voltage with the generation of a minimal amount of output ripple current. The principle objective of an active EMI filter, then, is to perform, one of these two functions. Since they are duals, only one needs to be considered to illustrate the basic principles and problems of active filtering.

5.2.2 The Active Approach

Considering the active voltage filter problem, a basic approach would be to use a series active device to cancel the ripple voltage. An obvious problem with this method would be the power dissipation in the device due to large power-frequency currents. Perhaps a better approach, then, is to have a small series inductor to pass the larger low frequency currents, and a parallel active device to drive a voltage across the inductor to cancel the high frequency ripple, as shown in Fig. 5-1. Alternately, this device may be a current source which circulates the ripple current of the inductor to keep it from going out toward the utility. Practically, the difference between the current drive and voltage drive methods is just the relative level of the output impedance, Z_{out}, of the driving source as compared to that of the inductor, L_d, being driven. If the circuit is operated at a frequency much higher than the drive pole $\frac{Zout}{L_d}$, for example, it would be considered a voltage-drive circuit.

This discussion has assumed that the active device is somehow controlled so that the ripple voltage is canceled. This control, however, requires some sort of current or voltage sensing to determine how much drive to apply. An obvious choice might be a feedforward approach in which an active circuit senses the ripple voltage across the capacitor and drives

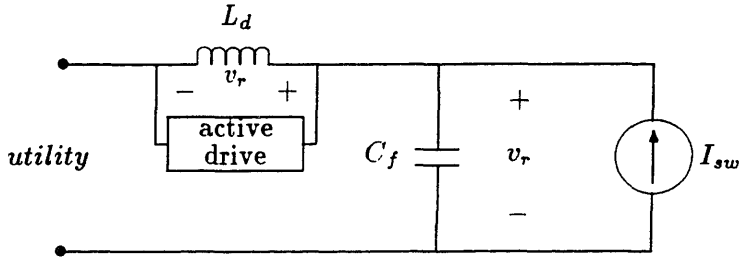

Figure 5-1: Objective of active voltage ripple cancellation

an equal voltage across a small inductor, as shown in Fig. 5-2. The problem with this approach is that it has an undesirable feedback mechanism: since the active circuit needs to have positive unity gain with zero phase, a resonance between the filter capacitor and an inductive utility impedance, for example, could increases the positive feedback gain above unity and result in instability. An alternate approach using negative feedback involves sensing the output ripple current to determine the level of active voltage drive across the inductor. To remove the power-frequency currents from the sensing circuit, a practical version of this circuit would actually include an additional inductor, L_s, as shown in Fig. 5-3, to pass the power-frequency currents. For the ideal case of infinitely high amplifier gain, A, the negative feedback drives the amplifier input voltage v_{in} , and hence the output ripple current i_r to zero.

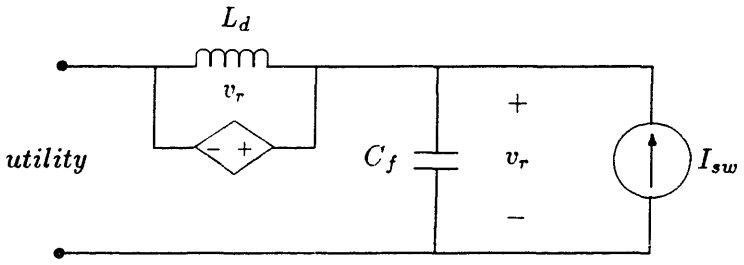

Figure 5-2: Objective of active voltage ripple cancellation

5.2.3 Gain of Active Circuit

An active filter like the one in Fig. 5-3 may be thought of as amplifying, or enhancing, the inductors, L_s and L_d.[2] An important parameter in evaluating the efficacy of the inductor

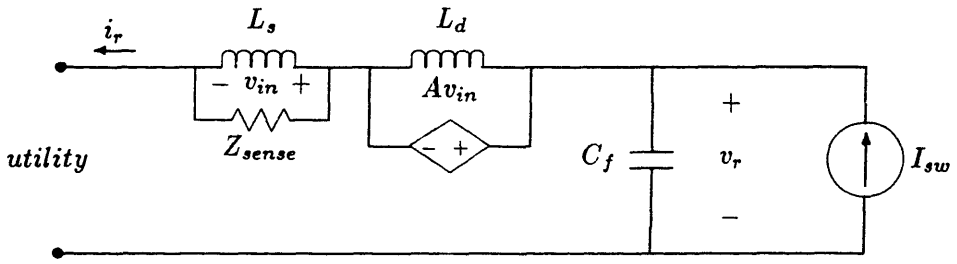

Figure 5-3: Objective of active voltage ripple cancellation

enhancement circuitry is its effective impedance Z_{eff} given by

$$Z_{eff} = \frac{v_r}{i_r} \tag{5.1}$$

where v_r is the unfiltered or partially filtered voltage presented to the enhanced inductor and i_r is the output ripple current. From this, an effective inductance $L_{eff} = Z_{eff}/s$ may be defined and the overall gain of the circuit with some total inductance, L_{actual} used is

$$gain = \frac{Z_{eff}}{sL_{actual}} = \frac{L_{eff}}{L_{actual}} \tag{5.2}$$

Equation (5.2) indicates how much larger the active circuitry has made the actual inductance appear to be. Note that this "gain" does not account for the cost of the active circuitry and any other extra components required.

5.2.4 Feedback Compensation

A very important aspect of the active filter of Fig. 5-3, as well as others which will be studied in this thesis, is that it is a negative feedback amplifier circuit. Proper compensation of the feedback loop must therefore be incorporated into any design, so that the closed loop system has a sufficient degree of stability. The chief method of stability analysis used in this work is to consider the loop transmission, the product of the amplifier frequency response, A(s), and its feedback gain F(s) by breaking the loop at some point and calculating the circuit gain. The closed loop gain, G(s), of the system is then related to this loop transmission

LT(s) by the following expression [15]:

$$G(s) = \frac{A(s)}{1 + LT(s)} \tag{5.3}$$

Thus, for example, a frequency $s = j\omega$ at which the loop transmission has unity magnitude and 180^o phase corresponds to imaginary axis poles of the gain, so that the transient response of this circuit includes undamped oscillation. A useful measure of the relative stability of the circuit to be used herein is the phase margin,

$$\phi_m = 180^o - \angle LT(j\omega_1) \tag{5.4}$$

where ω_1 is the frequency at which the magnitude of the loop transmission gain crosses unity. A phase margin of 45^o, for example, corresponds to an overshoot of about 25 % in the step response of the closed-loop circuit [1], and 0^o phase margin corresponds to an oscillatory step response, while a negative phase margin results in (unstable) growing exponential responses, bounded only by non-linear effects in the circuit such as saturation.

Note that a unity-gain-crossover point may be associated with the low-frequency rise of the loop-transmission, as well as with the high-frequency roll-off. As shown in Fig. 5-4, the gain, as well as the loop transmission, of the active circuit is expected to start out small at low frequencies and rise up to a midband level and then drop off at high frequencies before parasitics can cause instability. Furthermore, a study of the circuit in Fig. 5-3 shows that the feedback. and hence the loop transmission of the active circuit, depends on the external impedance of the utility. Finally, it should be noted that the amplifier gain A(s), the loop transmission gain LT(s), and the closed loop gain G(s) related in (5.3) are distinct from, although perhaps related to, the active filter gain defined in (5.2).

5.2.5 Other Basic Issues

The issues involved in the design of any amplifier circuit generally apply to active EMI filter circuits as well. In addition to gain and compensation, these issues include biasing, bandwidth (closely related to gain and compensation), parasitic effects of devices, input and output current and voltage levels, and power dissipation. An important point to note

[1] From graph in [15, pp. 157-158]

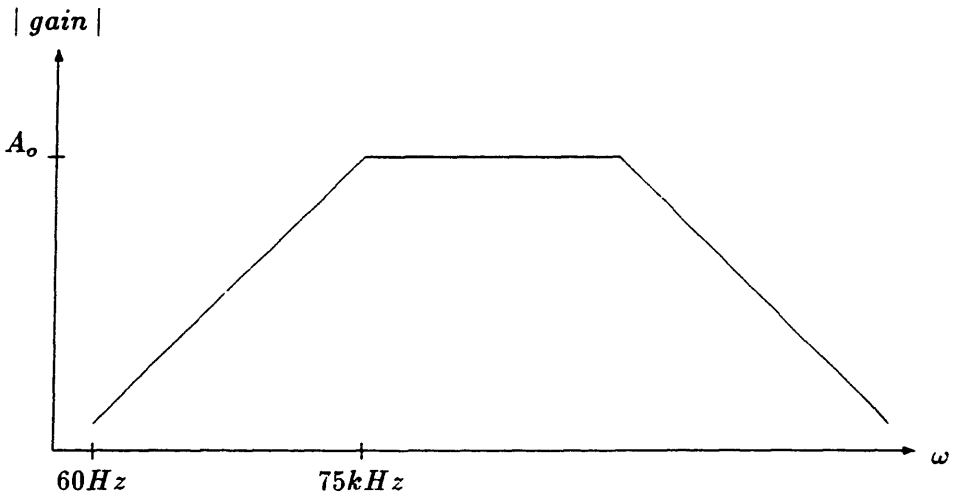

Figure 5-4: Amplifier frequency response desired for active EMI filtering

is that the active filter achieves ripple attenuation with smaller energy storage components by dissipating much of the excess ripple energy. For active filtering to be practical, then, it is generally necessary to use passive filtering to reduce the ripple energies and include the active enhancement on the side of the filter nearest the utility.

5.3 Previous work

The active filter study portion of this thesis is largely based on the master's thesis work of Leif E. LaWhite in [2, 4, 3]. LaWhite developed and analyzed several active filter topologies, as well as details of the associated amplifier design issues. In addition, he designed, built, and tested a second-order voltage ripple filter based on an active inductor-enhancement circuit. Additional previous work in this area by J. Walker in [18] predates LaWhite's thesis. While demonstrating the concept of using active gain circuitry for ripple attenuation, Walker did not demonstrate any overall improvement in cost, size, or performance. His circuit had a capacitor enhancement gain of only 4, [2, p. 10], which is not a substantial improvement, as will be shown later.

5.3.1 Topologies Developed

LaWhite developed and studied two viable inductor enhancement topologies and the capacitor enhancement duals of these circuits. The two classes of circuits developed, standard drive and alternate drive, both involve replacing a component of a second-order filter with two significantly smaller components of the same type and using active circuitry to make the total effective component value look much larger.

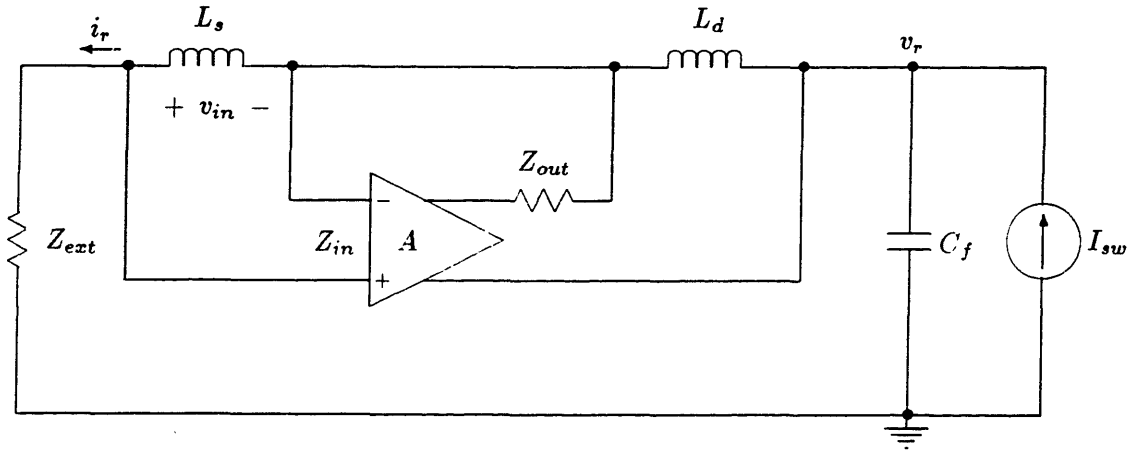

Figure 5-5: A standard-drive inductor-enhanced current-filter circuit

The standard drive topology, reproduced here in Fig. 5-5, is essentially the same as the circuit of Fig. 5-3 discussed in Section 5.2.2. Here, a fully-differential amplifier is used to represent the sense, amplification, and drive of the active circuit. The topological difference between this standard drive and the alternate drive shown in Fig. 5-6 is the placement of the output terminals of the active drive. In the alternate drive, the connection of the lower terminal of the amplifier output is slided across the filter capacitor C_f, so that the active circuit output is across the entire ripple voltage at the terminal where L_s and L_d connect rather than just the voltage across the sense inductor. The result is that the amplifier attempts to drive the sense inductor voltage to be A times smaller than the difference between the capacitor ripple voltage and the inductor ripple voltage, a significantly smaller quantity than the inductor ripple voltage alone. While the alternate-drive circuit therefore has the potential to provide greater overall gain than the standard-drive circuit for the same amplifier gain, it brings the additional complication of having the full line voltage across the active enhancement circuit, requiring that the output impedance include a capacitor.

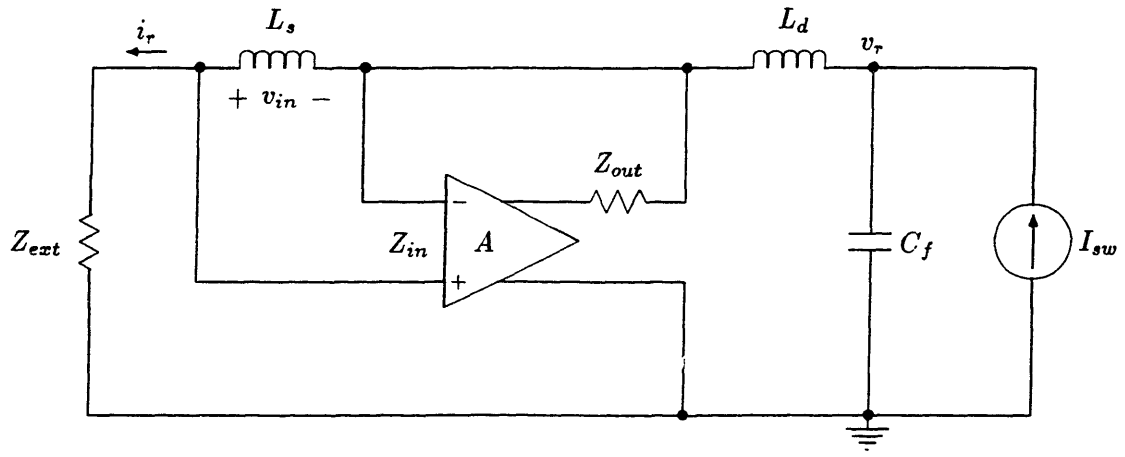

Figure 5-6: Alternate drive inductor-enhanced current filter circuit

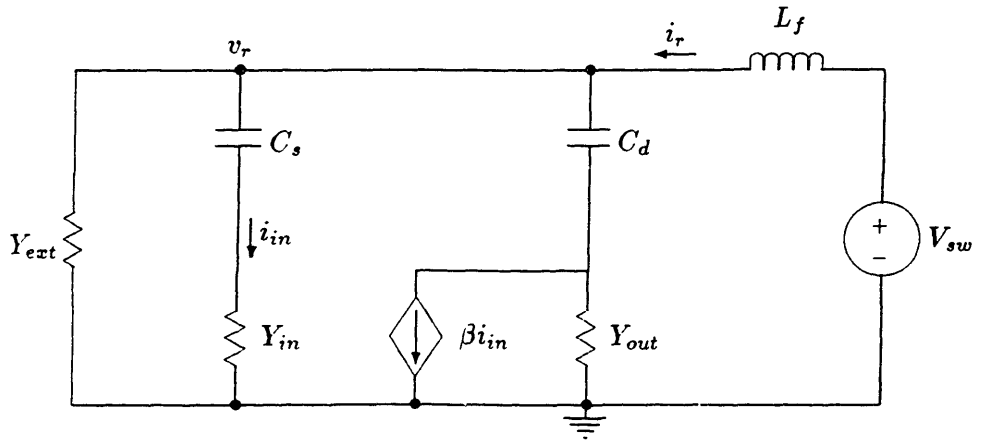

Figure 5-7: Standard drive capacitor-enhanced voltage filter circuit

The capacitor-enhancement duals of these two types of circuits are shown in Figs. 5-7 and 5-8. The principles of operation of these circuits are, of course, duals of the inductor-enhancement circuits described above. Note that the dual problem of the alternate drive capacitor-enhancement circuit is that the output drive is in the path of the large power-level currents, unless its output impedance Z_{out} is mostly inductive so as to shunt these currents. In any case, this complicates the dynamics of the circuit.

While the inductor-enhancing circuits shown in Figs. 5-5 and 5-6 have voltage source drives and the capacitor-enhancement circuits of Figs. 5-7 and 5-8 have current source

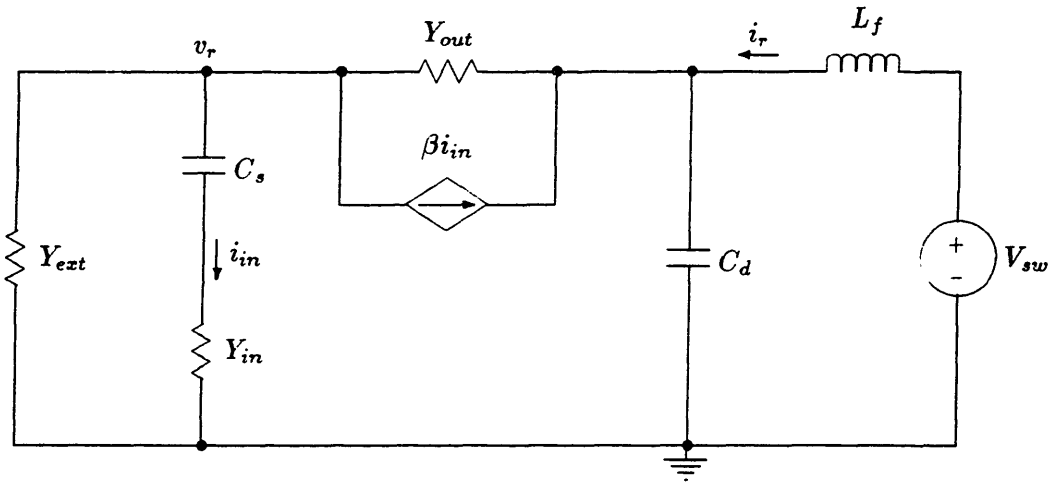

Figure 5-8: Alternate drive capacitor-enhanced voltage filter circuit

drives. Any of these topologies may be considered with either current drive or voltage drive implementations by transforming between Thevenin and Norton equivalents. As suggested in Section 5.2.2, the distinction should indicate the relative impedance levels of the active source and its load at the frequencies of filter operation. Similarly, any of the active topologies may be current-sensing or voltage-sensing, the difference being in the relative size of the sense pole, $\frac{Z_{in}}{L_s}$ for inductor enhancement and $\frac{Y_{in}}{C_s}$ for capacitor-enhancement, compared to the frequency of operation.

5.3.2 Evaluation of Demonstrated Circuit

The circuit built by LaWhite [2, p. 76] was a second-order current-ripple filter using an alternate drive inductor enhancement circuit based on the topology of Fig. 5-9. While the output of the active circuit was essentially a current-drive, the sense pole was very near the switching frequency of 1 MHz for which the circuit was designed.

The active enhancement was implemented with two RF transistors. The biasing and compensation network required a 0.3 W 15 volt dc power supply, five resistors, and five capacitors, including one 0.1 μF high-voltage blocking capacitor and a 10 μF electrolytic capacitor.

The resulting circuit, had a calculated gain of 520, using two 25 μH inductors to provide an effective inductance of 26 mH at 1 MHz. Used with a 0.3 μF filter capacitor, the expected 1 MHz ripple current attenuation of this filter was about 110 dB. The circuit was

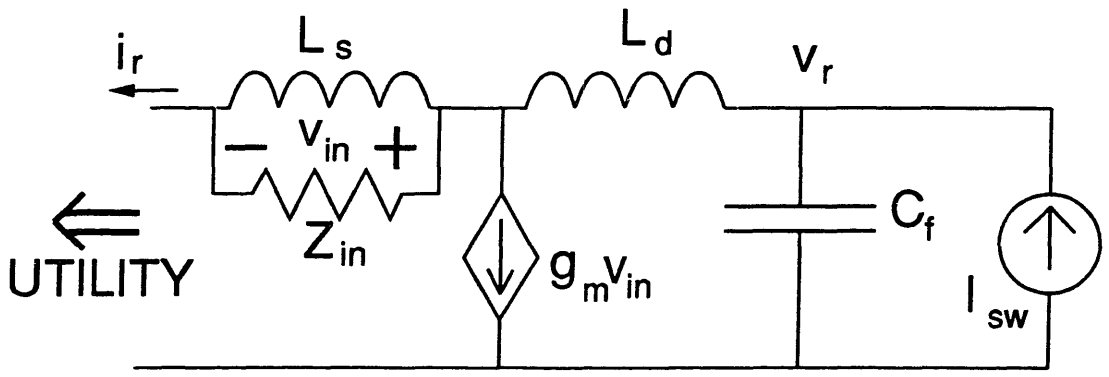

Figure 5-9: Basic topology of circuit built by Leif LaWhite

tested using a signal generator as the input source and a short circuit as the external line impedance. Oscilloscope measurement of the voltage across L_s with 1 volt peak-to-peak input signal imposed on the capacitor roughly confirmed the gain calculation.[2, p. 78] The circuit operated well with up to 2 volts peak-to-peak of capacitor ripple, requiring less than 7 mA of peak current from the output current drive. Note that the power dissipation of less than 0.4 W in this active circuit is substantially less than that dissipated in a 26 mH inductor conducting a few amperes.

In terms of feedback compensation, LaWhite's circuit was designed with a roll-off pole at 1 MHz, giving a high-frequency phase margin in excess of 65° at the loop transmission unity gain crossover frequency of 35 MHz. Due to parasitic zeros at higher frequencies, however, an additional pole was needed at 25 MHz to stabilize the circuit. [2, p. 77] The low-frequency compensation of the circuit was also somewhat lacking in robustness. Despite a very large gain margin in excess of 1000, the phase margin of the loop transmission was less than 5° at a unity-gain frequency of 25 kHz. [2, p. 93]

Clearly, this circuit is more complex than a second-order, or even a fourth-order LC filter and has many problems as well. Comparison with passive filters having the same attenuation is fundamental to determining the practicality of the active filter. To get the same attenuation with a second-order passive filter would require an LC product of 8000 μH - μF . If attained by the same L/C ratio as the active filter's 50 μH to 0.4 μF , this LC product would require as much as 20 times the inductance and 20 times the high-voltage capacitance of the active filter. This is, undoubtably, a substantial reduction in storage components.

Comparison to a fourth-order passive filter, however, does not show such a substantial reduction in energy storage components. While the 50 μH of inductance and 0.4 μF of capacitance in a fourth order filter, split evenly between stages, would give about 17 dB less attenuation at 1 MHz; because of the fourth-order nature of the filter, only 66% more total capacitance and 66% more total inductance would be necessary to match the 110 dB attenuation of the active filter at 1 MHz. Thus, the active circuit reduced the size of the energy storage components over the fourth-order passive filter by a bit less than a factor of two (40%). Although LaWhite recognized that the energy storage reduction compared to a fourth-order filter might not be considered a major improvement, he pointed out that the second-order dynamics of the active filter made compensation of the power converter's control circuit substantially easier than with a fourth-order filter and therefore made a good case for the active filter. [2, p. 83]

5.4 New Motivations

The results of the filter measurement study of chapter 3 illustrated some of the problems caused by the large components needed to provide sufficient attenuation at the fundamental frequency of the switching power supply. These components have large parasitics which degrade the performance of the filter at higher frequencies. Although the attenuation of LaWhite's active filter above 1 MHz was not documented, the high frequency compensation needed would make the effective inductance decrease with frequency by 20 dB per decade above 1 MHz. Thus, the effective impedance of the enhanced inductors, would have a flat frequency response between 1 MHz and the second pole of the amplifier. Nevertheless, an actual 26 mH inductor would, in general, have a capacitive impedance starting well below 1 MHz. While this comparison with the second-order passive equivalent exaggerates the point, it is clear that an additional advantage of reducing components, even if only by a factor of two, is the improved high frequency filter performance due to smaller component parasitics. Smaller components would have higher self-resonant frequencies and therefore larger bandwidths of ideal performance and, even above self-resonant frequencies, the parasitics would be smaller, making behavior somewhat closer to ideal. In the case of a common-mode inductor, lower leakage inductance could also reduce magnetic coupling problems which also deteriorate filter performance. Even the components which are not

directly enhanced may be reduced, as suggested above in Section 5.3.2, since an optimal design would probably maintain a similar ratio of inductance to capacitance.

The objective is then to use active circuitry to enhance smaller components at low frequencies and then roll off the gain as needed but take advantage of the better performance of these smaller components at higher frequencies. Since the EMI filters being considered in this study are for more conventional switching frequencies on the order of 50 to 100 kHz, it is hoped that larger gains may be obtained even with lower bandwidth amplifiers, so that storage components may be reduced by at least a factor of two or more. Since commercial EMI ripple specifications are flat above 500 kHz, as shown in Fig. 1-1, and switching frequency harmonics should drop off with frequency by at least about 20 dB per decade, depending on the shape of the waveform, even a flat frequency response of the filter above 500 kHz should be more than sufficient to meet the output ripple requirements. Note that parasitic effects in other filtering components, such as the rectifier capacitor which is typically considered a part of the power supply, should be taken into account when considering the high frequency filtering needs.

Filter topologies employing active circuitry need not be limited to second order filters, although it is likely that the optimal use of this technique may be in a second-order configuration like those considered so far. Another possible direction in taking advantage of active filtering may be to enhance more than one component. While the analysis and compensation of a filter with several actively-enhanced components may be quite complicated, the potential for energy storage reduction could be much greater, particularly with a fourth-order topology.

5.5 Challenges

While LaWhite's work was an excellent development and demonstration of the concept of active filtering, the filter was not tested in an actual power supply or connected to the utility. In fact many practical issues remain to be resolved. Among the fundamental challenges are robust compensation, variation of the external line impedance, power frequency rejection, and the application of active filtering to a three-ire power supply and utility system. Additional challenges include the power supply for the active circuit, and noise and transient susceptibility,

5.5.1 Compensation with Varying External Impedances

One of the greatest challenges of practical active filter development is that of compensating the associated feedback loop. The normal difficulties of robust compensation of a feedback system at a reasonable cost are exacerbated in the active filter by the variation and uncertainty of the external impedances. The previously built circuit, revised during the simulation phase to get a low-frequency phase margin of 5^o and after construction to eliminate high-frequency oscillations, was designed and tested with a shorted external power source impedance. Thus, even under the simplest of external impedance conditions, the robustness of this circuit was very questionable. It is quite likely that this circuit would have been unstable if tested with some non-zero line impedances.

To the extent that it may be predicted, all of the possible external impedances to which the active filter may be connected should be considered in developing and testing the active circuit's compensation. One design objective would, in fact, be to make the operation of the circuit insensitive to the external line impedance. In any case, resolution of this problem requires a study of the range of external impedances, including power line impedances and power converter output impedances, and the development of suitable line impedance models for design, simulation, and testing of active circuits.

5.5.2 Power-Frequency Rejection

Another fundamental practical issue is that of dealing with the large currents and voltages of the power circuit in which the active circuit is to be placed. In a sense, this is the function of the passive filter components – to separate the EMI ripple currents or voltages from those at the power frequency. The difficulty of this function is due to the large difference in magnitude between the two. To the extent that the EMI frequency and the power transmission frequency are separated, this filtering function is easier to accomplish, so that this issue is more of a challenge at the lower switching frequencies to be considered than it was in LaWhite's circuit.

There are two respects in which the power-frequency rejection issue needs to be considered. The current and voltage levels incidentally subjected to the drive and sense devices is one. These levels are purely functions of the power-frequency voltage and current, the input and output impedances of the active circuit, and the impedances of the passive filter-

ing components. For example, the circuit of Fig. 5-9 requires a capacitor in series with the current source drive, and if this capacitor is made too large in order to be a short-circuit at the filter's operating frequencies, it may pass too much current through the active device at the power frequency. These currents or voltages may affect the biasing levels of the devices and lead to non-linearities, reduced gain, or instability. The larger biasing currents required or the conducted power-frequency currents themselves may dictate the need for larger (and lower bandwidth) devices. An additional effect may be excessive power dissipation due to power-frequency currents in the devices.

The other respect in which the power-frequency rejection issue comes into play is that of the overall active circuit response to the large current through or voltage across the sensing circuit. If the attenuation of the amplifier is not small enough, and the power-frequency rejection of the sensing circuit is not sufficient, the output of the drive circuit may be large enough, depending also on its output impedance, to lead to any of the problems described above.

5.5.3 Three-Wire Application

The EMI filter applications considered herein are for systems with three-wires – hot, neutral, and ground. The EMI must be filtered between both of the current-carrying phases and ground; or, from the alternate perspective, both common-mode and differential-mode EMI need to be filtered. As discussed in Chapter 3, conventional EMI filter techniques have been developed to deal with and, in some cases, take advantage of the characteristics of a three wire power system and the applicable regulations. The practical active filter design needs to maneuver an active topology into one of these three wire filters or develop new techniques to actively filter both common-mode and differential-mode EMI. While complicating the problem, the three wire system may provide opportunities for increased improvement of an active approach over the passive equivalent.

5.5.4 Ancillary Issues

Other important issues include the power supply for the active circuitry and the protection of the circuit from external power line transients. While these issues are also important considerations in the practicality of an active EMI filter, their designs are not fundamentally tied in with the design of the active circuit itself and will not be considered in detail in this

study.

The power supply is related to the circuit mainly in the sense that the active circuit design dictates the type and amount of power required. Restrictions on this DC power supply are that it must float with the line and it obviously should not add more EMI to the line through any switching methods employed. More than one isolated power supply may be needed, if, for example, both the hot and neutral lines include separate active inductor circuits.

5.6 External Impedances

Two external impedances must be considered in designing the active filter, particularly in determining the compensation. The EMI source input of the filter connects to the power converter. While this impedance may vary for different power supplies, the designer presumably knows which types of power supplies the EMI filter will be used for. Having been discussed in Chapter 4, the issue of the power supply impedance will be covered only briefly at the end of this section in 5.6.3.

The other external impedance is that of the power source. For the purposes of ensuring sufficient attenuation to meet ripple requirements over the EMI frequency range, the LISN network described in Section 1.2.1 is the applicable impedance to consider. Nevertheless, the EMI filter must be designed to operate reasonably well with the full range of actual line impedances, as well as the LISN. This includes keeping the EMI levels reasonably low, not stressing active devices excessively, and not degrading the performance of the main power converter by, for example, oscillating between active circuit supply rails. These requirements mostly imply good biasing and feedback compensation insensitive to external impedances. Since the line impedance for the application considered here is the electric utility, an investigation into the full range of possible power line impedances is necessary. The minimal frequency range which should be investigated is from the smallest possible low-frequency loop-transmission unity gain cross-over frequency to the largest possible high frequency UGC. For completeness, the frequency range included was from the power-frequency of 60 Hz to the upper frequency of 30 MHz considered for conducted EMI. The power-line impedance study is broken up into high-impedance and low-impedance sections, where the breakpoint is 100 kHz, the approximate value of the switching frequency.

5.6.1 Consideration of LISN Impedance

The appearance of the LISN to the device under test was considered previously in terms of its impedance between 9 kHz and 30 MHz, which follows the specified simulated line impedances of 50 Ω || (50 μH + 5 Ω), with a ± 20% tolerance. The schematic of the particular LISN considered, a Polarad ESH2-Z5, was shown in Fig. 1-2. The magnitude of the impedance is shown again here along with the phase in Fig. 5-10. Note that the LISN

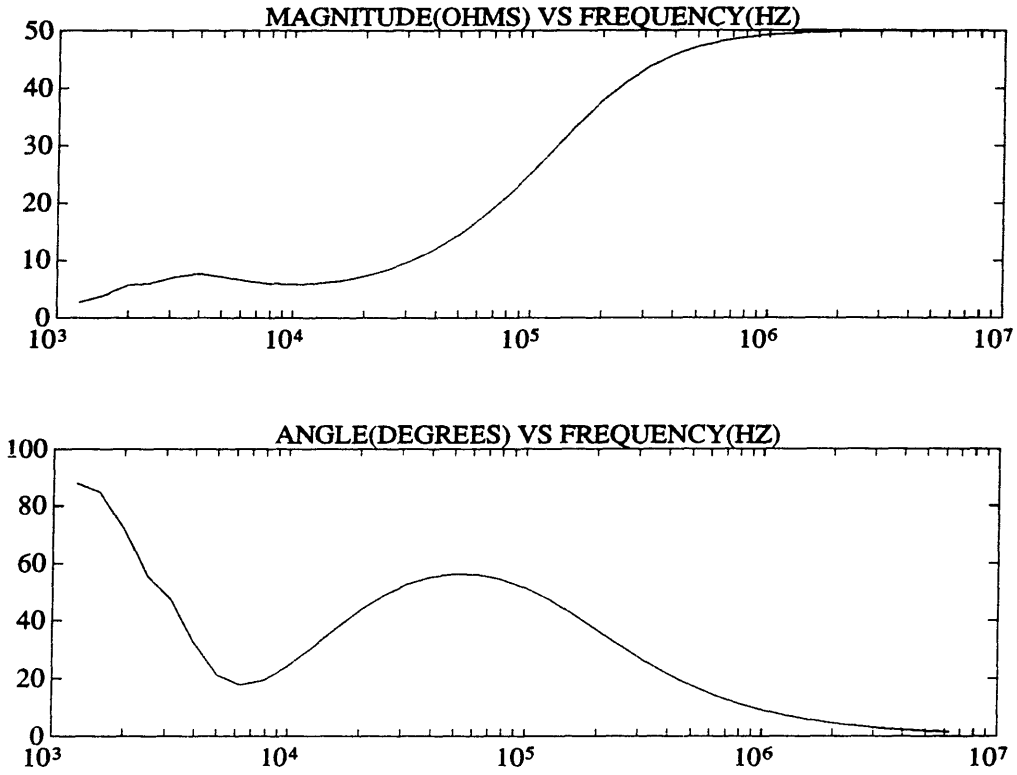

Figure 5-10: Impedance of LISN from d.u.t. with external line impedance shorted

changes from a purely resistive impedance of 50 Ω at very high frequencies to a mostly resistive impedance of 5 Ω at 10 kHz, passing through a partly inductive, partly resistive region at around 20 to 150 kHz. As the frequency drops below 9 kHz, the impedance becomes increasingly dependent on the series combination of the LISN filter inductance of 300 μH and the actual power line impedance. Thus if the line impedance is considered to be a short circuit, as for the plot of Fig. 5-10, the impedance near 1 kHz and lower is essentially inductive. However, to understand the realistic external impedance with the LISN at such low frequencies requires understanding of the utility impedance as well.

It is important also to note the difference in the common-mode versus differential-mode impedance during the LISN test. Since the LISN connects between each phase and ground, the common-mode network sees the parallel combination of two LISN's, each terminated with an external line impedance to ground. The differential-mode network sees these two LISN's in series and their external line terminations are in series separated by an external hot-to-neutral line impedance.

5.6.2 Power Line Impedance

While some articles were found which documented measurements of power line impedances above 10 kHz or 100 kHz, there was no hard data found on the impedance of the power line below 10 kHz. Information was pieced together, however, from the National Electrical Code Handbook [28] and conversations with experts from the Electric Power Research Institute and others referred to by them. In general, it was found from [19] that the impedance of the power line is dominated by the series combination of the resistance of the wiring and the impedance of a distribution transformer at low frequencies, but the inductance of these elements, particularly the wiring, becomes important around 1 to 10 kHz. Above 10 kHz the impedance is predominantly inductive until around 100 kHz to 1 MHz where the power line starts to look like a lossy transmission line.[19] The actual values of these impedances might vary over as much as two orders of magnitude. [20] The following sections will consider the available information and attempt to put some reasonable but conservative bounds on the range of possible line impedances.

Low Frequency Line Impedance

Since no power line measurement data below 10 kHz was found, information available was used to calculate impedances at 60Hz for utility connections in the United States. Information on distribution transformers was obtained from the EPRI [22]. These transformers may be sized for power levels between 5kVA and 100kVA. The typical values for the reactances and resistances of these two sizes of transformers leads to the following range for the complex impedance of the transformer at 60 Hz:

$$1.3m\Omega + j\omega(6\mu H) < Z < 60m\Omega + j\omega(120\mu H) \tag{5.5}$$

The 60 Hz wire impedance range was calculated based on National Electrical Code regulations and wiring data in [28]. The wiring between the distribution transformer and an electrical outlet consists of a feeder circuit between the transformer and a switch panel of fuses or circuit breakers; and a branch circuit, between the panel and the outlet, usually carrying only 15 to 20 A except for service to larger single loads. The minimum wire impedance would be nearly zero for loads that are close to the service equipment. The maximum impedance may be determined from regulations which limit the maximum voltage drop in the wiring to be 2% in the feeder and 3% in the branch circuit. [28, p. 82, art. 210-19]. Although, the feeder usually carries considerably more than 15 A, since the smallest distribution transformers (5 kVA) are rated for about 80 A, a worst-case analysis of the total maximum wire impedance would assume a 5% drop with a 15 A rating, which yields $(0.05)(120\ \mathrm{V})/(15\ \mathrm{A}) = 0.4\ \Omega$.

To determine the reactive and resistive parts of this impedance, the phase of the impedance of a pair of wires in a three wire electrical cable is considered. Based on 60 Hz wire resistance and inductance data in [28, p. 1101], this phase may vary from about 1^o for aluminum AWG # 12 wire in a PVC or aluminum conduit to about 69^o for uncoated copper 1000 kcmil wire in a steel conduit. For this case of 15 A in both feeder and branch circuits with maximal voltage drop through 1000 kcmil wire, the wire would have

$$(0.4\Omega)(sin69^o)/(2\pi \times 60Hz) \approx 1mH$$

of inductance and 0.023 Ω of resistance. This result is a very unlikely worst-case, since the 1000 kcmil wire, which has a diameter of 1.15 inches and a total impedance of only 0.049 Ω per 1000 feet, would not be used for a 15 A circuit unless needed to carry this small current over a distance of about 3000 feet. A more reasonable figure might be based on AWG # 1 wire, which would yield a maximum inductance of 360 μH , with a resistance of 270 mΩ. Combining this with the numbers for the transformer above yields the following rough range for the total complex external power line impedance Z_x at 60 Hz :

$$1.5m\Omega + j\omega(6\mu H) < Z_x < 350m\Omega + j\omega(500\mu H) \tag{5.6}$$

While the above information is certainly of interest, information on how this line impedance characteristic changes at higher frequencies is necessary for this work. Although

skin depth would have more of an effect on electrical distribution wiring and transformers than on the smaller inductors discussed in section 3.3.2, the resistance-increasing effect would be greatest for the thicker wires, which have a lower resistance per inductance anyway. Thus it is easy to imagine the inductance of the wiring becoming the dominant effect by 10 kHz, as is the case. [24, 19]

Most of the documented measurements of RF power line impedance include a frequency range down to 10 or 20 kHz. [21, 24, 25] Table 5.1 shows maximum, minimum, and mean inductances around this frequency based on data in these papers. [2] All but the measurements of [21] on the first line, are based on impedance magnitude measurements and the assumption that this impedance is inductive, which is supported by the shapes of the curves. Reference [21] measured real and imaginary parts of the impedance, finding a mean resistance of 0.6 Ω and a maximum of 1.6 Ω , two to three times smaller than the corresponding reactances at 10 kHz. This study also documented a few instances of capacitive impedance of about 0.25 Ω at 20 kHz, but capacitive power line impedances were not mentioned elsewhere. The data around 10~20 kHz, particularly for the U.S., suggests that either the 60 Hz line inductance analysis above was very conservative or that the inductance decreases substantially between 60 Hz and 10 kHz. The inductance measurements seem to be larger outside of the United States, possibly because the larger line voltages in foreign countries could allow for longer wiring, four times as long for the same power level and maximum percentage voltage drop.

High Frequency Line Impedance

[2] U.K. listings from [24] are for ±1 standard deviation from the mean value.

source	country	samples	frequency	max. L	mean L	min. L
[21]	U.S.	36	20 kHz	27 μH	13 μH	0.5 μH
[24]	U.K.	$\sim$ 100	20 kHz	64 μH	40 μH	24 μH
[24]	USSR	~100	10 kHz	-	160 μH	-
[24]	Holland	~100	10 kHz	-	96 μH	-
[25]	Japan	$\geq$ 4	10 kHz	64 μH	-	32 μH

Table 5.1: 10-20 kHz inductance statistics from documented line impedance measurements

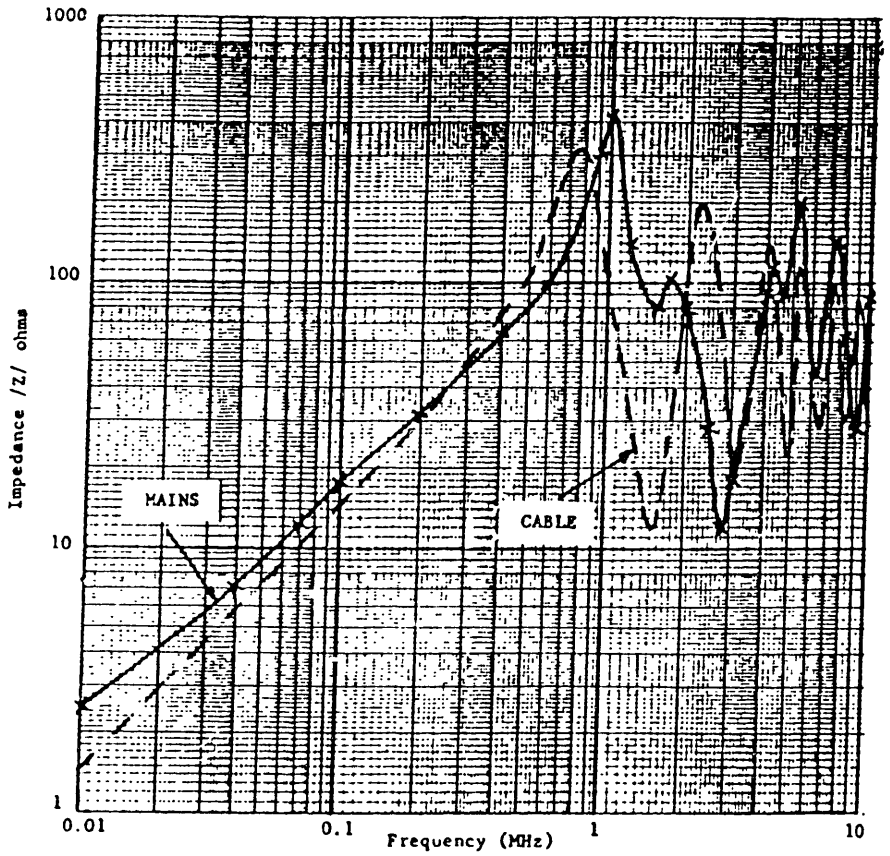

Figure 5-11: Measurement of line impedance mains

Measurements documented in several papers confirm that the line impedance increases inductively between 10 kHz and a few hundred kHz, and behaves like a lossy transmission line at higher frequencies [24, 21, 23]. Since the complex impedance of a transmission line varies periodically with the ratio of the length of the line to the wavelength of the excitation, it also varies periodically with frequency for a fixed length line. For a lossless line, this impedance would vary from an open circuit through all possible capacitances to a short circuit, then through all possible inductances up to an open circuit. [27] Fortunately, the power line is quite lossy, so that this variation is bounded by a resistive maximum impedance and a resistive minimum impedance, with partially capacitive and inductive impedances having magnitudes in between. The mean of the maximum and minimum impedances should equal the characteristic impedance of the transmission line, $Z_o = \sqrt{L/C}$, where L and C are the inductance and capacitance per unit length of the transmission line.[3] Figure

[3]This analysis is based on observation of a Smith Chart and the fact that increasing frequency rotates the impedance about the origin with a fixed radius for a fixed line length and frequency-independent transmission-line parameters.

5-11 taken from [24] shows a measurement of the impedance of a typical utility power line connection between 10 kHz and 10 MHz, comparing the result with the measurement of a 50 meter cable short-circuited at the end. Although the cable behaves more like the lossy transmission line described above with the lossiness increasing with frequency, the general behavior of the mains is quite similar. Appendix A shows reprints of several other plots of measurements of RF power line impedances.

Since the power line impedance at these transmission line frequencies, as documented in the literature, does not seem to have frequency-independent transmission-line parameters but does bounce up and down with frequency like a lossy line, a useful way to describe the variation of these impedances may be in terms of maximum and minimum values over certain frequency ranges. Table 5.2 shows the maximum and minimum values for various frequency ranges, as given by the plotted data in the various papers referred to. [4] Note that where specified, all sources indicated the same results for hot-to-ground or neutral-to-ground impedance measurements as for hot-to-neutral measurements.

Modeling of Line Impedance

Line impedance models are considered here for the purposes of analysis and simulation of active filter circuits. For frequencies below 100 kHz, it should be sufficient to model the power line impedance Z_x as the series combination of some resistance and inductance:

$$Z_x = R_x + j\omega L_x \tag{5.7}$$

[4] A few notes about the table here:

- U.K. listings from [24] are for ± 1 standard deviation from the mean value.
- Holland listings from [24] are maximum and minimum of mean impedance.
- U.S. listings from [23] were made at nine different outlets in the same building.

source	country	samples	0.1 ~ 1 MHz	1 ~ 10 MHz	10 ~ 30 MHz
[21]	U.S.	36	2 ~ 450 Ω	5 ~ 480 Ω	20 ~ 400 Ω
[24]	U.K.	~100	7 ~ 105 Ω	14 ~ 160 Ω	-
[24]	Holland	~100	-	23 ~ 70 Ω	-
[25]	Japan	≥ 4	2 ~ 100 Ω	1 ~ 500 Ω	-
[23]	U.S.	6	7 ~ 140 Ω	4 ~ 1200 Ω	1 ~ 1600 Ω

Table 5.2: High frequency maximum and minimum line impedance measurements

where R_x and L_x represent worst-case values based on the data here and the loop transmission of the particular circuit under consideration. Normally, the worst-case would be some combination of the high or low extremes of these parameters. If not, or if this is not self evident, it may be useful to run a computer program through a three-dimensional matrix of possible values of R_x, L_x, and frequency ω and calculate the phase of the loop transmission to determine the worst-case values at various frequencies over a range of concern.

To ease the use of this model for considering the LISN along with other line impedances, Fig. 5-12 shows the impedance of the LISN in terms of its resistive and inductive components throughout the frequency range of interest. Note that the impedance of the LISN below a few kiloHertz approaches that of the 300 μH inductor in series with the actual external power line impedance, which is substantially resistive at these lower frequencies.

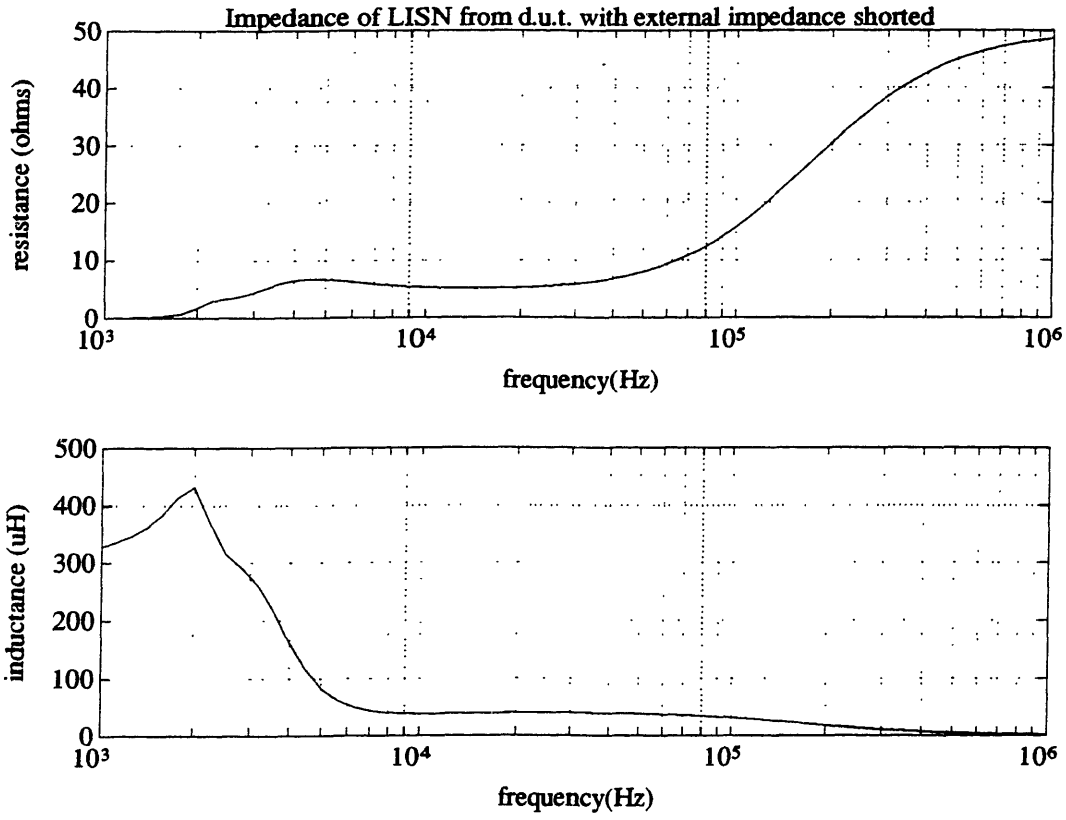

Figure 5-12: Line impedance model parameters, R_x and L_x , for LISN (with external line impedance shorted)

At higher frequencies, a similar model may be used except that the reactance may be positive or negative:

$$Z_x = R_x \pm jX_x \tag{5.8}$$

Here, R_x varies between some minimum and maximum possible impedance magnitude, as suggested by Table 5.2, and X_x varies over a somewhat less extreme version of this range. Again, the worst case values of these parameters would be considered. For the purpose of SPICE simulations, the model shown in Fig. 5-13 is considered. Here, Z_o, which represents

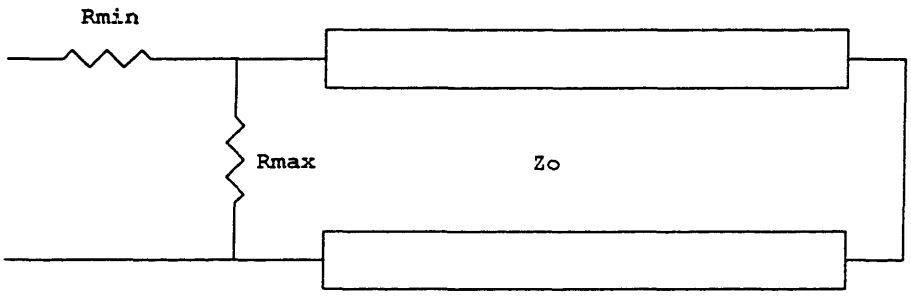

Figure 5-13: High frequency line impedance model for spice simulations

the characteristic impedance of the lossless transmission line, should be the geometric mean of the series and shunt resistors R_{min} and R_{max}. This model proves useful for transmission-line frequencies, as SPICE allows the inclusion of a lossless transmission line as a circuit element. By making the transmission line very long, such that the impedance varies very rapidly as a function of frequency above 100 kHz, and including a large number of data points, the range of impedance values between R_{min} and R_{max}, may be effectively tested over a wide frequency range.

Remaining Questions

Certain situations may not be accounted for in this study. These include the use of isolation transformers or uninterruptible power supplies, which might result in line impedances out of the range suggested here. In addition, the likelihood of there being a capacitive line impedance at low frequencies is suggested in a table in [21], which shows some positions of a table filled in for negative imaginary impedances at 20 kHz and 40 kHz. Other information, however, suggests that inductance [24, 19] dominates line impedances up until transmission-line frequencies. Further study of this issue is required to determine if and to at what

frequencies and levels capacitive power line impedances need to be considered.

5.6.3 Impedance of Power Supply

The output impedance of the power converter may also affect the loop transmission of an active circuit. The common-mode and differential-mode Thevenin impedances of the power supply were considered in Section 4.1. For the purposes of the active filter analysis herein, the differential-mode impedance of the power supply will be modeled with the rectifier capacitor but a parallel resistance will also be considered, including the smallest possible value for the case of full load. The common-mode output impedance of the power supply is not clear or easily determined. The need to know this impedance in order to assess the stability of active EMI filter circuits certainly provides strong motivation for the Thevenin characterization of EMI sources discussed in Chapter 4. The value of 50 pF, a typical figure for the aggregate parasitic capacitance to ground, will be used for the common-mode impedance, but some range around this should be considered as well.

5.7 Conclusion: Requirements and Expectations

The conclusion of this chapter should set the stage for an analysis of active filters and the determination of their practicality for a particular application or in general. The basic requirements of an active filter to be worthy of consideration are therefore set forth and the implications of these are considered. Also, a candidate passive filter for active replacement is presented.

5.7.1 Requirements of Active Filter

The material presented in this chapter points to several requirements or expectations of the practical active EMI filter. The compensation of the active filter should yield stability with all possible external impedances, including variations of load conditions. The active circuit should significantly reduce the total size of the energy storage components compared to its passive equivalent. This reduction must be significant in order to offset the extra size, cost, and complexity of the active devices and their compensation, biasing, and power supply. A minimal goal to start with is to reduce the total inductance and total capacitance by a factor of two each, or by some unequal but equivalent tradeoff of this. Despite the

smaller components, the attenuation of the active filter must be greater than or equal to that of the passive equivalent at the switching frequency. The attenuation should increase by at least 20 dB per decade up to 500 kHz and then be maintained at least to about 10 MHz, particularly because the generally large rectifier capacitor cannot be relied on to remain capacitive up to the MHz range. In addition, the active filter should have low power dissipation so that the required devices are small and its effect is to increase rather than decrease the overall efficiency of the power conversion. In short, the active enhancement must improve the performance per cost and size of the EMI filter to be worth developing.

5.7.2 Candidate Filter for Active Replacement

The schematic for an actual passive filter to be considered for active replacement is shown in Fig. 5-14 This filter is similar to that studied in Chapter 3 and shown in Fig. 3-1, with

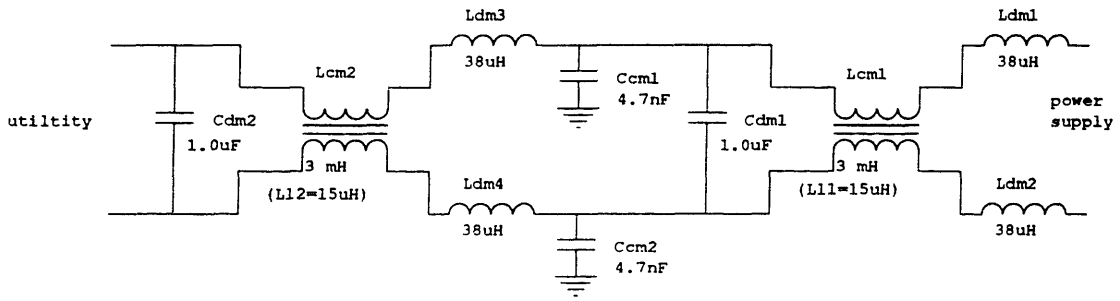

Figure 5-14: Candidate passive filter for active replacement

differences only in the use of the inductors. Based on the measurement and analysis of EMI filters throughout the previous chapters, this filter is a better representation of a good passive filter and therefore makes for a more fair comparison between active and passive filters. Note that the inductance and capacitance is split evenly between each stage for optimal attenuation per total energy storage. The common-mode chokes L_{c1} and L_{c2} are similar to the alternate choke described in section 3.3.2, which was was found to have 3 mH of common-mode inductance and smaller parasitics, 15 μH of leakage inductance and 15 pF of winding capacitance. While this lower leakage inductance should give the filter better high-frequency performance, it does result in a lower contribution to the differential-mode filtering. Thus, while the previously studied filter got by at the switching frequency with

just one pair of differential-mode inductors using a leakage inductance alone in one stage, this filter has a pair of differential-mode inductors in each stage. Otherwise, the components of this filter are the same as those measured in Chapter 3. This filter is also designed for use in a 75 kHz switching power supply with a 4.4 μF rectifier capacitor input.

The attenuations of the common-mode and differential-mode networks were found using SPICE simulations which included their respective LISN test impedances. Using a total inductance of 200 μH and a total capacitance of 2 μF, the differential-mode filter has an attenuation of -52 dB at 75 kHz. Note that the discrepancy of about about 2 dB from the $\omega^4 L^2 C^2$ product is due to the proximity of the switching frequency to the filter resonances. The attenuation of the third-order common-mode network, which employs 6 mH of common-mode inductance and 9.4 nF of capacitance, was similarly found by SPICE to be -79 dB at the switching frequency. These calculations were performed assuming a (zero impedance) voltage source driving the EMI filter. This is certainly a reasonable assumption for the differential-mode filter, which is driven by the voltage on the large 4.4 μF rectifier capacitor, which is indeed a low impedance at and above the switching frequency. For the common-mode filter, however, this may be a very poor assumption, as suggested by the discussion of common-mode power supply impedance in Sections 4.1 5.6.3, which expressed uncertainty about the common-mode power supply impedance and also gave the value of 50 pF as a rough order-of-magnitude figure. This capacitance would actually be a large source impedance relative to the filter's input impedance, not even resonating with the common-mode inductor until about 400 kHz. Thus, it is not clear how much this inductor contributes to the common-mode attenuation and therefore what the actual attenuation of this mode of the filter is.

The ripple current and voltage levels on the load side of this passive filter need to be considered in order to determine the specific requirements of the active filter. The hot-to-ground or neutral-to-ground ripple specification shown in Fig. 1-1 is about -57.5 dBV at 75 kHz. This is the strictest specification, class B. The class A specifications are 12 dB higher in this region. If the filter just meets this specification of -47.5 dBV and the output ripple voltage is predominantly differential-mode, the maximum hot-to-neutral voltage across the rectifier-capacitor at the fundamental frequency is about 4.5 dBV, or 1.7 V. If the output ripple is predominantly common-mode, then the maximum fundamental component of the common-mode voltage across the 'Y' capacitors is, based on a 75 kHz common-mode LISN

impedance of 20 Ω , about 295 mV. The common-mode voltage at the load side of the filter which would give this output ripple depends on the uncertain CM impedance of the power supply.

5.7.3 Expectations of Active Filter

Certain characteristics may be expected of an active replacement filter that meets the requirements described in Section 5.7.1. To reduce inductors and capacitors without excessive dissipation, the actively enhanced component needs to be near the external power line side of the filter, as mentioned earlier. Since the components that are further in the filter towards the power supply cannot be substantially reduced without bringing resonances too close to the switching frequency, a reduction of filter order from equivalent passive filters is also expected, at least for the higher order differential-mode subcircuit. This reduction of filter order must be made up for with high gain, so that gains on the order of a hundred would be needed and several hundred for large reductions of filter order, as with LaWhite's circuit.

Another goal in designing an active filter is to increase the output impedance of the filter to avoid the magnetic coupling problems described in Chapter 3. This effectively prohibits termination of the new filter design with a capacitor, and therefore makes capacitor-enhancement circuits impractical for this application, since an active filter needs to do the final small-signal-level filtering in order to be of practical use. Because the basic capacitor enhancement topologies are duals of the inductor enhancement topologies, much of the inductor enhancement analysis in the following chapter may be applied to capacitor enhancement to the extent that the external power source and load impedances are duals of those considered herein.

Chapter 6

Practical Active Filter Circuits

Based on the principles and objectives of active filtering discussed in the previous chapter, this chapter provides an analysis of the basic inductor enhancement topologies introduced, with special attention paid to the effects of the external source impedance which may vary as described in Section 5.6.2. The general approach for the analysis of each topology is to first consider the gain of the topology, demonstrating whether and under what conditions the circuit can yield practical amounts of gain. Given these conditions, the loop transmission is found and effects of the possible external impedances are considered. The practical limits on the gain of the active circuit are ultimately considered in order to assess the viability of active filtering. Initially, the analysis is applied to the active replacement of the passive canidate filter presented in the previous chapter; later, however, filters for converters with higher switching frequencies are considered as well. Where applicable, results from Leif LaWhite in [2] will be cited without derivation.

6.1 Standard Drive Inductor Enhancement

6.1.1 Gain

The basic standard-drive inductor enhancement current filter circuit of Fig. 5-5 is considered first. While the gain A and the impedances Z_{in} and Z_{out} may be functions of frequency, they are initially assumed to be constants. The gain of this circuit is relatively easy to derive, since the active circuitry and the enhanced inductor are contained within a two-terminal element, as shown in Fig. 6-1, An intuitive, superposition type of approach to

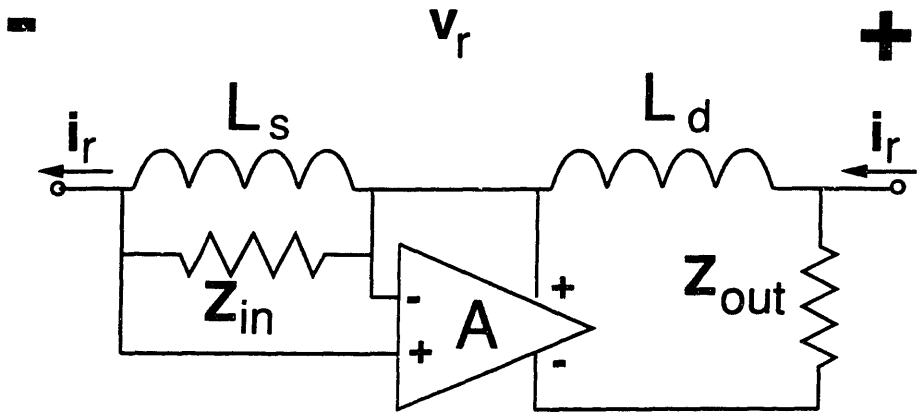

Figure 6-1: Isolated standard-drive enhanced inductor

the calculation of the effective impedance yields the following equation:

$$Z_{eff} = \frac{v_r}{i_r} = sL_s \parallel Z_{in} + sL_d \parallel Z_{out} + A(sL_s \parallel Z_{in})(\frac{sL_d}{sL_d + Z_{out}}) \tag{6.1}$$

By making the following reasonable assumption about the amplifier's characteristics:

$$(A+1)Z_{in} \gg Z_{out} \tag{6.2}$$

(6.1) may be rewritten in the following general form, similar to that derived in [2, p. 15]:

$$Z_{eff} = \frac{s(L_s + L_d)(1 + s/\omega_z)}{(1 + s/\omega_s)(1 + s/\omega_d)} \tag{6.3}$$

where $\omega_s = \frac{Z_{in}}{L_s}$ and $\omega_d = \frac{Z_{out}}{L_d}$ are the sense and drive poles referred to in Chapter 5 and ω_z is a zero frequency which may be simplified to $\frac{Z_{out}}{(A+1)L_p}$, where L_p is the parallel combination of the two inductors. Also, by this assumption the zero, ω_z, is much lower than either of the two poles. Note that this zero between the total parallel driven inductance and the amplifier's apparent output impedance (i.e., its actual output impedance reduced by its gain) is essentially the frequency at which the amplifier begins to have a noticeable effect on the circuit.

From (6.3) and (5.2), the gain G of the standard-drive inductor enhancement follows:

$$G = \frac{(1 + s/\omega_z)}{(1 + s/\omega_s)(1 + s/\omega_d)} \tag{6.4}$$

or, rewritten to emphasize the high frequency result,

$$G \approx (A+1)(\frac{Z_{in}}{L_s + L_d})(\frac{s+\omega_z}{(s+\omega_s)(s+\omega_d)}) \tag{6.5}$$

Since both poles are above the zero of this expression the peak gain will occur between the two poles. In addition, an intuitive approach suggests that this peak gain is maximized by designing the sense pole to be much larger than the drive pole:

$$\frac{Z_{in}}{L_s} \gg \frac{Z_{out}}{L_d} \tag{6.6}$$

so that the amplifier is more fully utilizing the sense inductor at the input and fully driving L_d at its output. This result is also proven in [2, p. 16].

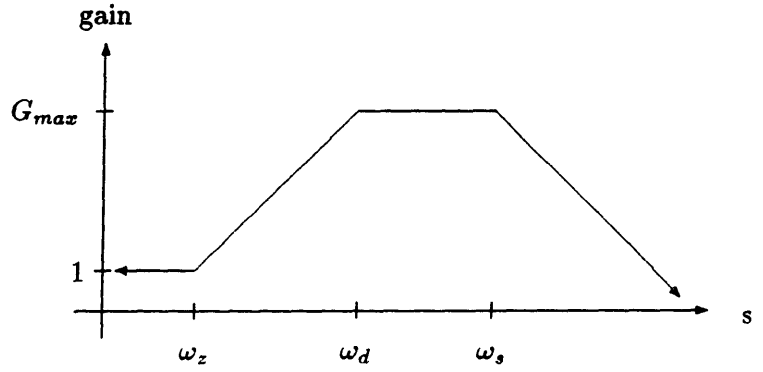

Figure 6-2: Bode plot of gain for standard-drive inductor-enhancing circuit

The assumption of (6.6) results in the bode plot of the gain shown in Fig. 6-2. Thus, the maximal gain of

$$G_{max} \approx (A+1)\frac{L_s}{L_s + L_d} \tag{6.7}$$

is attained over the range $\omega_d < \omega < \omega_s$. Figure (6-3) shows a bode plot for the effective impedance, indicating expressions for the impedance over each region. Below the amplifier output drive zero, ω_z, the effective impedance is just that of the two inductors in series. Above the drive pole, the active circuit essentially amplifies the sense impedance by the amplifier gain A; thus, between here and the sense pole, the impedance amplified is the sense inductor. Since the effective impedance above the drive pole is independent of L_d, this inductor may be very small as far as the circuit gain is concerned. Note that while the ulti-

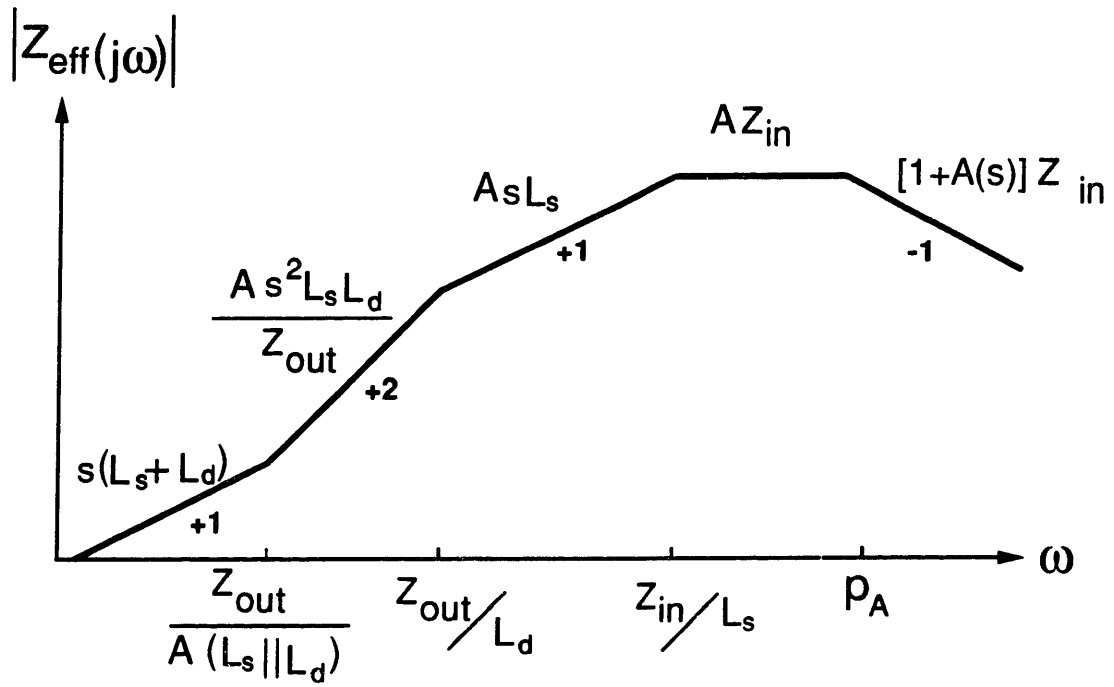

Figure 6-3: Bode plot for effective impedance of standard-drive enhanced inductor

mate attenuation of the inductor-enhanced filter depends on the external impedances, the gain of the standard-drive enhancement itself is independent of these impedances, assuming of course that the amplifier remains in stable, linear, operation.

6.1.2 Basic Loop Transmission Compensation

General LT Calculation

Having established that a standard-drive inductor enhancement may yield a gain very close to the amplifier gain A used in the circuit, consideration of the loop transmission of the circuit is in order. Initially, everything external to the enhanced inductor of Fig. 6-1 is grouped into one external impedance, Z_x'. From Fig. 5-5, this external impedance includes the power line impedance, Z_x in series with the parallel combination of the filter capacitor C_f and the power supply or any additional filter components further in. Breaking the feedback loop of the circuit at the input of the amplifier results in the loop transmission circuit of Fig. 6-4. The transfer function of this network gives a general expression for the

loop transmission:

$$LT = \frac{As^2 L_s L_d Z_{in}}{s^2 L_s L_d (Z_{in} + Z_{out} + Z'_x) + s[(L_s + L_d) Z_{in} Z_{out} + (L_d Z_{in} + L_s Z_{out}) Z'_x] + Z'_x Z_{in} Z_{out}} \tag{6.8}$$

The assumption of (6.6) and and also that L_d is no larger than L_s, as justified above for large gain, allows elimination of two terms of the denominator, leaving

$$LT(s) = \frac{As^2 L_s L_d Z_{in}}{s^2 L_s L_d (Z_{in} + Z'_x) + s[(L_s + L_d) Z_{in} Z_{out} + L_d Z_{in} Z'_x] + Z'_x Z_{in} Z_{out}} \tag{6.9}$$

Not much more can be done with this expression without making further approximations and substituting some parameters for Z'_x. The low-frequency and high-frequency loop transmissions are therefore considered separately so that the appropriate external impedance models can be used and some reasonable approximations made.

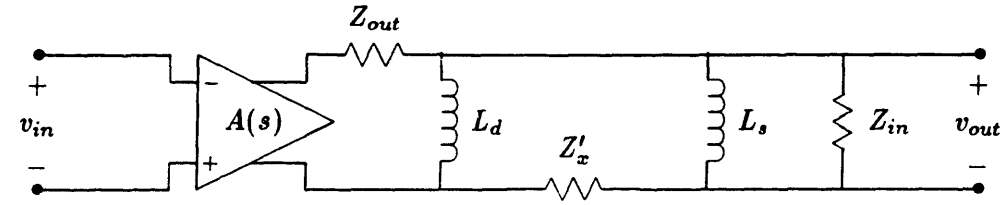

Figure 6-4: LT circuit for standard drive inductor enhancement circuit

High Frequencies

LT Approximation The high frequency approximation of the loop transmission is considered first. since it turns out to be the simplest. Assuming the frequency is larger than the drive pole:

$$\omega \gg \frac{Z_{out}}{L_d} \tag{6.10}$$

and that the external power line impedance Z_x is much larger than the impedance of the power supply (which is dominated by the filter capacitor), so that $Z'_x \approx Z_x$, (6.9) may be simplified to

$$LT(s) = A(s) \frac{sL_s Z_{in}}{sL_s(Z_{in} + Z_x) + Z_{in} Z_x} \tag{6.11}$$

where the frequency dependence of A is explicitly recognized for high frequencies.

Note that the second term in the product of (6.11) is the feedback F(s) and may be rewritten as

$$F(s) = \frac{Z_{sense}}{Z_{sense} + Z_x} \tag{6.12}$$

where

$$Z_{sense} \doteq sL_s \parallel Z_{in} \tag{6.13}$$

Z_{sense} is simply the impedance of the inductor below the sense pole; at higher frequencies, however, it becomes resistive or capacitive depending on the input impedance of the amplifier. Since the external power line impedance Z_x may range over a wide region due to its transmission-line behavior, assuming sufficient damping of resonances between Z_x and Z_{sense}, F(s) will range from very small to near unity throughout the high-frequency range. Therefore, the amplifier gain A(s) needs to be rolled-off below unity at a frequency before parasitics make the circuit too unpredictable and potentially unstable. Particularly since F(s) may bounce down to small values for large Z_x, (unless Z_{sense} is maintained very large), this roll-off must maintain substantial phase margin, $\phi_m = 180^o - \mid \angle LT \mid$ as long as A(s) is above unity.

Compensation Considerations Two approaches to the high frequency compensation are considered here. As suggested above, if $\mid Z_{sense} \mid$ is kept sufficiently larger than $\mid Z_x \mid$, then $F(s) \approx 1$ and the high frequency compensation is reduced to an amplifier design problem. For the other case, where the sense impedance cannot be kept much larger than Z_x due to parasitic effects or design requirements for gain or low frequency compensation, the effect of the external impedance must be considered.

Based on Section 5.6.2, note that the phase of the denominator of (6.12) may vary between $+90^o$ and -90^o, the extremes being where the line impedance is undamped and much larger than or of the same type as the sense impedance. For the worst case of an inductive denominator, then,

$$\phi_m = 90^o + \angle Z_{sense} + \angle A(s) \tag{6.14}$$

Thus, the more positive the phase of the sense impedance, the more allowance there is for gain roll-off with reasonable phase margin. If Z_{sense} must be small, then it is best kept

inductive so that the gain may be rolled-off with as much as $-\frac{3}{2}$ slope while still maintaining a phase margin of at least 45°. A capacitive Z_{sense} that is relatively small, on the other hand, would give poor results, even a flat A(s) would leave no phase margin and could result in oscillation if Z_x is large and inductive. A small resistive Z_{sense}, it follows, would allow for some gain roll-off of a slope of $-\frac{1}{2}$.

Note that the line impedance will have some reasonable amount of damping, so that the bounds of its phase would not actually be so close to ±90°. However, this conservative estimate may be offset by core losses of the sense inductor which reduce the phase of its impedance. In fact, the presence of both of these damping effects is very important to the stability of the system at very high frequencies; otherwise, the denominator of F(s) could blow up due to a resonance between Z_x and Z_{sense}, which, if undamped and above the UGC, could be accompanied by a very negative phase and lead to instability. Thus, the requirement for large amplifier gain with good high frequency compensation is that the sense impedance be designed to be much larger than the external impedance or to be inductive with damping ensured near and above the UGC frequency. The ultimate high-frequency compensation limit on the size of the gain then becomes the frequency response of the amplifier itself which is limited by the parasitic effects of the devices of which it is composed. Provided that EMI and power-frequency current levels in the amplifier are kept low and the sense impedance is carefully chosen, the bandwidth of the amplifier may be as large as that of LaWhite's, which was 35MHz, allowing roll-off of gains of several hundred from frequencies of a few hundred kiloHertz, assuming a $+\frac{3}{2}$ roll-off for at least some of this region.

Low Frequencies

While the high-frequency compensation essentially depends on the design of the amplifier, for the lower switching frequencies being considered here, the maximum gain that can be achieved in a robust circuit is most likely limited by the low frequency compensation.

LT Approximation For frequencies well below the sense pole:

$$\omega \ll \frac{Z_{in}}{L_s} \tag{6.15}$$

the amplifier's input impedance, Z_{in} may be neglected. In addition, given the result in (6.7) and the desire to maximize gain, the following approximation seems reasonable:

$$L_s \gg L_d \tag{6.16}$$

Equations (6.15) and (6.16) result in the following simplified loop transmission expression:

$$LT(s) = \frac{As^2 L_s L_d}{(sL_d + Z_{out})(sL_s + Z'_x)} \tag{6.17}$$

In addition, using the low frequency power line impedance model of Chapter 5 and assuming the power supply impedance is dominated by the capacitor C_f gives

$$Z'_x = sL_x + R_x + \frac{1}{sC_f} \tag{6.18}$$

which results in the following LT expression with the denominator factored into a first order pole and a double resonant pole:

$$LT(s) = A(\frac{L_s}{L_s + L_x})\frac{s^3}{(s + \omega_d)(s^2 + 2\alpha s + \omega_o^2)} \tag{6.19}$$

where

$$\omega_o = [(L_x + L_s)C_f]^{-\frac{1}{2}}$$

$$\alpha = \frac{R_x}{2(L_s + L_x)}$$

$$\omega_d = \frac{Z_{out}}{L_d}$$

The low frequency loop transmission thus depends on the order of the two pole frequencies, ω_d and ω_o, as well as the damping of the resonance and magnitude of the external inductance relative to the sense inductance. Figures 6-5 and 6-6 show bode plots for the two possible arrangements of these frequencies, assuming that the amplifier gain A remains constant. In both cases, the damping of the resonance would play an important role in the actual shapes of the frequency responses.

LT Analysis The case where the drive pole is below the LC resonance is considered in Fig. 6-5. For a sizable amplifier gain, the unity-gain crossover frequency of the loop transmission

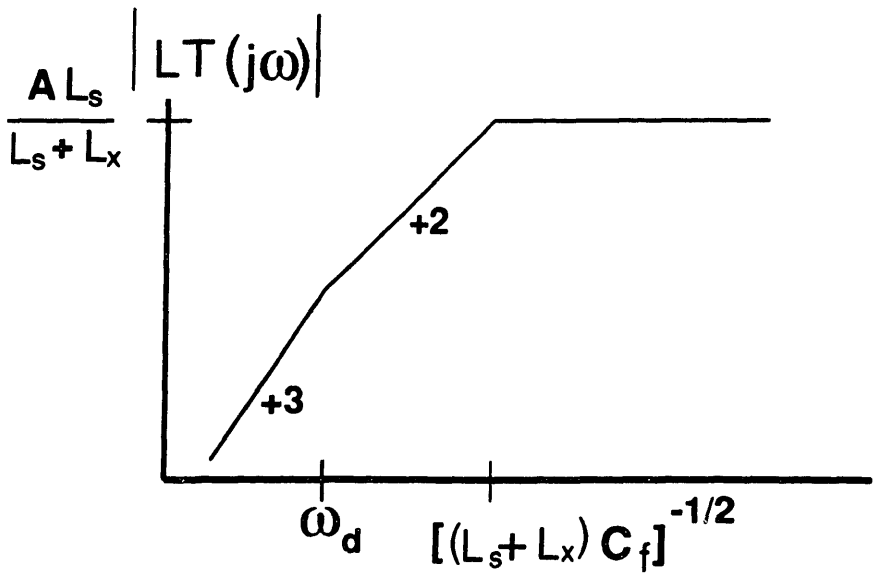

Figure 6-5: Low frequency loop transmission for drive pole below resonance in standard-drive inductor enhancement circuit

would be well below the resonant pole frequency and therefore in the +2 or +3 sloped region of the plot. Two conditions in which this might not be so are those of very large external inductance or very large external resistance. To the extent that L_x is large compared to L_s, the loop transmission curve is further lowered below A, but for this factor to significantly reduce the loop transmission, the effective inductance, AL_s, must be on the order of L_x in which case it is not doing much for the attenuation of EMI. If R_x is large enough to make the system overdamped, the resonance shown in the curve will be eliminated, leaving three single poles and a region of +1 slope in which the loop transmission may cross unity with reasonable phase margin. For the system to be significantly overdamped, however, the damping ratio ,ζ, must be much larger than one. For the second-order denominator polynomial of (6.19), the damping ratio is given by

$$\zeta = \frac{\alpha}{\omega_o} = \frac{R_x}{2\sqrt{(L_s + L_x)/C_f}} \tag{6.20}$$

Based on the line impedance information of section 5.6.2, the resistance of the power line even up to a few tens of kHz is unlikely to be more than a few ohms. For a storage-efficient filter design, however, the ratio $\sqrt{(L_s + L_x)/C_f}$ is on the order of the impedance V/I of the power supply, which is at least a few ohms for the broad range of power supply

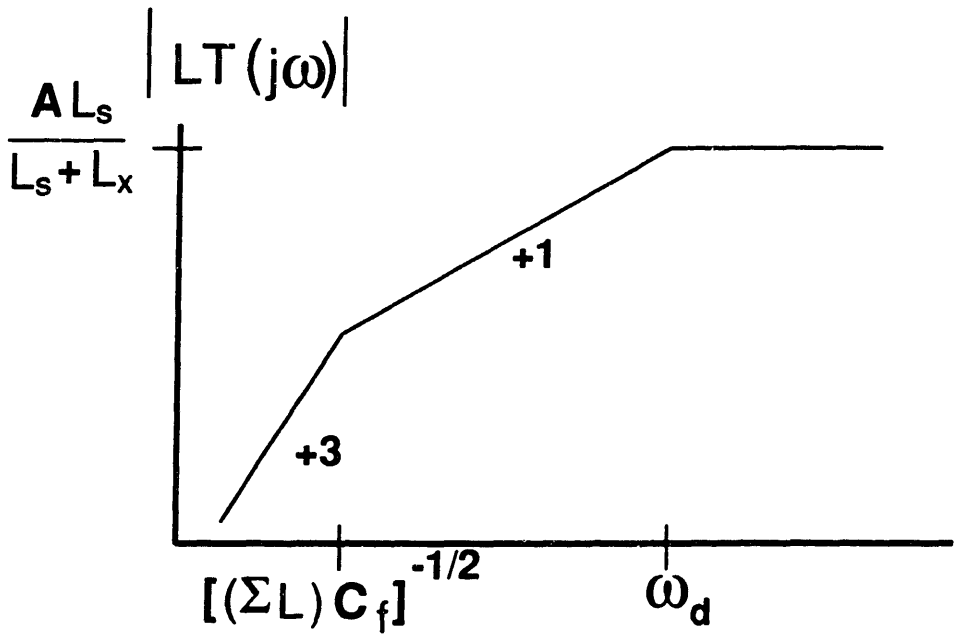

Figure 6-6: Low frequency loop transmission for drive pole above resonance in standard-drive inductor enhancement circuit

types considered here, so it is unlikely that the loop transmission resonance would even be critically damped ($\zeta = 1$). In any case, while a large external line impedance might improve the relative stability of the active circuit, it may not be relied on for compensation, so that the case considered in Fig. 6-5 is not an acceptable design.

The other case, shown in Fig. 6-6, is that of the drive pole being greater than the resonant frequency. Here, there is a potentially wide frequency band of $+1$ slope between the switching frequency and the resonant frequency, in which the loop transmission may cross unity with good phase margin. Since the aid of an external inductance cannot be relied upon, the width of this stable UGC band, which determines how large A can be, depends on the size of the product $L_s C_f$, as well as the damping ratio of the resonance. The advantage of the active filter over the passive filter, however, would be a substantially smaller total LC product. In fact, as the LC product becomes larger, a higher order passive filter becomes more advantageous relative to the active alternative, since the ωL's and ωC's are raised to larger powers in the higher order passive case in the calculation of the attenuation.

6.1.3 Need for Negative Phase Compensation

To illustrate the problem, a fourth order passive filter having inductance and capacitance split evenly between stages is compared with a second-order standard-drive inductor-enhanced filter with the above approximations so that the gain is that of (6.7) and the loop transmission is that shown in Fig. 6-6. First we define a measure of filter size, N, in terms of total capacitance C, total inductance L, and switching frequency ω_l:

$$N = \omega_l^2 LC \tag{6.21}$$

and let N_p represent the size of the passive filter and N_a represent the size of the active filter's energy storage components. Note that $N_a^{1/2}$ is also the width of the stable UGC band of the active filter, so that the the maximal gain of the active filter for zero damping is

$$A = \omega_l/\omega_o = \omega_l\sqrt{(LC)} = N_a^{1/2} \tag{6.22}$$

Relating a desired filter attenuation T to N_a then gives

$$T = (A\omega_l L)\omega_l C = N_a^{\frac{3}{2}} \tag{6.23}$$

For the fourth-order passive filter, this relationship is

$$T = \omega_l^4(\frac{L}{2})^2(\frac{C}{2})^2 = \frac{1}{16}N_p^2 \tag{6.24}$$

To compare the two types of filters for the same desired attenuation, the results of (6.23) and (6.24) are equated to give

$$N_a = (\frac{1}{4}N_p)^{\frac{4}{3}} \tag{6.25}$$

Defining β as the factor of reduction of total inductance and total capacitance achieved by the active filter over the passive equivalent (i.e., same attenuation T and switching frequency ω_l) gives

$$N_a = \frac{1}{\beta^2}N_p \tag{6.26}$$

Combining (6.25), (6.26), and (6.23) yields the maximum attenuation for an active filter with a factor of β reduction in energy storage components:

$$T = (\frac{2}{\beta})^{12} \tag{6.27}$$

While a very modest reduction of 20% ($\beta = 1.2$) could be made while achieving an attenuation of 460, or 53.2dB, the substantial desired reduction of a factor of 2 cannot be achieved, except for T=1, in which case the filter is useless.

Up to this point, the low frequency loop transmission analysis has assumed that the amplifier gain is constant. The gain constraints illustrated above become even more severe if the low-frequency roll-off of A(s) for power-frequency rejection is implemented near or above the UGC. It may seem that the loop transmission could be improved by using this roll-off to give a +1 slope above all three poles; however, this would limit the reduction of the storage components even more severely by requiring an even larger N = $\omega_l^2 LC$ for the active filter. In fact, rather than the $+90^{\circ}$ provided by this gain roll-off, the low frequency compensation requires the addition of some sort of negative phase compensation at low frequencies near and above the UGC, so that the amplifier gain may be larger than $\sqrt{N}$ while maintaining good phase margin, thus allowing substantial reductions in storage components sizes. Given sufficient negative phase compensation, the LT pole ordering of Fig. 6-6 ($\omega_o > \omega_d$) would be preferred, since it allows for smaller storage components.

6.2 Compensation Methods

Several methods of compensation are now considered. Two forms of negative phase compensation an all-pass filter and lag compensation, involve some transfer function to be cascaded into that of the amplifier A(s). Another, which involves the design of the amplifier output impedance, affects the loop transmission through the feedback transfer function F(s). Also included in this section are discussions of the power frequency rejection problems associated with the negative phase loop transmission compensation and of an amplifier input compensation method to improve the high frequency performance of the active filter.

6.2.1 All-Pass Filter

The bode plot and pole-zero plot for an all-pass filter with negative phase shift is shown in Fig. 6-7. An example of such an all-pass filter is given in [15, p. 536]. The phase

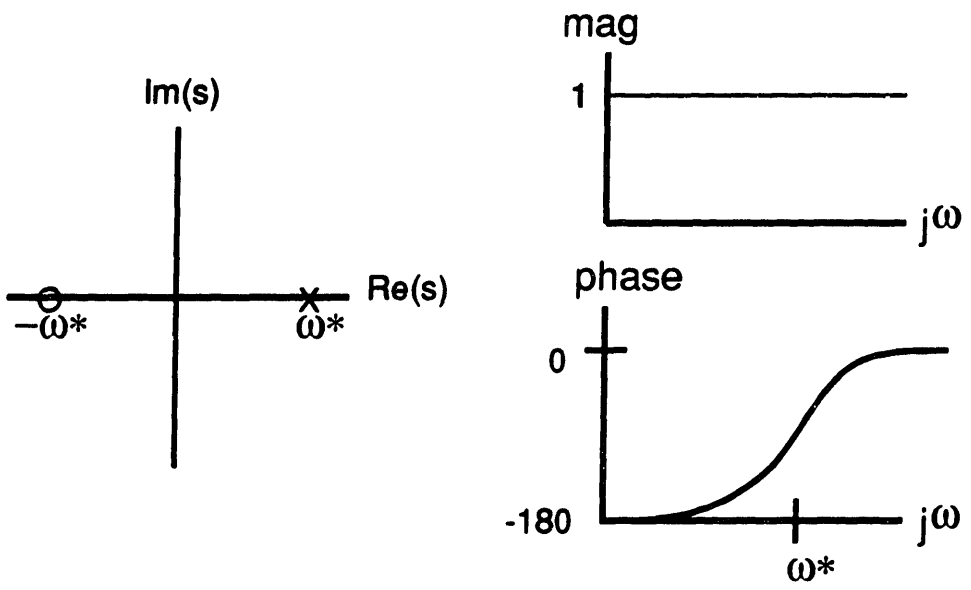

Figure 6-7: Pole-zero diagram and bode plot for negative-phase-shifting all-pass filter

of the transfer function is -180° at low frequencies but shifts to 0° around the breakpoint frequency, $\omega*$. The principal advantage of an all-pass filter is that it provides the desired negative phase shift without affecting the magnitude of the loop transmission. Its use might allow large gains, limited only by the high-frequency bandwidth, with relatively small LC products. A fundamental stability problem would exist, however, due to the right-half-plane pole added to the loop transmission by the all-pass filter. While this pole in a loop transmission would not automatically make a system unstable, it must move out of the right-half-plane when the loop is closed for the system to be stable. Fig. 6-8 shows a pole-zero diagram for the loop transmission including the all-pass filter and the root-locus contour for the pole of interest. When the loop is closed, the pole moves towards the origin where there are several zeros. For this pole to reach the origin, however, would require infinite gain A in the midband region; thus, for achievable gains, the pole from the all-pass filter would remain in the right-half-plane and the system would be unstable. For this reason no further consideration will be given to the all-pass-filter as a means To achieve negative phase compensation of the low-frequency loop transmission.

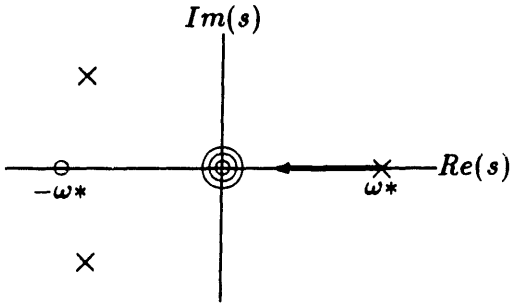

Figure 6-8: LT with all-pass filter and root-locus contour for RHP pole

6.2.2 Lag and Lead Compensation

The second method considered for obtaining the desired negative phase for low-frequency compensation is the cascading of a pole and a lagging zero. This technique, known as lag compensation, and its counterpart, lead compensation are discussed in [15]. Both are commonly used techniques for amplifier compensation. The transfer function for a generic lag compensation network of magnitude α may be represented by the following transfer function:

$$C(s) = \frac{s + \alpha\omega*}{s + \omega*} \tag{6.28}$$

A bode plot for C(s) is shown in Fig.6-9. While the left-half-plane pole and zero of the lag

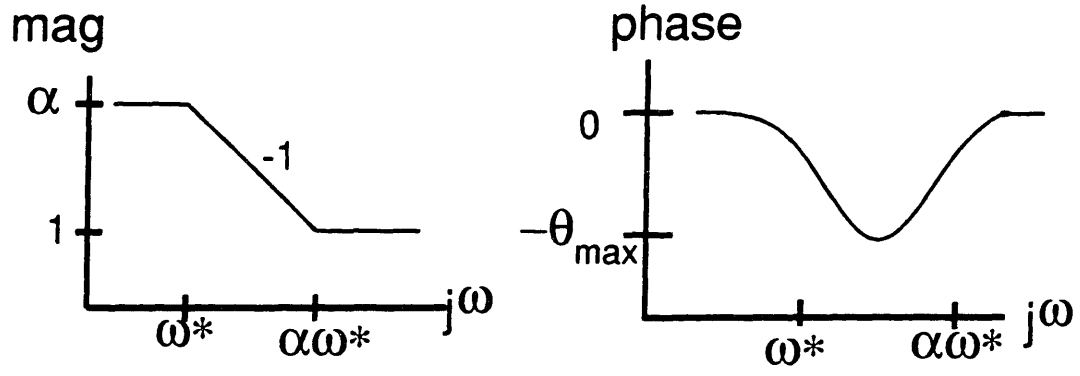

Figure 6-9: Bode plot for generic lag compensation network

compensation generally do not cause inherent stability trouble like the all-pass-filter does, this method has the drawback of sacrificing gain, that is the midband gain relative to the

power-frequency gain of the amplifier which needs to be minimized. The amount of gain α sacrificed for a desired peak negative phase θ at the pole-zero mean $(\sqrt{\alpha})\omega*$ is given by

$$\alpha = \frac{1+\sin\theta}{1-\sin\theta} \tag{6.29}$$

A peak of -30°, for example, requires $\alpha = 3$ and -60° requires $\alpha = 14$. This pair of examples illustrates the advantage of cascading low α lag compensations to achieve a desired large negative phase with minimal net attenuation. Cascading two $\alpha = 3$ compensations gives -60° with a total attenuation of only 3^2=9, while getting this much negative phase with a single lag sacrifices, 50% more, a factor of 14 in gain. This effect becomes most significant for phases close to -90°, as the phase of a single lag approaches this level only asymptotically with increasing α, while three $\alpha = 3$ lags could be used to get -90°. Of course, there is a tradeoff with the extra circuitry needed for each degree of lag compensation.

To some extent, the gain sacrificed by the lag compensation may be made up for with lead compensation at higher frequencies, between the final low-frequency pole and the switching frequency. The same analysis as done above applies to lead compensation except that the phase is positive and the magnitude rises with a +1 slope between $\omega*$ and $\alpha\omega*$. The amount of lead compensation that can be applied may is limited by the tolerance of the loop transmission to positive phase without coming too close to 180°, as a robust design requires that good phase margin be maintained even when the loop transmission magnitude is well above unity, in case it gets reduced by saturation or some other effect.

6.2.3 Output Impedance Compensation

Another method of compensation to be applied involves the design of the feedback function F(s). While the topology of the standard-drive inductor enhancement circuit dictates this transfer function as given in (6.19), the parameters of this transfer function are affected by the selection of components and amplifier characteristics. In particular, the drive pole ω_d depends on the output impedance of the amplifier, as well L_d. This parameter, Z_{out} represents a means of controlling the phase of the loop transmission without affecting the amplifier gain A(s) in the LT expression of (6.19) or in the gain expression of (6.7). As long as ω_d is below the switching frequency, the midband gain is unaffected by its value. If ω_d is in fact placed well below the UGC, then its negative phase effect may be fully taken advantage

of throughout the low-frequency LT to avoid additional negative phase compensation and the resulting midband gain reduction. For gains on the order of hundreds and a switching frequency of 75 kHz, however, the UGC of the LT may be expected to be around a couple kHz or less for a low frequency roll-off of +1 or $+\frac{3}{2}$. For ω_d to be well below the UGC frequency, then, it must be fairly close to 50 or 60 Hz, potentially resulting in a power-frequency rejection problem. If Z_{out} is not substantially larger than the impedance of L_d at the power-frequency, as determined by separation from the drive pole, too large a fraction of the power-line current will flow through the output stage of the amplifier.

In addition, if Z_{out} is too large on an absolute scale, the power frequency signals passed to the output voltage of the amplifier, seeing essentially Z_{out} as an impedance, may drive excessive currents through the amplifier output. While this current is proportional to the trans-impedance of the amplifier, that is, the amplifier output voltage due to a current through the sense impedance, it is also inversely proportional to Z_{out}.

A method to mitigate these power frequency rejection problems associated with the output impedance involves the use of a minor feedback loop within the amplifier, which allows separate control of the amplifier output impedance and the closed loop gain of the amplifier. To illustrate this concept, the basic inverting amplifier connection of Fig. 6-10 is considered as an example. For very large open-loop gain a(s), it can be shown that the

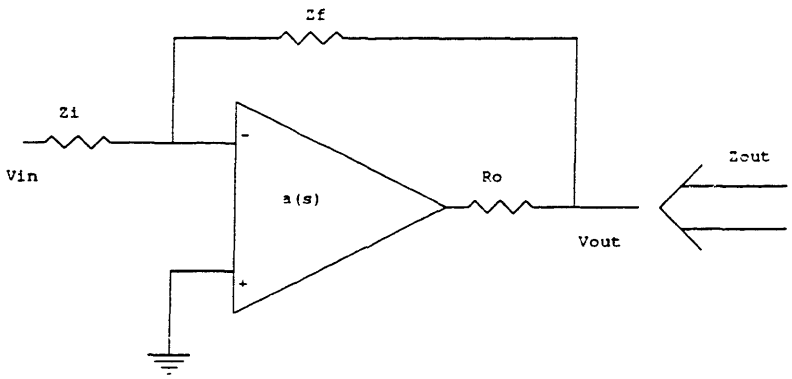

Figure 6-10: Basic inverting amplifier connection of op-amp

closed loop gain A(s) of the amplifier is approximately

$$A(s) \approx -\frac{Z_f}{Z_i} \tag{6.30}$$

and the output impedance Z_{out} of the amplifier is

$$Z_{out} \approx \frac{r_o}{a(s)}\frac{Z_f}{Z_i} \approx r_o A(s)/a(s) \tag{6.31}$$

So long as a(s) is maintained much larger than A(s) Z_{out} may be adjusted by changing a(s) without significantly affecting A(s). Adjustment to a(s) may be made through internal compensation of the op-amp, but caution should be taken to ensure good compensation of this minor loop as well as the loop transmission of the whole active filter.

By taking advantage of this technique, Z_{out} may be set so that its divider with L_d contributes substantial negative phase (or minimal positive phase if viewed as such) to the loop transmission at the UGC. Then at a somewhat lower frequency, the internal amplifier compensation begins to roll-up Z_{out} to a larger value at the power-frequency.

The same effect could be achieved, at least for first-order roll-up, by placing a capacitor in series with Z_{out}; however, the value of this capacitor would have to be very large, even considering that it does not support large voltages, or L_d would need to be large without any contribution to the gain in order to get their resonance below the UGC frequency. Still, it is helpful to use a series capacitor C_o to model the effect of first-order output impedance compensation. The LT thus has the following dependence:

$$LT \propto \frac{sL_d}{sL_d + Z_{out} + 1/(sC_o)} \tag{6.32}$$

An important point to note is that although the resonant effect of the output impedance compensation does not increase the phase of the LT above the 'resonance' any more than Z_{out} alone would, it increases the LT magnitude near that resonance, so the UGC should be at least about 3 times larger than that resonance to minimize the effect of this on the compensation. A factor of four difference, between the UGC and $(L_d C_o)^{-\frac{1}{2}}$, for example, would increase the LT at UGC by about 10%.

6.2.4 Power Frequency Compensation Problems

Even with the use of this output impedance compensation, the required negative phase compensation for gains on the order of a hundred at a switching frequency of 75 kHz requires a substantial amount of lag compensation. This lag compensation not only directly raises the magnitude of the amplifier gain at lower frequencies but also thereby causes the UGC frequency to be lower, in turn requiring more lag compensation. While simulations showed that the LT eventually makes it to unity because of its +3 slope for flat A(s) at low frequencies, the UGC may be as low as 1 kHz or less and the gain at this frequency may be even larger than the midband amplifier gain. To reduce this gain to unity or so at a 50-60 Hz power frequency requires a few dc (or very low frequency) zeros with canceling poles between the power frequency and the UGC. These extra dynamics, however, add more positive phase at the UGC. For example, a dc zero canceled by a pole at 250 Hz to give a mere factor of 4 in gain reduction at 60 Hz kills 14° of phase margin at a UGC of 1 kHz. Tailoring the amplifier compensation to meet the requirements may require dozens of components if it is even possible.

Twin-T Notch Filter

One potential solution to this problem might be the use of a twin-T notch filter. This network, discussed in [17, p. 161] and shown in Fig. 6-11, is a unique passive RC network in that it provides (ideally) infinite attenuation at the notch frequency. Furthermore, at distant frequencies the network has the characteristics of a first order system with a 3 dB point at 4 times (or one-fourth) the notch frequency $\frac{1}{RC}$. While twin-T notches are fabricated with notch depths of 60 dB, these require very stable components, one of which must be trimmable. If less costly components could be used to get even 40 dB of attenuation, this would have the same UGC phase shift but give far better 60 Hz attenuation than the 12 dB obtained by the dc zero canceled at 250 Hz.

One of the problems with the notch filter is that it is a fairly narrow notch. Circuits for 60 Hz and 50 Hz, for example, would require different components. A more fundamental problem with this scheme, however, is that the notch still passes harmonics of the power frequency. While the levels of the harmonic currents drawn by the power circuit might be on the order of 10 or more less than that of the power frequency, they are at higher frequencies,

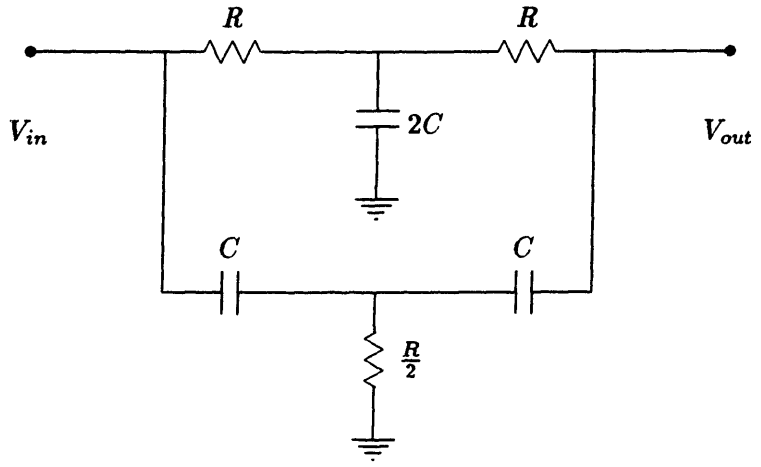

Figure 6-11: Twin-T notch filter considered for power frequency rejection

so that the active circuit is more susceptible to them due to larger gain and inductive sensing. As a series of twin-T notch filters would be too impractical, this approach to the power-frequency problem is only useful for power circuits with very good power factors, or more specifically, with very low total harmonic distortions (T.H.D.).

Approach

Thus, for the most part, the design attempts here will aim to reduce the amplifier gain of the active circuit below about 300 Hz by minimizing the use of negative phase compensation and using steep active (or small-signal passive) filters to tailor the frequency response of the amplifier, including the the addition of some dc zeros and canceling low-frequency poles. The appropriate design of this low-frequency compensation is very much a function of the harmonic content of the current waveform drawn by the power supply which determines how much gain can be tolerated at particular harmonic frequencies. If the current is purely 60 Hz, for example, it would be better in terms of UGC phase compensation to place a pair of dc-zero-canceling poles at 240 Hz rather than one at 960 Hz, even though both would give the same 60 Hz amplifier rejection. Whether or not the pair of compensators is worth the additional complexity depends on how close the UGC is, in this case, to 960 Hz.

6.2.5 High Frequency Amplifier Input Impedance Compensation

Returning briefly to the high frequency compensation, one of the problems of the active filter which may need to be dealt with is that posed by the input capacitance of the sense amplifier, which is likely to be substantially larger than the parasitic capacitance of the sense inductance. This capacitance limits the attenuation of the active filter at higher frequencies and may also lower the phase margin, to an extent which depends on its impedance in relation to the high-end of the power line impedance. A solution to this problem may be combined with the high-frequency compensation of the loop transmission. As pointed out earlier, a well-designed inductor enhancement circuit would have good phase margin even with a $-\frac{3}{2}$ high-frequency amplifier gain roll-off. The extra $-\frac{1}{2}$ of roll-off may be obtained with a lag compensation network which also decreases the input capacitance of the amplifier at high frequencies. The circuit shown in Fig. 6-13 accomplishes this by placing a small capacitor $C_c \ll C_{in}$ in series with the amplifier input and shunting this capacitor with a resistor $R_c \ll R_{in}$ to permit nearly full use of the amplifier gain at low frequencies. The resulting transfer function of the circuit is given by the bode plot of Fig. 6-12, where

$$\omega_p = [(R_{in} \parallel R_c)(C_{in} + C_c)]^{-1} \approx (R_c C_{in})^{-1}$$

and

$$\omega_c = (R_c C_c)^{-1}$$

The maximum negative phase of this network occurs at $\sqrt{\omega_p \omega_c}$, and is related to $\alpha = \omega_c/\omega_p$ by (6.29), which says that a compensation of $\alpha = 6$ may be obtained with a negative phase of 45°.

The effective input impedance of the amplifier with the lag compensation network is shown in the bode plot of Fig. 6-14, where the new symbols are defined by

$$\omega_{in} = (R_{in} C_{in})^{-1}$$

and

$$C_p = \frac{C_{in} C_c}{C_{in} + C_c}$$

Thus, at high frequencies, the input capacitance is reduced to a bit less than C_c. This

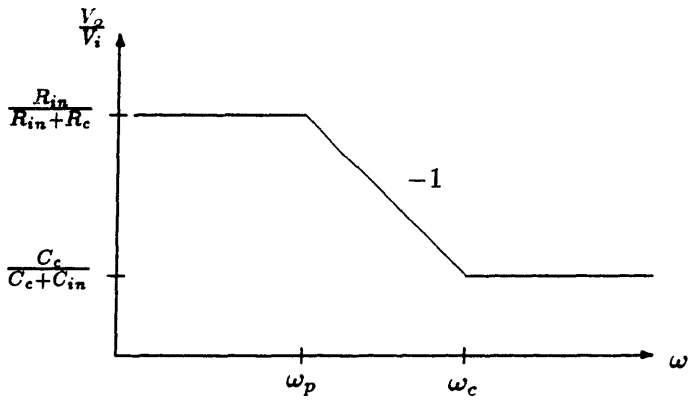

Figure 6-12: Bode plot of transfer function of lag network for amplifier input impedance compensation

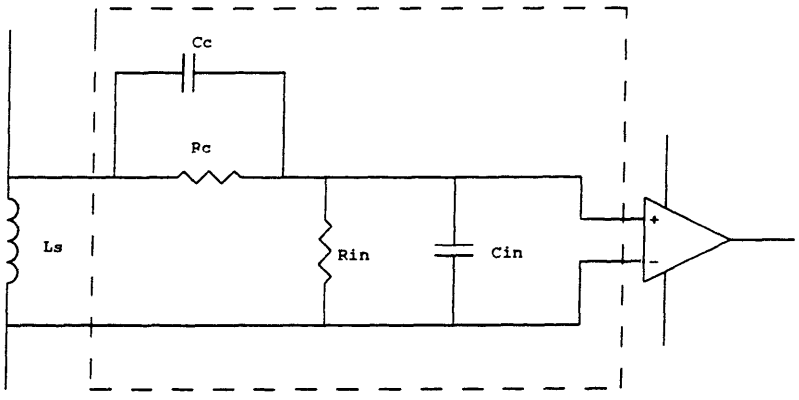

Figure 6-13: Lag compensation network to reduce high frequency input capacitance of amplifier

compensation capacitance may simply be the parasitic capacitance of the resistor R_c, which might be on the order of 1 pF, if this can be so arranged for a high input impedance amplifier.

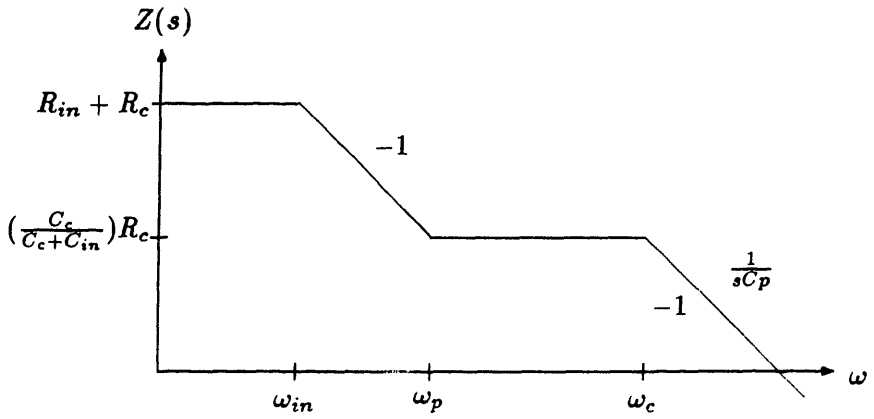

Figure 6-14: Bode plot of effective input impedance of amplifier with lag network

6.3 Practical Considerations of Standard Drive Enhancement

In this section, the above analysis and compensation methods are applied to the design of an actively enhanced filter to replace the passive filter of Fig. 5-14. First, practical three-wire topologies compatible to the power supply of interest are developed. SPICE simulations were run on designs based on two of these topologies. The results of analysis and simulations are used to evaluate the practicality of these topologies.

6.3.1 Practical Three-Wire Topologies

Because the standard-drive enhanced inductor is a two-terminal element playing the role of an inductor in the power circuit, the application of this topology to a three-wire filter is essentially the same as that of the passive inductor. As represented in Fig. 6-15 by L_{active}, an enhanced inductor circuit like that of Fig. 6-1 is placed in the series path of the hot and neutral lines to create a balanced filter. To ensure sufficient common-mode attenuation, the sense inductances, which are to be amplified, may need to consist partially of a common-

mode inductor. Note that this topology may be analyzed in terms of common-mode and differential-mode subcircuits, as was done with the passive filter in Chapter 3.

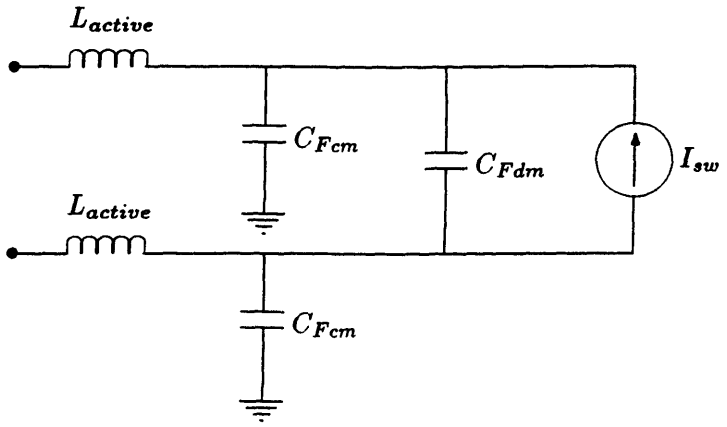

Figure 6-15: General form of a three-wire standard drive inductor enhancement

In terms of applying standard drive inductor enhancement to replace the passive filter of Fig. 5-14, two approaches are considered. One is to replace the candidate passive EMI filter with a pair of enhanced inductors and a pair of 'Y' capacitors for passive filtering and use the rectifier capacitor as the differential filter capacitor, as shown in Fig. 6-15, of which both the CM and DM subcircuits are the one analyzed in Section 6.1. Since this approach involves replacing the fourth-order differential filter with a 'first-order' enhanced inductor, a very large gain is needed for the total inductance used to be reasonably small. The other possibility is to add inductance between a filter stage like that of Fig. 6-15 and the power supply, represented here by I_{sw}. The net result is a fourth order differential-mode filter and a common-mode filter of the same (third) order as in the original passive EMI filter. Of course, this fourth order differential-mode actively enhanced filter ought to require less gain than the second-order version. The extra components in the passive stage of this filter, however, cannot be reduced very much due to the need to keep resonances down to low frequencies for both attenuation and compensation purposes.

Comparison of these two types of active topologies with the passive equivalent in terms of common-mode attenuation is quite difficult due to uncertainty of the EMI source impedance. Because of this uncertainty and the expectation that it may be a fairly small capacitance, likely on the order of the winding capacitance of the common-mode inductor, it is not clear

that the input-side common-mode inductor is contributing much to the filter's attenuation. If this contribution is small, then there is little difference between the two active topologies from a common-mode standpoint, and a pair of many-times smaller common-mode inductors can be used in the sense and drive positions and actively enhanced to achieve in conjunction with the pair of 'Y' capacitors, the same common-mode attenuation as the passive candidate filter, or it is likely that the parallel combination of the enhanced differential-mode inductance, a net amount of 8 mH in the above example, would be sufficient common-mode inductance. Even if the input common-mode inductor is doing substantial filtering work, enhancement of a relatively small common-mode inductance in the active stage might make up for the attenuation lost by removing the common-mode inductor from the input, as well as replace the output CM inductor.

The amount of common-mode inductance needed in the enhancement circuit may also be dictated by compensation, as the LT depends on resonance with the small 'Y' capacitors. Note also that if extra of either, but not both, a CM or DM inductance is placed between the capacitors, care must be taken that the filter resonance due to the 'parasitic' inductance in the undesired mode of the components is well damped, since this resonance would most likely be above the switching frequency. The analysis of the fourth order active filter and examples of each of the two proposed circuits are considered in the following sections.

6.3.2 Example of Second Order Filter with Standard Drive Enhancement

Circuit Design

An active replacement circuit for the passive candidate filter is considered here using standard drive inductor enhancement in a single stage stage filter, as was shown in Fig. 6-15. Because, the two large differential-mode capacitors are eliminated rather than reduced, an equivalent trade off to halving total inductance and capacitance might be met if the circuit uses no more differential-mode inductance than that of the passive equivalent circuit, or 200 μH Since the differential-mode impedance of the LISN is about 40 Ω at 75 kHz and that of the 200 μH inductance is about 100 Ω , the enhancement gain required to get 52 dB of DM attenuation from this voltage divider at this frequency is around 160. In terms of compensation, the 4.4 μF rectifier capacitor would give a resonant frequency of around 5 kHz with the 200 μH differential inductance. If the LT can be rolled up with a +2 slope

between here and the 75 kHz switching frequency, this may be low enough to allow for compensation of the feedback loop without destroying the power-frequency rejection of the amplifier.

The drive impedances, Z_{out} and L_d , must be selected very carefully because of the power frequency rejection problems associated with Z_{out}, as discussed in Section 6.2.3, and because of the need to minimize L_d , since it is an inductance which does not contribute to the attenuation in this topology. The value of 50 μH was chosen for $2L_d$, the total drive inductance, in the DM circuit. While this makes the total differential inductance 25% larger than that of the passive filter, this should be made up for by the great reduction of common-mode inductance made possible by the large enhancement gain. In fact, if the source impedance is large so that the load-side CM inductor is not doing much for the filter, the gain of 160 would give the pair of balanced 100 μH differential inductors a sufficient effective CM inductance of about 8 mH, since they appear in parallel to common-mode signals. A total value of $2Z_{out} = 0.25\ \Omega$ was chosen giving a 'drive pole' of $\omega_d \approx 800$ Hz. Note that $\frac{Z_{out}}{L_d}$ need not appear to be this low below the UGC frequency where output impedance compensation may be applied to increase Z_{out}.

Since this circuit is second-order, its sufficient performance up to high frequencies relies heavily on minimal parasitics. Aside from applying compensation to reduce amplifier input capacitance at high frequencies, the large 100 μH sense inductors on each line need to consist of two or three smaller lower capacitance components.

Differential-Mode Simulations

Simulations of the difference-mode attenuation and loop transmission for the circuit suggested above are shown in Appendix B. Section B.1 shows the subcircuits used in the simulation, including sources and components with parasitics, and networks used to simulate compensation functions which would probably be implemented in a more efficient but complicated way in an actual design. The next two sections use these subcircuits to calculate the LT with the worst-case line impedances, a short circuit and a LISN. The short circuit is a worst case because it makes the double-pole resonance of the low frequency LT occur at the highest possible frequency and with minimum damping; the LISN, on the other hand, gives the maximum damping at higher frequencies (above resonance) where the extra positive phase from the resistive line impedance may combine with that of the gain roll-up

or lead compensation to give poor phase margin. The compensation was adjusted so as to leave both of the resulting LT's with at least 30° of phase margin at and above unity gain and to minimize the amplifier gain at 60 Hz and its harmonics. The data calculated in the LT simulations are the magnitude and phase of the amplifier compensation, which are the same for both simulations, as well as the loop transmission. The 'midband', or uncompensated, amplifier gain A was chosen along with the compensation so that the filter attenuation with a LISN, as given in the simulation of Section B.4, would be the required 52dB at 75 kHz.

It is apparent from the simulations that a great deal of compensation was used in this circuit. Still, the results clearly indicate that it is not a practical design. While the compensation used in this simulation was not optimized, the results illustrate many of the problems with this type of active filter. The compromise between power frequency rejection achieved by the resulting compensated active circuit is marginally acceptable at best, depending on the power frequency harmonic content of the current waveform. A large gain value of A=600 is required because the lead compensation of about 540 near the switching frequency leaves the actual gain at 75 kHz many times short of its ideal 'bode plot' value. Without such a large lead compensation, the required low frequency compensation could not be achieved. The UGC is around 1.1 $\sim$ 1.2 kHz, but with an amplifier gain around of 25, which increases with decreasing frequency to 48 at 500 Hz because of the compensation needed to sufficiently stabilize the LT at a UGC so close to ω_d.

Power Frequency Rejection

The LT simulations did not include the effect of output impedance compensation; thus, the LT result assumes, as suggested in Section 6.2.3, that the output compensation be at least three times lower in frequency than the UGC, which would place it around 350 Hz. This is very low, already near the fifth harmonic of 60 Hz, which could be a substantial frequency component of the power line current spectrum. While the trans-impedance of 6.6 V/A in each amplifier at 300 Hz may give sufficiently low output voltage for a reasonable fifth harmonic current of 0.33 A, for example, the resulting 0.2 V would appear across a very small impedance. Even if a factor of two may be achieved in the output impedance compensation at this frequency, 0.8 A would have to be delivered across the 0.25Ω load of the output impedance to avoid nonlinear or self-destructive (i.e. overheating) amplifier

behavior.

High Frequency Attenuation Deficiency

One fundamental problem with the application of this topology is its insufficient high frequency attenuation. The deficiency is a result of its second-order nature and its consequential dependence on a high gain which must be rolled off at relatively low frequencies. While the attenuation should rise by at least 20 dB per decade up to 500 kHz, the data in Section B.4 shows the attenuation at 500 kHz only 8 dB higher than that at 75 kHz, despite a difference of 16.5 dB in frequency. The attenuation only drops below this frequency staying short of the attenuation criteria suggested in Section 5.7.1.

Common-Mode Compensation Trouble

Another fundamental problem with this second-order standard drive approach becomes evident upon consideration of the common-mode LT, which has the same form as that of the differential-mode, except for the passive component values L_s and C_f . In order for the compensation used in Sections B.2 and B.2 to be sufficient for the common-mode, the resonant frequency of the passive CM components must be less than or equal to that of the differential components, or (5 kHz). While no substantial CM inductance needs to be added for attenuation purposes, the limit of 10 nF on the CM capacitance requires a huge CM inductance of about 90 mH by this compensation criteria. In fact, even if the CM inductance were maintained at its candidate passive filter value of 3 mH, the resonance would be around 30 kHz, requiring much more lag and less lead compensation. This would have the spiraling effect described in Section 6.2.4 which substantially lowers the UGC and the power frequency rejection. The CM filter does not need as much gain as the DM, but because its gain is tied to the large DM gain, it requires a large LC product, in accordance with the simplified analysis of Section 6.1.3.

6.3.3 Consideration of a Fourth-Order Filter with Standard Drive

The fourth-order standard drive topology might lead to better results since it requires less gain. If the second-order standard-drive inductor enhanced topology is applied to the rectifier input of the power supply by placing a passive inductor between the two capacitors, as suggested earlier for this topology, the low frequency differential-mode loop transmission

needs to be reconsidered. Note that the common-mode loop transmission may be more or less unaffected by the addition of inductance between it and the power supply, since the large source impedance of the power supply, even with some inductance in series, may be dominated by the 'Y' capacitors, giving the same general results as developed for the second-order differential- or common-mode standard drive enhanced circuit in Section 6.1.2. Again, this result depends on the actual common-mode impedance of the power supply, which needs to be determined.

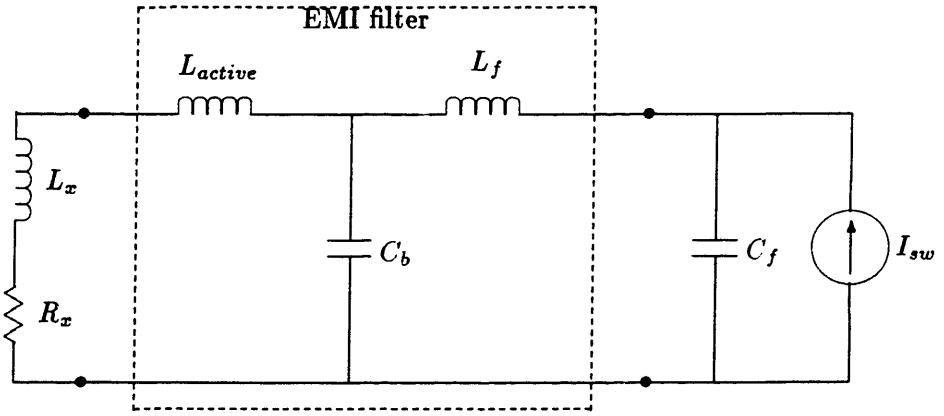

Figure 6-16: DM or CM subcircuit for fourth order filter with standard drive enhancement

LT Analysis

The fourth-order differential-mode inductor enhanced filter is shown in Fig. 6-16, where C_b is the smaller 'X' capacitor and C_f is the larger dc capacitor. Now, the impedance external to the inductor, Z_x' in (6.17), is equal at low frequencies to

$$Z_x' = sL_x + R_x + Z_f \tag{6.33}$$

where Z_f represents the filter and power supply impedance on the load side of the actively enhanced inductor. Rather than plugging in for Z_f and putting the whole mess into (6.17), the impedance term $(sL_s + Z_x')$ of the denominator is first considered separately. Above the drive pole, which may be quite low if the output impedance compensation of Section 6.2.3 is used, the rest of the loop transmission is just the effective impedance, AsL_s, in the

numerator, giving a phase of $+90^o$. Neglecting the damping effect of R_x , the denominator impedance expression is approximately given by the bode plot of Fig. 6-17, where

$$\omega_{o1} = [(L_\Sigma)C_f]^{(-\frac{1}{2})}$$

$$\omega_{o2} = [L_f C_b]^{(-\frac{1}{2})}$$

$$\omega_{o3} = [(L_s + L_x)C_b]^{(-\frac{1}{2})}$$

and

$$L_\Sigma = L_s + L_x + L_f$$

At low frequencies, the large capacitor C_f is the dominant impedance until it resonates with the inductances of the circuits which all appear in series so long as the impedance of C_b is considered negligibly large. At a higher frequency, C_b becomes important and resonates with the series combination of L_f and C_f. This bode plot is approximate because it assumes large spacing between the resonances. While ω_{o1} and ω_{o2} are likely to be spaced by a factor of at least 2 or 3 depending greatly on how much larger C_f is than C_b , ω_{o3} is likely to be close to ω_{o2} so that the effective capacitance of C_b at ω_{o3} may be very small, making ω_{o3} larger. In any case, above all of these resonances, the line impedance dominates the expression.

The results of Fig. 6-17 are applied to the loop transmission understanding by realizing that when the impedance of the denominator is inductive, the phase of the uncompensated loop transmission well above ω_d is between 0^o and 90^o depending on the level of damping by R_x in the line impedance. When the impedance is capacitive, however, the LT phase is above 90^o and approaches 180^o if R_x is very small. Thus, even if the drive pole is made very low, a considerable amount of negative phase compensation may be needed to ensure good phase margin throughout much of the low frequency roll-off of the loop transmission. If the UGC is between ω_d and ω_{o1}, which may be expected for a reasonable design, then the LT around the UGC is given by

$$LT \approx s^2 L_s C_f A(s) \tag{6.34}$$

The worst case of line impedance which should be considered is the lowest possible

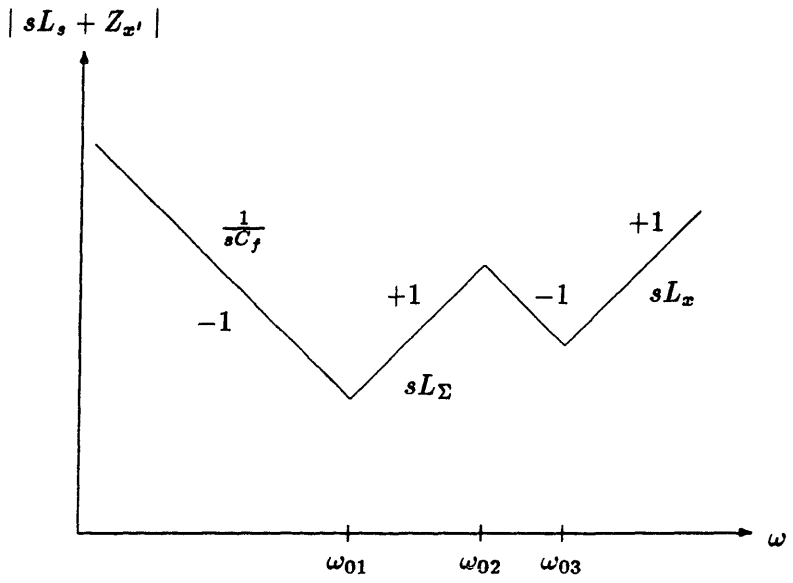

Figure 6-17: Magnitude of undamped impedance external to standard drive enhanced inductor in DM fourth order filter

impedance, which would essentially be a short circuit, so that ω_{o1} and ω_{o3} are at their maximum and damping is minimal. In addition, if substantial positive phase compensation to increase the midband gain is added in either of the inductive regions, between ω_{o1} and ω_{o2} or above ω_{o3}, the largest possible R_x must be considered to ensure that damping effects do not combine with this compensation to give poor phase margin. Depending on the frequencies of interest, this worst-case damped line impedance is likely to be the LISN network, which was shown in Section 5.6 to be considerably more resistive than the actual power line impedance. A single amplifier compensation needs to be designed for satisfactory performance with each of these worst-cases, as well as for the common-mode subcircuit.

Problems

Considering the second-order standard drive results of Section 6.3.2 and the above analysis, it is easily shown that the fourth order approach is also unworkable for the 75 kHz switching frequency, even if a minimal active improvement is undertaken to eliminate the output differential capacitor and to reduce the common-mode inductors by a factor of two. In this case, the 1.5 mH utility-side CM inductor and 9.4 nF of 'Y' capacitance give a resonance

around 42 kHz, below which lag compensation is needed to guarantee any phase margin, and above which there is little room for lead compensation to actually raise the gain before 75 kHz, without requiring that the actual uncompensated gain be much larger. The remaining third-order (fourth-order including C_f) differential-mode circuit requires a gain of at least 20 in order to make up for the elimination of the output capacitor, since the 40 Ω of DM LISN impedance is about 20 times larger than the 1 μF capacitor at 75 kHz. Even if no further gain increases would occur due to compensation, (6.34) shows that the UGC is below 1.7 kHz. In order to add sufficient negative phase between the CM resonance at 42 kHz and here, a gain increase of at least about 10 would be required, bringing the UGC below 1 kHz, with a gain on the order of 200. Furthermore, ω_d cannot be much lower than this if the circuit is to have any degree of power frequency rejection in line current conduction; the extra 30-40^o of phase from ω_d essentially makes compensation practically impossible, without having huge gains at the power frequencies.

6.4 Alternate Drive Inductor Enhancement

The second type of inductor enhancement circuit is analyzed here. While some of the compensation problems of the standard drive circuit are avoided in the alternate drive enhancement, the topology is somewhat more complex. The gain and LT are studied here applying some of the results from the standard drive. Practical application of this topology to replace the candidate passive filter is then considered.

6.4.1 Gain

The alternate drive inductor enhancement circuit of Fig. 5-6 is shown in Fig. 6-18 with the addition of a blocking capacitor in series with the amplifier output for power-frequency rejection, as suggested in Section 5.3.1 as well as in [2, p. 23] and [26, p. 122]. As in the circuit of Fig. 6-10, the effective output impedance of the amplifier here is roughly the impedance in series with its output divided by its gain. A reasonably small capacitor C_b will dominate over the series output impedance of the amplifier, so that this circuit effectively reduces the impedance of the capacitor by a factor of A, and may just as well be considered a capacitor-enhancement circuit. If, in addition, the amplifier input impedance Z_{in} is made large compared to that of the sense inductor L_s at the operating frequencies, the circuit

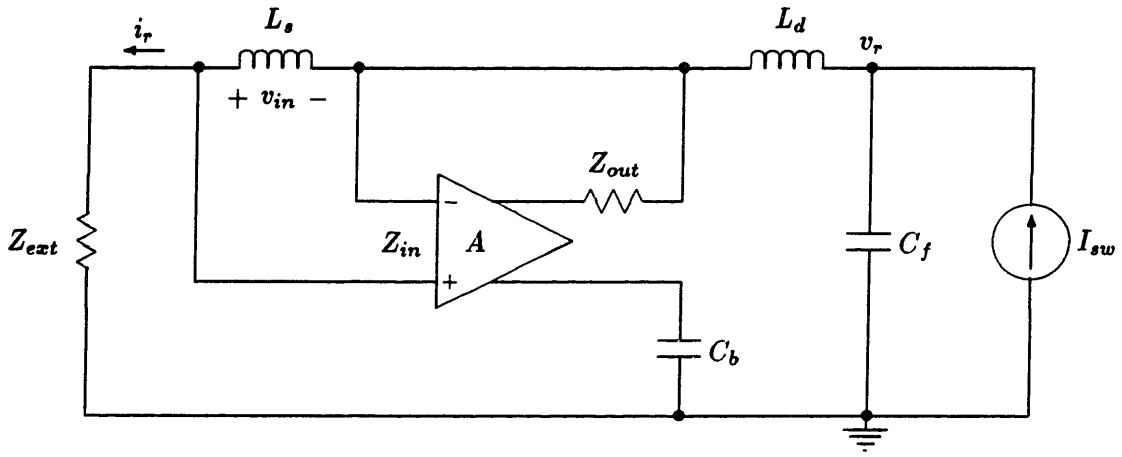

Figure 6-18: Alternate drive inductor-enhanced current filter circuit

may considered as a simple fourth order filter with the amplified capacitance, yielding an attenuation of $As^4L_sL_dC_fC_b$ above the resonant frequencies of the circuit. In active filter terms, the impedance from v_r to i_r is

$$Z_{eff} = As^3L_sL_dC_b \tag{6.35}$$

and the gain by which the amplifier and C_b enhance the total inductance is therefore

$$gain \approx As^2L_pC_b \tag{6.36}$$

where $L_p = (L_s \parallel L_d)$.

Unlike the standard-drive circuit, which amplifies only L_s, this circuit makes equal use of L_s and L_d , so that an optimal design, at least in terms of maximal attenuation, would be one that splits the total inductance as in a passive fourth order filter. Also, it is shown in in [2, p. 23] that the gain of (6.36) can be achieved above the resonant zero frequency of approximately $1/\sqrt{AL_pC_b}$. Based on this analysis, the alternate-drive circuit gives fourth order attenuations even at frequencies below the resonant frequencies of the passive network. Standard-drive enhancement, on the other hand, which operates only on a pair of series inductors, would require a passive LC filter operating well above resonance to get fourth-order attenuations. In terms of power supply control, however, the input impedance of the filter is still basically C_f in parallel with L_d. As with the standard drive,

the feedback compensation, to be discussed in the following section, may limit how much gain may be achieved with alternate drive inductor enhancement.

6.4.2 High Frequency Compensation

Note that the chief difference between the standard drive and alternate drive topologies is the inclusion of the filter capacitor C_f between the driving nodes of the amplifier. At high frequencies, however, this capacitor is a much lower impedance than L_d or the sense impedance $sL_s \parallel Z_{in}$. In addition, the blocking capacitor C_b may be neglected for the same reason. The resulting loop transmission is the same as that of the standard-drive circuit, which was shown in Fig. 6-4. Therefore, the high-frequency compensation analysis of Section 6.1.2 and the amplifier input compensation discussion of Section 6.2.5 directly apply to this circuit, as well.

6.4.3 Low Frequency Compensation

The extra capacitor C_b and the different placement of the amplifier with respect to C_f complicate the dynamics of the loop transmission of the alternate drive inductor enhancement circuit at lower frequencies, making it markedly different than that of the standard drive. This loop transmission circuit is shown in Fig. 6-19. Even with the low frequency assumptions that $Z_{in} \gg sL_s$ and $Z_{out} \ll \frac{1}{sC_b}$, this circuit results in the following fourth-order loop transmission: [1]

$$\frac{A(s)s^2L_sC_b(s^2L_dC_f+1)}{s^4(L_x+L_s)L_dC_bC_f+s^3L_dC_bC_fR_x+s^2[L_\Sigma C_f+(L_x+L_s)C_b]+s[(C_b+C_f)R_x]+1} \tag{6.37}$$

where

$$L_\Sigma = L_s + L_d + L_x$$

Without further analysis, this loop transmission expression can be described by no more than the partial bode plot of Fig. 6-20, where ω_{o2} is the resonant zero frequency given by the numerator of (6.37) Between a slope of +2 at low frequencies and 0 at high frequencies, the slopes of the bode plot depend on the relative positions of the four poles implicit in

[1] The LT for this circuit with an inductive line impedance and C_f neglected is considered briefly in [2, p. 30]. To show agreement with this result, apply the $Z_{in} \gg sL_s$ assumption to his result and substitute $Z_{out} \rightarrow \frac{1}{sC_b}, L_x \rightarrow (L_x + R_x/s), and L_d \rightarrow [L_d + 1/(s^2C_f)]$

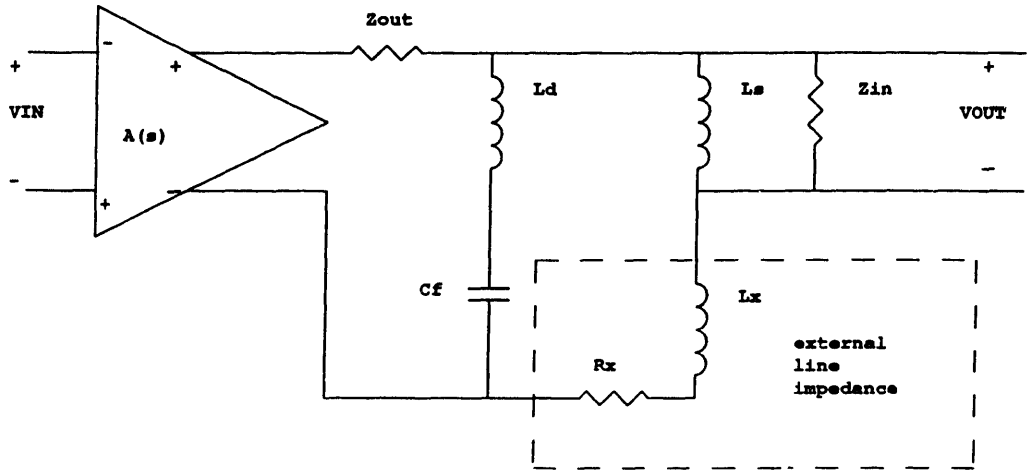

Figure 6-19: Low frequency loop transmission of alternate drive inductor-enhancement circuit

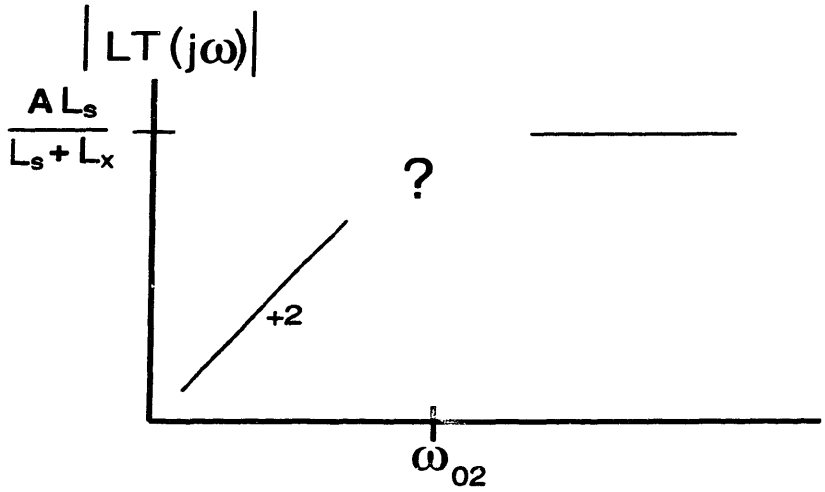

Figure 6-20: Low-frequency loop transmission of alternate drive inductor enhancement circuit

the denominator with respect to ω_{o2}. If, for example, all four poles are above ω_{o2}, then the loop transmission rises up to a slope of +4 and and then back down to 0, in which case instability is very likely.

Common-Mode Loop Transmission

For the case of a third-order common-mode alternate drive inductor enhancement, which would be connected directly to the rectifier-capacitor input of the power supply, a useful approximation is based on the fact that the presumably capacitive common-mode source impedance is quite large, so that in the circuit of Fig. 6-19, $C_b \gg C_f$. This approximation allows the denominator of (6.37) to be factored, resulting in a term which cancels the resonant zero, simplifying the equation to

$$LT = \frac{A(s)s^2 L_s C_b}{s^2(L_x + L_s)C_b + sC_b R_x + 1} \tag{6.38}$$

which is similar to the standard drive result in (6.19), except that the drive pole and its associated dc zero are absent here in (6.38). Again, considering the worst case of L_x =0 and R_x =0, for reasonably large gains and component size reductions, the resonant pole of (6.38) will be above the UGC, requiring some negative phase compensation between these two frequencies.

Differential-Mode Loop Transmission

The differential-mode LT is a bit more elusive to simplification. In order to better understand the behavior of the expression in (6.37) for differential-mode application, the case in which the line impedance is dominantly inductive is first considered. Specifically the approximation,

$$\omega(L_s + L_x) \gg R_x \tag{6.39}$$

allows the elimination of the damping terms, the first- and third-order ones in (6.37). Another approximation is based on the fact that C_b which must block power-frequency currents from the amplifier output, and which is being amplified anyway, would have a somewhat smaller value than the filter capacitor C_f , which need not be an 'X'-rated capacitor since it is on the dc side of the rectifier. While the difference in capacitor values may not be as great as for the common-mode, the following approximation is reasonable even if C_b is only

two or three times smaller than C_f :

$$C_f \gg [\frac{L_{px}}{L_\Sigma}]C_b \tag{6.40}$$

where

$$L_{px} = (L_s + L_x) \parallel L_d$$

and

$$L_\Sigma = L_s + L_x + L_d$$

because the multiplying factor $\frac{L_{px}}{L_\Sigma}$ can be no larger than $\frac{1}{4}$.

Lightly damped Loop Transmission The approximations of (6.39) and (6.40) allow the denominator of (6.37) to be factored yielding a more meaningful expression:

$$LT(s) = A(s)\frac{L_s}{L_s + L_x}\frac{s^2(s^2 + w_{o2}^2)}{(s^2 + \omega_{o1}^2)(s^2 + \omega_{o3}^2)} \tag{6.41}$$

where

$$\omega_{o1} = 1/\sqrt{L_\Sigma C_f}$$

$$\omega_{o2} = 1/\sqrt{L_d C_f}$$

and

$$\omega_{o3} = 1/\sqrt{L_{px} C_b}$$

This result makes clear the ordering of the loop transmission singularities,

$$\omega_{o1} < \omega_{o2} < \omega_{o3} \tag{6.42}$$

and gives the bode plot of Fig. 6-21 which shows that the phase of the loop transmission is never larger than 180°. Compensation of this loop transmission would likely be easier than that of the standard-drive loop transmission, which has a +3 below the resonant frequency and the drive pole. While the frequency of the final resonant-pole ω_{o3} in Fig. 6-21 may be quite large, the negative phase required to compensate the loop transmission is no larger than the desired phase margin at any frequency and is not needed between ω_{o1} and ω_{o2}

Because of the uncertainty of the power line impedance, however, the lightly damped

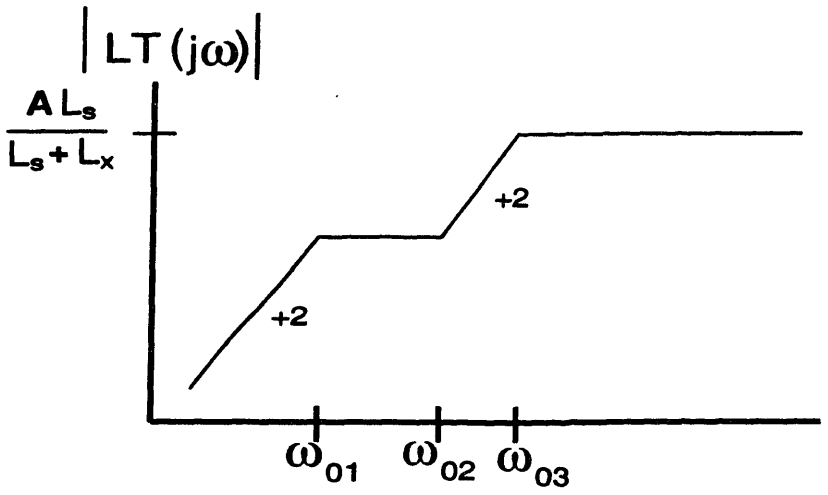

Figure 6-21: Low-frequency LT of alternate drive inductor enhancement with purely inductive line impedance

condition of (6.39) cannot be relied on. Even for frequencies high enough such that inductance dominates the line impedance (above 10 kHz), the impedance of the LISN, with which the active filter must perform at its best, must be taken into account. From the phase plot of Fig. 5-10, the LISN is a fairly resistive impedance above a few kHz, with its phase peaking at less than 60^o around 50kHz. In addition, as suggested in Section 4.1, the power supply may have a resistive input impedance which depends on its control scheme, and which may also cause damping in the loop transmission. The effect of damping on the loop transmission therefore needs to be considered.

Effect of Line Impedance Damping on LT The effect of a sizable R_x on the loop transmission of Fig. 6-21 would be to smooth out the slope transitions at the pole frequencies ω_{o1} and ω_{o3}. Because the resonant zero remains undamped, however, it will, by its occurrence, add $+180^o$ of phase to the loop transmission at a frequency w_{o2}, where a substantial amount of positive phase may remain un-canceled by the damped pole at w_{o1} While the damped pole at w_{o3} may contribute some negative phase here, it is likely to have less of an effect for $C_b \ll C_f$, in which case ω_{o1} may be considerably closer than ω_{o3} to ω_{o2}. A useful expression is the phase of the loop transmission denominator, particularly at ω_{o2}, just above which it is expected to bring about the worst-case (most positive) uncompensated loop transmission phase. This is calculated from (6.37); substituting $\omega = \omega_{o2}$ yields

a principal value of

$$| \tan \angle[denom.of LT(j\omega_{o2})] | = \frac{R_x\sqrt{L_dC_f}}{(L_x + L_s)} = \frac{R_x}{\omega_{o2}(L_x + L_s)} \tag{6.43}$$

which, is the amount of positive phase added to the base value of 180°. For $L_s \ll L_x$, this is essentially the complement of the angle of the line impedance. Note that this angle does not necessarily decrease with higher frequencies, particularly in the case of the LISN, which has a parallel inductor-resistor combination.

For a given design, the worst-case phase angle is given by (6.43) at ω_{o2} with the minimal L_x and the maximal simultaneous R_x or vice-versa. This angle, in addition to the desired amount of phase margin, dictates how much negative phase compensation is needed at ω_{o2}. Some negative phase is probably also needed below ω_{o1} to maintain good phase margin down to the UGC frequency. In fact, for the large gains required of the active filter, the UGC can be expected to be well below all three resonant frequencies of the circuit, especially since the required negative phase compensation implemented with the lag method raises the very low frequency gain A(s). Thus, the low-frequency UGC is nearly independent of the line impedance and may be found by taking the low frequency approximation of (6.37):

$$LT \approx A(s)s^2L_sC_b \tag{6.44}$$

6.5 Practical Considerations of Alternate Drive Enhancement

Advantages of Alternate Drive

In addition to the enhancement of a third-order unit to potentially achieve greater attenuation with smaller components and lower amplifier gains, a chief advantage of the alternate drive circuit over the standard drive is the elimination of output impedance problems by the use of the capacitor C_b as a blocking capacitor and an amplifier output impedance, as well as an attenuation component. The drive pole and its third-order LT effects are eliminated, as are the power frequency rejection problems associated with the small Z_{out} needed to keep the drive pole low. Other practical considerations are addressed here and the replacement of the candidate passive filter is considered as an example.

6.5.1 Design Trade-offs

For maximal gain, (6.36) dictates the use of equal L_s and L_d . For compensation, however, (6.43) suggests the use of a larger L_s , and small L_d and C_f , implying as well that for a given gain, C_b must be larger too. Nevertheless, this suggestion conflicts with the need to keep the amplifier output current levels low. At the power-frequency, a large C_b passes too much leakage current. At 60 Hz, for example, a 0.68 μF capacitor with 170 V peak line across it passes a peak current of 44 mA. In addition, at the fundamental switching frequency, a given switching current from the power supply results in an EMI ripple current in the active drive inversely proportional to $\omega^2 L_d C_f$. A minimum amount of this passive filtering is needed to keep the output current and power dissipation low in the active circuit. The amount of this passive filtering determines the maximum value on the resonant zero frequency ω_{o2}, and the resulting excess positive phase at this frequency must be compensated for.

6.5.2 Alternate Drive Three-Wire Topology

Because the alternate drive circuit does not replace a single component, as does the standard drive topology, taking full advantage of it in a three-wire system is somewhat more complex. One approach is to sense and amplify the voltages across a balanced pair of sense inductors, output the difference across a pair of balanced drive inductors in series with the EMI source, and output the sum between the utility-side terminal of each of these inductances and ground. The circuit of Fig. 6-22 integrates these functions into a pair of differential amplifiers which use the connection of common-mode and differential-mode blocking capacitors to add and subtract their voltages appropriately across the common-mode and differential-mode paths. The result is an L-C-L alternate-drive enhanced subcircuit for each mode, as shown in Figs. 6-23 and 6-24, where the differential-mode schematic also includes the dc side capacitor. Note that as with the passive filter, impedances add for the differential-mode and appear in parallel for the common-mode, except for the dual differential-mode capacitors and common-mode inductors, which are single elements affecting only one mode.

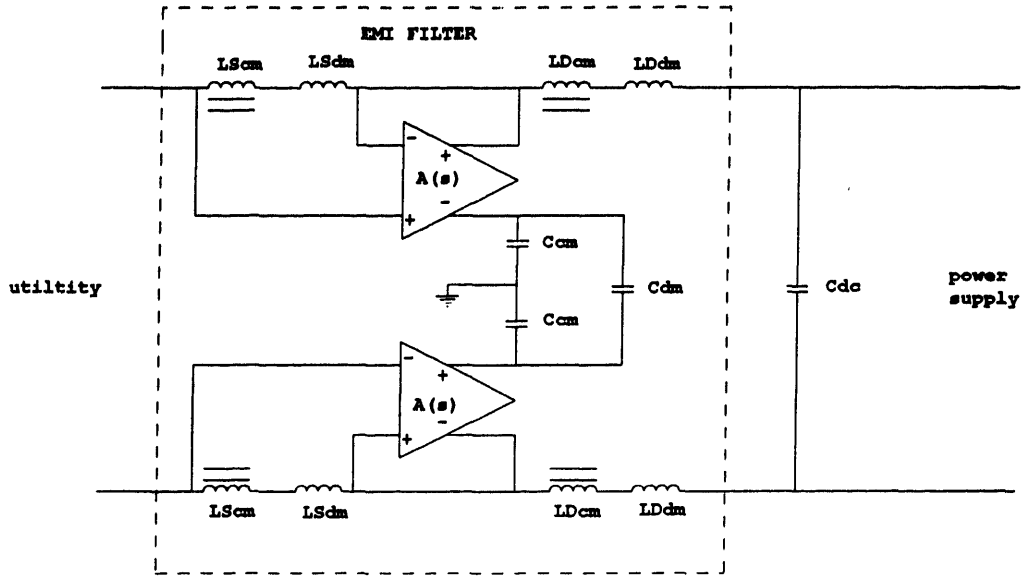

Figure 6-22: Three-wire alternate drive inductor enhancement topology

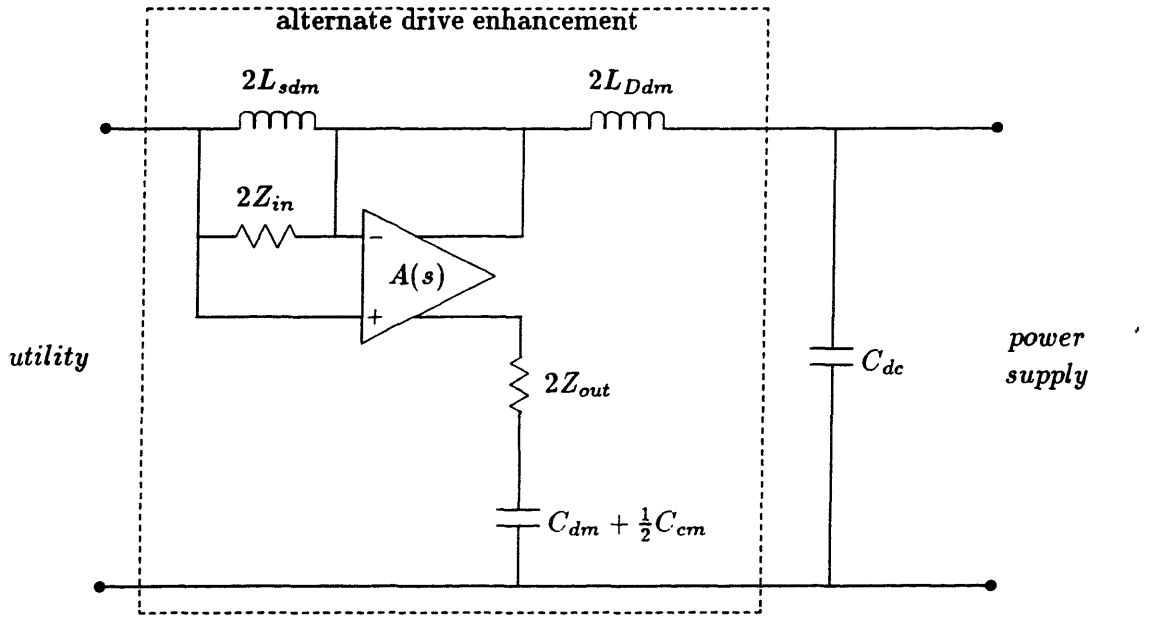

Figure 6-23: Differential-mode subcircuit of alternate drive inductor enhancement circuit

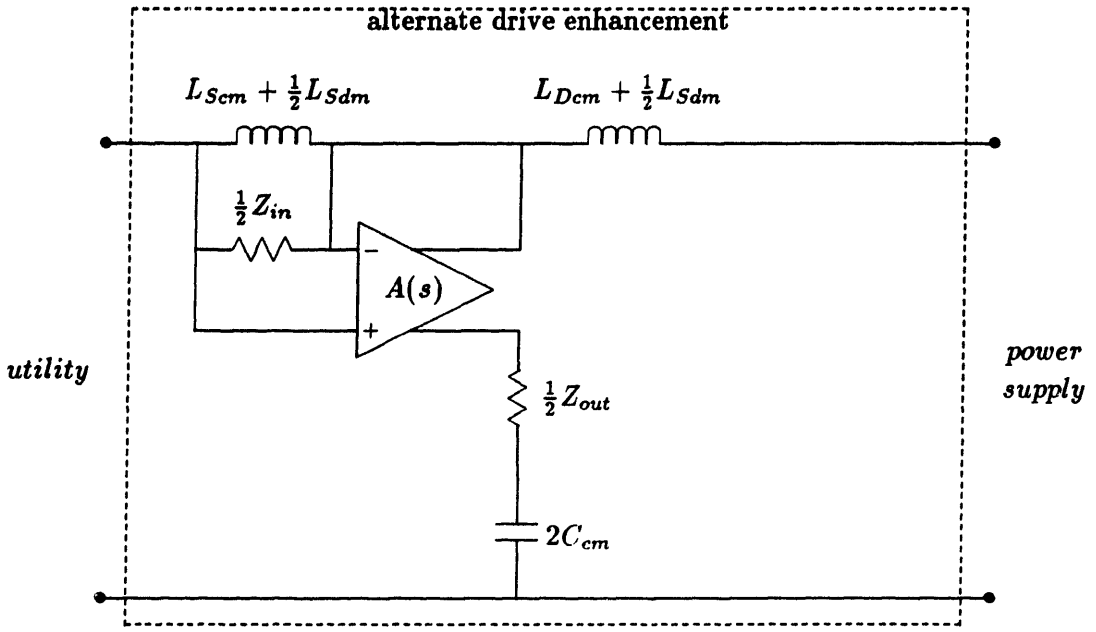

Figure 6-24: Common-mode subcircuit of alternate drive inductor enhancement circuit

By its relative simplicity, this circuit does sacrifice separate control of common-mode and differential-mode amplifier gains, which requires that the two filter subcircuits be designed in conjunction. Different gains for each mode would, in fact, require signal processing of the two voltages in the same circuitry. Besides the extra small-signal circuitry, this would require more blocking capacitors to couple the EMI signals across the two lines, although it might have the advantage of requiring only one power supply if all signal processing and output drive circuitry is floating with the same line. For the work herein, however, the single-gain circuit of Fig. 6-22 is considered.

6.5.3 Replacement of Candidate Passive Filter

Simulations confirm major problems associated with compensation of the alternate drive circuit for this application. A source of much trouble is the large positive phase of the differential-mode loop transmission just above the resonant zero, particularly with substantial damping in the circuit. For simplicity, it is assumed that the power supply operates as a high impedance current source above 60 Hz so that resistive line impedance on the utility side is the chief damping mechanism.

Due to the need to limit the power frequency current through the amplifier, a maximum value of C_b =0.33 μF was chosen to restrict this current for a 120 volt 60 Hz line to a maximum peak of about 25 mA. With the 2 μF of differential capacitance forcibly reduced by a factor of 6, use of 120 μF of differential inductance in the active filter is considered for a substantial reduction in storage components. Since L_d = 80 μH is needed to limit the fundamental DM ripple current through the active drive, based on the data of Section 5.7.2, to about 32 mA, L_s is left with 40 μH. The total gain required to get 52 dB of attenuation is then about 150. The problem is that, in this design, the resonant zero, ω_{o2} of (6.41), is around 8.5 kHz where the power line may be largely resistive and where the LISN impedance, in particular, is near a local minimum phase of less than 20°, as can be seen from Fig. 5-10. As shown in Section 6.5.1 this frequency cannot be changed much without subjecting the amplifier output to large ripple currents, making the active approach impractical.

Simulations similar to those of Appendix B were used to find the worst-case uncompensated loop transmissions. The following differential-mode line impedances were considered as worst cases for this circuit:

1. LISN with short-circuit external impedance
2. R_x = 4 Ω , L_x = 0
3. R_x = 4 Ω , L_x = 100 μH
4. R_x = 20 mΩ , L_x = 10 μH
5. R_x = 0.1 Ω , L_x = 100 μH
6. R_x = 0 , L_x = 0
7. LISN with (2) as external impedance
8. LISN with (3) as external impedance
9. LISN with (5) as external impedance
10. LISN with 250 μH external impedance

The curves which resulted in the highest phase value at some frequency with a phase greater than 100°are shown in Fig. 6-25. Although not shown in the plot, the common-mode loop

transmission would give its worst results with minimal line inductance, since it has a phase of about 180° up to the LC resonance which includes the line inductance as well as the L and C of the output (utility side) stage of the filter. Because L_{Scm} is so large and C_{cm} so small, this resonance is not expected to be significantly damped.

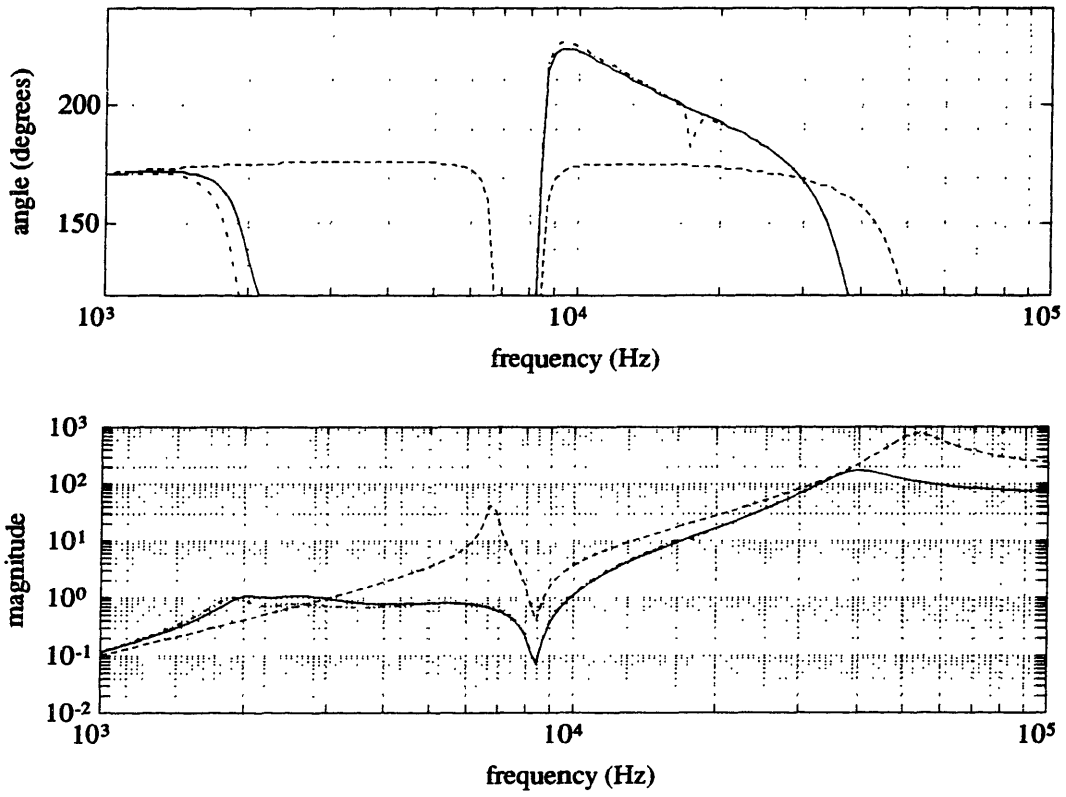

Figure 6-25: Phase plots for uncompensated alternate drive loop transmissions with various external line impedances: solid line = LISN , dashed line = short circuit , dot-dash-line = LISN + 4 ohms

The extent of the damped line impedance problem is clearly evident here, where all loop transmissions except the one with the purely resistive 4 Ω external impedance and those including the LISN, have maximum phases below 180°; the LISN, on the other hand, gives an LT phase near 225° and slightly larger than 225° when the line impedance external to the LISN is a purely resistive 4 Ω . Furthermore, the lightly damped zero just below the frequency of maximal phase brings the LT magnitude down quite low, even below unity, making good phase margin in this region especially critical. For 30° of phase margin, at least 75° of negative phase compensation is needed to accommodate the LISN impedance. Even if this negative phase compensation is split into three lags of α=2.5 to minimize

the associated magnitude effects, the gain increases by about 15. Because of the other possible impedances, the worst-case LT stays near 180° between the UGC and ω_{o3}, which is around 44 kHz, for the DM. For the CM, it stays near 180° up to at least about 50 kHz if common-mode inductors are reduced by a factor of two. Since the LT needs negative phase compensation up to two-thirds of the switching frequency, the use of lead compensation to make up for the lag is ruled out. Thus, even assuming that no additional lag compensation is needed at frequencies well below the resonant zero, which is unlikely, the gain reaches at least around 15x150=2250. The magnitude plot of 6-25, however, shows that even without the magnitude-increasing compensation, a gain of only 80 with the LISN requires a UGC as low as 2 kHz. The factor of at least 15 in magnitude increase due to the low frequency compensation, would lower this UGC by at least a factor of four. A UGC on the order of 500 Hz and an amplifier gain of 2250 here would result in power frequency amplification rather than power frequency rejection.

6.6 Application At Higher Frequencies

The main problem with the application of both the standard drive and the alternate drive topologies for the 75 kHz switching frequency is the lack of sufficient range between the switching frequency and the power frequency. This fact suggests that the active filtering techniques, that have been developed, could have practical use at higher switching frequencies, where there is a wider range of frequency available for compensated loop transmission roll-off followed by gain roll-off to get the gain down to low levels at the power frequency and its harmonics. It is worth noting that higher switching frequencies are, in fact, the direction in which the power supply industry is heading.

6.6.1 Effects of Higher Switching Frequencies

Component Scaling

Given the same control method and power level, a filter designed for a higher switching frequency, whether active or passive, will have smaller energy storage components. For the same external impedance and ripple specifications, the components can scale inverse proportionally with frequency. The impedance of the LISN, as well as the ripple specifications, do change with frequency, however, the LISN increasing toward 50 Ω per phase aysmp-

totically and the EMI limits becoming more strict by about 20 dB per decade up to 500 kHz, as shown in Fig. 1-1. The plot of Fig. 6-26 combines the variation of ripple voltage specification and LISN impedance to give the corresponding ripple current specifications. For the type of passive filter considered earlier, which has a capacitive DM termination, the LISN impedance has a negligible effect, on the filter requirements, since the impedance of the capacitor is much smaller than that of the LISN. Thus, to the extent that the LISN impedance increases with frequency, the active filters considered here would need larger component size increases than the passive equivalents. Still, the decrease in component size with the higher frequency has an additional benefit of improved power freqeuncy rejection. A smaller sense inductance, for example, leads to a lower amplifier trans-impedance.

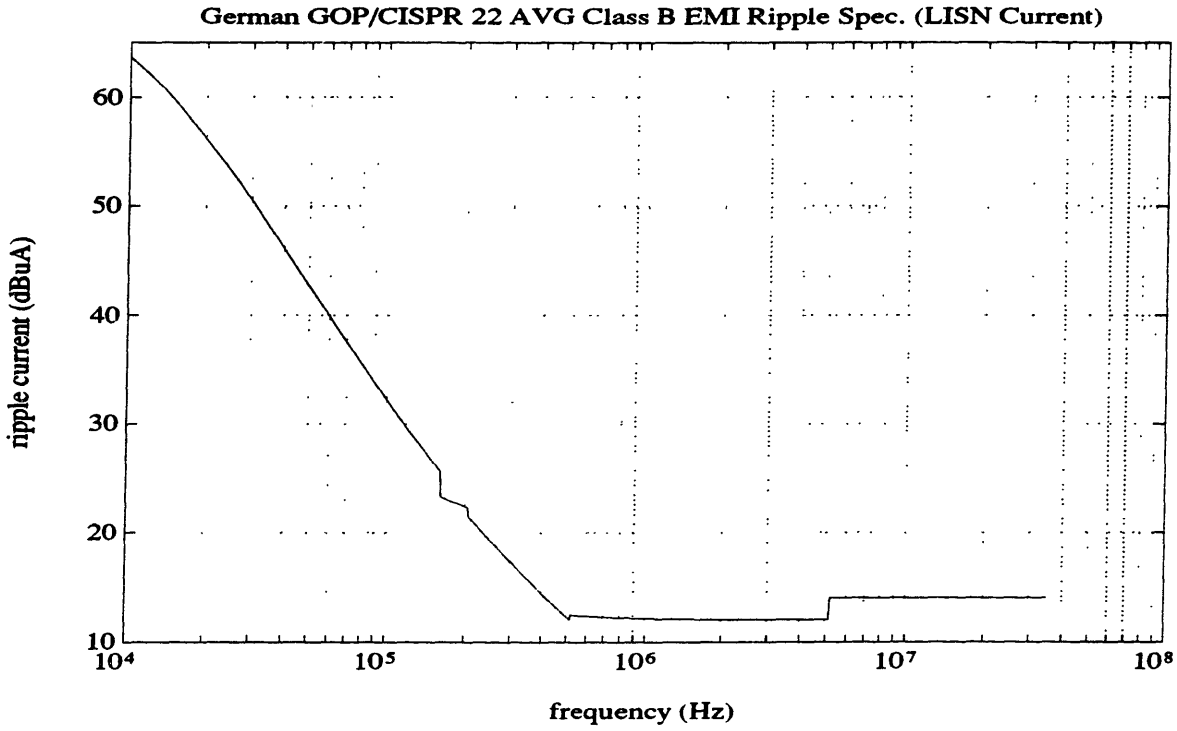

Figure 6-26: Current ripple specifications for commercial EMI testing with LISN

Drive Pole of the Standard Drive Enhancement

The compensation problems of the standard drive circuits relate largely to the drive pole, $\frac{Z_{out}}{L_d}$, but it is not clear that this problem is substantially improved with the move to higher frequency. As frequency increases, a practical standard drive circuit would have to decrease the size of the drive inductor L_d . Then, in order to maintain the drive pole at a certain

frequency, or to maintain a certain ratio of the impedances at the power frequency, Z_{out} must decrease as well. A further decrease of Z_{out} could not be tolerated unless the amplifier transimpedance is substantially decreased. The wider range of frequency would help some by giving a larger range over which to strike a compromise on the value of the drive pole and apply compensation, including output impedance compensation, well below the UGC to get power frequency rejection.

Resonant Zero of the Alternate Drive Enhancement

The reduction of components in the EMI filter, as well as the rectifier capacitor, moves the resonant zero of the alternate drive circuit up. An increase in this zero frequency by a factor of three to eight would bring it into the region in which the LISN becomes considerably inductive, with a phase of 45^o to 55^o. This would substantially decrease the excess positive phase just above the zero frequency, and eliminate the need for much of the compensation that kills the power frequency rejection of the circuit. This fact combined with the previously mentioned increase in the range available for low frequency compensation make this topology more attractive at higher frequencies. An example of an alternate drive inductor enhancement circuit is considered in the following section for a frequency around 500 kHz.

6.6.2 Design of A Higher-Frequency Alternate Drive Filter

Filter Requirements

The frequency of 450 kHz, exactly six times larger than the original switching frequency, was chosen to test the higher frequency potential of the alternate drive inductor enhancement topology with the compensation approach developed in the previous sections. Since the EMI ripple voltage specifications fall by about 20 dB per decade between 75 kHz and 450 kHz, the limit on the fundamental component of the output voltage of the filter for the higher frequency is six times lower in magnitude. Overall, the LISN current ripple specification, as given in Fig. 6-26, falls by about 23 dB between 75 kHz and 450 kHz.

Passive Filter for Comparison

To determine the practicality of the alternate drive inductor enhancement approach for a higher switching frequency of 450 kHz, an appropriate passive filter for comparison must first be determined. For the differential-mode filter, this is done by scaling down the components of the 75 kHz candidate passive filter of Fig. 5-14 and the rectifier capacitor, in proportion with the factor of 6 increase in frequency and distributing the burden of increased attenuation requirements among the components. Note that the frequency dependence of the LISN is negligible for the differential-mode because of the very low impedance of the output capacitor in parallel with it. Because five circuit elements are scaled, each one can be reduced by

$$\alpha = \frac{6}{6^{1/5}} = 6^{\frac{4}{5}} \approx 4.2$$

With some rounding off of numbers, this leaves a 1 μF rectifier capacitor, two 0.25 μF capacitors, and two balanced pairs of 12.5 μH inductors for the differential-mode filter.

The size of the common-mode filtering components is dominated by the common-mode inductors because of the limit on capacitance to ground. Thus, the component size reduction associated with the increased switching frequency is focused on the two common-mode inductors. Since, the common-mode filter terminates with a high impedance in series with the external impedance of the LISN, the relevant figure is the 23 dB reduction in the ripple current specification. If the 'Y' capacitors remain at 4.7 nF, the inductors may each be reduced by

$$\sqrt{6^3/14} \approx 4$$

Therefore, the common-mode chokes are reduced from 3 mH to 750 μH .

Design of Actively Enhanced Filter

The alternate drive topology of Fig. 6-22 is employed here to replace the 450 kHz passive filter described above. As suggested earlier, the active inductor enhancement is applied so as to eliminate or reduce the size of the most troublesome components, namely the common-mode inductors and the differential-mode capacitors, particularly the capacitor at the utility termination. Elimination of the utility termination capacitor, requires that the alternate drive active circuitry enhance the remaining third-order differential-mode EMI filter by about 64. This gain, applied to the common-mode filtering, as well, allows sub-

stantial reduction of the common-mode inductors, each by a factor of 8. As components reductions beyond a factor of two are marginally less valuable, however, part of this component reduction is sacrificed for compensation purposes so that the L-C resonance of the common-mode LT is no larger than that of the differential-mode LT, which is

$$\omega_o = 1/\sqrt{(25\mu H \parallel 25\mu H)(0.25\mu F)} = 2\pi \times 90kHz$$

Thus a value of 350 μH is chosen for the utility-side common-mode inductor, giving a resonance of around 88 kHz with the 9.4 nF of 'Y' capacitance. Note that the differential-mode sense and drive inductors may be set equal to each other for optimal attenuation per inductance, because the $\omega^2 L_d C_{dc}$ attenuation factor is left 1.27 times larger than that of the the 75 kHz alternate drive trial design, which required 80 μH along with the 4.4 μF to get sufficient attenuation of the ripple current through the active drive.

Compensation of this circuit should be considerably more feasible than the 75 kHz alternate drive circuit described earlier. Besides the greater frequency range available for LT and gain roll-off, the upward shifting of the resonant zero of the differential-mode LT substantially decreases the worst-case positive phase associated with that zero. Its value of $1/\sqrt{L_d C_{dc}}$ is around 32 kHz, leading to a maximum uncompensated phase of only about 200^o due to the increase in the phase of the LISN from its value at the previous zero frequency of around 10 kHz, which led to a phase of about 225^o. For a phase margin of 30^o, a negative phase compensation of 50^o is needed just above 32 kHz and 30^o elsewhere between the 90 kHz resonance and the lowest possible UGC.

6.6.3 Results

Worst-Case LT Simulations

Appendix C shows the SPICE and Matlab code used to study this active filter design. Four worst-case loop transmissions of this circuit were simulated in SPICE with high frequency compensation only. The SPICE input files for these four cases are shown in Appendices C.2 - C.5 with the subcircuits all shown together in Section C.1. The results of these simulations were then used to find a single low-frequency compensation appropriate for all cases by using the Matlab program shown in Appendix C.6, in which poles, zeros, and gain magnitude may be adjusted and the resulting low frequency LT magnitudes and phases

observed graphically or numerically. This was found to be a faster and less confusing design method than implementing the compensation with SPICE subcircuit networks as was done for the 75 kHz standard drive simulations of Appendix B. Note that the pole-zero pairs used in the compensation are separated into sets, since the transfer functions with all poles and zeros cannot be calculated at once, at least with a large number of singularities, because of dynamic range errors.

Given the results in Fig. 6-25 and the alternate drive LT analysis of the previous section, the line impedances for the worst-cases loop transmission simulations were chosen, based on the expectation that they would, over different frequency ranges, give the worst possible 'phase margins'. (Here the term is applied to the entire above-unity bandwidth of the LT rather than just the UGC frequency.) For the low frequency LT, this corresponds to the most positive angles over the low-frequency LT rise from unity to midband gain. The short circuit is a worst-case for both modes of the LT, as simulated by the code shown in Appendices C.3 and C.2, because the minimal damping keeps the LT very close to $+180^o$ below resonance and the minimal inductance makes this resonance be at its highest frequency. The maximal external inductance of 200 μH used in C.5 may be a worst-case for the differential-mode, because this inductance appears in series with the capacitor C_b in the low frequency LT expression of (6.44), effectively making the capacitor, and hence the LT, larger, so that the UGC is lower; also, this UGC phase is near 180^o because of the lack of damping. This maximal inductance worst-case is somewhat exaggerated, since a line impedance with a large inductance would contain long lengths of wire and therefore be fairly resistive; even if the wire is thick, the skin effect would increase the resistance at a few kHz to give some damping. The other worst case considered is that of the differential-mode LT in a LISN test with 100 μH of line inductance external to the LISN. As discussed earlier, the LISN gives a peak phase near the resonant zero due to damping. The 100 μH only affects the line impedance seen by the filter below a few kiloHertz because of the large inductance the LISN has in series with the external power line impedance Note that the short circuit is the only case considered for the common-mode because the CM LT has a considerably higher UGC because of the smaller LC product, and does not have the resonant zero problem of the differential-mode LT, so that the only place where the common-mode LT may be the worst-case is at the high-end of the LT roll-up just below the resonant pole of (6.38).

Compensation

The predetermined high frequency compensation was essentially implemented in the SPICE run using subcircuits to give a roll-off pole at 1.5 MHz and an input lag compensation of a factor of 6 between 1.5 MHz and 9 MHz. The low frequency compensation consists of the pole-zero pairs shown in the Matlab program in Section C.6. Many iterations of the Matlab program were run, trying to minimize the amount of compensation needed, particularly at the lowest frequencies where I.C. implementation would be more difficult, while aiming for phase margins no worse than about 30^o and reasonably low amplifier gains at the power frequency and its harmonics. The amplifier compensation finally used requires the six sets of poles and zeros shown in the Matlab program, in addition to the high frequency input lag compensation and roll-off pole. The bode plot of Fig. 6-27 illustrates the compensation of the amplifier gain in bode plot form and the calculated magnitude frequency response is shown in Fig. 6-28.

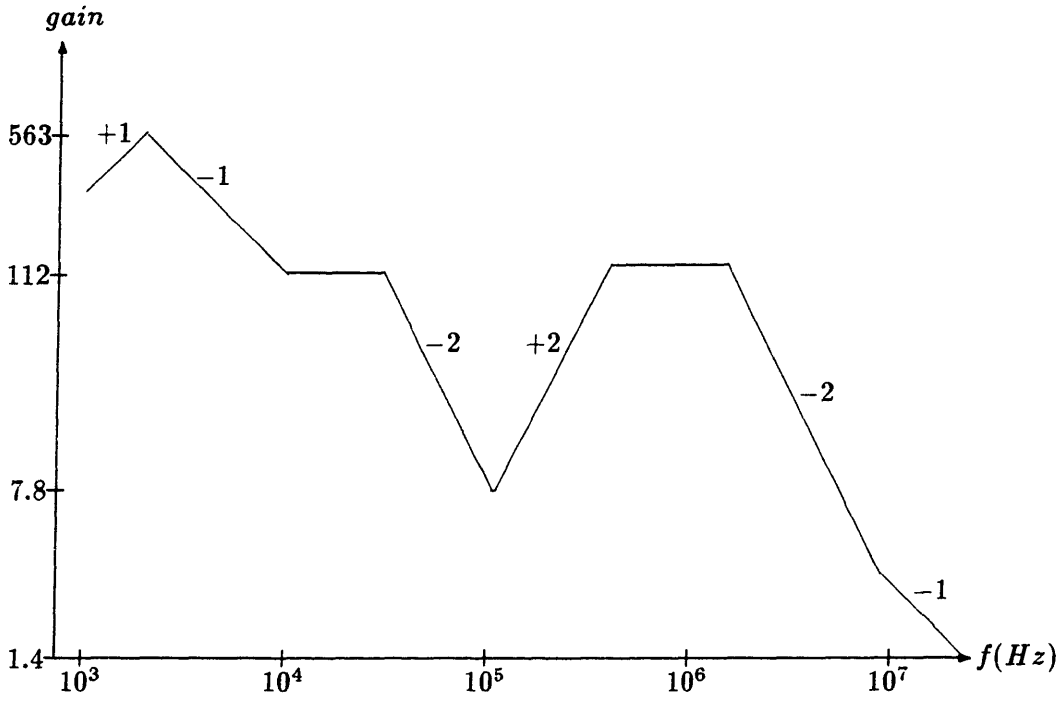

Figure 6-27: Bode plot of magnitude of compensated amplifier freqeuncy response

The resulting worst-case low frequency loop transmissions are shown in the magnitude and phase plots of Fig. 6-29 The worst phase margin is that of the DM LT with 200 μH

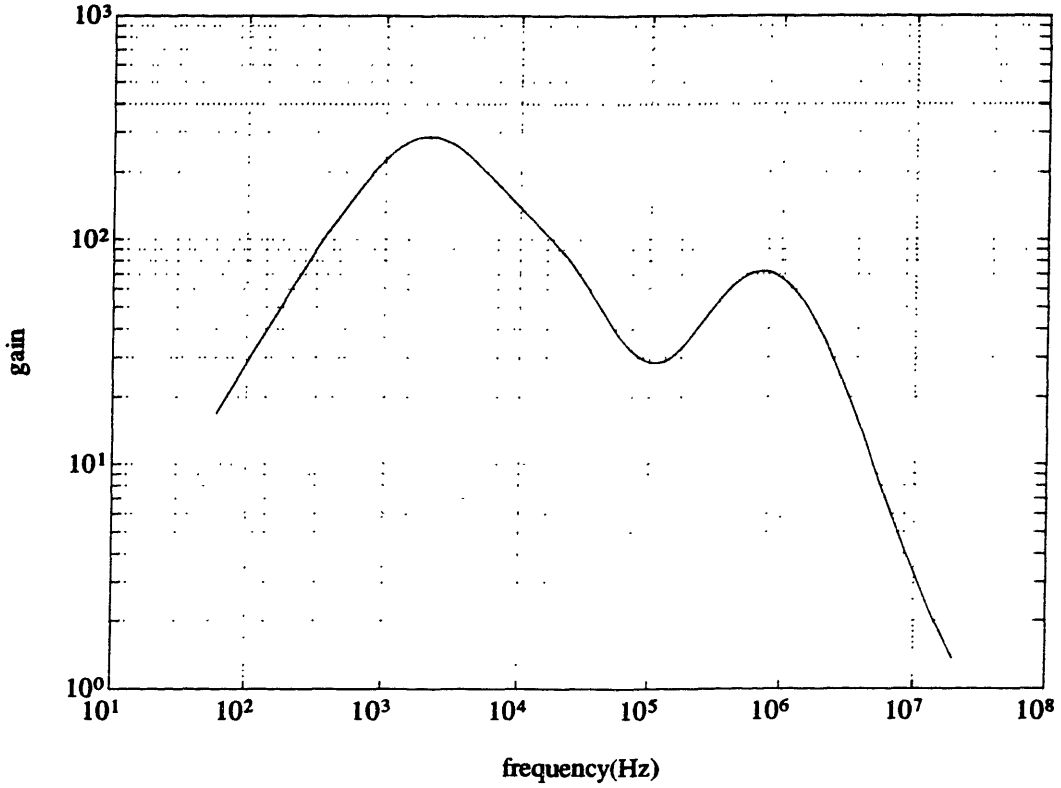

Figure 6-28: Compensated amplifier gain of 450 kHz alternate drive circuit

of external inductance, which is 27° at a UGC of 3.9 kHz. The damping of the resistance associated with this inductance, as mentioned earlier, would increase this phase margin. Otherwise the worst phase margins are 150-151° for the differential-mode, LISN case at 4.4 kHz and around 55 kHz.

It was shown in Section 6.1.2 that if the sense impedance is maintained either inductive or significantly larger than the line impedance, the high frequency LT is essentially the amplifier gain. After scaling the gain to account for the effects of lead compensation, as well as the high frequency lag and roll-off compensations, the nominal midband gain (i.e., what it would be without compensation) is actually 112, as shown in Fig. 6-27. Thus, with the factor of 6 of input lag compensation, the roll-off pole alone would result in a UGC of 28 MHz. Because of the greater uncertainty associated with parasitics at high frequencies, a good phase margin would be somewhat larger than the 30° accepted for the low frequency LT. For a phase margin of 45°, this amplifier must have its parasitic second pole at 20 MHz or higher.

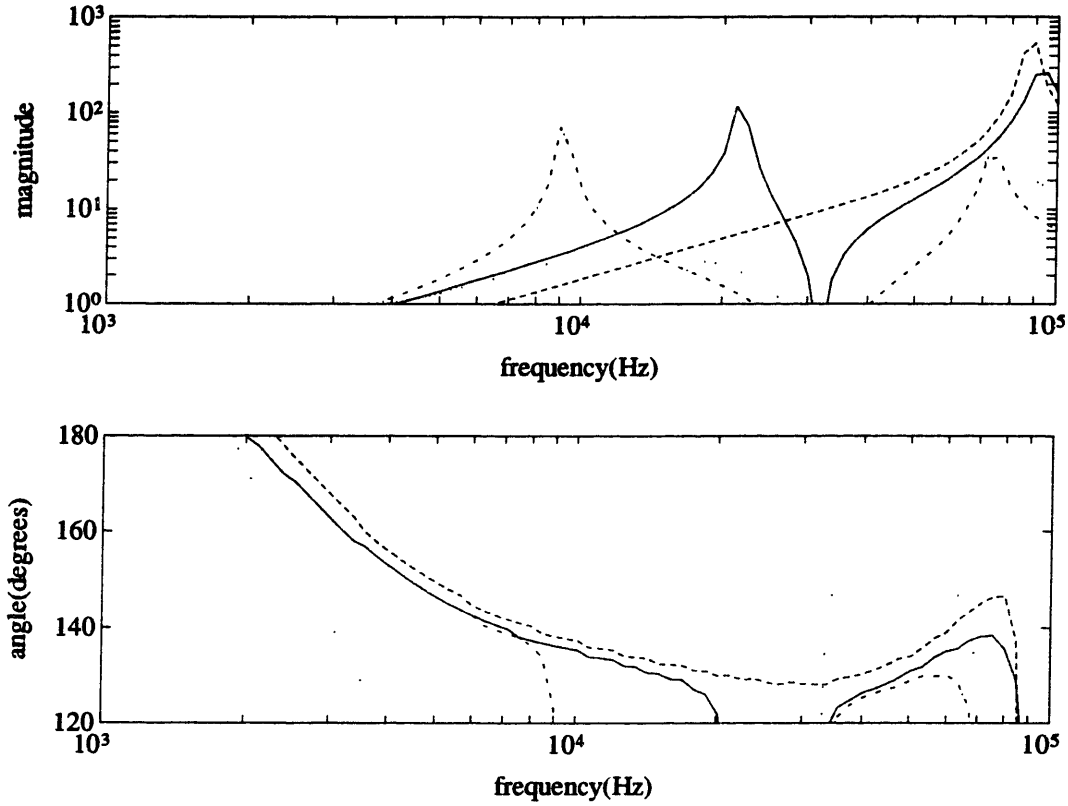

Figure 6-29: Compensated Worst-Case LT's for 450 kHz Alt. Dr.
solid line = DM, short-circuited external impedance
dashed line = CM, short-circuited external impedance
dotted line = DM, LISN + 100 μH external impedance
dash-dot line = DM, 200 μH external impedance

Power Frequency Rejection

The 0.25 μF capacitor limits the 60 Hz current through the amplifier output to a peak of 16 mA on a 120 Vrms utility connection. The other power frequency rejection issue is that of the output voltage on the amplifier due to the sensing of power frequency currents. Note that while the amplifier gain is quite large, on the order of 10$\sim$100 at the power transmission frequencies, the differential-mode sense inductance of each amplifier is quite small, at least compared to that of a 75 kHz version of this circuit. Thus, the transimpedance from power line input current to amplifier output voltage, as shown in Fig. 6-30, is quite reasonable. At 60 Hz, for example, 10 A of current drawn by the power supply results in 1.6 V at the output of the amplifier. At 300 Hz 0.5 A leads to 1 V at the output. Of course the amplifier will have to swing a few volts with the power cycle, but this should not be a problem.

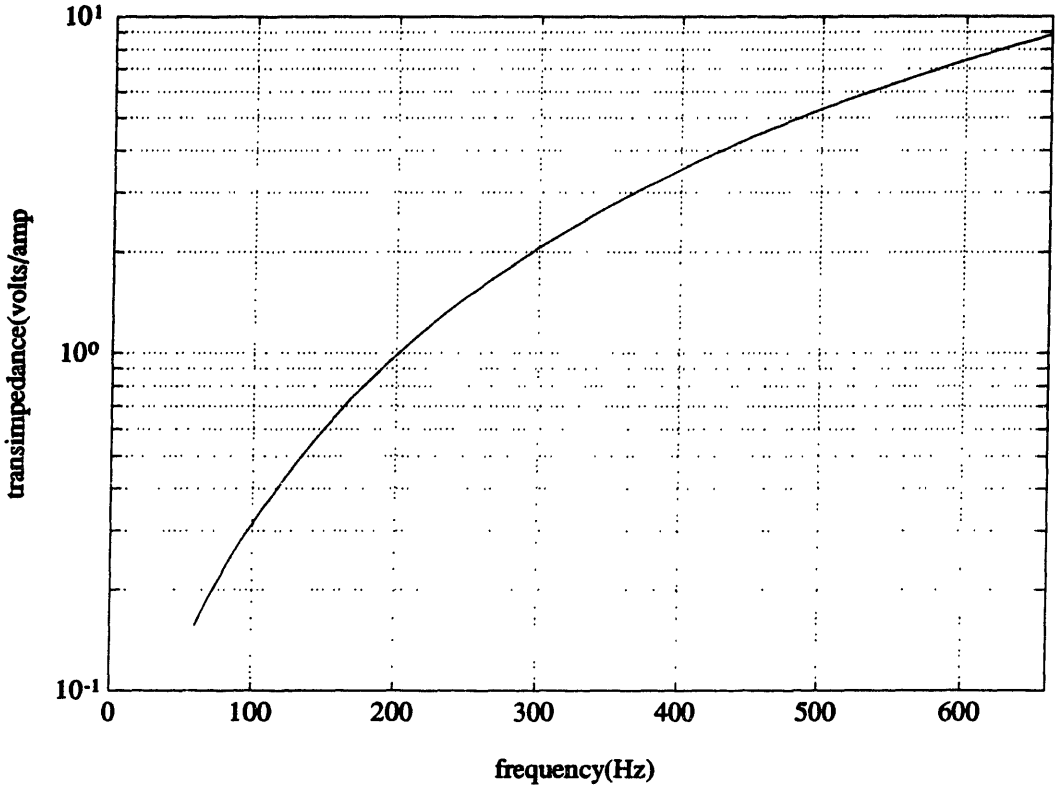

Figure 6-30: Transimpedance of 450 kHz alternate drive inductor enhancement circuit from line current to amplifier output

Attenuation

SPICE frequency response calculations were combined with the Matlab compensation to determine the attenuations of the filter. Figures 6-31 and 6-32 compare the differential-mode and common-mode attenuations, respectively, of the 450 kHz passive candidate filter to those of the proposed alternate drive active replacement. Because the common-mode active filter has the gain of the differential-mode without the reduction in filter order, the common-mode attenuation is significantly greater in the active filter than in the passive filter, exceeding it almost everywhere by 5 to 30 dB up until 30 MHz.

The differential-mode attenuation of the active filter matches that of the passive one at the switching frequency by design and increases by 50 dB per decade to about 2 MHz where it starts to fall off, coming back to the switching frequency value at 25 MHz. Note that the component-based attenuation would indicate that the passive DM filter has considerably better performance throughout the megaHertz range; based on the filter study

of Chapter 3, however, the low impedance of the differential-mode output capacitor and the greater leakage from the large 750 μH common-mode inductor would probably result in lesser attenuations limited by inductive coupling. In the active filter, the larger output impedance and the much smaller common-mode inductors, particularly the load-side one which carries substantial ripple current, should reduce inductive coupling substantially.

The SPICE code used to calculate these frequency responses is shown in Appendices C.7 and C.8 for the differential- and common-modes, respectively. Included are additional or modified definitions of subcircuits used in these calculations. These definitions show the parasitic models assumed for the components, which are mainly based on measurements

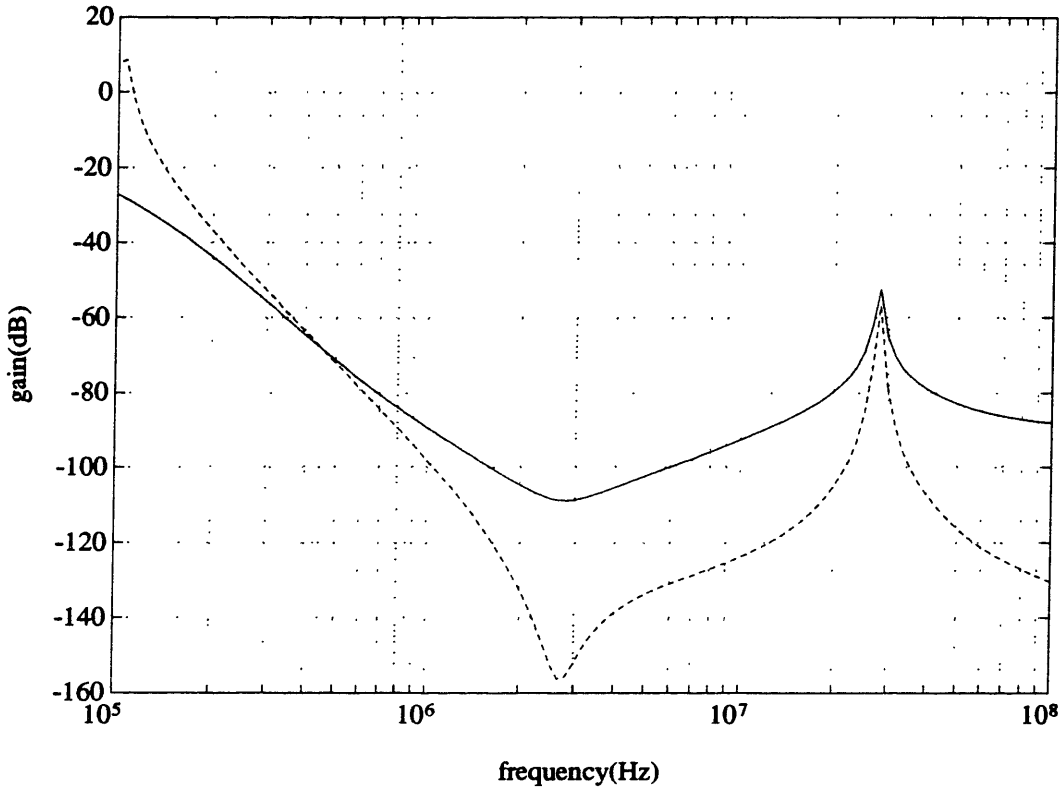

Figure 6-31: Component-based DM attenuation of 450 kHz passive filter (dashed line) and alternate drive active replacement (solid line)

from Chapter 3, and estimates of the scaling of the parasitic effects with component size. The parasitics associated with the capacitors are more likely to be accurate than those of the inductors, since [16] was used to determine typical characteristics of 'X' capacitors, and the 'Y' capacitors are the same as the one measured in Chapter 3. Also important is

the output impedance Z_{out} used in the attenuation simulations. This impedance, as well as those of the parasitic components, are critical to the high-frequency attenuation of the filter, since they become the dominant impedances of the circuit, although the parasitics are less important to the attenuation than in the passive filter. The resistive value of .05 Ω

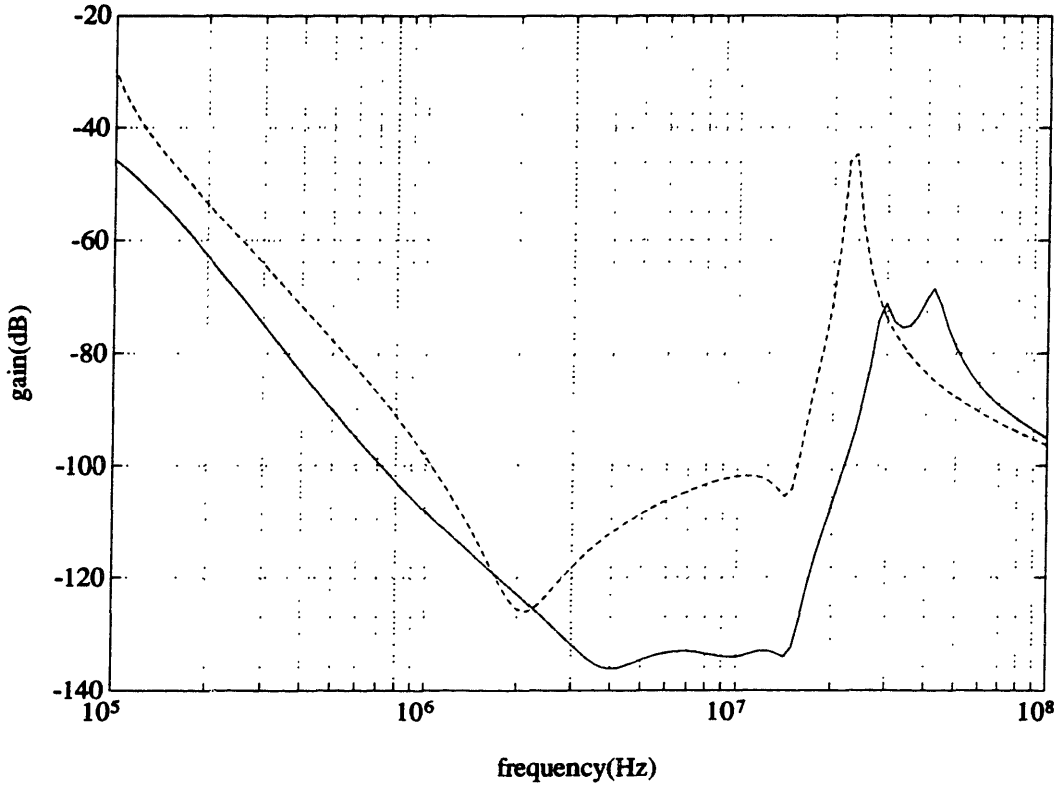

Figure 6-32: Component-based CM attenuation of 450 kHz passive filter (dashed line) and alternate drive active replacement (solid line)

assumed for the output impedance of each amplifier is quite low and it is not certain that this value can be maintained up to 30 MHz as the amplifier gain rolls off. For the most part, the high frequency attenuation of each mode of the filter was limited more by the parasitic inductance associated with the capacitance in series with the amplifier than by the amplifier's output impedance, but the attenuation due to the actual amplifier output impedance needs to be considered if this circuit is to be implemented.

6.7 Conclusion

The standard drive and alternate drive inductor enhancement topologies have been analyzed, with attempts made to apply these two circuits to the utility interface of a switch-mode power supply operating at a frequency of 75 kHz. Because of the the characteristics of the variable line impedance and the second-order nature of the L-C networks of each of these filters, compensation of the feedback loop of each active circuit was difficult to achieve with good phase margin throughout the low-frequency rise of the loop transmission, and with sufficient immunity to power frequency voltages and currents.

A study of the nature of these problems indicated that they would be less severe for higher switching frequencies. This fact was demonstrated by an example of an alternate-drive enhancement circuit for a switching frequency of 450 kHz. Compared to a passive filter with equivalent or worse attenuation at the fundamental frequency, the active enhancement halved the differential-mode capacitance and cut the total common-mode inductance by a factor of 3.3. Since these components dominated the filter's volume, filter size may be substantially reduced by active enhancement. The realization of this size, as well as cost, reduction also depends on the solution to the problem of providing power for the active circuitry.

Chapter 7

Conclusion

This thesis proposes a broad scientific approach to the problem of effective and efficient EMI reduction in switching power supplies. This approach involves the acquisition of practical knowledge through investigation and analysis, verification by experimentation, and the development of design processes to make use of results. The design processes would combine the knowledge base and the instrumentation in a CAD package or an 'expert system'.

The work in this thesis was aimed at developing some of the knowledge-base to understand EMI and the performance of EMI filters, as well as instrumentation, to measure both filters and power supplies. While several distinct projects were undertaken, they were all fundamentally related. The EMI filter measurement work of Chapter 3 led to an understanding of the influence of component and layout parasitics on the performance of EMI filters. Results relating problems of the filter at high frequencies to the largest components in the filter made a strong case for active filtering to enhance smaller components at low frequencies. The analysis of active filters, however, showed that the problem of low frequency compensation, particularly with the variable utility impedance in the feedback loop and with the need to bring the gain down at the ac power frequencies, limits their usefulness to switching frequencies of a few hundred kiloHertz. For the case of 450 kHz considered, active enhancement using the 'alternate drive' technique allowed elimination of a differential-mode output capacitor, shown earlier to be partly responsible for inductive coupling which ruins attenuation, and reduced by a factor of 7.5 the high-ripple-carrying common-mode inductor, suspected to be a major source of inductive coupling, in addition to halving the other common-mode inductor. Depending on the power frequency harmonic

content of the current waveform of the power supply and the amount of compensation that can be implemented at a low cost (using I.C. technology), some further component reductions would be possible. For both passive and active filtering, design optimization has been shown to require knowledge of the common-mode source impedance, as well as the source value, thus motivating the work of Chapter 4 on power supply EMI source measurement.

Appendix A

High Frequency Line Impedance Data

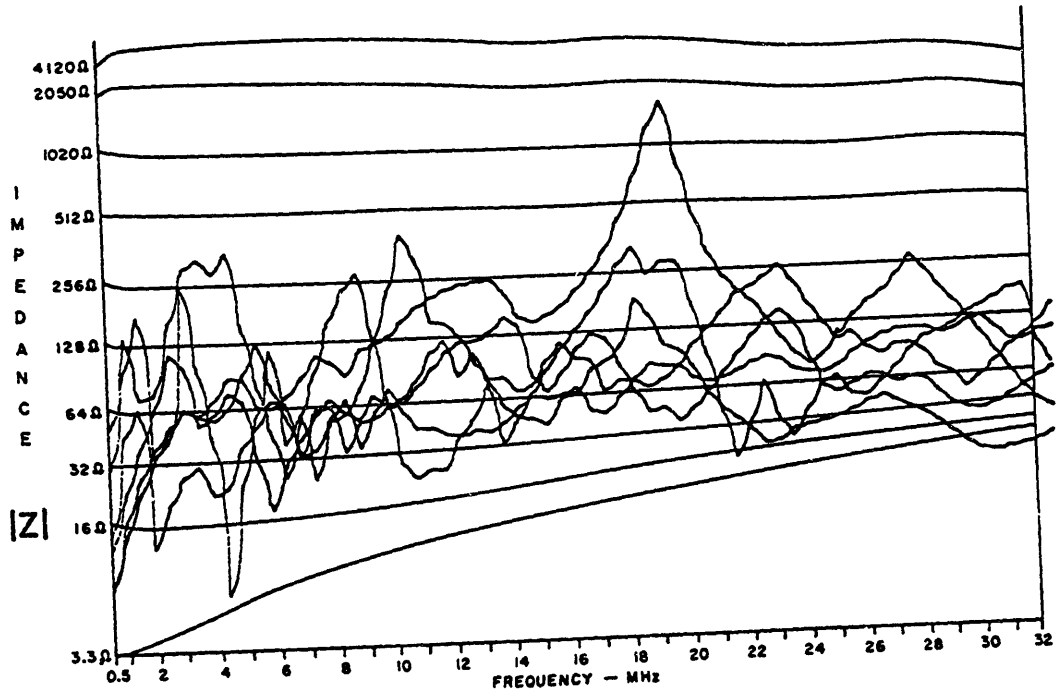

Figure A-1: High frequency measurements of impedance of single phase power line measured at several different outlets of a research building in San Antonio, Texas (taken from [23])

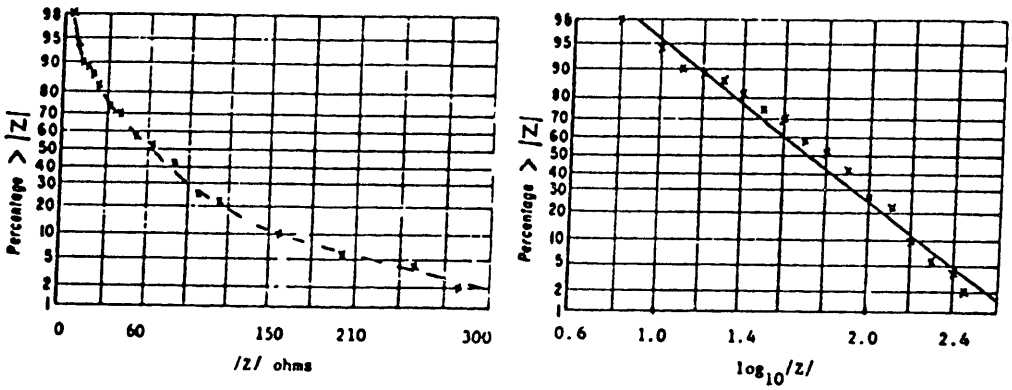

Figure A-2: U.K. mains impedance measurements results at 2 MHz: comparison of distribution of values on probability graphs with linear and logarithmic impedance scales (taken from [24])

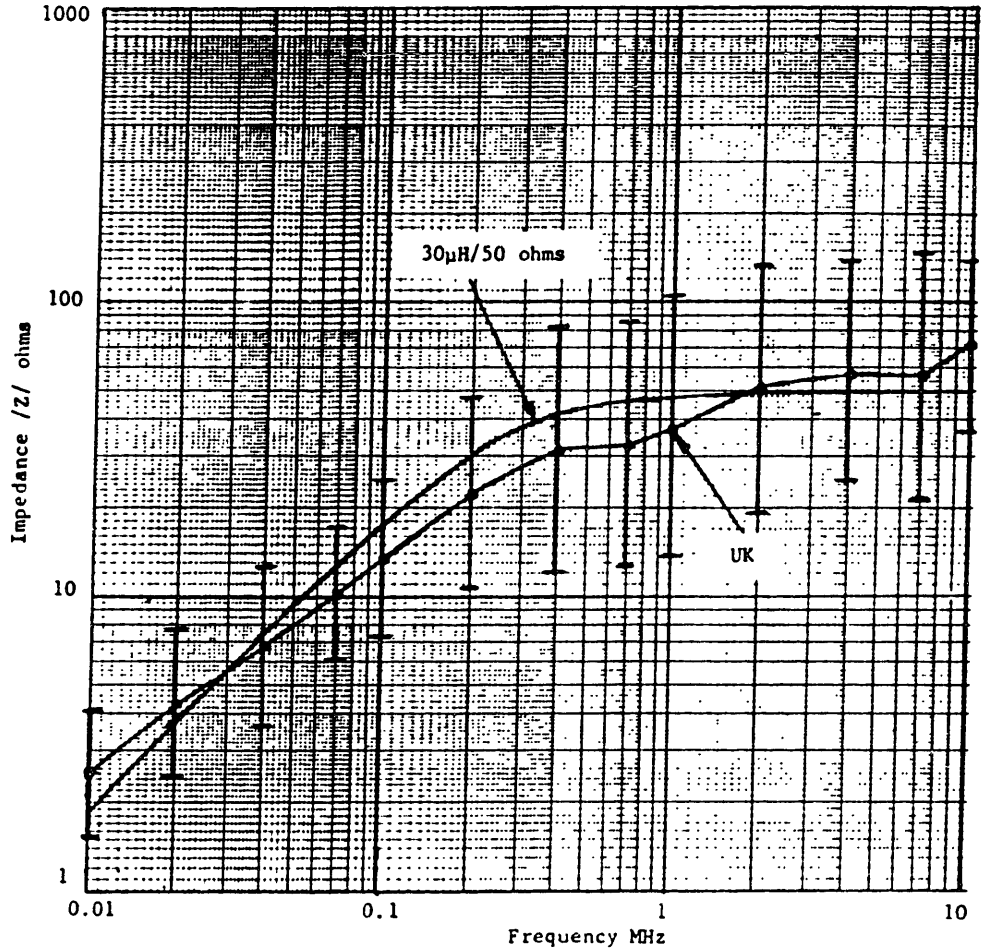

Figure A-3: Mean values of U.K.- mains impedance measurements (with spreads indicated by one standard deviation) compared with characteristic of 30 μH / 50 Ω network (taken from [24])

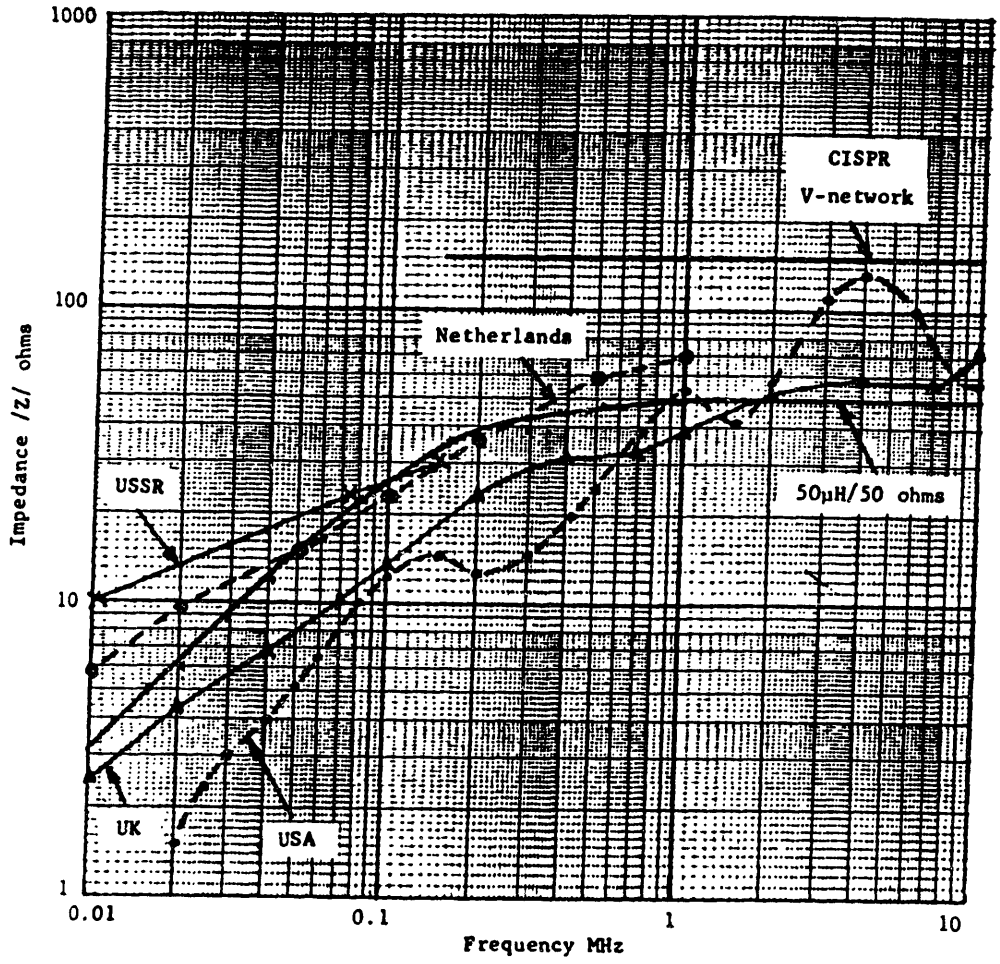

Figure A-4: Mean mains impedance characteristics from UK, USA, USSR, and Netherlands results measurement results compared with 30 μH / 50 Ω and CISPR measurement networks (taken from [24])

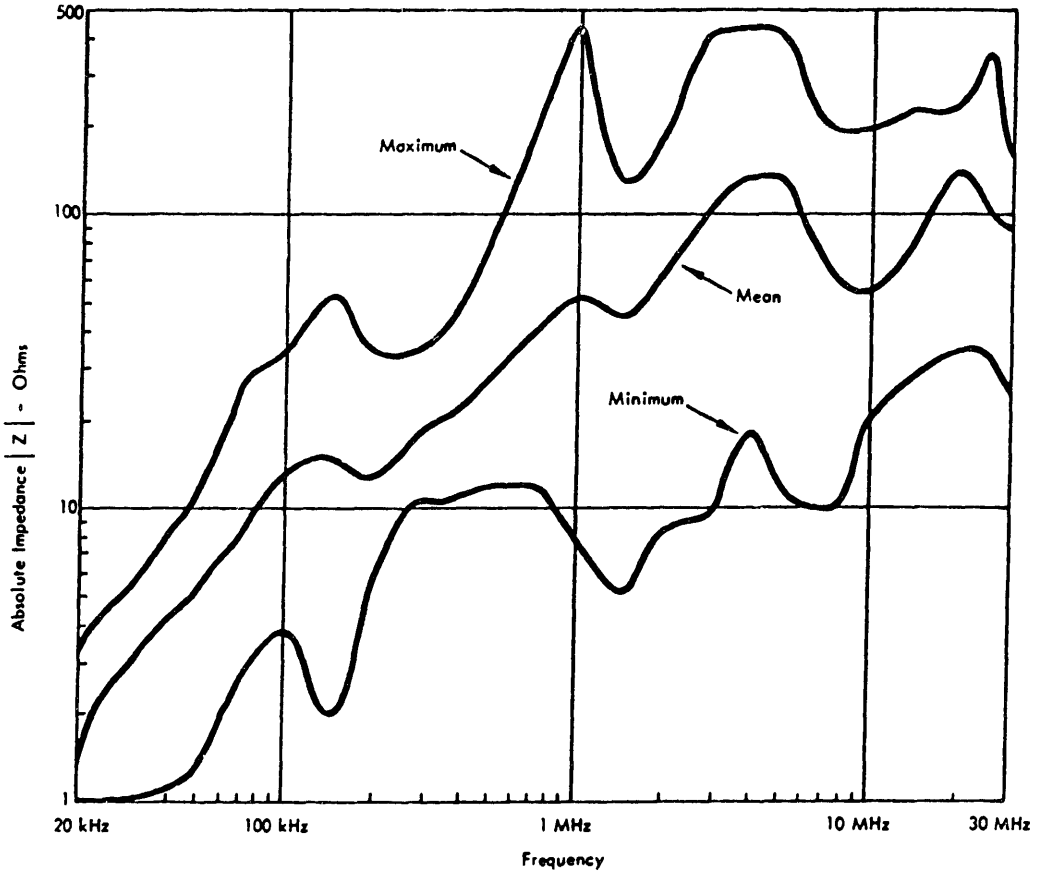

Figure A-5: Mean, maximum, and minimum of power line impedance measured at 36 commercial (U.S.) sites (taken from [21])

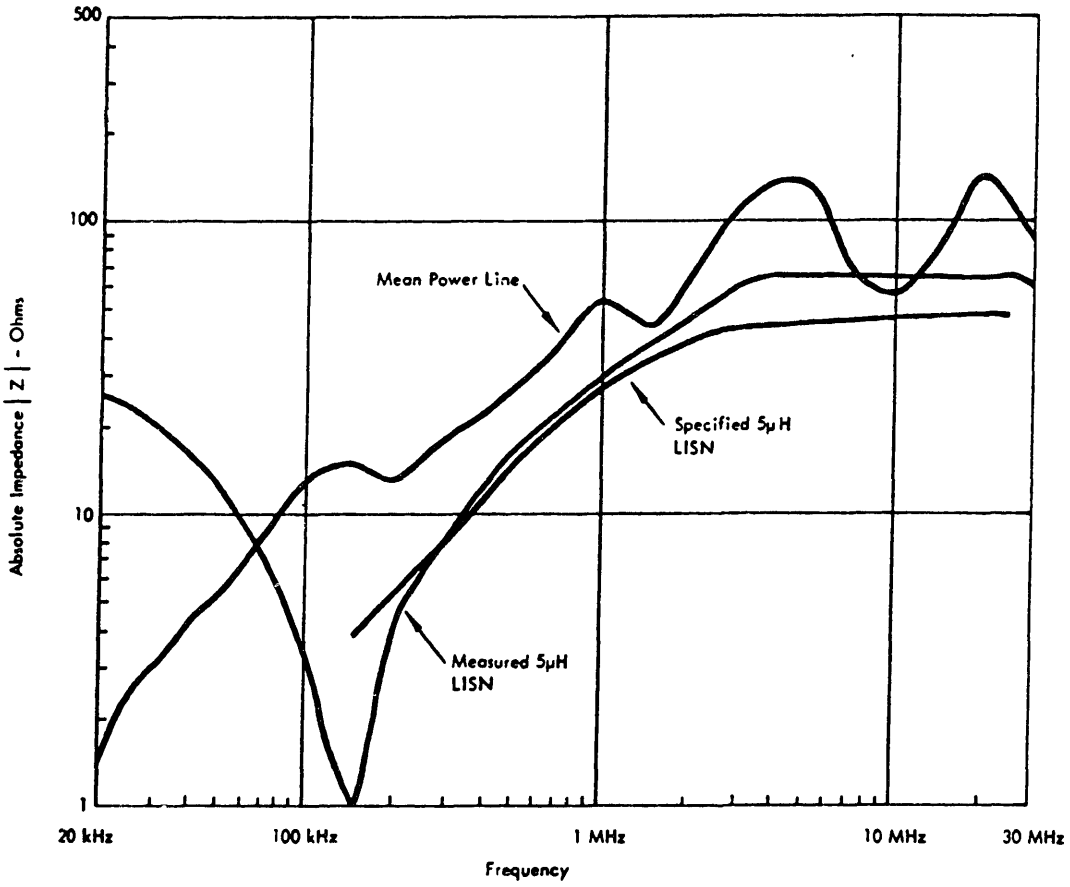

Figure A-6: Mean of power line impedance measured at 36 commercial (U.S.) sites compared with LISN network (taken from [21])

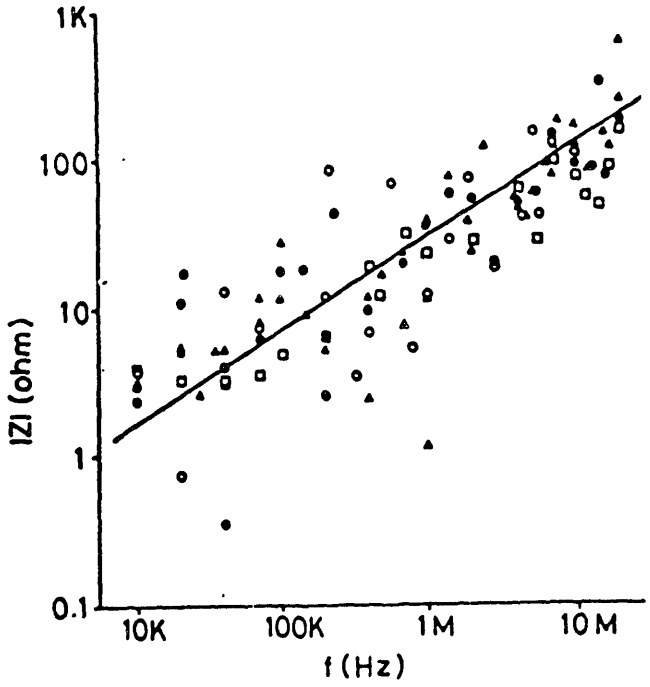

Figure A-7: Measurements of power line impedance at outlets in a research building in Japan (taken from [25])

Appendix B

Simulations of Second-order 75 kHz Standard Drive Circuit

B.1 Subcircuit Definitions

```
*** LISN Network as seen from EMI filter ***
*** (L3 connection to ac line is left open to add line impedance) ***

       .SUBCKT LISN 1 6 7
       C1 1 2 1.68U
       RDC1 1 2 1G
       C2 2 3 1.68U
       RDC2 2 3 1G
       L1 2 6 .002
       RM 3 6 50
       L2 1 4 50U
       C3 4 5 8U
       RDC3 4 5 1G
       R3 5 6 5
       L3 4 7 250U
       C4 7 6 2U
       RDC4 7 6 1G
       .ENDS LISN


*** Non-inverting Amplifier with Compensation Subcircuits **

       .SUBCKT COMPCAP 1 2
       CCOMP 1 2 159.15U
```

```
RDCPATH 1 2 100MEG
.ENDS COMPCAP

* dc zero & 400Hz pole
.SUBCKT DCCOMP1 1 2 3
XC1 1 4 COMPCAP
R1 4 2 2.5
E1 3 2 4 2 1
.ENDS DCCOMP1

* dc zero & 250Hz pole
* (may be replaced by Twin-T for 60 Hz rejection)
.SUBCKT DCCOMP2 1 2 3
XC1 1 4 COMPCAP
R1 4 2 4
E1 3 2 4 2 1
.ENDS DCCOMP2

* lag compensation to be applied around diff. mode low freq. UGC
* .54kHz-1.8kHz (factor of 3.3 centered at 1kHz)
.SUBCKT LAG33 1 2 3
R3 1 4 1.26
XC3 4 5 COMPCAP
R3A 5 2 0.55
E3 3 2 4 2 3.29
.ENDS LAG33

* lag compensation to be applied around diff. mode low freq. UGC
* 2.5kHz-8.2kHz (factor of 3.3 centered at 4.5kHz)
.SUBCKT LAG33C 1 2 3
R3 1 4 0.28
XC3 4 5 COMPCAP
R3A 5 2 0.123
E3 3 2 4 2 3.28
.ENDS LAG33C

* lag compensation to be applied around diff. mode low freq. UGC
* 3.7kHz-5.5kHz (factor of 1.5 centered at 4.5kHz)
.SUBCKT LAG15C 1 2 3
R3 1 4 0.09
XC3 4 5 COMPCAP
R3A 5 2 0.18
E3 3 2 4 2 1.5
.ENDS LAG15C

* lag compensation to be applied around diff. mode low freq. UGC
* .95kHz-2.4kHz (factor of 2.5 centered at 1.5kHz)
.SUBCKT LAG25 1 2 3
```

```
R3 1 4 0.625
XC3 4 5 COMPCAP
R3A 5 2 0.417
E3 3 2 4 2 2.47
.ENDS LAG25


* lead compensation to raise midband gain relative to 60 Hz gain
* 10kHz-20kHz (factor of about 2 centered around ~14kHz)
.SUBCKT LEAD2 1 2 3
R5 1 4 0.1
XC5 1 4 COMPCAP
R5A 4 2 0.1
E5 3 2 4 2 1
.ENDS LEAD2

* lead compensation to raise midband gain relative to 60 Hz gain
* 10kHz-30kHz (factor of about 3 centered around ~18kHz)
.SUBCKT LEAD3 1 2 3
R5 1 4 0.1
XC5 1 4 COMPCAP
R5A 4 2 0.05
E5 3 2 4 2 1
.ENDS LEAD3

* lead compensation to raise midband gain relative to 60 Hz gain
* 40kHz-80kHz (factor of about 2 centered around ~56kHz)
.SUBCKT LEAD2H 1 2 3
R5 1 4 0.025
XC5 1 4 COMPCAP
R5A 4 2 0.025
E5 3 2 4 2 1
.ENDS LEAD2H

* lead compensation to raise midband gain relative to 60 Hz gain
* 13kHz-20kHz (factor of about 1.5 centered around ~16kHz)
.SUBCKT LEAD15L 1 2 3
R5 1 4 0.075
XC5 1 4 COMPCAP
R5A 4 2 0.15
E5 3 2 4 2 1
.ENDS LEAD15L

* lead compensation to raise midband gain relative to 60 Hz gain
* 9.3kHz-83kHz (factor of about 9 centered around ~28 kHz)
.SUBCKT LEAD9 1 2 3
R5 1 4 0.108
XC5 1 4 COMPCAP
```

```
R5A 4 2 0.0135
E5 3 2 4 2 1
.ENDS LEAD9


* high-frequency roll-off compensation pole at 200kHz
.SUBCKT ROLLOFF 1 2 3
R6 1 4 0.005
XC6 4 2 COMPCAP
E6 3 2 4 2 1
.ENDS ROLLOFF

* buffer to fill space for deleted compensation subcircuits
.SUBCKT BUFFER 1 2 3
RBIG1 1 2 1G
RBIG2 3 2 1G
EBUFFER 3 2 1 2 1
.ENDS BUFFER

** Amplifier input impedance and high frequency lag comp. network
*** Pole at550kHz, zero at 4mHz
.SUBCKT INCOMP 1 2 3
RC 1 3 19.5K
CC 1 3 2P
RIN 3 2 500K
CIN 3 2 15P
.ENDS INCOMP

* main amplifier subcircuit
.SUBCKT AMP 1 2 3 4
XINHI 1 5 6 INCOMP
XINLO 2 5 7 INCOMP
EGAIN 8 4 6 7 600
XCOMP1 8 4 9 DCCOMP1
XCOMP2 9 4 10 DCCOMP1
XCOMP3 10 4 11 DCCOMP2
XCOMP4 11 4 12 LEAD9
XCOMP5 12 4 13 LEAD9
XCOMP6 13 4 14 LEAD3
XCOMP7 14 4 15 LEAD2
XCOMP8 15 4 16 LEAD15L
XCOMP9 16 4 17 LEAD2H
XCOMP10 17 4 18 LAG33C
XCOMP11 18 4 19 LAG33C
XCOMP12 19 4 20 LAG33
XCOMP13 20 4 21 LAG33
XCOMP14 21 4 22 LAG25
XCOMP15 22 4 23 LAG15C
```

```
        XCOMP16 23 4 24 ROLLOFF
        XCOMP17 24 4 25 BUFFER
        XCOMP18 25 4 26 BUFFER
        XCOMP19 26 4 3 BUFFER
        .ENDS AMP
        * Note XCOMP14 could be combined with XCOMP10 or XCOMP11

** Components with parasitics ****

        .SUBCKT IND50 1 3
        LIDEAL 1 2 50U
        RWIRE 2 3 .025
        RCORE 1 3 1.5K
        CWIND 1 3 1P
        .ENDS IND50

        .SUBCKT IND25 1 3
        LIDEAL 1 2 25U
        RWIRE 2 3 .012
        RCORE 1 3 1K
        CWIND 1 3 1P
        .ENDS IND25

        .SUBCKT IND200 1 5
        XL1 1 2 IND50
        XL2 2 3 IND50
        XL3 3 4 IND50
        XL4 4 5 IND50
        .ENDS IND200

        .SUBCKT CAP5N 1 2
        CIDEAL 1 3 4.7N
        RDCPATH 1 3 100MEG
        RSERIES 3 4 0.3
        LSERIES 4 2 25N
        .ENDS CAP5N

        .OPTIONS LIMPTS=1000

        .SUBCKT RIPVOLT 1 2
        VSW 1 2 AC 1
        RVSW 1 2 100MEG
        .ENDS RIPVOLT

        .SUBCKT ZPOWSUP 1 2
        CBULK 1 3 4.4U
        XCCM1 1 5 CAP5N
        XCCM2 2 5 CAP5N
```

```
CEXTRA 1 6 100N
RCEXTRA 6 2 0.05
RCBULK 3 2 .05
RSW 1 2 10000
.ENDS ZPOWSUP
```

B.2 Amplifier Gain and Low Frequency DM LT With Short-Circuit as External Impedance

```
    *** 4.4uF cap. inside rectifier, Ls=200uH, Ld=50uH, Zout=.25 , A=600
    *** Line impedance = short circuit

*** MAIN CIRCUIT DEFINITION **********************

   .OPTIONS NUMDGT=3 LIMPTS=1000

   XPSIMP 1 0 ZPOWSUP
   XLD 1 2 IND50
   ROUT 1 3 .25
   XVSW 7 8 RIPVOLT
   RDCPATH 8 0 1G
   XAMP 7 8 2 3 AMP
   XLS 2 5 IND200
   RZLINE  5 0 .0001

  .AC DEC 20 50 20MEG
  .PRINT AC VM(2,3) VP(2,3) VM(2,5) VP(2,5)

  .END


** V(2,3) columns are mag. and phase of amplifier gain
** V(2,5) columns are mag. and phase of DM LT

     FREQ        VM(2,3)    VP(2,3)    VM(2,5)    VP(2,5)
X

  5.000E+01     5.11E-01  -1.25E+02   9.17E-06   2.15E+01
  5.610E+01     7.14E-01  -1.30E+02   1.54E-05   2.34E+01
  6.295E+01     9.94E-01  -1.34E+02   2.61E-05   2.49E+01
  7.063E+01     1.38E+00  -1.40E+02   4.47E-05   2.60E+01
  7.924E+01     1.91E+00  -1.46E+02   7.72E-05   2.64E+01
```

8.891E+01	2.62E+00	-1.52E+02	1.34E-04	2.62E+01	
9.976E+01	3.58E+00	-1.59E+02	2.35E-04	2.50E+01	
1.119E+02	4.85E+00	-1.67E+02	4.13E-04	2.28E+01	
1.256E+02	6.51E+00	-1.76E+02	7.28E-04	1.95E+01	
1.409E+02	8.65E+00	1.75E+02	1.28E-03	1.50E+01	
1.581E+02	1.13E+01	1.64E+02	2.25E-03	9.17E+00	
1.774E+02	1.46E+01	1.53E+02	3.90E-03	1.99E+00	
1.991E+02	1.85E+01	1.41E+02	6.71E-03	-6.54E+00	
2.233E+02	2.29E+01	1.28E+02	1.14E-02	-1.64E+01	
2.506E+02	2.78E+01	1.15E+02	1.88E-02	-2.75E+01	
2.812E+02	3.28E+01	1.00E+02	3.06E-02	-3.97E+01	
3.155E+02	3.77E+01	8.59E+01	4.83E-02	-5.30E+01	
3.540E+02	4.20E+01	7.09E+01	7.41E-02	-6.71E+01	
3.972E+02	4.54E+01	5.58E+01	1.10E-01	-8.19E+01	
4.456E+02	4.75E+01	4.08E+01	1.58E-01	-9.71E+01	
5.000E+02	4.82E+01	2.60E+01	2.20E-01	-1.12E+02	
5.610E+02	4.73E+01	1.17E+01	2.95E-01	-1.28E+02	
6.295E+02	4.51E+01	-1.86E+00	3.83E-01	-1.43E+02	
7.063E+02	4.17E+01	-1.46E+01	4.80E-01	-1.57E+02	
7.924E+02	3.77E+01	-2.62E+01	5.84E-01	-1.70E+02	
8.891E+02	3.32E+01	-3.66E+01	6.91E-01	1.77E+02	
9.976E+02	2.87E+01	-4.57E+01	7.98E-01	1.66E+02	
1.119E+03	2.44E+01	-5.33E+01	9.03E-01	1.56E+02	
1.256E+03	2.04E+01	-5.95E+01	1.00E+00	1.47E+02	<< l.f. UGC
1.409E+03	1.70E+01	-6.41E+01	1.10E+00	1.40E+02	
1.581E+03	1.40E+01	-6.73E+01	1.20E+00	1.35E+02	
1.774E+03	1.15E+01	-6.89E+01	1.31E+00	1.31E+02	
1.991E+03	9.49E+00	-6.90E+01	1.43E+00	1.29E+02	
2.233E+03	7.82E+00	-6.76E+01	1.58E+00	1.28E+02	
2.506E+03	6.47E+00	-6.47E+01	1.77E+00	1.29E+02	
2.812E+03	5.39E+00	-6.04E+01	2.03E+00	1.31E+02	
3.155E+03	4.54E+00	-5.47E+01	2.41E+00	1.35E+02	
3.540E+03	3.87E+00	-4.75E+01	3.04E+00	1.40E+02	
3.972E+03	3.35E+00	-3.90E+01	4.20E+00	1.45E+02	
4.456E+03	2.96E+00	-2.91E+01	6.99E+00	1.50E+02	
5.000E+03	2.67E+00	-1.80E+01	1.95E+01	1.42E+02	
5.610E+03	2.48E+00	-5.76E+00	1.96E+01	2.87E+01	
6.295E+03	2.38E+00	7.38E+00	7.89E+00	2.37E+01	
7.063E+03	2.35E+00	2.12E+01	5.29E+00	3.29E+01	
7.924E+03	2.42E+00	3.53E+01	4.32E+00	4.47E+01	
8.891E+03	2.58E+00	4.95E+01	3.97E+00	5.73E+01	
9.976E+03	2.86E+00	6.34E+01	3.96E+00	7.01E+01	
1.119E+04	3.28E+00	7.67E+01	4.21E+00	8.25E+01	
1.256E+04	3.90E+00	8.90E+01	4.73E+00	9.40E+01	
1.409E+04	4.77E+00	1.00E+02	5.54E+00	1.04E+02	
1.581E+04	5.99E+00	1.10E+02	6.73E+00	1.14E+02	
1.774E+04	7.67E+00	1.18E+02	8.40E+00	1.21E+02	
1.991E+04	9.97E+00	1.24E+02	1.07E+01	1.27E+02	

2.233E+04	1.31E+01	1.29E+02	1.39E+01	1.31E+02	
2.506E+04	1.73E+01	1.31E+02	1.81E+01	1.34E+02	
2.812E+04	2.29E+01	1.33E+02	2.37E+01	1.35E+02	
3.155E+04	3.02E+01	1.32E+02	3.10E+01	1.34E+02	
3.540E+04	3.96E+01	1.30E+02	4.04E+01	1.32E+02	
3.972E+04	5.15E+01	1.27E+02	5.24E+01	1.28E+02	
4.456E+04	6.62E+01	1.22E+02	6.71E+01	1.23E+02	
5.000E+04	8.40E+01	1.16E+02	8.49E+01	1.17E+02	
5.610E+04	1.05E+02	1.09E+02	1.06E+02	1.10E+02	
6.295E+04	1.29E+02	1.01E+02	1.30E+02	1.02E+02	
7.063E+04	1.55E+02	9.19E+01	1.56E+02	9.27E+01	
7.924E+04	1.83E+02	8.21E+01	1.83E+02	8.28E+01	
8.891E+04	2.10E+02	7.16E+01	2.11E+02	7.23E+01	
9.976E+04	2.37E+02	6.07E+01	2.37E+02	6.13E+01	
1.119E+05	2.61E+02	4.95E+01	2.61E+02	5.00E+01	
1.256E+05	2.80E+02	3.81E+01	2.80E+02	3.86E+01	
1.409E+05	2.94E+02	2.66E+01	2.94E+02	2.70E+01	
1.581E+05	3.02E+02	1.51E+01	3.02E+02	1.55E+01	<< h.f. UGC
1.774E+05	3.04E+02	3.78E+00	3.04E+02	4.11E+00	
1.991E+05	3.00E+02	-7.34E+00	3.00E+02	-7.05E+00	
2.233E+05	2.90E+02	-1.82E+01	2.90E+02	-1.79E+01	
2.506E+05	2.75E+02	-2.87E+01	2.75E+02	-2.85E+01	
2.812E+05	2.57E+02	-3.88E+01	2.57E+02	-3.86E+01	
3.155E+05	2.36E+02	-4.86E+01	2.36E+02	-4.84E+01	
3.540E+05	2.13E+02	-5.78E+01	2.13E+02	-5.77E+01	
3.972E+05	1.90E+02	-6.66E+01	1.90E+02	-6.65E+01	
4.456E+05	1.67E+02	-7.49E+01	1.67E+02	-7.47E+01	
5.000E+05	1.45E+02	-8.26E+01	1.45E+02	-8.25E+01	
5.610E+05	1.25E+02	-8.98E+01	1.25E+02	-8.97E+01	
6.295E+05	1.06E+02	-9.63E+01	1.06E+02	-9.62E+01	
7.063E+05	8.94E+01	-1.02E+02	8.94E+01	-1.02E+02	
7.924E+05	7.48E+01	-1.08E+02	7.47E+01	-1.08E+02	
8.891E+05	6.21E+01	-1.12E+02	6.20E+01	-1.12E+02	
9.976E+05	5.12E+01	-1.16E+02	5.12E+01	-1.16E+02	
1.119E+06	4.21E+01	-1.20E+02	4.21E+01	-1.20E+02	
1.256E+06	3.45E+01	-1.23E+02	3.45E+01	-1.23E+02	
1.409E+06	2.82E+01	-1.25E+02	2.82E+01	-1.25E+02	
1.581E+06	2.31E+01	-1.27E+02	2.31E+01	-1.27E+02	
1.774E+06	1.88E+01	-1.28E+02	1.88E+01	-1.28E+02	
1.991E+06	1.54E+01	-1.28E+02	1.54E+01	-1.28E+02	
2.233E+06	1.26E+01	-1.28E+02	1.26E+01	-1.28E+02	
2.506E+06	1.04E+01	-1.28E+02	1.04E+01	-1.28E+02	
2.812E+06	8.60E+00	-1.27E+02	8.59E+00	-1.27E+02	
3.155E+06	7.13E+00	-1.26E+02	7.13E+00	-1.26E+02	
3.540E+06	5.95E+00	-1.24E+02	5.95E+00	-1.24E+02	
3.972E+06	5.00E+00	-1.23E+02	5.00E+00	-1.23E+02	
4.456E+06	4.22E+00	-1.21E+02	4.22E+00	-1.21E+02	
5.000E+06	3.59E+00	-1.19E+02	3.59E+00	-1.19E+02	

5.610E+06	3.07E+00	-1.17E+02	3.07E+00	-1.17E+02
6.295E+06	2.64E+00	-1.15E+02	2.64E+00	-1.15E+02
7.063E+06	2.28E+00	-1.13E+02	2.28E+00	-1.13E+02
7.924E+06	1.98E+00	-1.11E+02	1.98E+00	-1.11E+02
8.891E+06	1.73E+00	-1.09E+02	1.73E+00	-1.09E+02
9.976E+06	1.51E+00	-1.07E+02	1.51E+00	-1.07E+02
1.119E+07	1.33E+00	-1.05E+02	1.33E+00	-1.05E+02
1.256E+07	1.17E+00	-1.04E+02	1.17E+00	-1.04E+02
1.409E+07	1.03E+00	-1.02E+02	1.03E+00	-1.02E+02
1.581E+07	9.12E-01	-1.01E+02	9.12E-01	-1.01E+02
1.774E+07	8.08E-01	-1.00E+02	8.08E-01	-1.00E+02
1.991E+07	7.17E-01	-9.90E+01	7.16E-01	-9.90E+01
2.233E+07	6.36E-01	-9.80E+01	6.36E-01	-9.80E+01

B.3 Low Freq. DM LT with LISN + 4 Ω Ext. Imp.

```
*** 4.4uF cap. inside rectifier, Ls=200uH, Ld=50uH, Zout=.667, A=550
*** LINE IMPEDANCE = 2 series-connected LISN networks + 4 ohms

*** MAIN CIRCUIT DEFINITION **********************

.OPTIONS NUMDGT=3 LIMPTS=1000

XPSIMP 1 0 ZPOWSUP
Xld 1 2 IND50
ROUT 1 3 .25
XVSW 7 8 RIPVOLT
RDCPATH 8 0 1G
XAMP 7 8 2 3 AMP
XLS 2 5 IND200
XZX1 5 6 11 LISN
XZX2 0 6 12 LISN
RZLINE 11 13 4
LZLINE 13 12 0.001U

.AC DEC 20 500 200K
.PRINT AC VM(2,3) VP(2,3) VM(2,5) VP(2,5)

.END

** V(2,3) columns are mag. and phase of amplifier gain
** V(2,5) columns are mag. and phase of DM LT
```

FREQ	VM(2,3)	VP(2,3)	VM(2,5)	VP(2,5)	X
5.000E+02	4.82E+01	2.60E+01	2.25E-01	-1.16E+02	
5.610E+02	4.73E+01	1.17E+01	3.03E-01	-1.32E+02	
6.295E+02	4.51E+01	-1.86E+00	3.96E-01	-1.47E+02	
7.063E+02	4.17E+01	-1.46E+01	5.01E-01	-1.62E+02	
7.924E+02	3.77E+01	-2.62E+01	6.16E-01	-1.77E+02	
8.891E+02	3.32E+01	-3.66E+01	7.40E-01	1.70E+02	
9.976E+02	2.87E+01	-4.57E+01	8.69E-01	1.57E+02	
1.119E+03	2.44E+01	-5.33E+01	1.01E+00	1.45E+02	
1.256E+03	2.04E+01	-5.95E+01	1.15E+00	1.34E+02	
1.409E+03	1.70E+01	-6.41E+01	1.30E+00	1.23E+02	
1.581E+03	1.40E+01	-6.73E+01	1.46E+00	1.13E+02	
1.774E+03	1.15E+01	-6.89E+01	1.60E+00	1.01E+02	
1.991E+03	9.49E+00	-6.90E+01	1.65E+00	9.12E+01	
2.233E+03	7.82E+00	-6.76E+01	1.71E+00	8.52E+01	
2.506E+03	6.47E+00	-6.47E+01	1.87E+00	7.73E+01	
2.812E+03	5.39E+00	-6.04E+01	1.91E+00	6.62E+01	
3.155E+03	4.54E+00	-5.47E+01	1.78E+00	5.75E+01	
3.540E+03	3.87E+00	-4.75E+01	1.60E+00	5.40E+01	
3.972E+03	3.35E+00	-3.90E+01	1.47E+00	5.49E+01	
4.456E+03	2.96E+00	-2.91E+01	1.39E+00	5.86E+01	
5.000E+03	2.67E+00	-1.80E+01	1.37E+00	6.36E+01	
5.610E+03	2.48E+00	-5.76E+00	1.39E+00	6.94E+01	
6.295E+03	2.38E+00	7.38E+00	1.45E+00	7.55E+01	
7.063E+03	2.35E+00	2.12E+01	1.53E+00	8.21E+01	
7.924E+03	2.42E+00	3.53E+01	1.65E+00	8.91E+01	
8.891E+03	2.58E+00	4.95E+01	1.81E+00	9.68E+01	
9.976E+03	2.86E+00	6.34E+01	2.04E+00	1.05E+02	
1.119E+04	3.28E+00	7.67E+01	2.36E+00	1.13E+02	<< l.f. UGC
1.256E+04	3.90E+00	8.90E+01	2.81E+00	1.21E+02	
1.409E+04	4.77E+00	1.00E+02	3.44E+00	1.28E+02	
1.581E+04	5.99E+00	1.10E+02	4.31E+00	1.35E+02	
1.774E+04	7.67E+00	1.18E+02	5.50E+00	1.40E+02	
1.991E+04	9.97E+00	1.24E+02	7.14E+00	1.44E+02	
2.233E+04	1.31E+01	1.29E+02	9.35E+00	1.47E+02	
2.506E+04	1.73E+01	1.31E+02	1.23E+01	1.48E+02	
2.812E+04	2.29E+01	1.33E+02	1.63E+01	1.48E+02	
3.155E+04	3.02E+01	1.32E+02	2.15E+01	1.46E+02	
3.540E+04	3.96E+01	1.30E+02	2.82E+01	1.43E+02	
3.972E+04	5.15E+01	1.27E+02	3.67E+01	1.39E+02	
4.456E+04	6.62E+01	1.22E+02	4.73E+01	1.34E+02	
5.000E+04	8.40E+01	1.16E+02	6.02E+01	1.28E+02	
5.610E+04	1.05E+02	1.09E+02	7.55E+01	1.20E+02	
6.295E+04	1.29E+02	1.01E+02	9.31E+01	1.12E+02	
7.063E+04	1.55E+02	9.19E+01	1.13E+02	1.03E+02	

```
  7.924E+04     1.83E+02   8.21E+01   1.34E+02   9.29E+01
  8.891E+04     2.10E+02   7.16E+01   1.56E+02   8.25E+01
  9.976E+04     2.37E+02   6.07E+01   1.77E+02   7.18E+01
  1.119E+05     2.61E+02   4.95E+01   1.97E+02   6.07E+01
  1.256E+05     2.80E+02   3.81E+01   2.15E+02   4.94E+01
  1.409E+05     2.94E+02   2.66E+01   2.30E+02   3.80E+01
  1.581E+05     3.02E+02   1.51E+01   2.40E+02   2.66E+01
  1.774E+05     3.04E+02   3.78E+00   2.46E+02   1.53E+01
  1.991E+05     3.00E+02  -7.34E+00   2.47E+02   4.04E+00
  2.233E+05     2.90E+02  -1.82E+01   2.44E+02  -7.01E+00
```

B.4 DM Attenuation with Compensation

```
   *** 4.4uF cap. inside rectifier, Ls=200uH, Ld=50uH, Zout=.667, A=550
   *** line impedance = 2 LISN networks

   *** MAIN CIRCUIT DEFINITION **********************


   XSOURCE 1 0 RIPVOLT
   XLD 1 2 IND50
   ROUT 1 3 .25
   XAMP 2 5 2 3 AMP
   XLS 2 5 IND200
   XZX1 5 6 11 LISN
   XZX2 0 6 12 LISN
   RZLINE 11 13 0.001
   LZLINE 13 12 0.001U

  .AC DEC 40 50K 5MEG
  .PRINT AC VDB(5) VM(5) VP(5)

  .END


     FREQ        VDB(5)      VM(5)       VP(5)
X

  5.000E+04    -4.54E+01   5.38E-03   2.92E+01
  5.296E+04    -4.64E+01   4.77E-03   3.28E+01
  5.610E+04    -4.75E+01   4.24E-03   3.66E+01
  5.943E+04    -4.84E+01   3.79E-03   4.06E+01
  6.295E+04    -4.94E+01   3.40E-03   4.47E+01
```

```
6.668E+04    -5.03E+01   3.06E-03   4.89E+01
7.063E+04    -5.11E+01   2.77E-03   5.33E+01
7.481E+04    -5.20E+01   2.52E-03   5.77E+01
7.924E+04    -5.27E+01   2.31E-03   6.23E+01
8.394E+04    -5.35E+01   2.12E-03   6.69E+01
8.891E+04    -5.42E+01   1.95E-03   7.16E+01
9.418E+04    -5.48E+01   1.81E-03   7.63E+01
9.976E+04    -5.55E+01   1.69E-03   8.10E+01
1.057E+05    -5.60E+01   1.58E-03   8.58E+01
1.119E+05    -5.66E+01   1.49E-03   9.06E+01
1.186E+05    -5.71E+01   1.40E-03   9.53E+01
1.256E+05    -5.75E+01   1.33E-03   1.00E+02
1.330E+05    -5.79E+01   1.27E-03   1.05E+02
1.409E+05    -5.83E+01   1.21E-03   1.09E+02
1.493E+05    -5.87E+01   1.17E-03   1.14E+02
1.581E+05    -5.90E+01   1.12E-03   1.19E+02
1.675E+05    -5.93E+01   1.09E-03   1.23E+02
1.774E+05    -5.95E+01   1.06E-03   1.28E+02
1.879E+05    -5.97E+01   1.03E-03   1.32E+02
1.991E+05    -5.99E+01   1.01E-03   1.36E+02
2.108E+05    -6.01E+01   9.88E-04   1.41E+02
2.233E+05    -6.02E+01   9.73E-04   1.45E+02
2.366E+05    -6.04E+01   9.60E-04   1.49E+02
2.506E+05    -6.04E+01   9.50E-04   1.53E+02
2.654E+05    -6.05E+01   9.43E-04   1.57E+02
2.812E+05    -6.05E+01   9.39E-04   1.61E+02
2.978E+05    -6.06E+01   9.37E-04   1.65E+02
3.155E+05    -6.06E+01   9.38E-04   1.69E+02
3.342E+05    -6.05E+01   9.41E-04   1.72E+02
3.540E+05    -6.05E+01   9.47E-04   1.76E+02
3.749E+05    -6.04E+01   9.55E-04   1.80E+02
3.972E+05    -6.03E+01   9.66E-04  -1.77E+02
4.207E+05    -6.02E+01   9.79E-04  -1.73E+02
4.456E+05    -6.00E+01   9.95E-04  -1.70E+02
4.720E+05    -5.99E+01   1.01E-03  -1.66E+02
5.000E+05    -5.97E+01   1.03E-03  -1.63E+02
5.296E+05    -5.95E+01   1.06E-03  -1.60E+02
5.610E+05    -5.93E+01   1.08E-03  -1.57E+02
5.943E+05    -5.91E+01   1.11E-03  -1.54E+02
6.295E+05    -5.88E+01   1.15E-03  -1.51E+02
6.668E+05    -5.85E+01   1.18E-03  -1.48E+02
7.063E+05    -5.83E+01   1.22E-03  -1.45E+02
7.481E+05    -5.80E+01   1.26E-03  -1.43E+02 << sw. freq.
7.924E+05    -5.76E+01   1.31E-03  -1.40E+02
8.394E+05    -5.73E+01   1.36E-03  -1.37E+02
8.891E+05    -5.70E+01   1.41E-03  -1.35E+02
9.418E+05    -5.66E+01   1.47E-03  -1.33E+02
9.976E+05    -5.63E+01   1.53E-03  -1.30E+02
```

1.057E+06	-5.59E+01	1.60E-03	-1.28E+02
1.119E+06	-5.55E+01	1.67E-03	-1.26E+02
1.186E+06	-5.52E+01	1.74E-03	-1.24E+02
1.256E+06	-5.48E+01	1.82E-03	-1.22E+02
1.330E+06	-5.44E+01	1.91E-03	-1.20E+02
1.409E+06	-5.40E+01	2.00E-03	-1.18E+02
1.493E+06	-5.36E+01	2.09E-03	-1.17E+02
1.581E+06	-5.32E+01	2.19E-03	-1.15E+02
1.675E+06	-5.28E+01	2.29E-03	-1.13E+02
1.774E+06	-5.24E+01	2.40E-03	-1.12E+02
1.879E+06	-5.20E+01	2.51E-03	-1.10E+02
1.991E+06	-5.16E+01	2.63E-03	-1.08E+02
2.108E+06	-5.12E+01	2.76E-03	-1.07E+02
2.233E+06	-5.08E+01	2.89E-03	-1.05E+02
2.366E+06	-5.04E+01	3.02E-03	-1.04E+02
2.506E+06	-5.00E+01	3.16E-03	-1.02E+02
2.654E+06	-4.96E+01	3.31E-03	-1.01E+02
2.812E+06	-4.92E+01	3.46E-03	-9.89E+01
2.978E+06	-4.88E+01	3.61E-03	-9.73E+01
3.155E+06	-4.85E+01	3.78E-03	-9.56E+01
3.342E+06	-4.81E+01	3.95E-03	-9.39E+01
3.540E+06	-4.77E+01	4.12E-03	-9.22E+01
3.749E+06	-4.73E+01	4.31E-03	-9.03E+01
3.972E+06	-4.69E+01	4.50E-03	-8.84E+01
4.207E+06	-4.66E+01	4.69E-03	-8.64E+01
4.456E+06	-4.62E+01	4.90E-03	-8.44E+01
4.720E+06	-4.58E+01	5.12E-03	-8.22E+01
5.000E+06	-4.54E+01	5.34E-03	-8.00E+01

Appendix C

Simulations of 450 kHz Alternate Drive Circuit

C.1 SPICE Subcircuit Definitions

```
1*******26-AUG-91 *******  SPICE 2G.5 (10AUG81)  *******10:55:53*****

        *** SUBCIRCUIT DEFINITIONS

        *** LISN Network as seen from EMI filter ********************
        *** (L3 connection to ac line left open to add line impedance)
       .SUBCKT LISN 1 6 7
       C1 1 2 1.68U
       RDC1 1 2 1G
       C2 2 3 1.68U
       RDC2 2 3 1G
       L1 2 6 .002
       RM 3 6 50
       L2 1 4 50U
       C3 4 5 8U
       RDC3 4 5 1G
       R3 5 6 5
       L3 4 7 250U
       C4 7 6 2U
       RDC4 7 6 1G
       .ENDS LISN

    ** Components and parasitics ********************
```

```
        .SUBCKT CAP250 1 4
        CIDEAL 1 2 250N
        RSERIES 2 3 50N
        LSERIES 3 4 14N
        RDCPATH 1 4 100MEG
        CCM 1 4 2.35N
        .ENDS CAP250
           * self-resonance at 2.7MHz

       .SUBCKT IND12 1 5
       LIDEAL 1 2 12.5U
       RWIRE 2 3 0.008
       RCORE 1 3 .8K
       CWIND 1 3 1.5P
       LLCM 3 4 0.01U
       RLCM 4 5 0.01
       .ENDS IND12

       .SUBCKT INDDM 1 3
       XINDH 1 2 IND12
       XINDL 2 3 IND12
       .ENDS INDDM


       .SUBCKT CAP5N 1 2
       CIDEAL 1 3 4.7N
       RDCPATH 1 3 100MEG
       RSERIES 3 4 0.3
       LSERIES 4 2 25N
       .ENDS CAP5N

       .SUBCKT CMCAP 1 2
       XYCAPHI 1 2 CAP5N
       XYCAPLO 1 2 CAP5N
       .ENDS CMCAP

   ** EMI sources and impedances ***

.SUBCKT RIPVOLT 1 2
VSW 1 2 AC 1
RVSW 1 2 100MEG
.ENDS RIPVOLT

       .SUBCKT ZPOWSUPDM 1 4
       CBULK 1 2 1U
       RCBULK 3 2 .05
       LCBULK 3 4 38N
       RSW 1 2 10000
```

```
.ENDS ZPOWSUPDM
** Based on self-resonance estimate of 800kHz

 * high-frequency roll-off compensation pole at 1.5 MHz
 .SUBCKT ROLLOFF 1 2 3
 R6 1 4 0.00067
 C6 4 2 159U
 E6 3 2 4 2 1
 .ENDS ROLLOFF

** Amplifier input impedance and related lag compensation network
** For a factor of 6 in lag between 1.5 - 9 MHz
.SUBCKT INCOMP 1 2 3
RC 1 3 10.5K
CC 1 3 1.67P
RIN 3 2 500K
CIN 3 2 10P
.ENDS INCOMP

 * main amplifier subcircuit
 .SUBCKT AMPDMLT 1 2 3 4
 XINHI 1 5 6 INCOMP
 XINLO 2 5 7 INCOMP
 EGAIN 8 4 6 7 79
 XCOMP1 8 4 3 ROLLOFF
 .ENDS AMPDMLT


** CM stuff  ********************

.SUBCKT ZPOWSUPCM 1 4
CPAR 1 2 50P
RC 3 2 .05
LC 3 4 50N
RSW 1 2 10000
.ENDS ZPOWSUPCM
** Based on self-resonance estimate of 800kHz

 * main amplifier subcircuit
 .SUBCKT AMPCM 1 2 3 4
 XINHI 1 2 6 INCOMP
 XINLO 1 2 6 INCOMP
 EGAIN 8 4 6 2 79
 XCOMP1 8 4 3 ROLLOFF
 .ENDS AMPCM
```

C.2 Uncompensated DM LT With Short-Circuit as External Impedance

```
UNCOMP. LT OF 450KHZ "ALTERNATE DRIVE" INDUCTOR ENHANCEMENT CIRCUIT

       ** (Differential-mode sub-circuit)
           *** 25uH,25uH,220nF,Zout=0.5ohm,A=64 (needed 450kHz gain)
           *** Actual A=79
           *** Line impedance is 0.01 ohms resistive

         .OPTIONS NUMDGT=3 LIMPTS=1400

      ** Components and parasitics ********************


    *** MAIN CIRCUIT DEFINITION **********

     XPSIMP 1 0 ZPOWSUPDM
     XLD 1 2 INDDM
     ROUT 2 3 0.5
     XCF 4 0 CAP250
     XVSW 7 8 RIPVOLT
     RDCPATH 8 0 1G
     XAMP 8 7 3 4 AMPDM
     XLS 2 5 INDDM
     RZXMIN 5 0 0.01

     .AC DEC 40 60 20MEG
     .PRINT AC VM(4,3) VP(4,3) VM(5,2) VP(5,2)

     .END
```

C.3 Uncompensated CM LT With Short-Circuit as External Impedance

```
UNCOMP. LT OF 450KHZ "ALTERNATE DRIVE" INDUCTOR ENHANCEMENT CIRCUIT

      ** (Common-mode sub-circuit)
          *** 100uH, 320uH,9.4nF,Zout=0.5ohm,A=64(needed 450kHz gain)
```

```
        *** Actual A=79
        *** Line impedance is 0.05 ohms resistive

      .OPTIONS NUMDGT=3 LIMPTS=1400

  *** MAIN CIRCUIT DEFINITION **********

   XPSIMP 1 0 ZPOWSUPCM
   LD 1 2 100U
   ROUT 2 3 0.5
   XCF 4 0 CMCAP
   XVSW 7 8 RIPVOLT
   RDCPATH 8 0 1G
   XAMP 8 7 3 4 AMPCM
   LS 2 5 350U
   RZXMIN 5 0 0.05

   .AC DEC 40 60 20MEG
   .PRINT AC VM(4,3) VP(4,3) VM(5,2) VP(5,2)

   .END
```

C.4 Uncompensated DM LT With LISN Impedance

```
UNCOMP. LT OF 450KHZ "ALTERNATE DRIVE" INDUCTOR ENHANCEMENT CIRCUIT

    ** (Differential-mode sub-circuit)
        *** 25uH, 25uH,250nF,Zout=0.5ohm,A=64 (450kHz gain needed)
        *** Actual A = 79
        *** Line impedance is series combination of 2 LISNs & 100uH
        *** external impedance

      .OPTIONS NUMDGT=3 LIMPTS=1400


 *** MAIN CIRCUIT DEFINITION **********

   XPSIMP 1 0 ZPOWSUPDM
   XLD 1 2 INDDM
   ROUT 2 3 0.5
   XCF 4 0 CAP250
   XVSW 7 8 RIPVOLT
   RDCPATH 8 0 1G
```

```
XAMP 8 7 3 4 AMPDMLT
XLS 2 5 INDDM
XZXH 5 9 10 LISN
XZXL 0 9 11 LISN
LZLINE 10 11 100U

.AC DEC 40 60 20MEG
.PRINT AC VM(4,3) VP(4,3) VM(5,2) VP(5,2)

.END
```

C.5 Uncompensated DM LT With Max. Inductive Imp.

```
UNCOMP. LT OF 450KHZ "ALTERNATE DRIVE" INDUCTOR ENHANCEMENT CIRCUIT

      ** (Differential-mode sub-circuit)
      *** 25uH, 25uH,220nF, Zout=0.5ohm, A=64 (needed midband gain)
      *** Actual A=79
      *** Line impedance is 200uH inductive

        .OPTIONS NUMDGT=3 LIMPTS=1400

   *** MAIN CIRCUIT DEFINITION **********

    XPSIMP 1 0 ZPOWSUP
    XLD 1 2 INDDM
    ROUT 2 3 0.5
    XCF 4 0 CAP250
    XVSW 7 8 RIPVOLT
    RDCPATH 8 0 1G
    XAMP 8 7 3 4 AMP
    XLS 2 5 INDDM
    LZXMAX 5 0 200U

    .AC DEC 40 60 20MEG
    .PRINT AC VM(4,3) VP(4,3) VM(5,2) VP(5,2)

    .END
```

C.6 Matlab Compensation Program

```
% HERE IS SOME OF THE DATA RESULTING FROM THE BELOW PROGRAM
%midband gain (at 450 kHz)=   63.9317
% powfreqgains =  16.9049   50.1105   82.9524  114.7045
% worst p.m.'s are   151   deg. at  4.108 kHz for lisn  case
%                    153.3 @  3.900 for case of lx=200uH, rx=0
% Other cases considered: rmin=.01 ; lmax = 200uH ; cm with 1uohm
% H.F. LT:  mag=2 at 14.5 MHz (angle=-110 and rising to -90)
f=freq(m:n);
%
%
% HERE IS THE MAIN PROGRAM
%
a = 1.47;    % times factor of 79 used in SPICE simulation
%%% factor of 1.47 is to compensate for loss of midband
%%% gain due to compensation effects
%
s=j*2*pi*f;
%
dczeros = 2*pi*1e3 * [   0   ];
dcpoles = 2*pi*1e3 * [   2   ];
lagzeros = 2*pi*1e3 * [ 10 ];
lagpoles = 2*pi*1e3 * [ 2  ];
hlagzeros = 2*pi*1e3 * [ 105 105 ];
hlagpoles = 2*pi*1e3 * [ 29 29  ];
leadzeros = 2*pi*1e3 * [ 110 110 ];
leadpoles = 2*pi*1e3 * [ 400 400 ];
%
dcnum = poly(dczeros);
dcden = poly(dcpoles);
dcn = polyval(dcnum,s);
dcd = polyval(dcden,s);
dccomp = ( dcn ./ dcd ) ;
lagnum = poly(lagzeros);
lagden = poly(lagpoles);
lagn = polyval(lagnum,s);
lagd = polyval(lagden,s);
lagcomp = ( lagn ./ lagd ) ;
hlagnum = poly(hlagzeros);
hlagden = poly(hlagpoles);
hlagn = polyval(hlagnum,s);
hlagd = polyval(hlagden,s);
hlagcomp = ( hlagn ./ hlagd ) ;
leadnum = poly(leadzeros);
leadden = poly(leadpoles);
leadn = polyval(leadnum,s);
leadd = polyval(leadden,s);
leadcomp =  ( leadn ./ leadd ) ;
%
```

```
c = a * dccomp .* lagcomp .* leadcomp .* hlagcomp ;
cmag = abs(c);
[cang] = dewrap(180 * (angle(c))/pi);
% to unwrap phase calculated by matlab
cang = -cang';
%
g = cmag .* gain(m:n);
mbgain = g(156)
powfreqgains=[ g(1) g(20) g(29) g(35) ]
% 60, 180, 300, and 420 Hz gains
%
ugcplot;
gettransimp;
%
%
%SUBROUTINES
%
% This subroutine (ugcplot) plots worst case LT's with compensation
%
clg;
subplot(211);
axis([3 5 0 3]);
%axis([5 8 0 2]);
%loglog(f,cmag.*ltmfd,f,cmag.*ltmfc,f,cmag.*ltmad );
loglog(f,cmag.*ltmfd,f,cmag.*ltmfc,f,cmag.*ltmad,f,cmag.*ltmcd);
xlabel('frequency(Hz)');
ylabel('magnitude');
axis([ 3 5 120 180]);
%axis([ 5 8 -150 60]);
title('Compensated Worst-Case LT's for 450 kHz Alt. Dr.')
qq= cang + ltpfd(m:n);
semilogx(f,qq,f,(cang+ltpfc(m:n)),f,(cang+ltpad(m:n)),f,
       (cang+ltpcd(m:n)));
%semilogx(f,qq,f,(cang+ltpfc(m:n)),f,(cang+ltpad(m:n)));
xlabel('frequency(Hz)');
ylabel('angle(degrees)');
axis;
%
% This subroutine (gettransimp) was used to find and
% plot the trans-impedance
%
zls = abs ( 12.5e-6*2*pi*j*freq + .008);
transimp = g .* zls ;
semilogy(freq,transimp);
title('Transimpedance of alternate drive inductor enhnancement
circuit from line current to amplifier output')
xlabel('frequency(Hz)');
ylabel('transimpedance(volts/amp');
```

```
grid;
```

C.7 Calculation of Differential-Mode Attenuation

```
DM ATTENUATION OF 450KHZ "ALTERNATE DRIVE" INDUCTOR ENHANCEMENT CIRCUIT

            ** (Differential-mode sub-circuit)
            *** 25uH, 25uH,250nF, Zout=0.1 ohm
            *** Nominal A = 79
            *** Line impedance is series combination of 2 LISNs

          .OPTIONS NUMDGT=3 LIMPTS=1400

*****  MODIFIED SUBCIRCUITS ***********

         .SUBCKT CAP250 1 4
         CIDEAL 1 2 250N
         RSERIES 2 3 50M
         LSERIES 3 4 14N
         RDCPATH 1 4 100MEG
         CCM 1 4 2.35N
         .ENDS CAP250
            * self-resonance at 2.7MHz

        .SUBCKT IND12 1 5
        LIDEAL 1 2 12.5U

        RWIRE 2 3 0.008
        RCORE 1 3 .8K
        CWIND 1 3 1.5P
        LLCM 3 4 0.01U
        RLCM 4 5 0.01
        .ENDS IND12

        .SUBCKT INDDM 1 3
        XINDH 1 2 IND12
        XINDL 2 3 IND12
        .ENDS INDDM

          * main amplifier subcircuit
          .SUBCKT AMP 1 2 3 4
```

```
        XINHI 1 5 6 INCOMP
        XINLO 2 5 7 INCOMP
        EGAIN 8 4 6 7 115.77
        XCOMP1 8 4 3 ROLLOFF
        .ENDS AMP


******* MAIN CIRCUIT DEFINITION **********

      XEMISRC 1 0 RIPVOLT
      XLD 1 2 INDDM
      ROUT 2 3 0.1
      XCF 4 0 CAP250
      ESENSE 7 8 2 5 1
      RDCPATH 8 0 1G
      XAMP 8 7 3 4 AMP
      XLS 2 5 INDDM
      XZXH 5 9 10 LISN
      XZXL 0 9 11 LISN
      LZLINE 10 11 100U

      .AC DEC 40 100K 100MEG
      .PRINT AC VM(5) VM(2,5) VM(3,4)
      .END
```

C.8 Calculation of Common-Mode Attenuation

```
CM ATTENUATION OF 450KHZ "ALTERNATE DRIVE" INDUCTOR ENHANCEMENT CIRCUIT

        ** (Common-mode sub-circuit)
        *** 100uH, 350uH, 9.4nF, Zout=0.025ohm , A=115.7
        *** Line impedance is 2 parallel lisns


        .OPTIONS NUMDGT=3 LIMPTS=1400

******** MODIFIED SUBCIRCUIT DEFINITIONS **********************

   .SUBCKT IND750 1 5
   LIDEAL 1 2 750U
```

```
CWIND 1 2 8P
RCORE 1 2 20K
RWIRE 2 3 10M
LDM 3 4 6U
RDM 4 5 4M
.ENDS IND750
   * rcore is a guess here (3mH cm choke had 32K)

.SUBCKT IND350 1 5
LIDEAL 1 2 350U
CWIND 1 2 5P
RCORE 1 2 16K
RWIRE 2 3 5M
LDM 3 4 6U
RDM 4 5 4M
.ENDS IND350
   * rcore is a guess here (3mH cm choke had 32K)

.SUBCKT IND100 1 5
LIDEAL 1 2 100U
CWIND 1 2 2.5P
RCORE 1 2 12K
RWIRE 2 3 2M
LDM 3 4 6U
RDM 4 5 4M
.ENDS IND100
   * rcore is a guess here (3mH cm choke had 32K)

      * main amplifier subcircuit
      .SUBCKT AMP 1 2 3 4
      XINHI 1 2 6 INCOMP
      XINLO 1 2 6 INCOMP
      EGAIN 8 4 6 2 115.8
      XCOMP1 8 4 3 ROLLOFF
      .ENDS AMP


*** MAIN CIRCUIT DEFINITION **********

 XEMISRC 1 0 RIPVOLT
 XLD 1 2 IND100
 ROUT 2 3 0.025
 XCF 4 0 CMCAP
 ESENSE 7 8 2 5 1
 RDCPATH 8 0 1G
 XAMP 8 7 3 4 AMP
 XLS 2 5 IND350
 XZXH 5 0 9 LISN
```

```
XZXL 5 0 10 LISN
RSHORT 9 10 0.01

.AC DEC 40 100K 100MEG
.PRINT AC VM(5)

.END
```

Bibliography

[1] H. W. Ott. *Noise Reduction Techniques in Electronic Systems*, New York: John Wiley and Sons, 1988.

[2] L. E. LaWhite. *Active Filters for 1 MHz Power Circuits Under Strict Ripple Limitations*, MS Thesis, Massachusetts Institute of Technology, February 1987.

[3] L. E. LaWhite. "Design of Active Ripple Filters for Power Circuits Operating in the 1-10 MHz Range," *Proceedings of the 18th Annual IEEE Power Electronics Specialists Conference*, Blacksburg, Virginia, 1987, pp. 195-203.

[4] L. E. LaWhite. "Active Filters for 1 MHz Power Circuits With Strict Input/Output Ripple Requirements," *Proceedings of the 17th Annual IEEE Power Electronics Specialists Conference - PESC 1986.*

[5] C. R. Paul and K. B. Hardin. "Diagnosis and Reduction of Conducted Noise Emissions," *1988 IEEE International Symposium on Electromagnetic Compatibility*, Session 2A, pp. 19-23.

[6] G. Dash. "EMI Regulation and Control in Power Supplies and Computers for U.S. and Foreign Use," *Proceedings of the Power Electronics Show and Conference*, Boxborough, MA, April 27-29, 1987, pp. 187-206.

[7] C. M. Kendall and A. A. Schmid. "Characteristics and Control of EMI in a Switching Regulator Power Converter," *Proceedings of PowerCon 1983* Session G-4.

[8] W. D. Kimmel. "Focus on Ferrite Filters," *RF Design*, August 1990, pp. 32-34.

[9] "Manual: Artificial Mains Network ESH2-Z5." New York: Polarad Electronics, Inc.

[10] MIL-STD-462. *Military Standard: Electromagnetic Interference Characteristics, Measurement of.* July 31, 1967.

[11] "Capacitors for RfI Suppression of the AC Line: Basic Facts", EVOX/RIFA, inc., Lincolnshire, IL, second ed., Feb. 1990.

[12] K. H. Beeber and C. A. Forsberg. "Controlling Conducted EMI With Ferrite Cores and L-C Filter Networks", *Powercon 11 Proceedings*, April 10-12, 1984, Paper C1-2.

[13] J. L. Norman Violette, D. White, and M. F. Violette, *Electromagnetic Compatibility Handbook.* New York: Van Nostrand Reinhold Company, 1987.

[14] J. G. Kassakian, M. F. Schlecht, and G. C. Verghese. *Principles of Power Electronics.* Reading, MA: Addison-Wesley Publishing Company, Inc., 1991.

[15] J.K. Roberge. *Operational Amplifiers: Theory and Practice.* New York: John Wiley and Sons, Inc., 1975.

[16] "Capacitors 1990/91", RIFA catalogue. Kalmar, Sweden, 1990.

[17] P. Horowitz and W. Hill. *The Art of Electronics* Cambridge: Cambridge University Press, 1986.

[18] J. Walker. "Designing Practical and Effective Active EMI Filters." *Powercon 11 Proceedings*, April 10-12, 1984. Paper I-3.

[19] D. Gerke, P.E., B.S.E.E. Kimmel-Gerke Associates, St. Paul, MN. Consultant with expertise in power disturbances, ESD, FCC/VDE EMC requirements.

[20] F. Martzaloff. National Institute of Standards and Technology, Gaithersburg, MD. Leading researcher on lightning effects and surge impedances.

[21] J. R. Nicholson and J. A. Malack. "RF Impedance of Power Lines and Line Impedance Stabilization Networks in Conducted Interference Measurements." *IEEE Transactions on Electromagnetic Compatibility*, May 1973, pp. 84-86.

[22] G. Rau, EPRI.

[23] R. A. Southwick. "Impedance Characteristics of Single-Phase Powerlines." *IEEE EMC Symposium Record*, 1973, pp 241-252.

[24] J. H. Bull. "Impedance of the Supply Mains at Radio Frequencies." *1st Symposium And Technical Exhibition on Electromagnetic Compatibility*, Montreaux, May 20-22, 1975, pp. 357-362.

[25] M. Tanaka. "High Frequency Noise Power Spectrum, Impedance, and Transmission Loss of Power Line in Japan on Intrabuilding Power Line Communitcation." *IEEE Transactions on Consumer Electronics*, Vol 34, No. 2, May 1988, pp. 321-326.

[26] J. G. Kassakian and M. F. Schlecht. "High-Frequency High-Density Converters for Distributed Power Supply Systems." *Proceedings of the IEEE*, vol. 76, no. 4, April 1988.

[27] D. H Staelin, J. A. Kong, A. W. Morgenthaler. *Electromagnetic Waves.* (Course notes.) Cambridge, MA: M.I.T, 1989.

[28] M. W. Earley, R. H. Murray., and J. M. Caloggero. *The 1990 National Electrical Code Handbook.* Quincy, MA: National Fire Protection Association, 1989.